UNIVERSITY OF LIVERPOOL

The Role of Genetic Background and Hypoxia in the Chemotherapeutic Efficiency in Paediatric Brain Tumours

Thesis submitted in accordance with the requirements of the University of Liverpool

For the degree of Doctor in Philosophy by

Yuen Ngan Carol Fan

December 2013

Abstract

Medulloblastoma (MB) is the most common malignant brain tumour in children. MBs arise in the cerebellum, originating from neural stem cells progenitors. It has previously been shown that the lack of integrity of signalling pathways due to genetic alterations play a key role in MB chemosensitivity. An example is the p53 signalling, with p53 mutations and or deletions which are associated with drug resistance. Here, we explored the role of p53 induction by chemotherapeutic drugs such as etoposide in MB and the way to bypass the need for intact p53 to trigger apoptosis. We specifically demonstrated that a downstream miRNA target transcribed by p53, miR-34a, is able to reduce the number of viable cells in cultures of MB cells lacking functional p53, although the effect was limited.

Beyond the genetic background of a tumour, it is more and more described that the tumour microenvironment plays a key role in drug resistance. MB is a solid tumour and hence will contain areas deprived in oxygen (hypoxic). It has been widely documented that hypoxia is associated with poor prognosis and resistance to treatment in other cancer models and we here aimed to investigate the specific role of hypoxia in MB response to etoposide. We demonstrated that MB (p53 WT) cell lines became more resistant in chronic but not acute hypoxia and this was associated with a decrease in the recruitment of double strand DNA damage sensing machinery and subsequent impairment to transactivate p53 and transcription of pro-apoptotic genes.

A transcriptomic microarray profiling study further revealed that chronic hypoxia induced broad and significant changes in global gene expression affecting many biological pathways including stem cell maintenance, neuronal development and phosphoinositol-3 phosphate kinase.

List of Abbreviations

AA	Amino Acids
ABC	ATP-binding cassette
APS	Ammonium Persulphate
ARNT	Aryl-hydrocarbon receptor nuclear translocator
bHLH	Basic helix-loop-helix
BBB	Blood brain barrier
BSA	Bovine Serum Albumin
CBP	CREB Binding Protein
CMV	Cytomegalo Virus
CREB	cAMP Response Element Binding Protein
DMEM	Dulbecco's Modified Eagle Medium
DMSO	Dimethyl sulphoxide
DNA	Deoxyribose Nucleic Acid
dNTP	Deoxribonucleotide Triphosphate
DsRedXP	DsRed-Express
E.coli	Escherichia coli
EGFP	Enhanced Green Fluorescent Protein
ETO	Etoposide
FITC	Fluorescein Isothiocyanante
FCS	Fetal Calf Serum
HAT	Histone Acetyl Transferase
HDAC	Histone Deacetylase
HRE	Hypoxia Response Element
HRP	Horseradish Peroxidase
Hrs	Hours
IR	Ionization Radiation
Luc	Luciferase
LSM	Laser Scanning Microscopy

MEM	Modified Eagle's Medium
mRNA	Messenger Ribose Nucleic Acid
NLS	Nuclear Localisation Sequence
ODDD	Oxygen dependent degradation domain
PAS	PER-ARNT-SIM
PBS	Phosphate Buffered Saline
PCR	Polymerase Chain Reaction
PER	Period circadian protein
PHD	Prolyl Hydroxylase Domain
PK	Protein Kinase
RNA	Ribonuclei Acid
RNApol	RNA polymerase
RPM	Revolutions per minute
RT-PCR	Reverse Transcription Polymerase Chain Reaction
SD	Standard Deviation
SDS	Sodium Dodecyl Sulphate
SEM	Standard error of the mean
SUMO	Small Ubiquitin-Like Protein
TAD	Transcriptional activation domain
TEMED	Tetramethylethylenediamine
Tris	Tris(hydroxymethyl)aminomethane
UV	Ultra Violet Light
V/V	Volume per Volume
WT	Wild-type
W/V	Weight per Volume
YFP	Yellow Fluorescent Protein

Contents

ABSTRACT ii

LIST OF ABBREVIATIONS iii

Chapter 1: Introduction 1

1.1 Human cancer 2

1.2 Cancer cell biology 2

1.2.1 Tumour growth 3

1.2.2 Tumour microenvironment 4

1.2.2.1 Cellular energetics of cancer cells 5

1.2.2.2 Angiogenesis 5

1.2.2.3 Tissue invasion and metastasis 6

1.3 Cellular oxygen regulation 7

1.3.1 The HIF family of protein 8

1.3.2 The HIF signalling pathway 9

1.4 Brain tumours 11

1.4.1 Gliomas 11

1.4.1.1 Glioblastoma multiforme (GBM) 11

1.4.1.2 Origin of GBM 12

1.4.1.3 GBM treatment 12

1.5 Brain tumour in children 13

1.5.1 Medulloblastoma 13

1.5.1.1 Histopathology 14

1.5.1.2 MB subgroup classification and genetic markers 15

1.5.1.3 MB subgroup characterisation 17

1.5.1.4 Genetic Predisposition of MB 18

1.5.1.5 Symptoms of patients with MB 19

1.5.1.6 Prognosis 19

1.5.2 Current Treatment 20

1.5.2.1 Etoposide 21

1.5.2.2 Cisplatin 21

1.5.2.3 Methotrexate 21

1.5.2.4 Problems with current MB treatment 21

1.5.2.5 Tumour hypoxia and chemoresistance 22

1.6 DNA Damage response 24

1.6.1 Double stranded breaks 24

1.6.1.1 Non-homologous End-Joining (NHEJ) repair 25
1.6.1.2 Homologous recombination repair 25
1.6.1.3 Pathological relevance of *NBN* 28
1.7 The p53 signalling pathway 29
1.7.1 Structure of p53 29
1.7.2 Regulation of p53 31
1.7.2.1 p53 regulation by MDM2 31
1.7.2.2 Activation of p53 32
1.7.2.3 Oscillations of p53 34
1.7.3 p53 mutations in cancer 34
1.8 MicroRNA 37
1.8.1 Biogenesis of miRNA 37
1.8.2 MicroRNA expression in cancer 38
1.8.2.1 Hypoxia regulated miRNAs 39
1.8.2.2 MicroRNA expression in brain tumours 39
1.8.2.3 miR-34 microRNA family 40
1.9 Project aims and hypothesis 42
Chapter 2: Materials and Methods 44
2.1 Chemical and Reagents 45
2.2 Drug and Chemical Treatments 45
2.3 Cell Lines and growth requirements 45
2.3.1 Routine sub-culturing protocol 46
2.3.1.1 Sub-culturing protocol for non-adherent cells 46
2.3.1.2 Sub-culturing protocol for adherent cells 47
2.4 Molecular Biology techniques 48
2.4.1 DNA propagation 48
2.4.1.1 Transformation of Competent Cells 48
2.4.1.2 Purification of Plasmid DNA (Plasmid Maxi Preparation) 48
2.4.2 Plasmid Transfection 49
2.4.3 Oligonucleotides (miRNA, siRNA) Transfection 50
2.5 Real time PCR (qPCR) 51
2.5.1 Total RNA extraction 51
2.5.1.1 Reverse Transcription 51
2.5.2 MicroRNA extraction 51
2.5.2.1 Reverse Transcription-First Strand cDNA synthesis 52
2.5.2.2 Quality Quantification of Nucleic Acid 52

2.5.3 qPCR 52
2.6 Microarray study 54
2.6.1 Design of the microarray study 54
2.6.2 Microarray sample preparations 55
2.6.2.1 Messenger RNA extraction with Rneasy Plus 55
2.6.2.2 Transcriptome amplification 55
2.6.2.3 PCR purification 56
2.6.2.4 Agarose Gel electrophoresis 56
2.6.3 Microarray analyses 56
2.6.3.1 Microarray Raw data 56
2.6.3.2 Transcript expression plots 58
2.6.3.3 Statistical analysis of Microarray Data 59
2.6.3.4 Biological analysis with Ingenuity Pathway Analysis 61
2.7 Single cell Imaging 62
2.7.1 Immunocytofluorescence 62
2.7.2 Comet Assay 62
2.7.3 Confocal Imaging 63
2.7.3.1 Tracking analysis-calculating threshold 63
2.8 Western blotting 64
2.8.1 Sample preparation 64
2.8.1.1 Protein concentration assay 64
2.8.2 Protein separation by SDS-PAGE 64
2.8.3 Protein transfer onto nitrocellulose membrane 65
2.8.4 Antibody incubations and protein detection 65
2.9 Cell Viability assays 66
2.9.1 MTS Assay 66
2.9.2 ViaCount viability assay 66
2.10 Cell cycle Analysis 67
2.11 Statistical analysis 67
Chapter 3: Chemoresistance in MB 68
3.1 Introduction 69
3.2 Results 70
3.2.1 D283 response to etoposide treatment 70
3.2.2 Effect of etoposide on the p53 signalling pathway in MB cells 71
3.2.2.1 Etoposide-induced p53 protein levels 71
3.2.2.2 Etoposide-induced p53 transcriptional activity 72

3.2.2.3 Restoration of p53 pathway 74
3.2.3 Bypassing p53 activation 78
3.2.3.1 Induction of miR-34a by etoposide 79
3.2.3.2 Etoposide-induced miR-34a is p53 dependent 80
3.2.3.3 Functional role of miR-34a 81
3.2.3.4 The effect of SIRT1 inhibitors on cell number 83
3.2.3.5 The effect of miR-34a on cell number 86
3.2.4 Role of miR-34a in other brain tumours 88
3.3 Chapter 3 Discussion 90
3.3.1 p53 status and chemoresistance 90
3.3.2 Inhibition of a pro survival gene, SIRT1 91
3.3.3 Introduction of miR-34a 92
Chapter 4: Hypoxia-induced Chemoresistance 93
4.1 Introduction 94
4.2 Results 95
4.2.1 Effects of Hypoxia on Cell Fate 95
4.2.1.1 Growth Analysis of D283 cells in hypoxia 95
4.2.1.2 Cell Cycle profile of D283 cells in hypoxia 97
4.2.2 Effect of hypoxia on response to chemotherapy 100
4.2.2.1 Sensitivity of Etoposide treatment in hypoxia 100
4.2.2.2 Etoposide-induced G2/M accumulation 102
4.2.3 Validating etoposide drug action in hypoxia 104
4.2.3.1 Visualising DNA breaks induced by etoposide in normoxia and hypoxia 105
4.2.4 Effect of chronic hypoxia on p53 signalling pathway 108
4.2.4.1 Etoposide-induced p53 transcriptional activity in hypoxia 108
4.2.4.2 Etoposide-induced p53 phosphorylation in chronic hypoxia 110
4.2.5 Bridging DNA damage to p53 activation 111
4.2.5.1 ATM activities in chronic hypoxia 112
4.2.6 Role of hypoxia on p53 activation in other brain tumours 114
4.2.6.1 Etoposide-induced p53 expression in Glioblastoma 114
4.2.6.2 Etoposide-induced p53 activity in Glioblastoma 115
4.2.6.3 Chemosensitivity of U87 cells in hypoxia 116
4.3 Chapter 4 Discussion 117
4.3.1 Hypoxia duration and acquired chemoresistance 117
4.3.2 The relationship of hypoxia and p53 118
4.3.3 ATM activation and p53 induced apoptosis 119

4.3.4 The effect of hypoxia on cancer cell biology 121
Chapter 5: Gene Expression in Hypoxia Associated with Drug Resistance 122
5.1 Introduction 123
5.2 Results 125
5.2.1 HIF signalling in chronic hypoxia 125
5.2.1.1 HIF-1α expression in chronic hypoxia 125
5.2.1.2 HIF-1α target genes expression in chronic hypoxia 126
5.2.2 Microarray Gene Expression study 128
5.2.3 Expression of multidrug drug resistance genes 129
5.2.4 Expression of hypoxia-induced drug resistance genes 130
5.2.5 Significantly expressed genes 134
5.2.5.1 Producing heat map clustergrams 134
5.2.5.2 Optimising heatmap clustergrams 135
5.2.6 Expression of p53 and DNA damage genes in chronic hypoxia 137
5.2.6.1 p53 pathway analysis 137
5.2.6.2 DSB repair pathways 139
5.2.7 Microarray target validation 143
5.2.7.1 Target gene validation by qRT-PCR 143
5.2.7.2 Nibrin protein levels in hypoxia 144
5.2.8 Role of nibrin in other cell lines 145
5.3 Chapter 5 Discussion 147
5.3.1 HIF kinetics 147
5.3.2 Hypoxia-induced chemoresistance genes 148
5.3.3 DNA repair in hypoxia 149
5.3.4 Role of nibrin and p53 150
5.3.5 Prognostic value of nibrin 151
Chapter 6: Global Gene Expression in Acute and Chronic Hypoxia 153
6.1 Introduction 154
6.2 Results 155
6.2.1 Microarray further analysis 155
6.2.1.1 Profile Clustering by hypoxic time points 155
6.2.1.2 Grouping by expression pattern using k-means clustering 158
6.2.2 Biological analysis of acute and chronic hypoxia gene expression 160
6.2.2.1 Network and canonical pathway analysis in acute hypoxia 160
6.2.2.2 Upstream transcription factor analysis in acute hypoxia 163
6.2.2.3 Canonical pathway analysis for chronic hypoxia 163

6.2.2.4 Upstream transcription factor analysis in chronic hypoxia 168
6.3 Chapter 6 Discussion 171
6.3.1 A global view of microarray analysis 171
6.3.1.1 Signalling pathways affected by chronic hypoxia 172
6.3.1.2 Transcription factor regulation in chronic hypoxic conditions: and the role of ZNF217 and EZH2 transcription repressor 174
6.3.1.3 Limitations of microarray 175
Chapter 7: General Discussion 176
7.1 Project overview 177
7.1.1 The significance of p53 in MB 177
7.1.2 The global cellular effect of hypoxia 178
7.1.3 Future perspective for MB treatment 179
7.1.3.1 Targeted therapy 179
7.1.4 Moving towards *in vivo* study 180
7.1.5 Final Remarks 181
REFERENCES 182
APPENDIX 229

Chapter 1: Introduction

1.1 Human cancer

Cancer is a disease characterised by abnormal cell growth, caused by multiple changes in gene expression leading to deregulation of the cellular program controlling cell fate. These genetic changes result in imbalance of cell proliferation and cell death, promoting the growth of malignant tumour cell populations that can invade neighbouring tissues and metastasise to other distant parts of the body.

Cancer can occur in almost any part of the human body and, as the disease progresses, can affect the functions of vital organs and is usually life threatening. In the UK, cancer was responsible for 150,000 deaths in 2010, contributing to the major cause of mortality with the exclusion of infantile death under one year. Cancer of the brain and central nervous system (CNS) remains the leading killer of childhood cancers in the UK (Stiller, 2007). This project was developed in collaboration with paediatric oncologists and surgeons from the Alder Hey Children's hospital, and therefore this thesis focus on paediatric brain tumours.

1.2 Cancer cell biology

Cancer cells have a distinct altered cell biology compared to normal cells. The functional capabilities of cancer cells were first described and classified around 10 years ago by *Hanahan and Weinberg* (Hanahan and Weinberg, 2000). In their review, they have described six hallmarks of cancer cells: self-sufficiency in growth signals, insensitivity to anti-growth signals, evading apoptosis, limitless replicative potential, sustained angiogenesis and tissue invasion & metastasis. Over the last decade, advancing studies have further lead to the emergence of two additional hallmarks: deregulating cellular energetics and avoiding immune destruction (**Figure 1.1**) (Hanahan and Weinberg, 2011). It is these acquired functions of cancer cells that enable them to survive and proliferate during the course of tumour development. In this thesis, we will consider how some of these hallmarks are enabled in brain tumours, hence promoting survival and tumourgenesis.

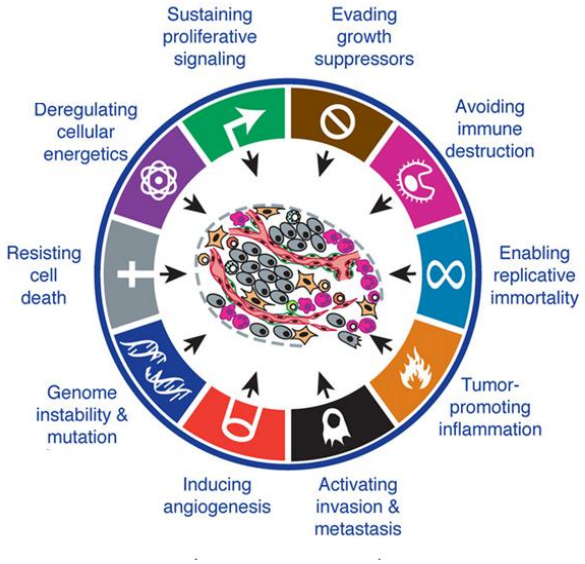

Figure 1.1 Hallmarks of Cancer. *A diagram illustrating the ten hallmarks of cancer capabilities which contribute to tumourgenesis, as described by Hanahan and Weinberg. This figure is from the original paper* (Hanahan and Weinberg, 2011).

1.2.1 Tumour growth

One of the most eminent capabilities of cancer is deregulated cell proliferation. Normally, cell growth and division are controlled to ensure the maintenance of tissue homeostasis. Cells remain non-proliferative until growth is triggered by extracellular mitogenic signals. These signals are generally growth factors (GFs), which will bind to GF receptors located on the cell membrane, where they will transmit the signals within the cells. The growth signals will then activate a series of signalling cascades to activate cell proliferation. In the context of a developing brain, the brain expresses a large selection of these mitogenic growth signals, such as fibroblasts growth factors (FGF), insulin growth factors (IGFs), platelet-derived growth factors (PDGFs) and epidermal growth factors (EGF) (Altaba *et al.*, 2002, Cheng *et al.*, 2001, Xu *et al.*, 2000). Many of these factors dictate cell proliferation and cell differentiation, therefore, the probability of a fault in one of these signalling pathways/ response is high. Indeed, amplification and upregulation of growth factors and growth factor receptors is associated with many brain tumours (Tuzi *et al.*, 1991, Diedrich *et al.*, 1995, Ekstrand *et al.*, 1991). Moreover, the loss of functions and or deletions of tumour suppressor genes such as *p53*, *PTCH* and *PTEN* are often observed in brain cancer (section 1.4.1 and 1.5.1).

1.2.2 Tumour microenvironment

Tumour microenvironment describes the whole structure of the tumour, including the heterogeneity of the cell types within and the surrounding oxygen concentration. Where oxygen tension falls below the cell's regular demands, cells experience hypoxia. Hypoxia is a common characteristic of solid tumours (such as brain tumours), this is due to the rapidly dividing nature of cancer cells outgrowing its vasculature. In addition to this, although angiogenesis (formation of new blood vessels) in the tumour is promoted, these blood vessels in tumours tend to be weaker, leaky and have blockages (Dvorak *et al.*, 1991), therefore oxygen supply to the cells is often not sufficient. Depending on the distance between tumour cells and the nearest blood vessels, tumour cells experience a varied gradient of oxygen concentration across the mass of the tumour, with the centre core being the most hypoxic (**Figure 1.2**). Additionally, tumour cells can also experience 'intermittent hypoxia' due to changes in blood flow of microvessels within a tumour, or they can experience 'anoxia', when there is a complete lack of oxygen (Kimura *et al.*, 1996, Dewhirst *et al.*, 2008, Kiani *et al.*, 1994). Hypoxia is known to contribute to several aspects of cancer cell hallmarks including: deregulating cellular energetics; inducing angiogenesis and activating invasion & metastasis.

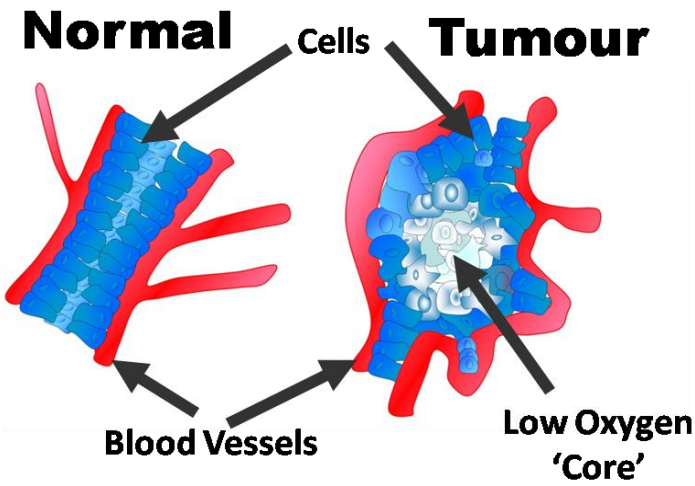

Figure 1.2 Tumour hypoxia*. A schematic diagram showing oxygenation of tumour cells. Blood vessels are in red. Cells closest to the blood vessels are well oxygenated (dark blue), cells away from the blood vessels are hypoxic (light blue). The tumour core (white) is the most hypoxic.*

1.2.2.1 Cellular energetics of cancer cells

More than 50 years ago, it was observed that cancer cells utilise energy differently to normal cells (Warburg, 1930, Warburg, 1956a, Warburg, 1956b). In normal cells, oxidative phosphorylation is the major energy metabolism used, where mitochondria consume oxygen to produce 36-38 ATP molecules. It is only under anaerobic conditions that glucose is used as fuel, producing relatively little energy by the process of glycolysis. During glycolysis, glucose is metabolized to produce pyruvate, where it is further oxidized in the mitochondria to generate only 2 ATP molecules. Interestingly, cancer cells have a preference for utilizing glucose for energy metabolism even in the presence of oxygen. Furthermore, the pyruvate produced by glycolysis in cancer cells is directed away from mitochondria and used to produce lactate instead. This favoured aerobic-glycolysis and lactate production in cancer cells is termed the "Warburg effect" (Warburg, 1930, Warburg, 1956a, Warburg, 1956b). In solid tumours, where the cells are hypoxic, the lack of oxygen availability will also drive the cells toward glycolytic activity. This is partially aided by upregulated expression of glucose transporters (GLUT1) and dehydrogenaseA (LDHA) to enhance glucose uptake and glycolysis in hypoxia (Jones and Thompson, 2009, Hsu and Sabatini, 2008).

1.2.2.2 Angiogenesis

To enhance the delivery of oxygen and nutrient supply, which is required by the rapidly dividing cells, tumour cells can promote new vasculature by angiogenesis. In adult human cells, angiogenesis is normally only switched on transiently when required, such as during would healing. However, in cancer cells, this process remains constantly turned on (Hanahan and Folkman, 1996, Baeriswyl and Christofori, 2009). At a molecular level, angiogenesis is controlled by the vascular endothelial growth factor-A (VEGF-A) and fibroblast growth factor-2 (FGF-2), which are both induced by hypoxia (Connolly *et al.*, 1989, Klagsbrun and Soker, 1993, Shweiki *et al.*, 1992, Veikkola and Alitalo, 1999, Kuwabara *et al.*, 1995). These growth factors bind to tyrosine kinase receptors on endothelial cells, stimulating endothelial cell proliferation, migration to hypoxic region and new blood vessel formation (Veikkola and Alitalo, 1999, Singh *et al.*, 1995, Volpert *et al.*, 1997, Baeriswyl and Christofori, 2009). Additionally, tumour cells can further promote new vasculature by downregulating angiogenesis inhibitors, such as thrombospondin-1 and β-interferon (TSP-1) (Laderoute *et al.*, 2000, Lawler, 2002). The development of new vasculature encourages fresh nutrient supply, thus supporting the growth of tumour cells (Hanahan and Folkman,

1996). The induction of angiogenesis is found at the early and mid stage of cancer, during the premalignant phase of invasive cancer, therefore this process is often viewed as an indication of macroscopic tumour progression (Raica *et al.*, 2009, Hanahan and Folkman, 1996).

1.2.2.3 Tissue invasion and metastasis

The process of metastasis involves multiple complicated steps and is not completely understood. These steps include Epithelial-mesenchymal transition (EMT), endothelial transmigration, survival in the circulatory system, extravasation and proliferation at new sites (van Zijl *et al.*, 2011, Semenza, 2012a). Invasive and metastatic properties of tumour cells generally involve the alteration of three classes of proteins: cell to cell adhesion molecules (CAM), integrins and proteases (Behrens, 1993, Hood and Cheresh, 2002, Stetler-Stevenson and Yu, 2001). Firstly, EMT is a process where epithelial cells lose their cell-to-cell adhering ability and undergo biochemical changes in order to enhance migratory and invasive properties (Klymkowsky and Savagner, 2009, Polyak and Weinberg, 2009, Thiery *et al.*, 2009, Barrallo-Gimeno and Nieto, 2005). EMT is mediated by the reduction of E-cadherin expression. The role of E-cadherin is to maintain the structure of epithelial cell sheets by forming adherens junctions to adjacent cells (Christofori and Semb, 1999, Berx and van Roy, 2009, Cavallaro and Christofori, 2004). There are a number of factors mediating EMT. For example, hypoxia induces EMT regulators such as Snail, Slug and Twist, which in turn transcriptionally repress the expression of E-cadherin (van Zijl *et al.*, 2011, Tsai and Wu, 2012). Furthermore, other hypoxia-induced targets such as FGF, VEGF and EGF also induce EMT. FGF induces Snail, leading to repression of E-cadherin (Ciruna and Rossant, 2001); both VEFG and EGF induce expression of Snail and Twist (Yang, A. D. *et al.*, 2006, Wanami *et al.*, 2008); and EGF can also promote E-cadherin endocytosis (Lu *et al.*, 2003, Lee *et al.*, 2008, Lo *et al.*, 2007).

Secondly, endothelial transmigration describes the invasion of cancer cells into the blood or lymphatic vessel, by which the cells can then be transported to distant parts of the body to form secondary tumours. The overview of this process is that malignant cells attach themselves to the endothelial membrane where they can pass through and enter into vasculature. The mechanism of this migration into the blood vessels is thought possible by passive movement and/or active process (intravasation) (Bockhorn *et al.*, 2007). Both passive and active movements of cancer cells are shown to be mediated by the microenvironment, such as hypoxia. Hypoxia can mediate passive entry by inducing VEGF,

which promotes blood vessel formation, providing a route for cancers cells to enter into circulation (Issa *et al.*, 2009, Hicklin and Ellis, 2005). Many reports support the idea that intravasation is associated with increased expression of growth factors and receptors, including ones that are induced by hypoxia, such as EGF, EGF-R and TGF-β (Joyce and Pollard, 2009, Giampieri *et al.*, 2009). Other studies in breast cancer have also demonstrated that cancer cells can directly enter lymphatic vessels, and suggest this is mediated by hypoxia-induced ALOX15 (arachidonate lipogenases) enzyme, which subsequently reduces VE cadherin expression, damaging the integrity of the lymphatic endothelial cell layer and allowing cell invasion (Hulten *et al.*, 2010, Kerjaschki *et al.*, 2011). Once the cancer cells have disseminated into the circulatory system, the metastasis into the new sites is termed extravasation. A process begins by cancer cells adhering to endothelial cells (EC), disrupting EC interactions and then migrating through the EC layer. The adhesion can be mediated by hypoxia mediated expression of adhesion molecules such as L1CAM (L1 cell adhesion molecule) (Zhang *et al.*, 2012) and angiopoietin-like 4 (ANGPTL4) (Padua *et al.*, 2008). ANGPTL4 dissociates the cell-cell interaction of EC thus promoting the process of extravasation. Although many of the details and exact mechanisms of metastasis and invasion remains open, accumulating evidence supports that these processes can be mediated by hypoxia through regulation of growth factors, growth factor receptors and cytokines.

1.3 Cellular oxygen regulation

The level of oxygen demand within a cellular system is dependent on the cell metabolic activity, and determined by the location of the cells in relation to the nearest blood vessels, as oxygen has a limited diffusing distance of 150µm (Folkman *et al.*, 2000). As the oxygen requirement varies between cells and tissues, the term 'hypoxia' will mean different oxygen levels for each cell type. Some examples of physiological oxygen levels in humans include: 1% to 5% in the brain (Sharp and Bernaudin, 2004, Panchision, 2009, Jezek *et al.*, 2010); 19.7% in the airway; 5.6 % in the lungs; 3.8% in muscles; and 1.9% in the heart (Carreau *et al.*, 2011, Wiener *et al.*, 1976). Hypoxia is encountered in many biological processes, including developmental biology, stem cell biology and immunity (Iyer *et al.*, 1998, Dunwoodie, 2009, Gustafsson *et al.*, 2005, Liu, L. X. *et al.*, 2008, Mohyeldin *et al.*, 2010, Zinkernagel *et al.*, 2007). Hypoxia is also associated with diseases such as myocardial infarction (Semenza, 2000), stroke (brain ischemia) (Sun, 1999, Markus *et al.*, 2004) and

cancer as mentioned above (Sharp and Bernaudin, 2004, Safran and Kaelin, 2003, Bruick, 2003).

1.3.1 The HIF family of protein

The cellular sensing and response to oxygen level changes is mediated by a transcription factor called Hypoxia-Inducible Factor (HIF), first discovered in 1992 by *Greg Semenza* (Semenza and Wang, 1992). Under normal circumstances, HIF plays a vital role in allowing cellular adaptation and survival in low oxygen conditions by promoting the transcription of genes involved in processes such as angiogenesis, red blood cell maturation and energy metabolism (Shweiki *et al.*, 1992, Forsythe *et al.*, 1996, Semenza *et al.*, 1991, Goldberg *et al.*, 1998, Weidemann and Johnson, 2008, Wenger, 2002). As mentioned earlier, the same properties are developed in tumour cells and enhance tumourgenesis.

HIF is a heterodimeric protein belonging to the basic helix-loop-helix (bHLH) family (Wang *et al.*, 1995). It consists of a constitutively expressed oxygen sensitive alpha subunit and an oxygen insensitive beta subunit. Currently three α-subunit isoforms (HIF-1α, HIF-2α, and HIF-3α) and two β-subunits (HIF-1β, HIF-2β) are known (Wang *et al.*, 1995, Jiang *et al.*, 1996, Gu *et al.*, 1998, Makino *et al.*, 2002). The HIF-1α is the most characterised isoform, it is 826 amino acids long and consists of the bHLH domain, PAS domain (PER-ARNT-SIM), oxygen-dependent degradation domain (ODDD), N-TAD (amino-terminal transcriptional activation domain) and C-TAD (carboxy-terminal transcriptional activation domain) (**Figure 1.3**). The basic region of the bHLH motif is essential for DNA binding and PAS is the central domain which facilitates dimerisation with HIF-1β (Wang *et al.*, 1995). The ODDD contains two hydroxylation sites (proline 402 and 564) and the N-TAD region. Lastly, there is the C-TAD, which contains another hydroxylation site (asparagine 803).

Figure 1.3 HIF-1α Domain Structure. *Schematic diagram showing the core domains of HIF-1α. (bHLH = basic helix-loop-helix, PAS=PER-ARNT-SIM, ODDD= oxygen dependent degradation domain, N-TAD = amino terminal transcriptional activation domain, C-TAD = carboxyl terminal transcriptional activation domain). The key hydroxylation sites are indicated (Pro= proline, Asn= asparagine).*

1.3.2 The HIF signalling pathway

Although HIF-1α is constitutively expressed in normoxia, it is also continually degraded. HIF-1α protein levels and activity are tightly controlled by a group of prolyl hydroxylases (PHD1, PHD2, PHD3) and Factor inhibiting HIF (FIH). In normoxia, PHDs use oxygen as a co-substrate to hydroxylate the two key proline residues located in the ODDD (**Figure 1.3**) of the HIF-1α subunit (Masson and Ratcliffe, 2003). This hydroxylation acts as a signal, allowing interaction with the E3 ubiquitin ligase, Von Hippel-Lindau protein (VHL). VHL promotes lysine-linked polyubiquitination thus mediating HIF-1α for targeted degradation by 26S proteasome (Maxwell *et al.*, 1999, Tanimoto *et al.*, 2000) (**Figure 1.4**). Additionally, in the presence of oxygen, FIH hydroxylates the asparagine residue of HIF-1α, preventing HIF-1α from interacting with transcriptional co-activators such as p300 and CREB binding protein (CBP) (Arany *et al.*, 1996, Schofield and Ratcliffe, 2004, Lee *et al.*, 2004, Taylor and Pouyssegur, 2007). Taken together, when oxygen is available, HIF-1α is rapidly degraded and is transcriptionally inactive.

Under hypoxic conditions, the lack of oxygen substrate means that PHDs and FIH can no longer hydroxylate HIF-1α efficiently, allowing HIF-1α to evade degradation and accumulate. HIF-1α binds to HIF-1β subunit, forming a functionally active heterodimeric transcription factor (Wang *et al.*, 1995, Arany *et al.*, 1996). In the nucleus, it binds to the promoter region of target genes, by recognition of the Hypoxia Response Element (HRE) sequence (-RCTTG-), interacts with its coactivators p300 and CBP, which together leads to transcriptional activation (Pugh *et al.*, 1991, Semenza *et al.*, 1991, Wenger *et al.*, 2005) (**Figure 1.4**). Over 200 HIF-1α target genes have been described and predicted, among which are its own regulators, PHDs, therefore forming a negative feed-back loop with itself (Schofield and Ratcliffe, 2004, Ortiz-Barahona *et al.*, 2010, Elvidge *et al.*, 2006, Benita *et al.*, 2009). Other well-known target genes include: erythropoietin (EPO) that controls erythropoiesis; vascular endothelial growth factor (VEGF) that promotes angiogenesis; and glucose transporter1 (GLUT1), which regulates glucose uptake and glycolysis. Whilst HIF-1α plays a crucial role in maintaining and facilitating cell homeostasis when cells are deprived of oxygen, HIF-1α can regulate induction of proapoptotic factors such as nineteen kD protein-3 (BNIP3), if cells experience near anoxic levels (Sowter *et al.*, 2001, Azad *et al.*, 2008, Guo *et al.*, 2001, Greijer and van der Wall, 2004).

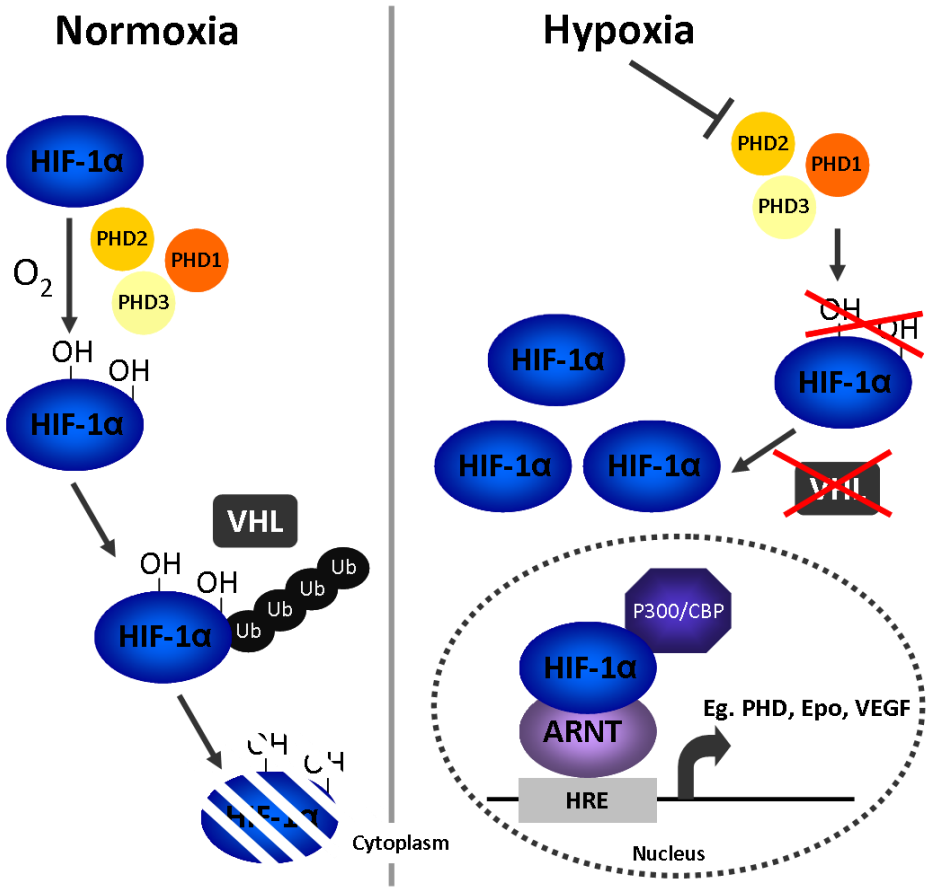

Figure 1.4 A schematic representation of HIF-1α regulation in normoxia (left) and hypoxia (right). *In normoxia, HIF-1α is hydroxylated by the PHD proteins and targeted for ubiquitination by VHL, which targets the alpha subunit for proteosomal degradation. In hypoxia, the activity of the PHD proteins is reduced and HIF-1α is not hydroxylated causing it to accumulate. In the nucleus the HIF-1α / HIF-1β heterodimer binds to the HRE of target genes, associates with co-activators p300/ CREB-binding protein (CBP) and activates transcription of hypoxia inducible genes.*

1.4 Brain tumours

Brain tumour types are usually named dependent on the tumour cells origin or by their location. They are further classified into benign low grade (grade I and II) and malignant high grade (grade III and IV), following the conventional cancer grading system (Louis *et al.*, 2007). Although not all brain tumours are malignant, a low grade tumour itself can often still cause serious symptoms if located in a crucial part of the brain.

1.4.1 Gliomas

Gliomas contribute to half of all primary brain tumours. The three main types are Astrocytoma, Ependymoma and Oligodendroglioma, developed from astrocytes, ependymal cells and oligodendrocytes respectively. Astrocytomas are the most common type of glioma in adult and it is graded and classified into different types by histology. They are Pilocytic astrocytomas (grade 1); Low-grade diffuse astrocytomas (grade II); anaplastic astrocytomas (grade III); and Gliomastoma multiforme (GBM) (grade IV) (Kleihues and Ohgaki, 2000). GBM is the most malignant form of gliomas and it will be one of the brain tumours investigated in this thesis.

1.4.1.1 Glioblastoma multiforme (GBM)

Glioblastoma (GBM) is a highly aggressive hypoxic tumour, found more commonly in adults than children. GBM is characterised by its high invasiveness property and poor response to treatment. Molecularly, GBMs are characterised and classified into one of four subtypes based on genetic markers (Verhaak *et al.*, 2010). Proneural subtypes show p53 mutation, loss of *PTEN* and *PDGF*-receptors amplifications; classical subtypes show epidermal growth factor (EGFR) amplification/ mutations, loss of PTEN, NOTCH and SHH pathway activation; neural subtypes are characterised by overexpression of HER2 (human epidermal growth factor receptor 2) and mesenchymal subtypes are indicated by loss of *TP53*/ *PTEN* and NFκB activation (Furnari *et al.*, 2007, Brennan *et al.*, 2009, Agnihotri *et al.*, 2012). Another mutation found in 12% of GBM, is the mutation of the *IDH1* (isocitrate dehydrogenase) gene (Parsons *et al.*, 2008, Nobusawa *et al.*, 2009), this enzyme is involved in the citrate acid cycle and it is also mutated in 70% of gliomas (Yan *et al.*, 2009, Thompson, 2009).

1.4.1.2 Origin of GBM

The cell of origin for GBM remains elusive, but there is increased support of GBM and the cancer stem cells (CSC) hypothesis (Dirks, 2001, Dirks, 2008, Stiles and Rowitch, 2008). GBM is a heterogeneous tumour and several groups have found that it contain a CSC population. These cancer stem cells are known as GBM stem cells (GSCs) (Yuan *et al.*, 2004, Altaner, 2008, Huang *et al.*, 2010). GSCs are similar to normal stem cells and neural stem cells phenotypically, possessing self-renewal and proliferation properties. It is hypothesised that these stem cells come from mature glial cells dedifferentiating or from mutations in neural progenitors or from mutations in adult neural stem cells (Dirks, 2001, Dirks, 2008, Stiles and Rowitch, 2008). The induction of CSC phenotypes is further enhanced by the cell micrcoenvironment such as hypoxia (Li, P. *et al.*, 2013, Keith and Simon, 2007). Regions of hypoxia in GBM are often associated with increased expression of stem-cell markers (McCord *et al.*, 2009, Bar *et al.*, 2010).

1.4.1.3 GBM treatment

The standard immediate treatment for GBM is surgical resection followed by radiation or combined radiotherapy and chemotherapy (Hargrave and Zacharoulis, 2007, Stupp *et al.*, 2005). Patients with newly diagnosed GBM treated with radiotherapy followed by temozolomide, (an alkylating agent which is the sole drug used to treat GBM), have a 26% 2-year survival rate (Hargrave and Zacharoulis, 2007, Stupp *et al.*, 2005). However, treatment response is poorer in children, with only a 12% 2-year survival rate (Hargrave and Zacharoulis, 2007, Nicholson *et al.*, 2007, Broniscer *et al.*, 2006, Ruggiero *et al.*, 2006). Moreover, hypoxia-induced HIF overexpression is correlated to increased angiogenesis, tumour dispersal, treatment resistance and a worse prognosis in GBM (Birner *et al.*, 2001, Zagzag *et al.*, 2000, Thorns *et al.*, 2003, Kaur *et al.*, 2005, Agnihotri *et al.*, 2012, Hu *et al.*, 2012).

1.5 Brain tumour in children

1.5.1 Medulloblastoma

Medulloblastoma (MB) is the most common malignant paediatric brain tumour, it accounts for 15-20% of cancer of the CNS in children (**Figure 1.5**) (Pizer and Clifford, 2008). It has the highest prevalence among children between ages 4 to 7 years and it is more common in boys than girls. MB's arises in the posterior fossa of the brain, which consists of the cerebellum and brain stem (Medulla). They are neuroepithelial tumours originating from neural stem cell progenitors in the granule cell layer of the cerebellum (Raffel, 2004). Hence MB is often located in the cerebellar vermis, in the roof of the forth ventricle presenting as a midline tumour. In less often cases, it can arise in the cerebellar hemisphere in older children. MB has a tendency to metastasis throughout the CNS via the cerebrospinal fluids (CSF), but rarely to other parts of the body outside CNS (Kleinman *et al.*, 1981).

Some of the earliest study of MB molecular genetics revealed the loss of tumour suppressor genes such as *APC* (Adenomatous Polyposis Coli) and *NF1* (Neurofibromin 1) are observed in primary MB (Huang *et al.*, 2000, Martinez-lage *et al.*, 2002). Other chromosomal losses such as 17q, 10 and 11 were also detected in MB (Gilbertson *et al.*, 2001, Langdon *et al.*, 2006). The classification of MB, into subgroup and responses to treatment, was later found to be closely related to several important developmental pathways. Deregulation in Hedgehog (Shh), Notch and Wingless (Wnt) developmental signalling pathways has been linked to MB growth (Yokota *et al.*, 2002, Rossi *et al.*, 2008, Guessous *et al.*, 2008). Additionally, other oncogenic pathways such as MYC (v-myc avian myelocytomatosis viral oncogene homolog) and RTK (receptor tyrosine kinase) are also involved in the progression of MB (Guessous *et al.*, 2008, Gilbertson, 2004).

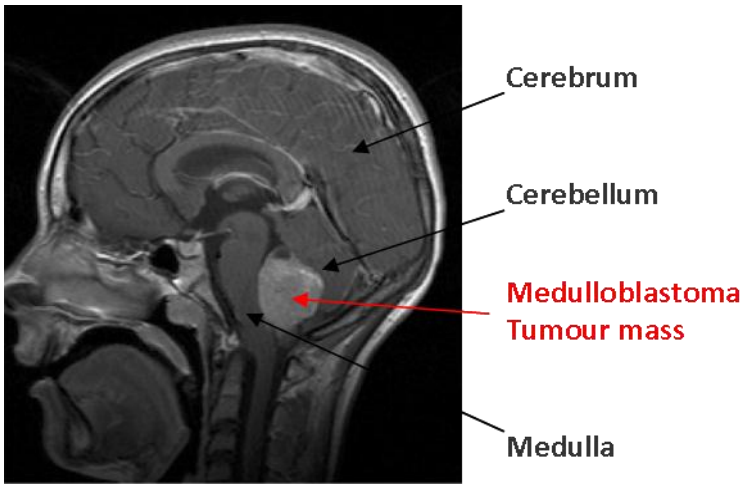

Figure 1.5 An example of medulloblastoma. *A T1-weighted sagittal MRI scan showing a medulloblastoma tumour mass situated next to the medulla and cerebellum. Adapted from Pizer et al. 2008. (Pizer and Clifford, 2008)*

1.5.1.1 Histopathology

Five histopathological variants of MB are currently classified by the World Health Organisation (WHO): (i) Classical medulloblastoma (**Figure 1.6A**) (ii) Medulloblastoma with extensive nodularity (iii) Desmoplastic/nodular medulloblastoma (**Figure 1.6B**) (iv) Anaplastic medulloblastoma (**Figure 1.6C**) and (v) Large cells medulloblastoma (Louis *et al.*, 2007, Gilbertson, 2004).

Representing ~80% of MB diagnosed, the type (i) classical MB is the most observed phenotype. These tumours are presented as sheets of small round cells with nuclei as big as the cell and little cytoplasm (**Figure 1.6A**). Type (iii) desmoplastic MB occurs mostly in very young children under the age of 3 (Rutkowski *et al.*, 2005). Type (iv) anaplasia is observed in ~15% of cases and is characterised by nuclei with varied size and shape, this MB is associated with poor prognosis. Finally, the large cells type (v), only occurs in 5% of cases but it is associated with the worst outcome (McManamy *et al.*, 2003, Eberhart, 2003).

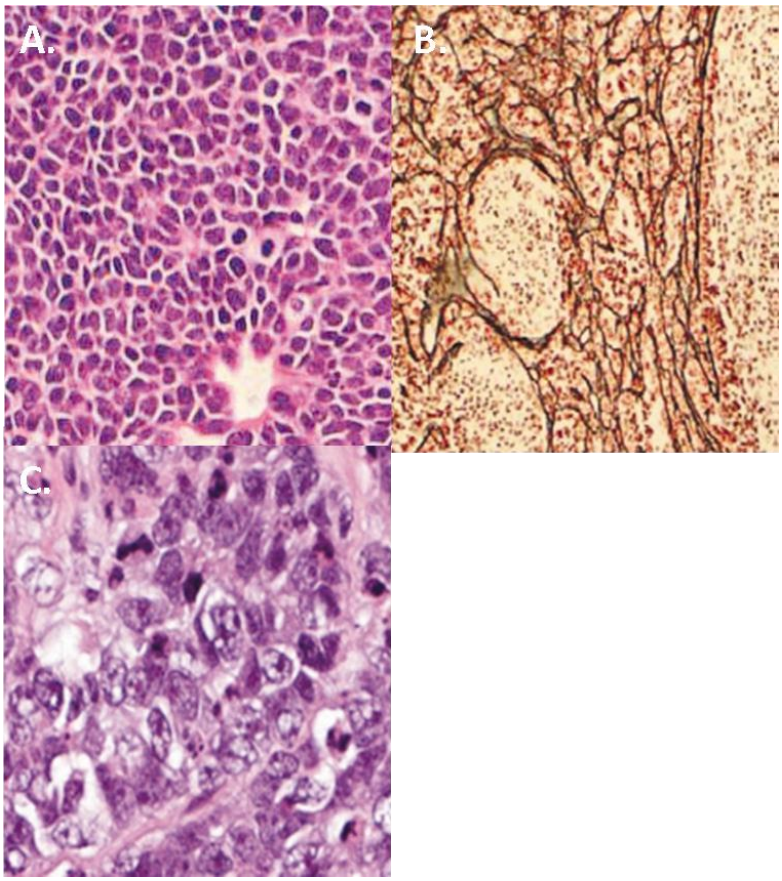

Figure 1.6 Common MB histopathological variants. *Three histological sections of MB stained with hematoxylin and eosin.* ***(A)*** *Classic, small round nuclei arranged sheets.* ***(B)*** *Desmoplastic, MB show neurocytic differentiation, surrounded by collagen matrix.* ***(C)*** *Anaplastic, large tumour cells with pleiomorphic nuclei. Adapted from Gilbertson (Gilbertson, 2004).*

1.5.1.2 MB subgroup classification and genetic markers

Currently in clinic, the classification of MB is based on their histopathology. In the last decade, several groups have utilised transcriptomic studies to further classify MB into subgroups but final conclusions was varied between studies (Kool *et al.*, 2008, Northcott *et al.*, 2011, Thompson *et al.*, 2006). Recently, a consensus has emerged that there are 4 principal subgroups of MB, which are: Shh, WNT, Group 3 and Group 4 (Taylor *et al.*, 2012). Based on clustergram algorithm, the subgroups appear to further differentiate into subtypes, but these are not yet classified and are currently named as α, β and γ (**Figure 1.7**) (Cho *et al.*, 2011, Taylor *et al.*, 2012).

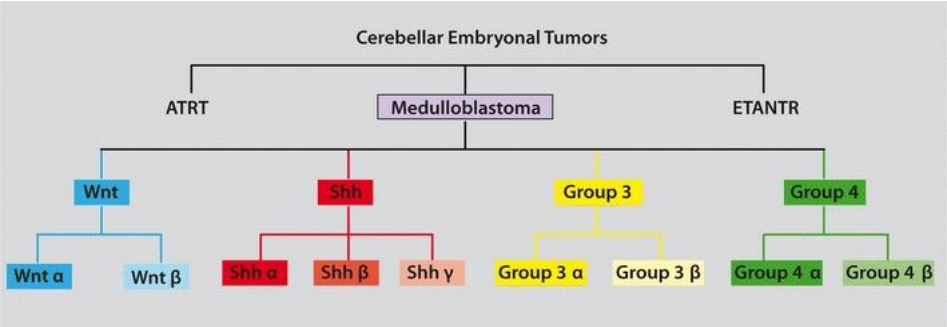

Figure 1.7 *Classification of Cerebellar embryonal tumours. MB are spilt into four subgroups, Wnt, Shh, Group 3 and Group 4. Each subgroup is classified to subtype α, β or γ. Figure obtained from Taylor et al. (Taylor et al., 2012)*

Wnt subgroup, generally with classical appearance is the best known group with good prognosis. Wnt group express high level of MYC and mutations of the *CTNNB1* gene is often found in this group (Northcott *et al.*, 2011). Additionally this group shows positive nuclear stain with β-catenin and monosomy six (one copy of chromosome 6 is deleted) (Taylor *et al.*, 2012, Ellison, D. *et al.*, 2011, Ellison, D. W. *et al.*, 2011, Clifford *et al.*, 2006). Shh subgroups carry mutation involving the Sonic Hedgehog signalling pathway and express high level of MYCN (MYC Neuroblastoma derived). Its identification is obtained by immunohistology staining for SFRP1 (secreted frizzled-related protein 1) or GAB1 (Growth factor receptor-bound protein 2-associated binding protein 1) (Northcott *et al.*, 2011, Thompson *et al.*, 2006, Ellison, D. W. *et al.*, 2011). Group 3 commonly shows classical histopathology and high expression of MYC, FOXG1B (Forkhead box G1B) and OTX2 (orthodenticle homeobox 2) (Cho *et al.*, 2011, Kool *et al.*, 2008, Northcott *et al.*, 2011). The key marker to differentiate Group 3 is with NPR3 (nucleolin related protein 3) staining and by transcriptional profiling clustering (Northcott *et al.*, 2011). Group 4 also expresses high level of OTX2 and FOXG1B (Adesina *et al.*, 2007, Northcott *et al.*, 2011). The genetic markers for Group 4 are less well classified, the current immunohistochemical marker used for this group is KCNA1 (potassium voltage-gated channel). This group is often associated with high incidence loss of chromosome X and 17q. (Cho *et al.*, 2011, Kool *et al.*, 2008, Northcott *et al.*, 2011).

1.5.1.3 MB subgroup characterisation

The Medulloblastoma Advanced Genomics International Consortium group carried out an extensive somatic copy number aberration (SNCA) study involving over 1000 MB samples in attempt to identify the molecular genetics of MB (Northcott *et al.*, 2012). SNCA is the study of chromosomal changes including DNA duplications, chromosomal deletions or translocation. They have discovered 62 regions of SCNA which are common in MB. Some of which are specific to certain subgroup (**Table 1.1**).

Gene	SCNA types	Subtype
PTEN	Homozygous deletions	Shh
PTCH1	Homozygous deletions	Shh
CDKN2A/B	Homozygous deletions	Shh
MYCL1	Amplifications	Shh
PPM1D	Amplifications	Shh
MDM4	Amplifications	Shh
MYCN	Amplifications	Shh, Group 4
SCNAIP	Tandem duplications	Group 4
PVT1	Translocation	Group 3

Table 1.1 Somatic copy number aberrations (SCNAs) in MB. *Example of enriched-SCNAs in MB subtype. (Northcott et al., 2012)*

In MB, recurrent homozygous deletion is relatively rare but not completely omitted (**Table 1.1**). More strikingly, recurrent high-level amplifications were identified in 28 regions. This include *MYCN* in the Shh subgroup and Group 4; *MYCL1* (MYC lung carcinoma derived) in Shh; and *MYC* in Group 3. The Shh group remains the most easily identified with other enriched SCNAs amplification such as *GLI2 (GLI family zinc finger 2)*, *MYCL1* and *PPM1D* (protein phosphotase 1D) (Ruark *et al.*, 2013). The pathogenesis of Group 4 is poorly understood, however, *SNCAIP* (synuclein, alpha interacting protein) tandem duplication is associated with this group (Northcott *et al.*, 2012).

Besides alteration in copy numbers, translocation assisted by the process of chromothripsis is observed in Group 3. Chromothripsis is a phenomenon where a chromosome 'shatters' and the fragments rearrange but with a potential deletion (Stephens *et al.*, 2011, Forment

et al., 2012). Chromosome 8 chromothripsis has led to the gene fusion of *PVT1* (a non-protein coding RNA) fusion with *NDRG1 (N-myc downstream regulated 1) or PVT1 with MYC (Northcott et al., 2012).* Moreover, chromosome 8 chromothripsis is further correlated to the deletion of chromosome 17p, hence the loss of *TP53*. Finally, the WNT group shows no significant frequent deletion and thus there are no specific SCNA's related to this group.

In contrast to SCNA, which is common in MB, single nucleotide variants (SNV) are relatively less prevalent. Sanger sequencing study consisting of 22 MB tumours has only detected 8 SNVs per tumour (Parsons *et al.*, 2011). Nonetheless, some of these SNVs are enriched in certain subgroups. For example, SNVs in *PTCH1 (protein patched homolog 1)*, *CTNNB1* (catenin (cadherin-associated protein) beta 1) gene are found predominately in Shh group (Parsons *et al.*, 2011, Northcott *et al.*, 2012).

Furthermore, exon sequencing study of MB has shown a list of 12 specific somatic mutations. Some of these genes are mentioned earlier (*TP53*, *PTCH*, *CTNNB1*) but some newly identified candidates such as *DDX3X* (DEAD box polypeptitde 3 X-linked), a RNA helicase; *GPS2 (G protein pathway suppressor 2)* and *BCOR* (BCL6 corepressor) have been identified (Pugh *et al.*, 2012).

1.5.1.4 Genetic Predisposition of MB

The majority of MB arises spontaneously with unknown causes, with only 5% of cases due to genetic predisposition (Pizer and Clifford, 2008). Gorlin, Turcot and Li-Fraumeni Syndromes are three genetic disorders, which have shown higher incidence of MB formation. These diseases are caused by germline mutations in Patched homolog 1 (*PTCH*), *APC* and tumour suppressor *TP53* genes respectively (Zurawel *et al.*, 2000, Huang *et al.*, 2000, Barel *et al.*, 1998).

Gorlin's syndrome is associated with skeletal abnormalities due to the mutation of *PTCH* gene which encodes a transmembrane protein. PTCH is a key growth regulator of external granular cell layer cells, which binds a family of protein belonging to the Shh pathway. Normally, Shh pathway remains in an 'off state', this is achieved by the binding of PTCH with smoothened protein (SMO). However, upon SHH binding to PTCH receptor, PTCH is relieved allowing a signal transduction to the nucleus promoting granule cell proliferation (Kenney *et al.*, 2003). Therefore, deletion of PTCH and deregulation of the Shh pathway leads to constitutive activation and proliferation of granule cells hence MB formation.

Turcot's syndrome is linked to mutations of the *APC* gene, a component of Wnt pathway. The Wnt pathway coordinates a series of developmental processes including the proliferation of progenitor cells in the central nervous system (Huang *et al.*, 2000, Yokota *et al.*, 2002). Wnt activation is achieved through a serial cascade of activity, ultimately activating expression of genes which are involved in proliferation, inhibition of cell death and differentiation of cells. Both mutations in the *APC* gene and other members of Wnt signalling pathway have been shown to be associated with MB (Huang *et al.*, 2000, Yokota *et al.*, 2002, Dahmen *et al.*, 2001).

1.5.1.5 Symptoms of patients with MB

Similar to general brain tumours symptoms, MB patients often exhibit intermittent and subtle headaches, vomiting and drowsiness, this is due to the increased intracranial pressure within the skull. As the cerebellum is a centre for voluntary motor movement, contributing to fine tune motor activity, coordination, timing, equilibrium and balance, patients can display a lack of coordinated muscle movement or cranial nerve palsy (involuntary muscle spasm).

1.5.1.6 Prognosis

The stage of the disease and the age of the patient upon diagnosis are important contributing factors in the prediction of MB outcome. Thus the prognosis of MB patients relies on a combined assessment of patient's age, histopathology, subgroups, biological markers and the stage of the disease. For a simple overview, MB patients are typically split into three groups: (1) Standard/ average risks, if patient is older than 3 years and without evidence of metastasis; (2) high risk, patients with evidence of CSF spread; and (3) patients under 3 years at the point of diagnosis (with the exception of type III desmoplasia).

The favourable MB type is the desmoplastic form found in patient under 3 years, they are often associated with good outcome (Rutkowski *et al.*, 2005, McManamy *et al.*, 2003). Also, the Wnt subgroup with activation of Wnt/Wingless pathway (beta-catenin) markers displays a favourable outcome (Clifford *et al.*, 2006, Ellison, D. W. *et al.*, 2011). Furthermore, there is evidence that good prognosis upon treatment is associated with certain growth factor receptors, such as TrkC (neurotrophin-3 receptor) expression via induction of apoptosis (Kim *et al.*, 1999). Shh and Group 4 MB patients appear to have similar intermediate outcome, where their prognosis are worse than Wnt but better than Group 3.

MB Group 3, which occurs more commonly in boys than girls have the least favoured prognosis, with frequent metastatic activity and cancer reoccurrence (Northcott *et al.*, 2011). In particular if MYC is amplified in Group 3 patients, this is highly associated with death (Taylor *et al.*, 2012). Other factors linking to poor treatment prognosis is the expression of the HER2, platelet derived growth factor receptor (PDGF-R) and insulin-like growth factor receptor-1 (IGFR-1).

1.5.2 Current Treatment

The treatment options for patients are determined by the grade of the tumour and the patient's age. Where possible, complete or near complete tumour excision by surgical resection is the first line of treatment, followed by craniospinal radiotherapy (CSRT). This standard treatment results in a 5-year survival rate of 50-60% (Gilbertson, 2004, Hargrave and Zacharoulis, 2007). Resection is achieved with surgical techniques aided by neuronavigation. Then after surgery, a CSRT dose of 54-55 Gy is applied to the primary tumour site and a lower dose of 34-36 Gy is directed at and along the spinal cord, to minimise potential spreads through the CSF (Hargrave and Zacharoulis, 2007).

Another more advanced radiotherapy procedure uses intensity modulated radiotherapy IMRT (Pizer and Clifford, 2008). IMRT is a more precise method that uses a computer-controlled linear accelerator to deliver doses of radiation in multiple small volumes. This method can target the three dimensional shape of the tumours precisely using a computer generated planning system (Huang *et al.*, 2002). IMRT is needed for tumours which are situated in a location surrounded by normal critical brain structure. Lastly, in North America, tight doses of proton beams are also used to target the posterior fossa and spinal components (St Clair *et al.*, 2004).

Chemotherapy treatment is generally applied to younger patients, recurring MB or high risk patients (in combination with radiotherapy) (Hargrave and Zacharoulis, 2007). The majority of the drugs used to treat MBs tend to be DNA damaging agents. MB is a relatively sensitive tumour, showing sensitivities to single drug treatment with cisplatin, cyclophosphamide and methotrexate (Kortmann *et al.*, 2000, Strother *et al.*, 2001). The cocktail combination of cyclophosphamide, carboplatinum and etoposide shows good treatment response of 65% 5-year survival rate for average risk MB (Kortmann *et al.*, 2000,

Taylor *et al.*, 2003). Other drugs such as cisplatin, lomustine and vincristine are also commonly used (Rossi *et al.*, 2008, Packer *et al.*, 1994).

1.5.2.1 Etoposide

Etoposide is a topoisomerase II inhibitor, affecting its enzyme regulatory function. During normal DNA replication, highly tensile supercoiled DNA is created. Topoisomerase II induces double stranded breaks (DSB) within the supercoiled DNA, allowing it to unwind and relax before re-ligation. In the presence of etoposide, topoisomerase II religation ability is inhibited, thus allowing the number of DSB breaks to accumulate within the cell. Through this mechanism, etoposide triggers the activation of the p53 pathway and subsequently apoptosis.

1.5.2.2 Cisplatin

Cisplatin (cis-diamminedichloroplatinum(II) or CDDP) is a compound that contain a platinum atom with two chloride ions and two amine groups (Siddik, 2003). Within the cells, cisplatin chloride ions are displaced by water, and this allows the binding of platinum atoms to DNA bases resulting in DNA cross links. Cisplatin can form both DNA inter or intra-strand cross linking, altering the DNA conformation and preventing DNA synthesis (Eastman, 1987, Pinto and Lippard, 1984).

1.5.2.3 Methotrexate

Methotrexate (MTX) is an antimetabolite and antifolate drug, which inhibits purine and pyrimidine synthesis (Barnhart *et al.*, 2001, Tian and Cronstein, 2007, Pagnoux and Guillevin, 2009). It is a competitive inhibitor of the dihydrofolate reductase (DHFR), an enzyme that reduces dihydrofolic acid to tetrahydrofolate. The production of tetrahydrofolate is required for the de novo synthesis of purines, which are needed for DNA/RNA synthesis during S phase (Chen *et al.*, 1984).

1.5.2.4 Problems with current MB treatment

In young patients, the brain is still developing, therefore the current treatments available can cause long term side effects (Frange *et al.*, 2009, Gilbertson, 2004). Surgery leaves 20% of patients with limb weakness, cranial nerve palsies, personality changes and involuntary movements (Pizer and Clifford, 2008). Moreover, molecular mechanisms of resistance to chemotherapeutic drugs have been reported (Friedman *et al.*, 1992, Dong *et al.*, 1999, Bacolod *et al.*, 2009, See, 2012).

One of the earliest observations was resistance to cyclophosphamide, a common alkylating drug used at that time. This compound is processed by the body in multisteps to generate alkylating metabolites, which are damaging to the DNA thus causing cytotoxity. However, resistance is acquired by overexpression of the aldehyde dehydrogenase enzyme (ALDH). ALDH catalyses the oxidation of alkylating metabolites, thus detoxifying the function of this drug (Friedman *et al.*, 1992). In addition to overexpression of ALDH, another alkylating agent drug resistance mechanism acquired by MB was observed: the overexpression of O6-methylguanine-DNA-methyltransferease (MGMT) (Dong *et al.*, 1999). MGMT transfers the alkyl group from DNA into a cysteine residue within the enzyme, thus protecting DNA against alkylated guanine. Finally, another cyclophosphamide resistance mechanism is due to overexpression of the metallothionein (Bacolod *et al.*, 2009). Metallothionein contains thiol groups in its cysteine residues, which can covalently bind to cyclophosphamide, detoxiyifing it to a non-toxic derivative (Bacolod *et al.*, 2009). Apart from acquired molecular drug resistance mechanisms, inadequate drug administration can itself be problematic. For example, the blood-brain barrier (BBB) can restrict the entry of hydrophilic or large lipophilic compounds into the brain (Schinkel, 1999, Gottesman *et al.*, 2002), hence reducing the concentration of drugs delivered to tumour sites (Gatti and Zunino, 2005, Mellor and Callaghan, 2008).

1.5.2.5 Tumour hypoxia and chemoresistance

Tumour hypoxia is often associated with resistance to treatment and poor prognosis (Brown, 1999, Sullivan *et al.*, 2008, Rohwer and Cramer, 2011, An *et al.*, 1998, Greijer and van der Wall, 2004, Piret *et al.*, 2006, Semenza, 2003). Although the study of hypoxia and chemoresistance in MB is not extensive, we will consider the general role of hypoxia-induced treatment resistance in tumours. On a physical level, treatment can be compromised due to the poor tumour vasculature of solid tumours, as drug delivery to the cells far away from the blood vessels becomes difficult. Moreover, certain drugs require oxygen as a co-substrate for their mechanism of action, these drugs, such as tirapazamine will therefore become ineffective in an environment lacking oxygen (Hicks *et al.*, 2004, Koch, 1993, Teicher, 1994).

Molecularly, hypoxia associated chemoresistance has been reported to be mediated by HIF expression. An early study demonstrated HIF-induced multidrug resistance 1 (*MDR1*) gene contributing to drug resistance (Comerford *et al.*, 2002). MDR1 is a glycoprotein encoded by the *ABCB1* gene, an efflux pump which has been evolved to remove 'harmful' substances

such as chemotherapeutic drugs. Later on, other studies have shown that more genes such as multidrug-resistance associated protein 1 (*MRP1*) (another ABC transporter) and Lung resistance protein (*LRP*) were also upregulated by HIF and contribute to hypoxia-induced resistance (Chen, L. *et al.*, 2009, Zhu *et al.*, 2005, Liu, L. L. *et al.*, 2008). Besides the upregulation of drug resistance genes, the strong involvement of hypoxia in cellular energetic, cellular response, tissues invasion and metastasis can all potentially play contributions to chemoresistance in hypoxic tumour cells (section 1.2.2).

1.6 DNA Damage response

The DNA damage response (DDR) is a vital mechanism for maintaining genomic integrity in mammalian cells. This is co-ordinated by a complex system, involving a large range of proteins categorised into DNA damage sensors, transducers, mediators and effectors. DDR senses damage in DNA and subsequently triggers DNA repair or cell death. For this reason, many chemotherapeutic drugs employ the mechanisms of DDR to trigger cell death in tumour cells, highlighting the importance of DDR machinery for successful chemotherapeutic treatments.

Under normal circumstances, DNA is constantly challenged by DNA damage, with several thousands of lesions arising in every human cell per day (Lindahl and Barnes, 2000). Endogenous DNA damage can be caused by errors which naturally arise during DNA replication or physical DNA attacks by free radicals generated from cellular metabolism. Exogenously, DNA damage could result from carcinogenic substances, such as nitrosamine in tobacco, UV radiation or X-rays. The type of DNA damage created can be classified into single stranded breaks (SSBs) or double stranded breaks (DSBs). Dependent on the type of breaks and when damage occurs, in terms of cell cycle phase, different repair mechanisms are employed by the cell. In the following sections, we will focus on DSBs and their mechanisms of repair.

1.6.1 Double stranded breaks

DSBs are of greater concern than SSBs, as they can increase the chance of chromosome breakage, neurodegeneration, immunodeficiency and cancer predisposition (Jackson and Bartek, 2009). DSBs can arise during normal physiological processes, for example during replication, when an unrepaired SSB meets the progression replication fork, it is converted into a DSB. Therefore during this time the DNA is stringently monitored for DSBs (and SSBs) by DNA glycosylase, which initiates base excision repair (Almeida and Sobol, 2007, Hitomi *et al.*, 2007, Jacobs and Schar, 2012). Damaged DNA activates processes which halt cell cycle progression, allowing time for DNA repair before the cells continue to go through their cycle. Extrinsically, DSBs can also be induced by: radiation or radiometric compounds such as bleomycin, alkylating agents (e.g. methyl methane sulphate) and topoisomerase II inhibitors (e.g. etoposide), as described in (section 1.5.2) (Vanankeren *et al.*, 1988, Mirabelli *et al.*, 1985).

The two major pathways involved in sensing and repairing DSBs are homologous recombination (HR) and non-homologous end-joining (NHEJ) (Hartlerode and Scully, 2009, Pardo *et al.*, 2009).

1.6.1.1 Non-homologous End-Joining (NHEJ) repair

Non-homologous End-Joining (NHEJ) repair is active throughout the cell cycle but with increased activity as the cells progress through G0/G1 to S and G2/M phase. NHEJ directly ligates broken ends back together without the use of a homologous template to guide repair, therefore this method is error prone and can generate small insertions or deletions in the repaired DNA (Riches *et al.*, 2008, Hartlerode and Scully, 2009, Pardo *et al.*, 2009).

During NHEJ, the first events involve the DNA binding proteins Ku70 and Ku80 associating with the DNA break site (Walker *et al.*, 2001). The Ku70/ Ku80 heterodimer binds each exposed end of the DNA terminus of the break site and its function is to aid the alignment of DNA strands, protect them from degradation plus to prepare the strands for ligation (van Gent and van der Burg, 2007, Weterings and Chen, 2008). The association of Ku70/ Ku80 with the DNA also attracts DNA protein kinase (DNA-PK) to the break site, which later plays a role in both the processing and ligation of DNA. The processing of DNA is performed by the nuclease Artemis, which trims the DNA followed by the DNA ligase IV/XRCC4 complex, which ligates the blunt ends (Yannone *et al.*, 2008). Once the ligation has occurred, the repair process is completed (**Figure 1.8A**).

1.6.1.2 Homologous recombination repair

This mechanism is more complex than NHEJ, but it is more accurate and less prone to errors as it utilises a homologous sister chromatid template. However, this means that the HR repair mechanism is only active during the S and G2/M phase of the cell cycle, when sister chromatids are available (these are identical copies of chromatids generated by DNA replication) (Filippo *et al.*, 2008).

Recognition of DSBs, by the MRN complex, happens within minutes after the damage has occurred. The MRN complex consists of meiotic recombination 11 (MRE11), RAD50 and Nibrin (NBN) (Lavin, 2007). The MRN complex plays a key role in sensing, signalling and promoting repair of DNA breaks. In the case where repair mechanisms are triggered, the DSBs ends are first processed by resection from 5' to 3' ends to produce 3' single strand tails. This is initiated by MRN complex and CtBP-interacting protein (CtIP). With the aid of Rad51, the 3' ssDNA then undergo strand invasion, branch migration and DNA synthesis.

Following these processes, the crossover DNAs are resolved and the initial broken DNA are repaired (**Figure 1.8 B**).

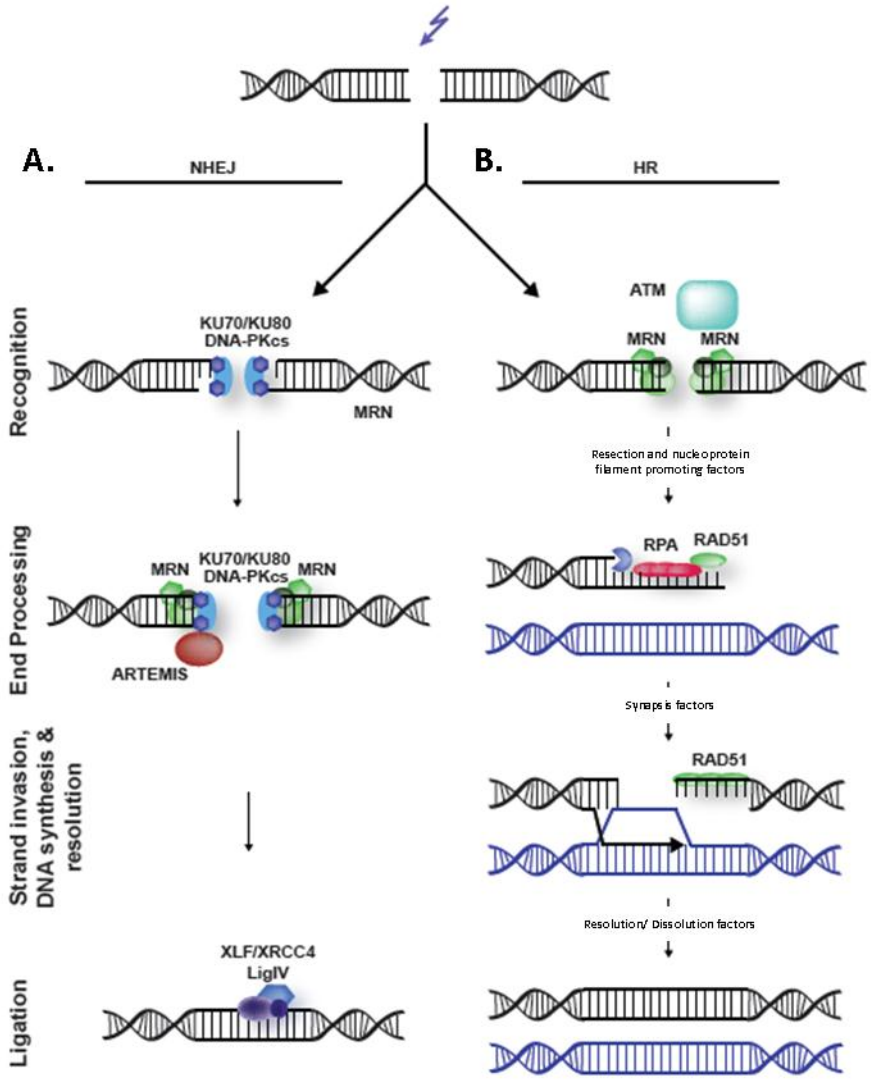

Figure 1.8 Mammalian DNA Double Stranded Breaks Repair. ***(A) NHEJ repair****, DSB recognised by KU70/KU80, processed by DNA-PK and ARTEMIS followed by relegation by XRCC4/Lig4 complex.* ***(B) HR repair****, DSB recognised by MRN complex followed by resection, strand invasion and extension mediated by RPA and RAD51. After extension, the strands are resolved. Adapted from Lans et al. Epigenetics & Chromatin 2012 5:4*

Besides triggering repair, once MRN is associated with the exposed ends of DNA, its NBN component activates the catalytic function of a kinase called ataxia telangiectasia mutated (ATM) (Horejsi *et al.*, 2004, Costanzo *et al.*, 2004). Additionally, it retains the ATM at the site of the DSB, which allows for signal amplification and downstream ATM response

(Horejsi *et al.*, 2004, Berkovich *et al.*, 2007). When ATM is activated, it phosphorylates targets such as a histone variant called H2AX, as well as carrying out autophosphorylation of itself. Thus, ATM plays a central role in DSBs response where it can phosphorylate other proteins such as Chk2, BRCA1 and p53, involved in repair, cell cycle checkpoint and apoptotic responses (Jowsey *et al.*, 2007, Buscemi *et al.*, 2004, Stiff *et al.*, 2004)(**Figure 1.9**).

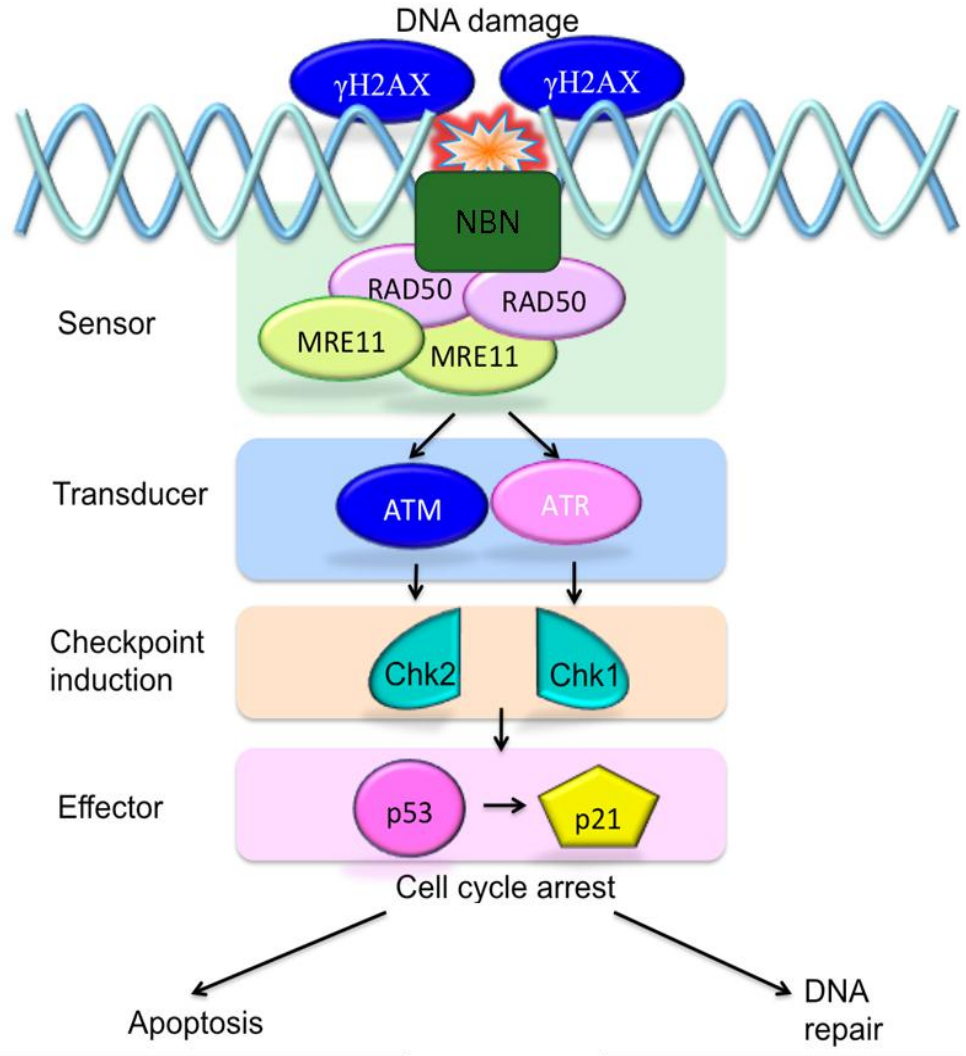

Figure 1.9 Overview of DSB response. *A schematic diagram demonstrating the signalling cascade of DSB response. DNA damage is detected by sensor proteins (MRN complex: NBN, Rad50 & Mre11), where signals are transduced by ATM which activate Chk2 (left) or ATR which activates Chk1 (right). Activation of Chk2 or Chk1 will then activate p53 signalling response. (http://www.intechopen.com/books/senescence-and-senescence-related-disorders/molecular-mechanisms-of-cellular-senescence).*

1.6.1.3 Pathological relevance of *NBN*

Nijmegen Breakage Syndrome (NBS) is a rare autosomal recessive disease where the *NBN* gene is mutated (Weemaes *et al.*, 1981). Patients with NBS display facial dysmorphism, microcephaly and growth retardation. NBS has been documented to be associated with increased cancer incidence, in particular B-cell non-Hodgkin's lymphoma (Paulli *et al.*, 2000, Hama *et al.*, 2000, Kruger *et al.*, 2007). *NBN* mutations have been reported in gastrointestinal cancer, breast cancer and lymphoblastic leukemia (Ebi *et al.*, 2007, Bogdanova *et al.*, 2008, Varon *et al.*, 2001). Moreover, NBN is also often found to be mutated in many GBM cases (Watanabe *et al.*, 2009) and in some cases of MB patients (Distel *et al.*, 2003, Bakhshi *et al.*, 2003, Huang *et al.*, 2008). In the study by *Huang et al.*, they screened 42 MB patients and discovered that 7 carried NBN mutations. They then hypothesised that NBN mutations might be involved in MB pathogenesis (Huang *et al.*, 2008).

1.7 The p53 signalling pathway

The p53 protein was first discovered in 1979, when it was found complex to the Simian virus 40 large T-antigen (Lane and Crawford, 1979, Linzer and Levine, 1979). It was initially falsely considered to be an oncogenic protein due to couple of reasons. Firstly, it was found that this 'p53' protein was highly expressed in tumour cells. Secondly, cloning and transfection of the p53 gene into cells has enabled them to gain immortality (Eliyahu *et al.*, 1984, Jenkins *et al.*, 1984). It wasn't until the late 1980's, that it was realised that the p53 gene used in those studies was a mutant form of p53 and not the WT p53 (Finlay *et al.*, 1989). Since then, the studies on p53 have expanded and it became clear that p53 is in fact a tumour suppressor protein. It is now well established that the p53 protein plays a central role in maintaining genomic integrity in response to cellular stress (Lane, 1992, Levine, 1997). p53 is activated by a variety of stimuli such as DNA damage, heat shock, nutrient depletion and oxidative stress. Activated p53 transactivates many downstream targets according to the type of stress signals. One important role of p53 is its involvement in response to DNA damage, senescence and apoptosis in the presence of genotoxic stress. The activation of DNA repair proteins can induce cell cycle arrest hence allowing time for the cells to repair their DNA damage before cell cycle progression. Furthermore, when DNA damage is beyond repair, p53 can induce cellular senescence or apoptosis (Harris and Levine, 2005, Oren, 2003). For these reasons, mutations or malfunction of the p53 pathway are often associated with neoplastic disease and can lead to cancer development.

1.7.1 Structure of p53

The p53 protein is encoded by the *TP53* gene located on the short arm of chromosome 17; 17p13.1 (McBride *et al.*, 1986). The *TP53* gene is highly conserved, composed of 11 exons and 10 introns (Lamb and Crawford, 1986). The encoded p53 transcription factor comprises of three functional domains: N-terminus, central core and C-terminus (**Figure 1.10**).

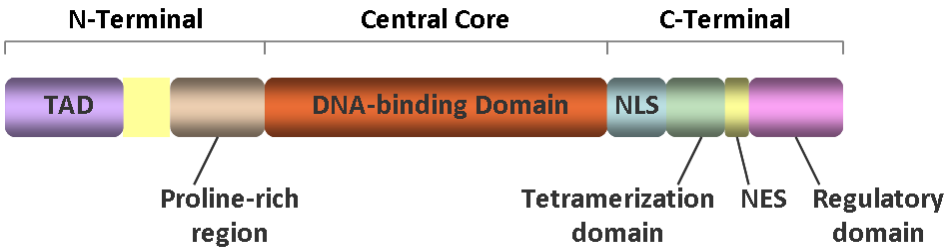

Figure 1.10 p53 domain structure. *A schematic representation of p53 protein with its functional domains. TAD= Transactivation domain, NLS= Nuclear Localisation signal, NES= Nuclear export signals.*

The N-terminus contains the transactivation domain (TAD) and a proline rich region. The highly conserved and largest domain is the DNA binding domain (residue 102-292) found in the central part of the protein. Lastly, located in the C-terminal, is an oligomerisation domain (OD), 3 nuclear localization signals (NLS), nuclear export sequence (NES) and a regulatory domain (**Figure 1.10**). In summary, the N-terminal is responsible for activation of transcription factors, the central region binds and interacts with target DNA and the C-terminal allows tetramerisation as well as being involved in negative regulation. The details and functions of each region are described in **Table 1.2**.

Domains	Residues	Descriptions
Transactivation	1-42	An acidic transactivation domain and MDM2 protein binding sites
Proline-rich	63-97	Repeated proline rich region and second transactivation domain
DNA binding domain	98-292	Central region, contains DNA binding domain
Tetramerization	324-355	Consists of a beta-stand, alpha helix and a nuclear export signal (NES)
Regulatory	363-393	A strongly basic carboxyl- terminal domain. Involved in downregulation of DNA binding

Table 1.2 Description of p53 domains and their basic functions

1.7.2 Regulation of p53

1.7.2.1 p53 regulation by MDM2

The p53 gene is constitutively transcribed, but its levels are tightly regulated by the oncoprotein murine double minute-2 (MDM2). In the absence of genotoxic stress, MDM2 protein regulates p53 expression on several levels, targeting p53 for degradation, inhibiting translation and inhibiting transcriptional activity. Firstly, MDM2 binds to the N-terminus of p53 protein and targets p53 for ubiquitination and subsequent proteasomal degradation (**Figure 1.11**) (Chen *et al.*, 1995, Haupt *et al.*, 1997, Honda *et al.*, 1997). Secondly, MDM2 can inhibit p53 transcriptional activity by physically blocking p53 interaction with its target DNA binding domain (**Figure 1.11**) (Momand *et al.*, 1992). Lastly, MDM2 can bind to the L26 ribosomal protein (a subunit of the ribosomal 60s translation machinery), inhibiting its function of translating p53 mRNA (**Figure 1.12**) (Takagi *et al.*, 2005, Chen *et al.*, 2012).

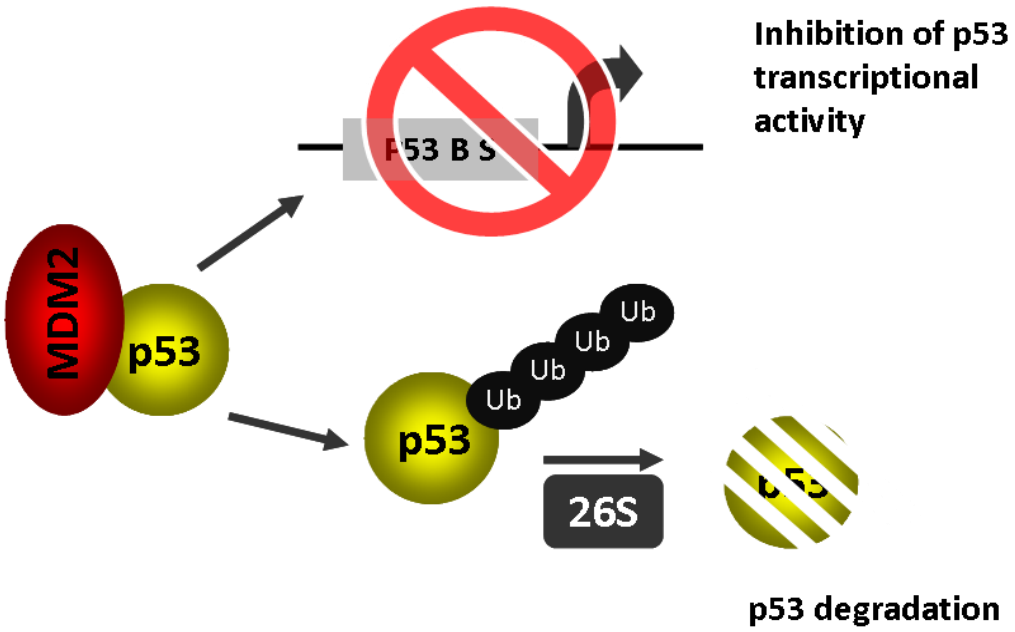

Figure 1.11 MDM2 regulation of p53 expression. *A simplified diagram depicting how MDM2 regulates p53 expression. MDM2 physically blocks transcriptional activity or by binding to p53 N-terminal which targets p53 for ubiquitination and degradation.*

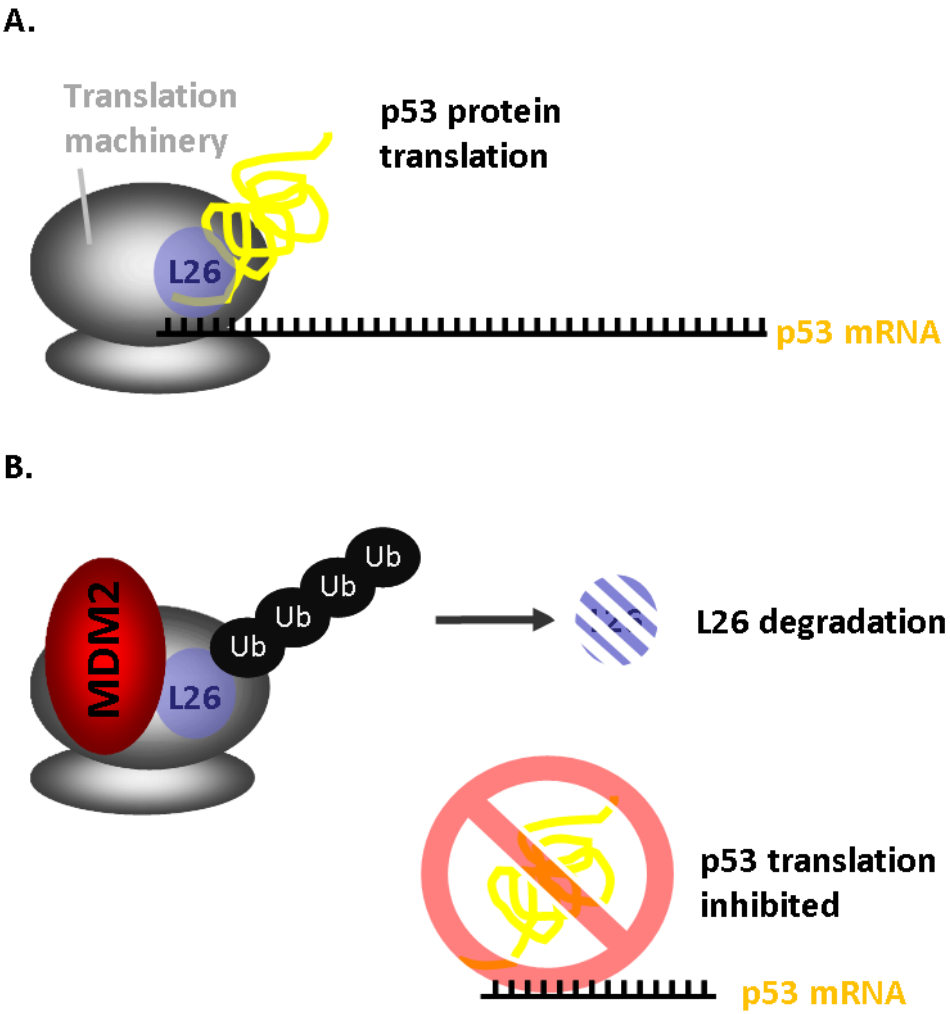

Figure 1.12 MDM2 inhibits p53 translation via mediating L26 degradation. *A simplified diagram demonstrating* ***(A)*** *p53 translation by translation (ribosomal) machinery* ***(B)*** *MDM2 binds L26 ribosomal subunit, leading to its degradation. Consequently, p53 translation is inhibited.*

1.7.2.2 Activation of p53

Induction of p53 activity occurs via the dissociation from its negative regulator MDM2. This process is mediated by p53 post translational modifications in the presence of intrinsic or extrinsic genotoxic insults. p53 activity and stability is controlled by a series of phosphorylation, acetylation, methylation, glycosylation, sumolyation, neddylation and poly-ribosylation events (Appella and Anderson, 2001). The combination of these various types of modifications dictates the functional outcome of p53 but the exact post-modifications and their corresponding downstream target activation is unclear (Maclaine and Hupp, 2009). Although there are multiple p53 phosphorylation sites, specific sites have been identified to play a key role in p53 activation, for example serine 15 (Thompson *et al.*,

2004). Phosphorylation of this residue is mediated by ATM and ataxia telangiectasia Rad3 related (ATR) kinases and promotes subsequent modifications of other residues such as serine 9, 20 and 46 (Sakaguchi *et al.*, 1998, Saito *et al.*, 2002, Saito *et al.*, 2003, Sakaguchi *et al.*, 2000). Furthermore, ATM mediated serine 15 phosphorylation recruits p300 and CBP histone acetyl transferase, which are required for p53 transactivation.

One example of p53 activation through this pathway is upon DNA damage induced by UV/gamma radiation or chemical treatment. DNA damage is detected by the sensor proteins, ATM and ATR, which phosphorylate the checkpoint kinase 2 (Chk2) and checkpoint kinase 1 (Chk1), respectively (**Figure 1.9**) (Appella and Anderson, 2001, MacLaine and Hupp, 2011). Consequently, Chk2 and Chk1 kinases phosphorylate p53, inhibiting the binding of MDM2 to p53 thus preventing the degradation of p53 (**Figure 1.13**). This allows the protein to stabilise and accumulate, and then to interact with its co-activators, CBP/p300. This further transactivates downstream target genes such as p21, BAX and PUMA as well as non coding microRNAs (Harris and Levine, 2005, He *et al.*, 2007). Also, p53 induces its own regulator, MDM2, therefore forming a negative feedback loop (**Figure 1.13**) (Wu *et al.*, 1993).

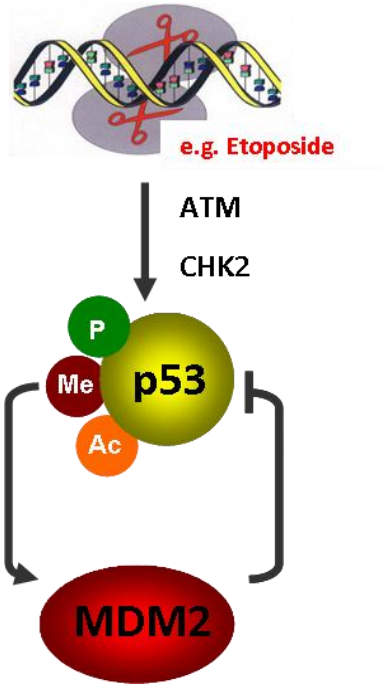

Figure 1.13 Activation of p53. *A diagram demonstrating activation of p53 by etoposide via ATM and Chk2 phosphorylation. The p53 and MDM2 regulatory negative feedback loop is shown.*

1.7.2.3 Oscillations of p53

Oscillations in the cellular localisation of transcription factors including p53 have been observed (Hoffmann *et al.*, 2002, Bar-Or *et al.*, 2000, Lahav *et al.*, 2004, Geva-Zatorsky *et al.*, 2006, Hamstra *et al.*, 2006). The negative feedback loop between p53 and MDM2 is central for the oscillations to take place. Oscillations in p53 was first reported by *Lev Bar-Or et al.*, where dampened p53 oscillations were observed post DNA damage induction by γ-irradiation on a cell population level (Bar-Or *et al.*, 2000). Later work based on single cell image analysis clarified that dampened p53 oscillations are due to varied frequencies of oscillation and the loss of synchronicity of oscillation over time within a cell population (Lahav *et al.*, 2004, Geva-Zatorsky *et al.*, 2006). *Lahav et al.* proposed that the p53:MDM2 feedback loop resulted in 'digital' oscillations, with the number of oscillations increasing when DNA damage increased (Lahav *et al.*, 2004). p53 oscillation signalling allow a repeated but short duration of p53 transactivation. *Purvis et al.* demonstrated that oscillatory function in p53 can alter the pattern of downstream gene expression and cellular fate decisions (Purvis *et al.*, 2012). Cells that experience repeated p53 pulses express cell cycle arrest related genes and recover from DNA damage, whilst cells with sustained p53 signalling undergo senescence through activation of apoptotic genes (Purvis *et al.*, 2012). However, the question of whether p53 indeed oscillates or whether it is due to repeated individually repetitive triggers still remains to be elucidated.

1.7.3 p53 mutations in cancer

Defects in the p53 pathway are a common feature in tumours, *TP53* gene mutations are found in over 50% of all human cancers including brain tumours (Tabori *et al.*, 2010, Baker *et al.*, 1989, Bennett *et al.*, 1999, Nigro *et al.*, 1989, Toledo and Bardot, 2009, Oren and Rotter, 1999, Vogelstein *et al.*, 2000). Commonly, p53 mutations found in cancer are missense mutations or single base-pair substitutions. In some cases, loss of the chromosome 17 have been observed, such as in ovarian cancer and breast cancer (Russell *et al.*, 1990, Tavassoli *et al.*, 1993, Negri *et al.*, 2010). Additionally, impairment of p53 function can be also due to an elevated MDM2 expression (Oliner *et al.*, 1992, Momand *et al.*, 1992, Haupt *et al.*, 1997).

For most other tumour suppressor genes, mutations observed tend to be the result of gene 'truncation' or 'deletion' (Weinberg, 1991), therefore leading to an inactivated protein or

little/ no gene expression. However, because the majority of *TP53* mutations are often due to missense resided to residues belonging to the 'functional domain', *TP53* mutations regularly result in a full length protein, which lacks specific DNA binding function (Freed-Pastor and Prives, 2012). Many of these p53 mutants have been further shown to cause two functional outcomes: a dominant negative (DN) or a gain of function (GOF) effect.

Mutant p53 often have an increased half life and thus prolonged protein stability, which is unlike its WT counterpart (Strano *et al.*, 2007). Due to the increased stability, these excess mutant proteins can exert DN effects on the remaining WT protein and mask its function (Brosh and Rotter, 2009). A DN effect can result when mutant p53 forms a tetramer with the WT p53 (of varied combination), thus resulting in an altered functional p53 protein (Chan and Lung, 2004, Xu *et al.*, 2011). Moreover, missense mutations in *TP53* are commonly followed by 'loss of heterozygosity' (Baker *et al.*, 1989, Brosh and Rotter, 2009). This leads to the mutant p53 'Gain of function' hypothesis, where mutant p53 not only reduces WT functions but are selected for expressions. Mutant p53 GOF is well documented, and is generally referred to as functions gained by these proteins in the absence of WT p53. GOF mutants have been demonstrated to interact with a selection of proteins, forming complexes with their partners and altering their functions. For example, mutant p53 is found to interact with p63 and p73, inhibiting their usual function of mediating transcription of p53 target genes (Gaiddon *et al.*, 2001, Strano *et al.*, 2002, Di Como and Prives, 1998, Marin *et al.*, 2000). Moreover, as mutant p53 is transcriptionally active, the different mutant forms are found to be associated with activation of a wide variety of downstream targets, including genes involved in proliferation, metabolism, cell-cell/ cell-ECM signalling and anti-apoptotic functions (**Table 1.3**) (Bossi *et al.*, 2008, Sampath *et al.*, 2001, Sun *et al.*, 2000). Altogether, p53 mutations and its mutant protein demonstrate roles in tumourgenesis and thus enhance cancer progression through DN and GOF effects.

Gene	Description	Biological process	Mutant	Reference
MAP2K3	Mitogen-activated protein kinase 3	Cell proliferation	R175H, R273H, R280K	(Bossi *et al.*, 2008, Gurtner *et al.*, 2010)
PCNA	Proliferating cell nuclear antigen	Cell proliferation	D281G, R248W	(Deb *et al.*, 1992)
BCL2L1	Bcl-xl	Anti-apoptotic	R175H, R273H	(Bossi *et al.*, 2008)
MDR1	Multidrug resistance protein 1	Chemoresistance	R273H, R273H	(Chin *et al.*, 1992, Strauss *et al.*, 1995)
IDI1	Isopentenyl-pyrophosphate isomerase	Metabolism	R273H	(Freed-Pastor and Prives, 2012)
MMP3	Matrix metalloproteinase 3	Cell-ECM signalling	R175H	(Sun *et al.*, 2000)
ITGA6	Intergin α 6	Cell-cell signalling	D281G	(Scian *et al.*, 2005)

Table 1.3 Example of p53 mutant transcriptional targets. *A table demonstrating different p53 mutant target genes involved in a wide range biological of processes. The Mutant column shows the site of missense mutation (R= arginine; H= histidine; D=aspartic acid; G= glycine; W=tryptophan).*

1.8 MicroRNA

MicroRNA (miRNA) is a class of small non-coding RNA first discovered 20 years ago in *C.elegans* (Lee *et al.*, 1993). Their mature form is between 18-21 nucleotides long and their main function is to control gene expression at the post transcriptional level (Lee *et al.*, 1993, Hammond *et al.*, 2000, Bartel, 2004, Lewis *et al.*, 2005). A key feature of miRNAs is their ability to control the expression of multiple gene targets (Bartel, 2004, Xie *et al.*, 2005, Lewis *et al.*, 2003). These post transcriptional regulators are found to have roles in cell fate and are associated with cancer (Cho, 2007, Tsuchiya *et al.*, 2006).

1.8.1 Biogenesis of miRNA

The regulation of miRNA transcription is similar to coding mRNA, whereby miRNA coding sequences are regulated by promoter regions and their expression is controlled by transcription factors. A hairpin structured pri-miRNA is transcribed by RNA polymerase II and processed by Drosha/DGCR8 protein complex into a pre-miRNA within the nucleus (Lee *et al.*, 2002, Lee *et al.*, 2003) (**Figure 1.14**). The export of pre-miRNA into the cytoplasm is assisted by exportin-5-RAN-GTP (Yi *et al.*, 2003, Bohnsack *et al.*, 2004, Lund *et al.*, 2004). After nuclear export, the pre-miRNA hairpin loop is cleaved by DICER, releasing a miRNA duplex (Hutvagner *et al.*, 2001, Knight and Bass, 2001, Ketting *et al.*, 2001). The duplex miRNA is loaded onto Argonaute (Ago) protein, while the antisense strand of the miRNA duplex is degraded, the mature miRNA (sense strand) remain on the Ago protein. The Ago protein with miRNA, combined with the TRBP and Dicer, is known as the RNA-induced Silencing (RISC) complex (**Figure 1.14**) (Lingel *et al.*, 2004, Bartel, 2004, Kim *et al.*, 2009, Chendrimada *et al.*, 2005). RISC-miRNA can guide and bind to the 5'UTR region of target mRNA, by perfect or incomplete base complementation, subsequently inducing mRNA degradation or translational repression of target genes (Hammond *et al.*, 2000, Bartel, 2004).

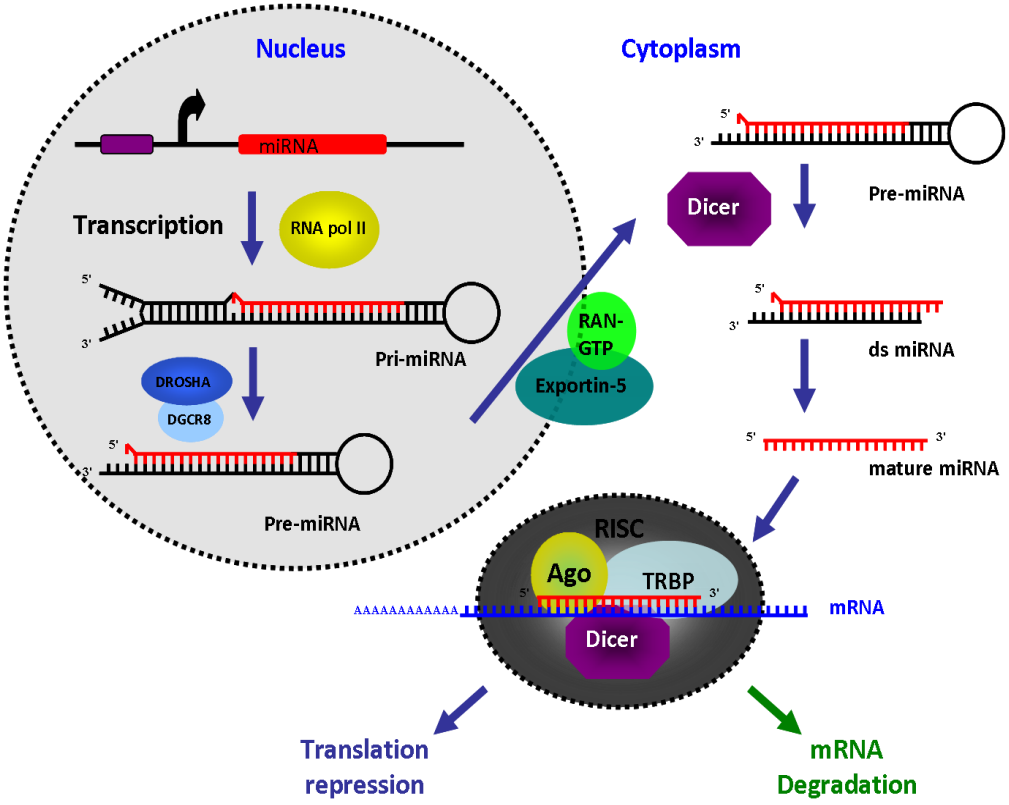

Figure 1.14 Schematic diagram of miRNA processing. *pri-miRNA is transcribed by RNA pol II and cleaved by DROSHA/DGCR8 into pre-mRNA. Pre-miRNA is exported by RAN-GTP/Exportin5 into the cytoplasm and processed by Dicer. Mature miRNA incorporates onto RISC complex and targets mRNA for degradation or translation repression.*

1.8.2 MicroRNA expression in cancer

Recent expression profiling of miRNAs has revealed their association with tumour progression and prognosis (Calin and Croce, 2006, Yanaihara *et al.*, 2006, Volinia *et al.*, 2006). Many studies have reported varied expression of miRNAs in human cancers, for example increased levels of miR-155 have been observed in B cell lymphoma (Kluiver *et al.*, 2005), whilst reduced levels of miR-335 & miR-126 are found in metastatic breast cancer (Tavazoie *et al.*, 2008). Alteration of miRNA expression can be due to genetic mutations, for instance, frequent chromosome deletions such as 13q14 in chronic lymphocytic leukaemia patients results in no detectable expression of miR-15a and miR-16 cluster (Calin *et al.*, 2005, Cimmino *et al.*, 2005).

Specific miRNAs (Oncomirs) involved in targeting tumour suppressor genes, genes controlling cellular differentiation or apoptosis are often up-regulated in cancer. Reversely,

miRNAs targeting oncogenes might be down-regulated. In addition to their roles in controlling cell fate, miRNAs have also been demonstrated to be involved in angiogenesis, invasion and metastasis, genomic instability and evasion of the immune system, which are all hallmarks of cancer mentioned in section 1.2 (**Figure 1.1**).

1.8.2.1 Hypoxia regulated miRNAs

Several microRNAs have been found to be regulated under hypoxia. These miRNA are termed as hypoxia-responsive miRNA (HRM) (Kulshreshtha *et al.*, 2007, Chen *et al.*, 2013, Ghosh *et al.*, 2010, Camps *et al.*, 2008, Huang *et al.*, 2009). *Kulshreshtha et al.* used a microarray-based screen method and examined miRNA expression of selected cancer cell lines incubated in hypoxia (0.2%). They have identified 27 HRM which were upregulated in at least two of the four cell lines investigated (Kulshreshtha *et al.*, 2007). These include miR-21, miR-107, miR-155 and miR-210, which are commonly found to be associated with cancer (Si *et al.*, 2007, Volinia *et al.*, 2006, Huang *et al.*, 2009, Gee *et al.*, 2010, Bruning *et al.*, 2011). Although there are reports of hypoxia/ HIF-induced miRNA, there is no extensive evidence of a general miRNA signature of hypoxic cells.

1.8.2.2 MicroRNA expression in brain tumours

In brain tumours, many miRNAs are found to be dysregulated (**Table 1.4**). The miRNA expression profiling study on primary MB performed by *Ferretti et al.* has demonstrated typical miRNA expression patterns classifying MB histotypes (Ferretti *et al.*, 2009). The majority of miRNAs in MB are found to be downregulated, two of which are miR-9 and miR-125 (Ferretti *et al.*, 2009), which are also downregulated in neuroblastoma (Laneve *et al.*, 2007). Table 1.4 demonstrates some of the miRNAs commonly found to be differentially expressed in brain tumours (**Table 1.4**).

MicroRNAs	Cancer	Expression	Reference
miR-9	*Medulloblastoma/ Neuroblastoma*	Reduced expression	(Ferretti *et al.*, 2009)
miR-17/92	*Medulloblastoma*	Overexpressed	(Ferretti *et al.*, 2009, Uziel *et al.*, 2009, Northcott *et al.*, 2009)
miR-30b/ d	*Medulloblastoma*	Overexpressed	(Lu *et al.*, 2009)
miR-34a	*Glioma, Neuroblastoma*	Reduced expression	(Welch *et al.*, 2007, Li *et al.*, 2009)
miR-124a	*Medulloblastoma*	Reduced expression	(Pierson *et al.*, 2008)
miR-125a/b	*Medulloblastoma, Neuroblastoma*	Reduced expression in MB	(Ferretti *et al.*, 2009)
miR-199b	*Medulloblastoma*	Reduced expression	(Garzia *et al.*, 2009)

Table 1.4 miRNA involved in brain tumours. *Examples of miRNA expression in brain tumours.*

1.8.2.3 miR-34 microRNA family

MiR-34a is a miRNA that has caught the interest of many researchers, as it is commonly expressed at reduced levels in glioma and neuroblastoma. MiR-34a has been demonstrated to down-regulate many oncogenes and pro-survival genes (**Table 1.5**), illustrating its role as a tumour suppressor. Moreover, miR-34a expression is regulated by p53. It has been shown that p53 binds directly to a p53 responsive element, located upstream of the miR-34a transcription start site (Bommer *et al.*, 2007, Raver-Shapira *et al.*, 2007). Independent studies have confirmed that miR-34a expression is correlated with p53 status and that induction is dependent on p53 activation both *in vivo* and *in vitro* (He *et al.*, 2007, Bommer *et al.*, 2007, Wei *et al.*, 2006).

MiR-34a is a family of three transcripts consisting of miR-34a, miR-34b and miR-34c, with the latter two located on the same chromosome while miR-34a is located in chromosome 1p36. The tumour suppressor role of miR-34a was first described by *Welch et al 2007*, where the deletion of chromosome 1p results in a reduced level of miR-34a in neuroblastoma patients. Later, low levels of miR-34a were also reported in other cancer types such as pancreatic, colon and lung cancer (Bommer *et al.*, 2007, Chang *et al.*, 2007, Tazawa *et al.*, 2007). Additionally, miR-34a expression is found to be silenced in melanoma

and prostate cancer (Lodygin *et al.*, 2008). Although miR-34b and miR-34c are less well documented, there is evidence of reduced expression in 40% of non-small cell lung carcinoma patients (Bommer *et al.*, 2007). Many independent studies have since confirmed the link between cancer and miR-34a, demonstrating an important role in cell cycle arrest, senescence and apoptosis (Bommer *et al.*, 2007, Chang *et al.*, 2007, Raver-Shapira *et al.*, 2007).

miR-34a target genes	Description of target genes	Reference
SIRT1	Pro-survival	(Raver-Shapira *et al.*, 2007, Yamakuchi *et al.*, 2008)
MYCN	Oncogene	(Wei *et al.*, 2008)
BCL2	Anti-apoptotic	(Raver-Shapira *et al.*, 2007, Li, L. *et al.*, 2013)
MAGE-A	Oncogene	(Weeraratne *et al.*, 2011)
E2F3	A transcription factor involved in cell cycle progression	(Tazawa *et al.*, 2007, Welch *et al.*, 2007)
CDK6	A cyclin dependent kinase, involved in cell cycle progression	(Sun, F. *et al.*, 2008)
c-Met	A tyrosine-kinase growth factor receptor involved in cell proliferation	(Li *et al.*, 2009)

Table 1.5 miR-34a target mRNA. *Examples of miR-34a target gene and a description of their role.*

1.9 Project aims and hypothesis

The major theme of this thesis is to understand the causes of MB resistance to chemotherapeutic agents and how this could be overcome. In young MB patients, treatment is dependent solely on chemotherapy due to the high risks involved with the other therapeutic methods highlighting the importance of chemotherapy. Moreover, chemoresistance has been observed in MB patients and derived cell lines, emphasising the need for a better understanding of this phenomenon to improve treatment strategy.

As mentioned in section 1.4.1, although MB of different subgroups shares identical histopathology, studies have revealed that these subgroups are highly variable in terms of their biology. The treatment response and prognosis of these subgroups can be very different, and this is governed by the differences in their genetic background. For example, chemoresistance in MB and MB cell lines have been shown to be associated with mutations in the p53 pathway (Tabori *et al.*, 2010, Meley *et al.*, 2010).

Here, we aim to further understand the molecular mechanisms, which contribute to MB chemoresistance. One aim being to overcome the resistance arising from p53 mutations. The second line of approach is to consider the role of the tumour environment such as hypoxia in mediating drug insensitivity. Most *in vitro* pharmacological studies are performed under atmospheric conditions, thus neglecting the classical pathological environment within solid tumours where hypoxic regions exist. Importantly, the role of hypoxia and its associated effect on chemoresistance and cancer malignancy have been well documented in GBM, yet little is known in MB. We hypothesised that hypoxia might also play a role in MB chemotherapy response and that it might be due to a potential crosstalk between the hypoxic and the p53-dependent signalling networks.

The specific project aims were to:

1. Investigate the importance of p53 in MB cell death induction, and to find new molecular targets that could bypass p53 activation to induce cell death in p53 mutated cells.

2. Assess the importance of hypoxia in MB chemosensitivity and to define the link between hypoxia and p53 activity in MB and GBM.

3. Explore the effects of hypoxia on global gene expression and to identify potential targets involved in chemoresistance in hypoxia that could be used to re-sensitise resistant cells.

Chapter 2: Materials and Methods

2.1 Chemical and Reagents

All tissue culture media was purchased from Gibco (Invitrogen, UK) and foetal calf serum from Harlan Seralab (UK) or PAA cell culture company (Austria). Restriction enzymes, real time PCR reagents were purchased from Roche (UK). DNA oligonucleotides, shRNA plasmids and all other reagents were purchased from Sigma-Aldrich (UK) unless otherwise stated.

2.2 Drug and Chemical Treatments

A variety of chemotherapeutic drugs and chemical were used for cell treatments. Typical and optimised concentrations of drug and chemicals used are listed in **Table 2.1**.

Drugs/ Chemicals	Molecular Action	Concentration used	Source
Etoposide	Topoisomerase inhibitor	20µM	Sigma E1383
Nicotinamide	SIRT1 inhibitor	10-100mM	Sigma 479865-U
EX527	SIRT1 inhibitor	50-100µM	Tocris 2780
Sirtinol	SIRT1 inhibitor	50-100µM	Sigma S7942

Table 2.1 A List of drugs used in this project*. The purpose of the drugs and the general dosages used are shown.*

2.3 Cell Lines and growth requirements

Medulloblastoma, Glioblastoma, breast cancer, 293TN-HEK and HeLa cultured cell lines are used in this project. A summary of the cell lines and culturing medium and supplements required are listed in **Table 2.2** and **Table 2.3**.

MB Cell line	Culture Medium	Source
D283-MED	EMEM, 10%FCS, 1% NEAA, 1% NaPyr	ATCC-HTB-185
MEB-Med8A	DMEM, 10%FCS	Provided by Prof T. Pietsch (University of Bonn, Germany)
MHH-Med1	DMEM, 10%FCS	Provided by Prof T. Pietsch (University of Bonn, Germany)

Table 2.2 Summary and sources of MB cell lines.

GM Cell line	Culture Medium	Source
U87MG	EMEM, 10%FCS, 1% NaPyr	ATCC-HTB-14
T98G	EMEM, 10%FCS, 1% NaPyr	ATCC-CRL-1690

Table 2.3 Summary and sources of GB cell lines.

2.3.1 Routine sub-culturing protocol

Cell lines are typically cultured in 75cm^2 tissue culture flasks (Corning, UK) and maintained in a growth condition of 37^{o}C, 5% CO2 in a humidified incubator (SAYO, Japan). The following table contains a brief summary of the sub-culturing schedule for each of the cell lines in a typical week (**Table 2.4**).

Cell Lines	Monday	Wednesday	Friday
D283-MED	*Sub-culture*	Add media	*Sub-culture*
MEB-Med8A	*Sub-culture*	Add media	*Sub-culture*
MHH-Med1	*Sub-culture*	Add media	*Sub-culture*
U87MG	*Sub-culture*	*Sub-culture*	*Sub-culture*
T98G	*Sub-culture*	Replace media	*Sub-culture*

Table 2.4 Summary of sub-culturing procedure in a typical week.

2.3.1.1 Sub-culturing protocol for non-adherent cells

Non-adherent cells are collected in a tube and pelleted by centrifugation for 5 minutes at 100g and the supernatant was removed. The pellet was resuspended with 10ml of fresh media and cell counts were determined using a particle cell counter (Beckman Coulter). Cells are transferred to new flask to maintain the cell culture or distributed to other culture dishes for experiments (**Table 2.5**)

Cells	Plates	Number of Cells Plated	Volume (ml)
D283 / Med 1	96-well	1-2 x10^4	0.1
	24-well	0.5 x10^6	1
	6-well	1-2 x10^6	2
	35mm dish	1-2 x10^6	2
	75cm^2 Flask	10-15 x10^6	20

Table 2.5 Commonly used culture vessels. *Typical plating density is shown.*

2.3.1.2 Sub-culturing protocol for adherent cells

The media of adherent cells was removed from the flask and washed with Ca^{2+} free phosphate buffered saline (PBS). All adherent cell lines were incubated for 2- 5 min at 37°C with 1ml of 1x trypsin/ EDTA (Sigma, UK) to allow cells to detach from the flask. A further 9ml of media was added to inhibit trypsin activity and the cells were counted using a cell counter (Beckman Cell Coulter counter). Cells were transferred to new flasks to maintain the cell culture or distributed to other culture dishes for experiments (**Table 2.6**).

Cells	Plates	Number of Cells plated	Volume (ml)
Med8A	96-well	2 x10^4	0.1
U87MG / T98G	96-well	5 x10^3	0.1
U87MG / T98G /Med8A	6-well	0.5-0.8 x10^6	2
	35mm dish	0.5-0.8 x10^6	2
	75cm^2 Flask	2.5 x10^6	15

Table 2.6 Commonly used culture vessels. *Typical plating density is shown.*

2.4 Molecular Biology techniques

2.4.1 DNA propagation

2.4.1.1 Transformation of Competent Cells

Plasmid DNA propagation was performed by transforming *Escherichia coli* (*E.coli)* DH5α competent cells (Invitrogen). DH5α competent cells were thawed on ice and incubated for 30min with the addition of 10ng of DNA plasmid in a 1.5ml microfuge tube. The cells were submitted to a heat-shock at 42°C for 60 seconds and chilled on ice immediately for another 2 minutes prior to addition of 900µl LB broth (1% (w/v) bactotryptone; 0.5% (w/v) yeast extract; 1% (w/v) NaCl, pH 7.0). The cells were incubated at 37°C in a shaking incubator for 30 minutes then pelleted at 1000g for 1 minute and 900µl of supernatant was then removed. The pellet was resuspended with the remaining supernanant and plated onto LB-agar plates containing the appropriate antibiotic (100µg/ml ampicillin or 50µg/ml kanamycin). The plate was then incubated at 37°C overnight.

2.4.1.2 Purification of Plasmid DNA (Plasmid Maxi Preparation)

One colony of transformed *E.coli* cells were inoculated in 5ml of LB broth with appropriate antibiotic selection for 6-8 hours prior to transfer to a 2L conical flask containing 250 LB broth containing the appropriate antibiotic. The flasks were cultured overnight at 37°C in a shaking incubator at 225rpm. The cells were harvested by centrifugation at 6000g for 15 minutes at 4°C. Plasmid purification was carried out following the manufacture's instruction with either Plasmid Maxi Kit (Qiagen) or PureLine Maxi Kit (Invitrogen). Plasmids were typically dissolved in 100µl of TE. The plasmid concentration was quantified using a Nanodrop spectrometer (ThermoScientific) and adjusted to a final concentration of 1µg/µl.

2.4.2 Plasmid Transfection

Cells were transfected using FuGene®6 (Roche, UK) or Lipofectamine 2000 (Invitrogen, UK) following the manufacturer's instruction. The ratio of transfection reagent (µl) to DNA (µg) used was dependent on cell types (**Table 2.7**). Total transfection reaction volume was determined empirically based on surface area of culture vessels (adherent cells) or cell culture volume (suspension cells). The table demonstrates a typical transfection of a 35mm dish with 2 ml cell culture medium.

Cells	FuGene6/Lipofectamine (µl): DNA (µg)	Volume of serum free medium (µl)
D283	4:2	100
Med8	4:2	100

Table 2.7 Reagents and DNA ratio used for plasmid transfection.

The required volume of transfection reagents are added to serum free medium and incubated at room temperature for 5 min. DNA was added to the pre-incubated mixture and further incubated at room temperature for 30 minutes (**Figure 2.1**). The complete transfection mix was then added onto the cells in a dropwise manner. Fresh media was added to the plate hours after transfection.

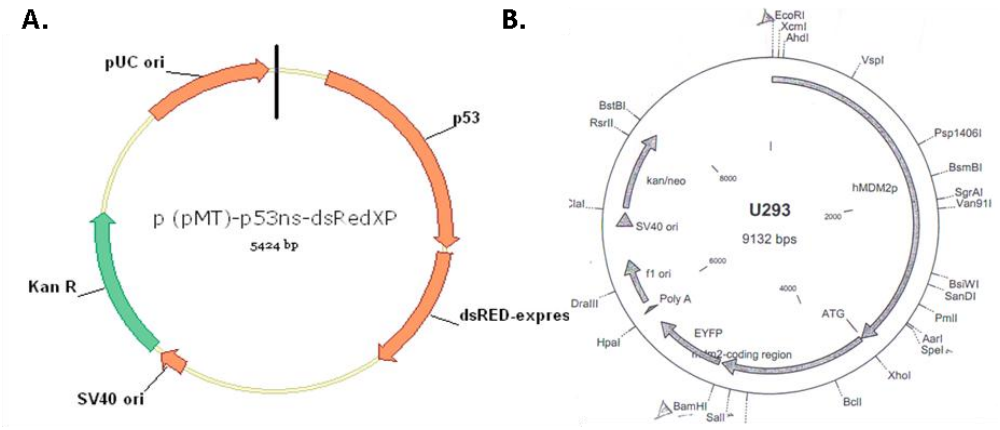

Figure 2.1.Expression plasmid (A) *pMT-p53-dsREDXP* ***(B)*** *mdm2-MDM2-YFP*

2.4.3 Oligonucleotides (miRNA, siRNA) Transfection

Small nucleotides RNA mimics and inhibitors {**Table 2.8**} were transfected into cells using HiPerfect (Qiagen) transfection reagents.

siRNA	Source	Cat no
miR-34a mimic	Dharmacon	C-300551-07
mimic control	Dharmacon	CP001000-02-05
mimic transfection control with Dy547	Dharmacon	CP-004500-01
miR-34a inhibitor	Dharmacon	IH-300551-08-0005
miR-34a Hairpin negatives	Dharmacon	IN-0010050105
Sip53	Invitrogen	1299001
scrambled siRNA	Dharmacon	D001810-10-05

***Table 2.8 siRNA and miRNA used**. Sources are shown.*

The required volume of transfection reagents and oligonucleotides (final conc [100nM]) are added to opti-MEM, mixed and incubated at room temperature for 15 min then added on to the cells gently (**Table 2.9**). Transfection medium was replaced (adherent cells) or topped up (suspension cells) 6 hours after transfection. Expression time is typically between 48-72 hours.

Reagents	Volume (µl)
Opti-MEM	100
HiPerFect	15
siRNA/ miRNA mimics or inhibitors [100nM]	5

Table 2.9 Reagents and DNA ratio used for siRNA or miRNA transfection.

2.5 Real time PCR (qPCR)

2.5.1 Total RNA extraction

The RNeasy Mini kit (Qiagen, Germany) was used to extract mRNA from D283 cells. The cells were typically treated with drugs or hypoxic exposure one day after plating on a 35mm dish. Prior to lysis, the cells were pelleted for 5 minutes at 300g, washed with 1ml of PBS and further centrifuged as previously described. After removal of PBS, the cells were lysed with 350µl of buffer RLT containing 1% β-Mercaptoethanol (v/v). The lysates were typically frozen at -80°C at this point until the rest of the samples were collected for mRNA extraction. Sample homogenisation was achieved by using a QIAshredder (Qiagen) and the 'Spin Protocol' extraction procedure was carried out as detailed in the manufacturer protocol. RNA was eluted with 30µl of RNase free water and the sample purity was quantified using spectrophotometry.

2.5.1.1 Reverse Transcription

The reverse transcription of mRNA to cDNA was carried out using SuperScript® VILO cDNA synthesis Kit (Invitrogen). Each conversion reaction consisted of 1µg of RNA, 1xSuperScript® enzyme, 1x VILO™ reaction mix (containing random primers, RNase inhibitor and recombinant ribonuclease inhibitor) made up to 20µl total volume with DEPC-treated water. PCR reactions were performed using a Px2 Thermal Cycler (Thermo) for 10 minutes at 25°C, 60 minutes at 42°C and 5 minutes at 80°C. The cDNA was then diluted 20-fold with DEPC-treated water and stored at -20°C prior usage in qPCR.

2.5.2 MicroRNA extraction

The miRNeasy Mini kit (Qiagen, Germany) was used to extract mRNA from D283 cells. The cells were typically treated one day after plating on 35mm dish. Prior to lysis, the cells were pelleted for 5 minutes at 300g, washed with 1ml of PBS and further centrifuged as previously described. After removal of PBS, the cells were lysed with 700µl of Qiazol. Sample homogenisation was achieved by passing the samples through a 10 gauge needle using a syringe for ten times. The lysates were frozen at -80°C at this point until all samples were collected. MiRNA extraction was carried out following the manufacturer's protocol.

RNA was eluted with 30µl of RNase free water and the sample purity was quantified using spectrophotometry.

2.5.2.1 Reverse Transcription-First Strand cDNA synthesis

The reverse transcription of miRNA to cDNA was carried out using Ncode™ miRNA First-Strand cDNA synthesis Kit (Invitrogen). Poly (A) tailing reaction consist of 1µg of RNA, 5x miRNA reaction buffer, 2.5mM $MnCl_2$, 80µM ATP, 0.5µl Poly A polymerase made up to 25µl total volume with DEPC-treated water and incubated at 37°C for 15 minutes using a Px2 Thermal Cycler (Thermo). Immediately after, 4µl of the polyadenylated RNA was added to 1µl of Annealing buffer, 9µM of Universal RT Primer made up in a total volume of 8µl and incubated at 65°C for 5 minutes and then placed on ice for 1 minute. 2x First-Strand Reaction mix and 2µl SuperScript™ III RT/ RNaseOUT™ Enzyme Mix was added to the reaction tubes, RT reactions were performed using a Px2 Thermal Cycler (Thermo) for 50 minutes at 50°C and 5 minutes at 85°C. The cDNA was then diluted 10-fold with DEPC-treated water and stored at -20°C prior usage in qPCR.

2.5.2.2 Quality Quantification of Nucleic Acid

The concentration and purity of RNA and DNA samples were quantified using a Nanodrop spectrometer (Thermo Scientific). High yields DNA from maxiprep were diluted to suitable concentration with a reading range between 2ng/µl to 1000ng/µl. Purity of nucleic acids was determined by absorbance value at different wavelengths, the ratio at 260/280 nm indicates presence of protein and at 260/230 nm of organic solvents.

2.5.3 qPCR

PCR primers were designed using primer 3 software, to search for primer size of 18-25 nucleotide long with a product melting temperature between 56-60°C (http://bioinfo.ut.ee/primer3-0.4.0/) (Koressaar and Remm, 2007, Rozen and Skaletsky, 2000) and quality of primers was determined by Primer stat (http://www.bioinformatics.org/sms2/pcr_primer_stats.html) (Stothard, 2000). Primers used are listed on **Table 2.10**.

Target genes	Forward Primers	Reverse Primers
Cyclophilin A	GCTTTGGGTCCAGGAATGG	GTTGTCCACAGTCAGCAATGGT
miR-34a	TGGCAGTGTCTTAGCTGGTTGT	Universal primer (Invitrogen)
MDM2	GCAAATGTGCAATACCAACA	CTTTGGTCTAACCAGGGTCTC
MDR1	GTGGGGCAAGTCAGTTCATT	TTCCAATGTGTTCGGCATTA
NBN	AGAATTGGCTTTTCCCGAACT	CAAGAAGAGCATGCAACCA
p21	GACTCTCAGGGTCGAAAACG	TAGGGCTTCCTCTTCCAGAA
PHD2	GGAAGATGGAGAACCTGCTG	GCTTGTGCTTCTTCCAGTCC
PUMA	CCTGGAGGGTCCTGTACAAT	CACCTAATTGGGCTCATCT
SIRT1	TTTGGAAATGTTTCAGTTGCTTTA	CACTCTCCCCAGTAGAAGTACCAT
VEGF	GGGCAGAATCATCACGAAGT	CACACAGGATGGCTTGAAGA

Table 2.10 A list of primers and their sequences is shown.

All q-PCR reactions were carried out in triplicate. Each reaction consists of 1xSYBR®Green PCR master mix (Roche), 200nM forward and reverse primers, 2µl of DNA made up in a total volume of 20µl with RNase free water. Real time PCR was performed using a LightCycler 480 (Roche) using the following temperature cycling parameters in **Table 2.11**.

Step	Temperature (°C)	Duration (s)	Ramp Rate (°C/s)	No. of Cycles
Pre-incubation	95	600	4.4	1
Amplification	95 60	5 30	4.4 2.2	45
Melt Curve	95 65 97	5 60 continuous	4.4 2.2 0.11	1
Cooling	40	10	1.5	1

Table 2.11 Typical qPCR cycling parameters used with SYBR®Green.

Results were analysed using the LightCycler480 software (version 1.5.0.39), Advanced Relative Quantification function. Fold change was calculated based on the threshold of amplification cycle for each reaction using the 2-CT method (Pfaffl *et al.*, 2002). The fold changes of target genes were normalised to cyclophilin A (a house keeping gene) and over untreated or time zero control.

2.6 Microarray study

Microarray is a high-throughput screening technique which allows the study of transcriptome, proteome or microRNAome. In a DNA microarray, cDNA samples are first labelled with a one-colour fluorescent dye prior to being placed on the microarray slide, typically made out of glass, silicon or plastic. The fluorescently labelled cDNA samples are hybridized with the microscopic spots (probes) pre-attached on the surface of array slide. The slide is then washed and the fluorescent intensity of each spot on the microarray slide is scanned and measured using a computer. The intensity signals of each spot therefore serves as an indication of the relative abundant of target gene present in the sample.

2.6.1 Design of the microarray study

D283 cells were incubated for a varied hypoxic duration (0, 6, 64 and 96 hours in triplicate), cDNA samples were prepared and sent directly to NimbleGen.

The NimbleGen 12 plex format microarray glass slide, which supports 12 arrays was chosen for the purpose of our experiment (**Figure 2.2**). Each array contains 135000 oligonucleotide probes which are of 60mer long. These relatively long oligonucleotides provide an increased sensitivity, specificity and can help reduced signal to noise ratio.

Figure 2.2 NimbleGen 12x135K Format array slide. *A schematic diagram of a 12 sample array slide containing 135,000 probes spotted on each chip. Glass slide sized 25 x 75mm.*

2.6.2 Microarray sample preparations

2.6.2.1 Messenger RNA extraction with Rneasy Plus

RNA extraction using Rneasy Plus (Qiagen, Germany) kit was identical to extraction using Rneasy kit as described earlier with the exception of one extra step. After homogenisation with QIAshredder (Qiagen), the homogenized lysate was transferred to a DNA Eliminator spin column, centrifuged for 3 seconds at 10,000rpm. The flow through was collected and used for RNA extraction following the 'Spin Protocol' as described in the manufacturer handbook. RNA was eluted with 30µl of RNase free water and the sample purity is quantified using spectrophotometry.

2.6.2.2 Transcriptome amplification

The reverse transcription and amplification of the cDNA library was carried out using a Transplex® Whole Transcriptome Amplification kit (Sigma). Following the manufacturer's protocol, each conversion reaction consisted of 300ng of RNA, 2.5µl WTA Library Synthesis Buffer, 2.5µl WTA Library Stabilisation Solution and 1µl WTA Synthesis Enzyme. Cycling conditions were 24°C for 5 minutes; 42°C for 120 minutes and 95°C for 5 minutes. The amplification step was carried out using all cDNA library products from the reverse transcription step. Each reaction consists of cDNA library, 300µl water, 37.5µl WTA amplification Master Mix, 7.5µl dNTP Mix and 12.5 units of Jumpstart Taq DNA polymerase (Sigma). The reaction was incubated in a thermal cycler with the conditions listed in **Table 2.12**.

Step	Temperature (°C)	Duration (s)	No. of Cycles
Pre-incubation	95	180	1
Amplification	94 65	20 5	17
Hold	4	-	1

Table 2.12 PCR cycling parameters for transcriptomic amplification

2.6.2.3 PCR purification

PCR purification was carried out using QIAquick PCR purification kit (Qiagen) to remove residual primers and nucleotides. The manufacturer's protocol was followed and the amplification product was purified and quantified using spectrophotometry.

2.6.2.4 Agarose Gel electrophoresis

Gel electrophoresis (1% w/v) is used to separate DNA fragments. Agarose is dissolved in 1xTAE buffer by heating it for 3-5 minutes using a microwave, 1x SYBR safe (Invitrogen) was added to the agarose solution before setting to gel. Hyperladder I DNA Ladder (Bioline) and DNA samples combined with 5x Loading Buffer (Bioline) are separated by electrophoresis at 100V for 90minutes. Gels were imaged using Syngene G:box imaging system (Syngene, UK).

2.6.3 Microarray analyses

2.6.3.1 Microarray Raw data

In our microarray, the expression of ~45k transcripts representing ~25k genes (of which, 23,611 are unique genes) were measured. Within the 135k probes, each transcript binds to 3 unique probes that are scattered randomly on the array. Among the 135k probes, there were also random probes (2500) which are spread across the array, for the purpose of experimental control and normalisation between and within cards. The expression values measured by each probe are generated using the Robust Multichip Average algorithm and quantile normalisation (Irizarry *et al.*, 2003a, Irizarry *et al.*, 2003b, Bolstad *et al.*, 2003). The raw results are sent back as an excel format where the expression data of each probe are listed, arranged according to transcripts ID. One can appreciate the scale of this data set (135k by 12) which therefore requires organisation before interpretation.

Dr Boris Noyvert (University of Warwick) provided a customized visualization code to enable generation of a more easily accessible html file by collecting the data together by gene names. Transcripts belonging to the same gene were grouped together and organised alphabetically into their own html page (**Figure 2.3A & B**). In each page, gene names, gene IDs and annotation are displayed among with their transcript expression plots (**Figure 2.3C**).

A.

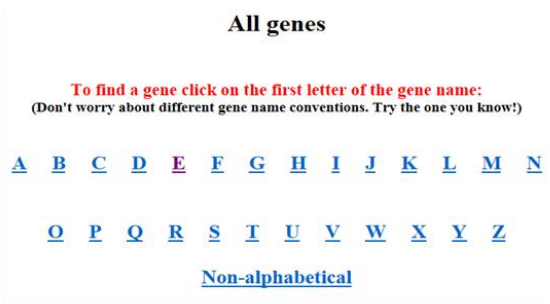

B.

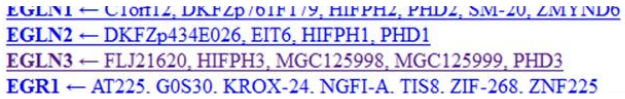

C.

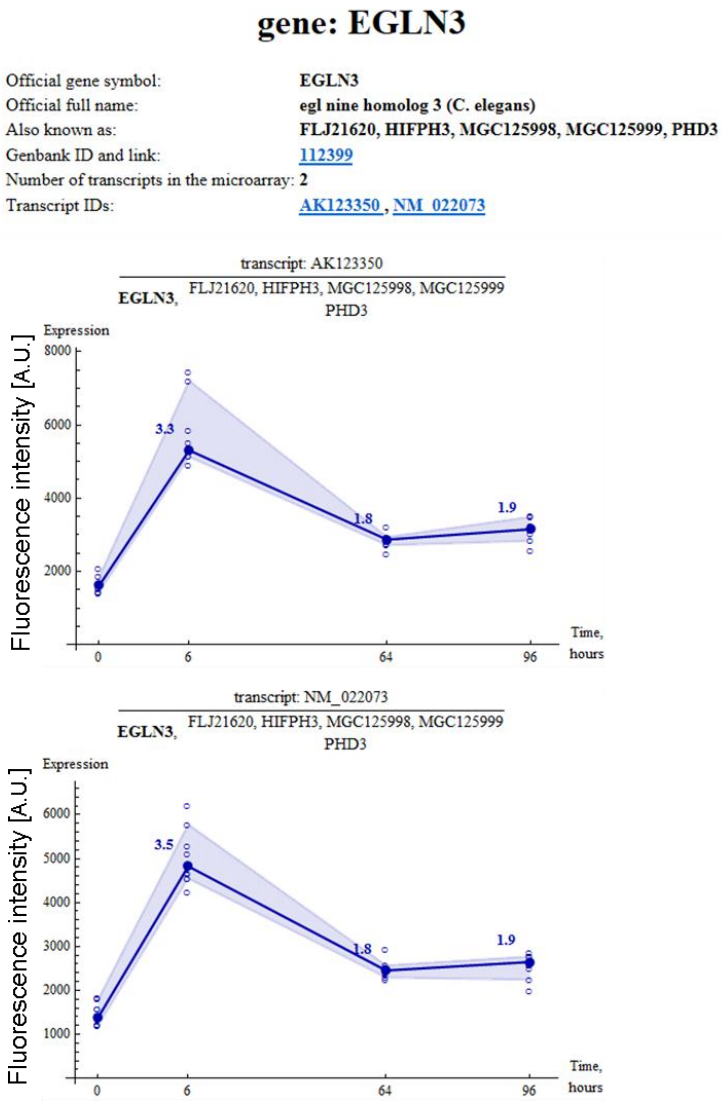

Figure 2.3 Screenshots and Examples of Microarray data on html page. ***(A)*** *Screenshot of search tools classified by gene names* ***(B)*** *Screenshots of part of gene lists organised alphabetically* ***(C)*** *Screenshots of EGLN3 transcripts html page displaying gene information and expression plots.*

2.6.3.2 Transcript expression plots

As there were 3 replicates for each hypoxic time point and that transcript was measured by 3 probes, 9 measurements are generated for each time point. However, the absolute expression value measured for each probe can be quite different, for example, values can be in the range of tens in one probe while it is in the thousands for another. This problem is overcame by rescaling the data of each probe for every transcript by multiplying it to a factor 'X_{probe}', making it possible to plot a meaningful 'average probe expression' on the same graph (**Figure 2.4**).

$$A = \frac{(\text{Mean of probe a}) + (\text{Mean of probe b}) + (\text{Mean of probe c})}{3}$$

$$X_{\text{probe a}} = \frac{A}{(\text{mean of probe a})}$$

$$X_{\text{probe b}} = \frac{A}{(\text{mean of probe b})}$$

$$X_{\text{probe c}} = \frac{A}{(\text{mean of probe c})}$$

Figure 2.4 Calculating average expression plot. *'A' is the average mean of all three probes. 'X_{probe}' is the multiplication factor which is to be used for scaling up the raw expression data for that probe.*

The expression plot on the graph is thus showing the mean of the three median expression levels for all 3 probes (after rescaling) (**Figure 2.5**). The purpose of the html pages allows quick searches and visual interpretation on expression pattern of the gene of interest, however the plots do not bear statistical significance.

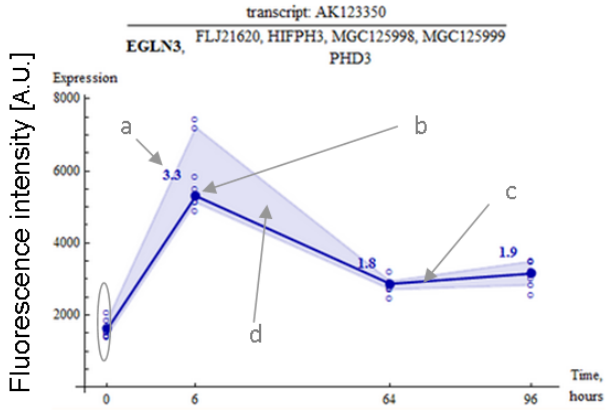

Keys	Description
circled	Data for individual probes at one time point
a	Fold ratio over T0
b	Average data of all probes at one time point
c	Average expression plot
d	Range of data variation

Figure 2.5 Expression plots on html page. *An example of a transcript expression plot with a description of the meaning of the different parts.*

2.6.3.3 Statistical analysis of Microarray Data

As mentioned earlier, a large data set was generated from the microarray study with sample repetition for each time point, multiple probes for each transcript and potentially more than one transcript per gene (**Figure 2.6**). The purpose of having separate probes binding to the same transcript allows a more reliable signal detection and confidence of the results. For example, we would expect the three individual probes targeted for the same transcript will all give rise to three similar expression profiles.

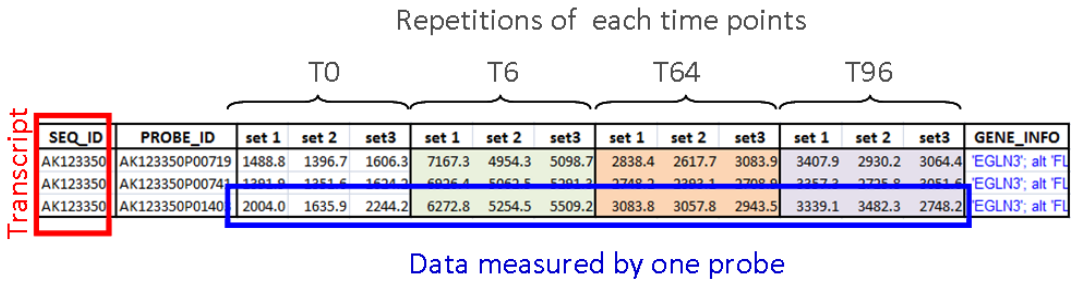

***Figure 2.6 An example of data values for one single transcript. Transcript ID is listed** vertically (red box), each horizontal row shows values measured by one single probe (blue box). Every 3 columns are data obtained from one time point.*

An important aspect of handling microarray data is choosing an appropriate statistical method to allow the selection of genes with a significant differential expression. There are many software or mathematic programs such as GeneSpring, Spotfire, R and Bioconductor, which can be used to analyse/ interpret an array. Here, we have employed the use of MATLAB, combining the use of its built-in features of the statistical and bioinfomatics tool box with manually created programming codes to analyse our microarray data (Damon Daniels, University of Manchester). See Appendix 1.1 to 1.3 for MATLAB codes.

A workflow of microarray data handling is illustrated in (**Figure 2.7**), the details of each step will be described throughout the next sections. Initially, an ANOVA (analysis of variance) test was performed on the log2 transformed data of each probe. ANOVA test makes comparison of the means of several groups of data and provide a statistical test to determine whether the variations between the groups are significantly different. The data values obtained at each time point for every probe were combined and used for analysis. An ANOVA test between every time point is carried out for each of the probes and a list of p values is produced for every probe in the microarray.

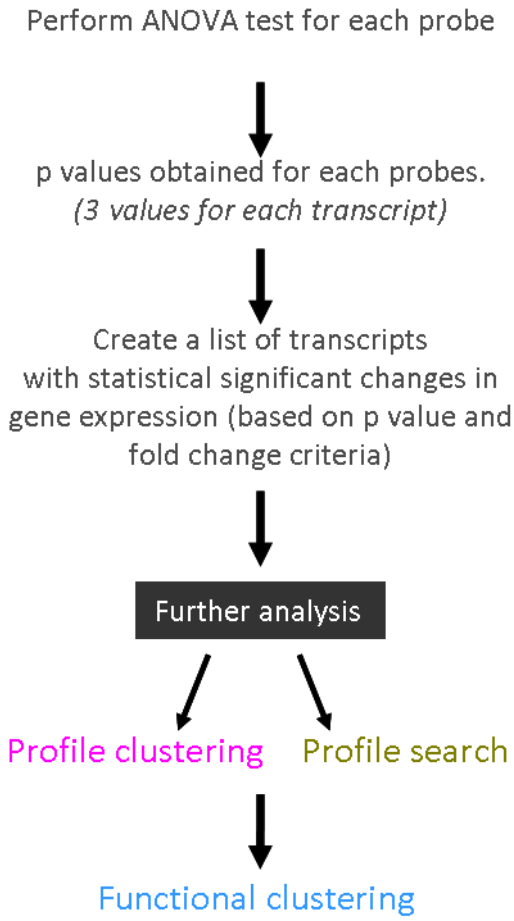

Figure 2.7 A workflow of microarray analysis.

As each gene transcript in the microarray is tested using three separate probes, three p values are therefore obtained for every transcript. In our analysis, a gene transcript is considered to be significantly differentially expressed (at any given time points) under two conditions: (1) if the p value for all 3 probes is <0.01 or if the p value of 2 out of 3 probes is <0.001. The latter criteria minimise false negatives in the cases where one 'faulty' probe might be present for a particular transcript. (2), a minimum of two fold change in gene expression must be met (**Table 2.13**).

Criteria	Value	Description
p value	*≤0.01*	p-value for all 3 probes for one single transcript
	Or	
p value	*≤0.0001*	p- value for all 2/3 probes for one single transcript
	And	
Fold change	*2*	Minimum fold change at any given time point

Table 2.13 Criteria for calculating significantly expressed genes

2.6.3.4 Biological analysis with Ingenuity Pathway Analysis

Data were analyzed through the use of IPA (Ingenuity Systems®, www.ingenuity.com). The significantly expressed data of T6 and combined T64+T96 hours time point resulted from MatLab were selected for analysis. The transcript IDs were converted to Entrez gene ID using Clone/Gene ID converter (Alibes *et al.*, 2007), and their fold change is listed along side in excel. The excel files were submitted to IPA and the results generated were analysed by manual interpretation.

In IPA, Fisher's Extact test statistical methods were chosen to calculate the significance of data observation (Fisher, 1922). The null hypothesis of this method state: "is the proportion of genes (with significant expression) mapped to a particular pathway in the data similar to the proportion that map in the entire population?" The p-value threshold was set to 0.05 in all analysis.

2.7 Single cell Imaging

2.7.1 Immunocytofluorescence

Coverslips were placed in 12 well plates and coated with 1ml polyornithine [100µg/ml] for 2 hours. After removal of polyornithine, cover slips were washed with PBS then MEM. Coverslips were then incubated with fresh MEM for 30 minutes prior to seeding cells onto it. Cells were plated on pre-coated coverslips 16 hours prior to experimental treatments. Cells were rinsed with PBS prior to a 15 minute fixation with paraformaldehyde (4%), then washed with PBS three times. Cells were blocked and permeabilised with PBS containing 1%BSA and 0.1% Triton-X for 20minutes. Cells were incubated with primary antibody (as indicated in (**Table 2.14**) for one hour, washed in PBS for 5 minutes three times then incubated with secondary antibody (as indicated in **Table 2.14**) for 30minutes protected from light. After secondary incubation, the cells were washed with PBS for 5 minutes and stained with DAPI (Hoechst, 1µl/ml in PBS) for 5 minutes, washed with PBS for 5minutes twice more. The coverslips were rinsed with RO water prior to mounting on glass slides with mounting medium (Dako). Image analysis was carried out with LSM 710 (Zeiss) or Leica DM2500 (Leica) microscope and quantified using AQM Advance 6 software (Kinetic Imaging Ltd, UK).

Antibody	Dilution	Host Species	Source	Cat No.
Cy3-anti mouse	1:500	Sheep	Sigma	C2181
Alexa Fluor 488-anti rabbit	1:500	Goat	Invitrogen	A11008
SIRT1	1:200	Rabbit	Abcam	ab13749
γH2AX	1:1000	Mouse	Millipore	05-636

Table 2.14 Summary of antibodies and sources.

2.7.2 Comet Assay

Comet assays were performed using OxiSelectTM comet assay kit (Cell Biolabs). The cells (300k/ml) were plated in 12 well plates directly prior to treatment. After incubation, the cells were collected and centrifuged at 700g for 3 minutes, supernatant removed and sample resuspended in 1ml ice-cold PBS. The samples were diluted with pre-warmed agarose and loaded on the slide provided. The subsequent procedure was carried out as

per manufacturer's protocol followed by alkaline electrophoresis. Vista dye was added immediately before the slides were observed by Leica DM2500 microscope. Images were analysed and quantified using the ImageJ 1.45s open source software (National Institutes of Health, USA).

2.7.3 Confocal Imaging

Time-lapse confocal microscopy was carried using a LSM510 system (Zeiss, Germany). Transfected cells in glass bottom dishes (Iwaki, Japan) were kept in a microscope mounted incubator at 37°C, 5% CO_2 and 21% O_2 and imaged using a 63x Plan Apochromatic oil immersion objective (NA 1.4). YFP-tagged protein was excited using an Argon ion laser (488nm) and dsRedXP-tagged protein was excited using a green-neon laser (543nm). Emitted light was detected through a 505-550nm band-pass filter or 560nm long pass filter through a dichroic mirror for YFP and dsRedXP fluorescence respectively. Imaging data were quantified using CellTracker v.6 software (http://dbkgroup.org/celltracker), (Hailin Shen, Douglas Kell).

2.7.3.1 Tracking analysis-calculating threshold

A threshold for fluorescent intensity is used for determining whether a plasmid is expressed above background level. The threshold was calculated using the raw data exported by CellTracker software. For each cell, the average fluorescent intensity and the standard deviation prior to stimulation were calculated. In our experiment, the threshold is set to be the average intensity prior to treatment plus 2 times standard deviation.

2.8 Western blotting

2.8.1 Sample preparation

Cells were seeded in 35mm dishes in 3ml medium in normoxia or hypoxia with or without etoposide treatment as indicated for each experiment. Cells were pelleted by centrifugation for 5 minutes at 300g, washed with 1ml PBS and a repeat centrifugation was performed. The cells were lysed with 100µl of lysis buffer (Tris-HCl 50mM pH7.5, EDTA 1mM, EGTA 1mM, Sodium Orthovanadate 0.5mM, Triton X-100 1%, sodium fluoride 50mM, Sodium Pyrophosphate 5mM, Sodium β-glycerophosphate 10mM, PMSF 0.1mM and protease inhibitor cocktail 1/100). The samples were rotated for one hour at 4°C on a rotation wheel and centrifuged at 14000g for 20 minutes at 4°C , the supernatant was then collected.

2.8.1.1 Protein concentration assay

Protein concentration was quantified using BCA assays (Thermo Scientific). The BCA assay was performed in a 96 well plate, in which 5µl of protein sample was diluted in 20µl of water. A triplicate standard curve was performed, using BSA protein at a total volume of 20µl and concentrations (µg/µl) of: 0.00, 0.25, 0.50, 1.00 and 1.50. BCA and copper sulphate solution reagent mix was added to samples prior to incubation at 37°C for 30 minutes. The absorbance measurement at 570nm was measured using Multiskan plate reader (Thermo Scientific).

2.8.2 Protein separation by SDS-PAGE

Protein samples were boiled for 5 minutes in the presence of 2x Laemmli buffer (Tris-HCL 0.125M, SDS 4%, glycerol 20%, β-Mercaptoethanol 0.02% and bromophenol blue 0.001%). Using the Mini-PROTEAN 3 system (BioRad), the gels were cast using glass plates with 1.5mm spacers. A 10% SDS resolving gel (0.38M Tris base, 0.1% SDS, 10% acrylamide, 0.25mg/ml APS and 0.125% Temed) and 4% stacking gel (0.14M Tris base, 4% acrylamide, 0.75mg/ml APS and 4% Temed) were prepared in water. 30-50µg of proteins were loaded into each well. The gel was submerged in running buffer (Tris 25mM, Glycine 192mM, 1% SDS) and the sample was resolved for 90 minutes at 120 volts.

2.8.3 Protein transfer onto nitrocellulose membrane

The transfer was performed at 4°C using a Bio-Rad transfer tank filled with pre-chilled transfer buffer (20% (v/v) methanol, Tris 25mM and glycine 200mM). The proteins resolved on the acrylamide gel were transferred by electrophoresis onto nitrocellulose membrane (Bio-Rad 162-0112) at 300mA for 90 minutes at 4°C.

2.8.4 Antibody incubations and protein detection

Nitrocellulose membranes were washed in TBS-T (Tris 20mM, NaCl 140mM, adjusted to pH7.6 and 0.1% Tween) and blocked with 5% (w/v) dry skimmed milk for 60 minutes. After removal of blocking buffer, membranes were rinsed with TBS-T and incubated with primary antibody at 4°C overnight (as indicated in **Table 2.15**). Membranes were washed 3x in TBS-T then incubated with either anti-mouse or anti-rabbit secondary antibody (**Table 2.15**) for 1 hour. Membranes were further washed 3 times in TBS-T. Membranes were developed with ECL (Thermo Scientific) and imaged with Syngene gel imaging G:box.

Antibody	Dilution	Host Species	Source	Cat No.
Anti-mouse HRP	1:5000	Sheep	Abcam	ab6808
Anti-rabbit HRP	1:3000	Goat	Cell Signalling	CS7074
Anti-goat HRP	1:1000	Donkey	Santa Cruz	SC2020
HIF-1α	1:1000	Mouse	BD Biosciences	610959
p53	1:1000	Mouse	Santa Cruz	SC126
p53 serine 15	1:1000	Rabbit	CalBiochem	PC386
SIRT1	1:1000	Rabbit	Abcam	ab13749
β-Actin	1:10000	Mouse	Abcam	Ab8226
β-Actin	1:1000	Goat	Abcam	Ab8229
Cyclophilin A	1:1000	Rabbit	Abcam	Ab3563

***Table 2.15 Summary of western blot antibodies and sources**. Typical concentrations used are also shown.*

2.9 Cell Viability assays

2.9.1 MTS Assay

Viable cells were determined by measuring the cell's metabolic activity using the CellTiter 96®Aqueous One Solution Cell Proliferation Assay Kit (Promega). The assay contains a tetrazolium compound, [3-(4, 5-dimethylthiazol-2-yl)-5-(3-carboxymethoxyphenyl)-2-(4-sulfophenyl)-2H-tetrazolium (MTS), which is reduced to a coloured formazan product by mitochondrial reductase activity. Absorbance values of formazan indicate the level of mitochondrial activity and hence viable cells. Cells were plated in 96 well plates followed by the appropriate treatment in a total volume of 100µl. For the MTS assay, 20µl of substrate was added to each well and the plates were incubated for 120 minutes at 37^{o}C before measurement of the absorbance value at 492nm using a Multiskan plate reader (Thermo scientific).

2.9.2 ViaCount viability assay

Appropriate culture conditions and treatments were applied to cells in a 6 well plate. For the viability assay, 500µl of sample was taken from the plate, centrifuged at 300g for 3 minutes and resuspended in 500µl-1000µl of HBSS. Subsequently, 25µl of the cell suspension was placed in a 96 well plate in duplicate prior to 5min incubation with 225µl of Guava ViaCount Reagent (Millipore). Samples were run using a ViaCount analysis on a GUAVA instrument (Guava EasyCyte Plus). Percentages of viable cells were measured using the Guava ViaCount software.

2.10 Cell cycle Analysis

Desired culture conditions and treatments were applied to cells plated in a 6 well plate. Cells were collected, centrifuged at 3000rpm for 3min and resuspended in an appropriate volume of HBSS to obtain a cell concentration between 100-500 cells per µl, 200 µl of each sample was stained with 25 µl of a solution containing propidium iodide [10µg/ml], ribonuclease A [0.1mg/ml] and 0.1% (v/v) Triton-X 100 in PBS in a 96 well plate. FACS analysis was performed immediately using a GUAVA instrument (Guava EasyCyte Plus) and a population of 5000 cells was used for analysis. Percentages of cells in each cell cycle phase were calculated using the Guava Express Pro software.

2.11 Statistical analysis

Statistical significance test was performed using one-way ANOVA followed by Bonferroni test using built-in statistical analysis in OriginPro 8.6.0 (OriginLab Corporation, USA). With the exception of qPCR data, non parametric *Krustal-Wallis* ANOVA was used (OriginLab Corporation, USA), as data are not normally distributed.

Chapter 3: Chemoresistance in MB

3.1 Introduction

Currently, a combination of surgery and radiotherapy provides a relatively good outcome for MB patients, but often leaves long term neurological side effects (Frange *et al.*, 2009, Rutkowski, 2006, Gilbertson, 2004). Moreover, for younger children and complicated tumour location, surgery is not possible and treatment relies on chemotherapy only.

Unfortunately, resistance to chemotherapeutic intervention has been observed in MB (Meley *et al.*, 2010, Dong *et al.*, 1999, Bobola *et al.*, 2005). One factor of MB chemoresistance is directly linked to the p53 genotype and this is also associated with poor survival (Friedman *et al.*, 1992, Tabori *et al.*, 2010, Pfaff *et al.*, 2010).

Generally, p53 signalling pathway is upregulated by drugs such as etoposide, and it plays a key role in activating genes involved in cell cycle arrest and apoptotic response. As a transcription factor, p53 not only induces transcription of downstream target's mRNA but also of non-coding RNA such as miRNAs. One such direct p53 target is miR-34a, which represses many genes involved in tumourgenesis (Yamakuchi and Lowenstein, 2009, Tazawa *et al.*, 2007, Raver-Shapira *et al.*, 2007).

The aim of this chapter is to investigate potential novel drug targeting downstream of p53 activation, to overcome the chemoresistance due to p53 malfunction. We hypothesised that direct activation of a miRNA downstream of p53, might have sufficient broad effects due to the nature of miRNA function compared to a single mRNA. More specifically, it might be possible to escape the need for p53 activation for triggering cell death by using a miR-34a mimic. The advantage of manipulating miRNA is that it represses hundreds of targets, potentially exerting a global effect compared to targeting one gene only.

Objectives:

1. To test MB cell lines for their sensitivity to chemotherapeutic drugs and to assess the consequences of p53 mutation for cell death induction in MB cells.
2. To understand the role of p53-induced miR-34a for triggering cell death in MB.
3. Attempt to re-sensitise resistant MB cells through miR-34a induction.

3.2 Results

Previously, *Meley et al.* have shown that some MB cell lines displayed resistance to etoposide (Meley *et al.*, 2010), cisplatin and methotrexate (unpublished data, Meley). *Meley et al.* have shown that D283 cell line (p53 WT) was the most sensitive to treatment, showing only ~20% of viable cells with etoposide after 24 hours of treatment. However, another p53 WT cell line, Med1, showed ~60% of cell viability upon 24 hours of etoposide treatment. The difference in etoposide response in these two p53 WT cell lines was explained by the additional signalling pathways, which are likely to be required for inducing cell death (Meley *et al.*, 2010). Med1 cells were shown to carry a NF-kappa β/p65 mutation and hence to be more resistant to etoposide (Meley *et al.*, 2010). Med8 is a cell line with a carrying a truncated p53 protein and showed the highest resistance, ~70% of viable cells were observed after 48 hours of etoposide treatment. These results demonstrated that different MB cell lines display a varied sensitivity to etoposide, with D283 cells being the most sensitive to treatment.

3.2.1 D283 response to etoposide treatment

Etoposide is one of the drugs within the chemotherapeutic cocktail combination used for treating MB in the clinic. It is also the most cytotoxic drug out of the three drugs *Meley et al.* have tested. Since D283 was the most sensitive to etoposide, we used D283 cell line to further investigate the mechanisms for cell death induction.

The cells were treated with a varied concentration of etoposide [1 to 20μM] for a 48 hours time course and the resulting cell viability was measured by MTS assay (**Figure 3.1**). Following 6 hours of treatment, there was no significant difference in the levels of cell numbers in the 3 drug concentrations. After 24 hours treatment, 20μM etoposide exerted a strong cytotoxic effect with a reduction in viable cell number to ~30%, whilst at the lower concentration of 5μM and 1μM etoposide, ~50% and ~85% of cells remained viable. However, after 48 hours of treatment, the levels of viable cells observed with 5μM etoposide and 20μM treatment were similar (~20%), with no significant difference. Taken together, the chemosensitivity response of D283 cells to etoposide treatment is both dose- and time-dependent.

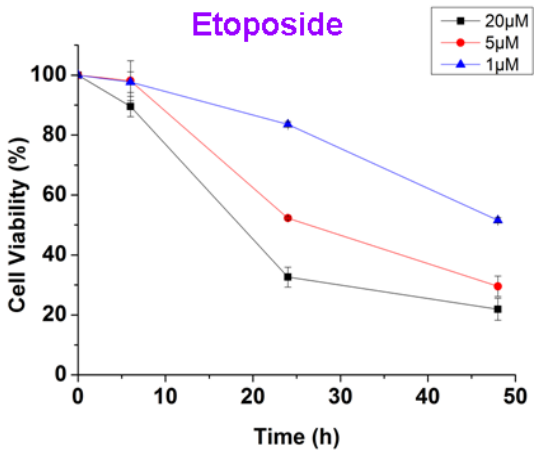

Figure 3.1 Sensitivity of D283 cells to etoposide treatment. *D283 cells were treated with [20µM], [5µM] or [1µM] Etoposide for a 48 hours time course. The percentage of cell viability was measured by MTS assay over the untreated control. Data shown are the mean of three independent experiments ± S.E.M.*

3.2.2 Effect of etoposide on the p53 signalling pathway in MB cells

The established etoposide mechanism of action is to inhibit the topoisomerase II, allowing double strand breaks to accumulate and, as a result, leading to the activation of the pro-apoptotic p53 protein. We first sought to measure p53 activation in the different cell lines upon etoposide treatment.

3.2.2.1 Etoposide-induced p53 protein levels

We measured the total p53 protein levels upon etoposide treatment by western blot. D283 and Med8 MB cell lines were treated with etoposide [20µM] for 4, 7 or 24 hours before assessment of total p53 protein levels normalised to a housekeeping protein and untreated control. For D283 cells, we saw a strong and transient increase of p53 protein by 4 and 7 hours, which further decreased towards basal levels by 24 hours (**Figure 3.2A**). In Med8 cells, the p53 induction was delayed with no increase detected until 24 hours and the molecular weight of the immunoreactive p53 band was lower than that observed for D283 cells (**Figure 3.2B**). It has to be noted that *Meley et al*. also previously observed that the p53 band in Med8 cells was running at a lower molecular weight than in other cell types, suggesting a truncated p53 isoform in Med8 cells.

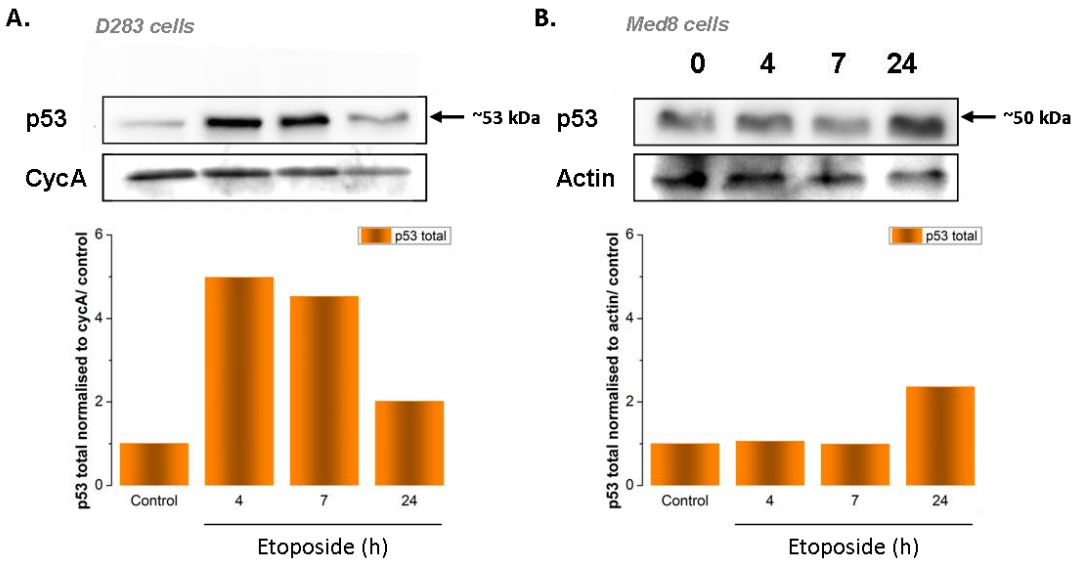

Figure 3.2 Etoposide-induced total p53 protein levels. ***(A)*** *D283 cells* ***(B)*** *Med8 cells were treated with etoposide [20μM] for indicated time points. Total p53 protein, cyclophilin A and actin are probed by western blot. Quantification are normalised to T0 and untreated control. The plots are representative of repeated experiments (N=2 for each cell line).*

3.2.2.2 Etoposide-induced p53 transcriptional activity

We then investigated if the increase of p53 levels were associated with an induction of its activity. The p53 protein is regulated by post-translational modifications such as phosphorylation, methylation and acetylation (Yang, 2003, Dai and Gu, 2010, MacLaine and Hupp, 2011), which direct the ability of p53 to activate downstream targets (Thompson *et al.*, 2004, Ashcroft *et al.*, 1999, Maclaine and Hupp, 2009). MDM2 is known to be one of the main targets of p53 and part of its feedback loop regulation, therefore MDM2 was used here as a readout of p53 activity. The relative MDM2 mRNA levels normalised to untreated control were measured by real time PCR (**Figure 3.3**).

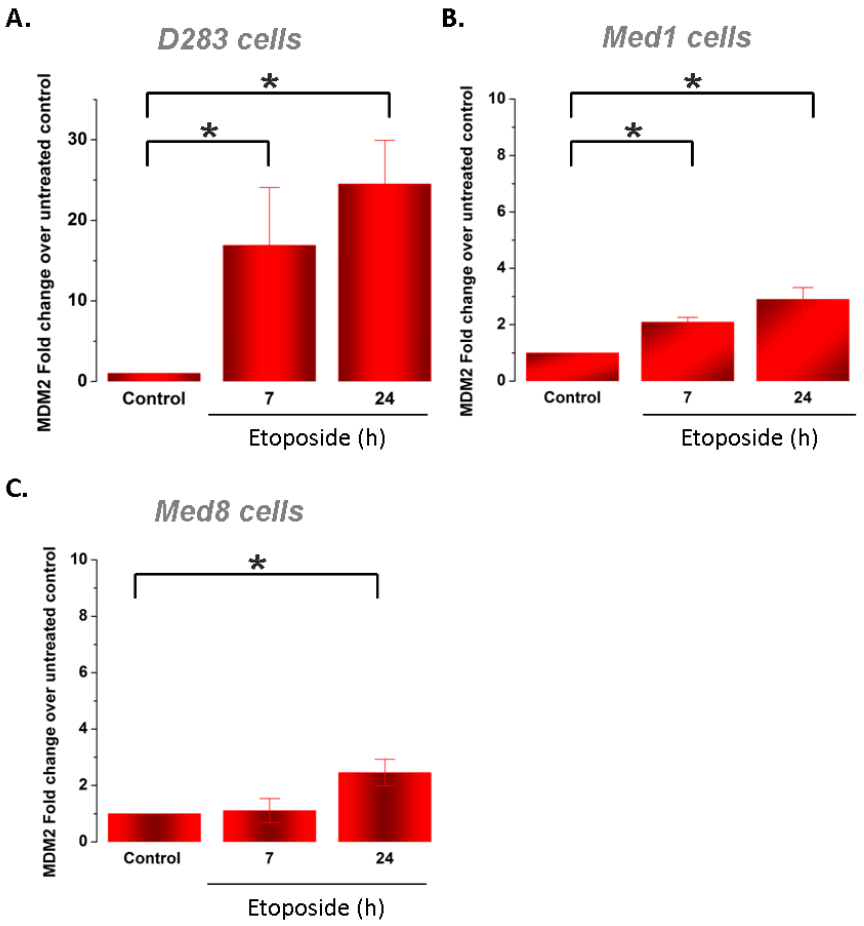

Figure 3.3 Levels of MDM2 upon etoposide-induced p53 activation. *MB cells were treated with etoposide [20μM] for 7 and 24 hours. The transcription of MDM2 was assessed by qPCR. Fold changes were normalised to cyclophilin A and over the untreated control.* ***(A)*** *D283 cells* ***(B)*** *Med1 cells* ***(C)*** *Med8 cells. Data shown are the mean ± S.E.M of three independent experiments for each cell line. Kruskal-Wallis ANOVA test was performed (*indicates p<0.05).*

In D283 cells, MDM2 mRNA levels increased ~17 fold by 7 hours, reaching up to 25 fold at 24 hours (**Figure 3.3A**). This increase was also present in Med1 cells but with a lower amplitude of ~2-3 fold induction (**Figure 3.3B**). In Med8 cells, no MDM2 induction was detected at 7 hours but a delayed and small yet significant increase of MDM2 was observed after 24 hours of etoposide treatment (**Figure 3.3C**). These results support the conclusion that both D283 and Med1 cells have a functional p53 pathway and that etoposide can indeed induce p53 transcriptional activity promptly in these cell lines. In Med8 cells, etoposide-induced p53 activation is not completely abolished but it appears to be delayed compared to D283 and Med1 cells, consistent with the western blot data in **Figure 3.2**. This delay of MDM2 mRNA level induction suggests that the truncated p53 isoform in Med8

could be functionally less active or that the cells might carry mutations elsewhere within the p53 pathway, thus resulting in a delayed p53 transactivation. Another alternative explanation is that the induction of MDM2 is contributed by other p53 protein family members such as p63 or p73. Further investigations and confirmation is required to elucidate the delayed p53 transactivation in Med8 cells.

3.2.2.3 Restoration of p53 pathway

We hypothesised that the Med8 cells might be re-sensitised to etoposide by expressing an exogenous full WT p53 protein. Med8 and D283 cells were transiently transfected with pMT-p53-dsRedXP and pmdm2-MDM2-YFP plasmids to express fluorescently tagged p53 and MDM2 proteins. The fluorescent fusions allow visualisation of increased levels of p53 due to the stabilising effect of etoposide treatment in D283 cells, previously observed by western blot (**Figure 3.2**). Using time-lapse confocal microscopy, the cells were imaged every 5 min, with etoposide [5µM] stimulation during the experiment. The fluorescence levels of both p53-dsRedXP and MDM2-YFP were measured over time, and quantified by cell tracker analysis (chapter 2.7.3). A strong p53 induction of 10-fold or more above background levels was observed in 30 of 33 D283 cells analysed and MDM2 was also induced with a slight delay compared to p53. Two examples of single cell traces are shown on **Figure 3.4A**. On average, increase in p53 and MDM2 above background was measured at 1.2 hours and 2.3 hours after etoposide treatment respectively (N=2; n=33; p53, SE=0.34; MDM2, SE=0.51). The delay of MDM2 induction is likely to be due to the time needed for p53 to activate the MDM2-YFP promoter. In 10% of the cells, no detectable MDM2 induction was measured even if p53 levels increased. A typical example is shown **Figure 3.4B**. In D283 cells, an increase in p53 and MDM2 was observed in ~90% of the transfected cells after etoposide stimulation (**Figure 3.6**). Many cells underwent apoptosis or showed apoptotic morphology within 24 hours, due to their sensitivity to etoposide.

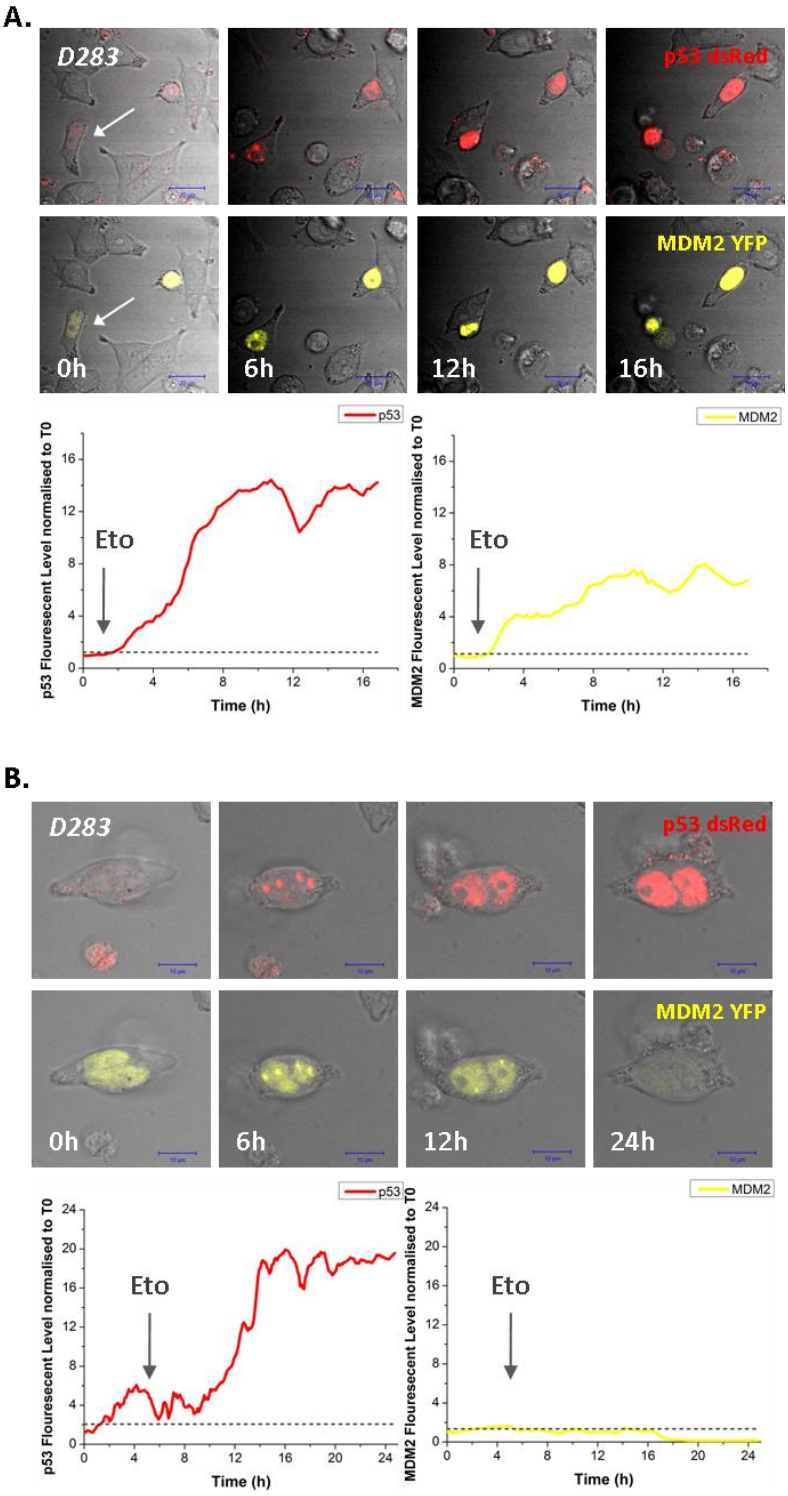

Figure 3.4 Etoposide-induced p53 activity at a single cell level in D283 cells. *D283 cells were co-transfected with p53-dsRedXP and MDM2-YFP and imaged by time lapse microscopy. Etoposide [5µM] stimulation is indicated.* ***(A)*** *A cell (indicated by arrow) showing p53 and MDM2 response* ***(B)*** *A cell showing p53 response but no MDM2 response. The level of p53 was assessed by the intensity of fluorescent protein expression measured by Cell Tracker normalised to untreated control, threshold was calculated as average intensity of untreated control + 2SD (N=2, n=33).*

We observed an induction of p53 in 78% of transfected Med8 cells (**Figure 3.6**), with only 35% MDM2 induction detected (**Figure 3.5A** and **Figure 3.6**) (N=2, n=22). The p53 increase in this cell line was lower compared to D283 cells, with 76% of cells showing increased p53 levels (**Figure 3.5B** and **Figure 3.6**). The timing of p53 and MDM2 induction in Med8 cells was also much slower, with an average of 2.6 hours after stimulation for p53 increase and 4.8 hours for MDM2 (N=2; p53, n=17; SE=0.57; MDM2, n=6, SE=1.61) to be compared with 1.6 hours (for MDM2) and 1.1 hours (for p53) in the D283 cells. These results further support the theory that the p53 protein in Med8 is functionally less active and that the lack of negative feedback mechanism observed suggests that Med8 bares a mutated p53 pathway. Furthermore exogenous expression of WT p53 in Med8 did not restore normal p53 activation, nor re-sensitise these cells to etoposide treatment as little apoptosis was observed up to 24 hours.

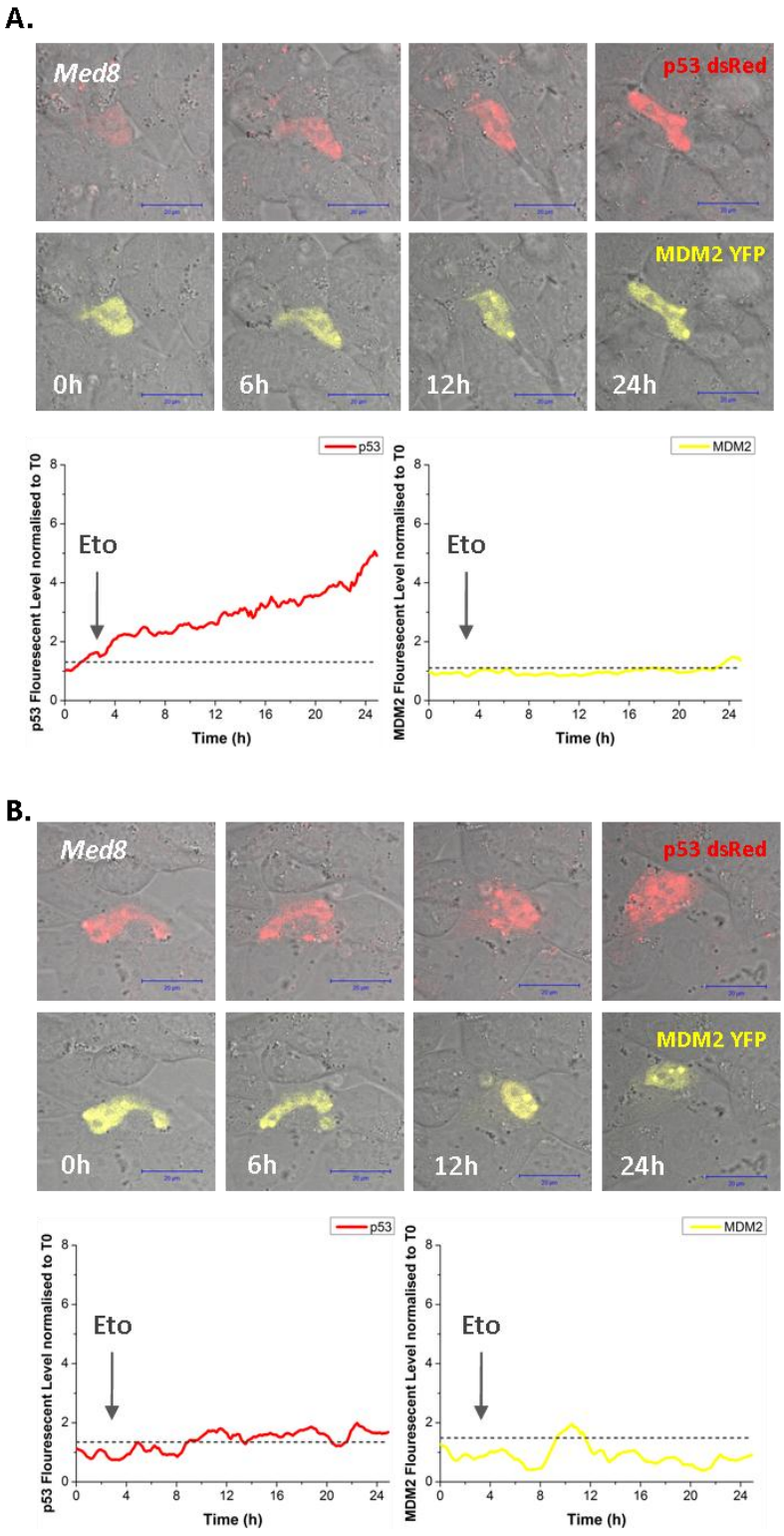

Figure 3.5 Etoposide-induced p53 activity at a single cell level in Med8 cells. *Med8 cells were co-transfected with p53-dsRedXP and MDM2-YFP and imaged by time lapse microscopy* ***(A)*** *A cell showing p53 response* ***(B)*** *A cell showing a weak p53 response just above threshold. The level of p53 was assessed by the intensity of fluorescent protein expression measured by Cell Tracker normalised to untreated control, threshold was calculated as average intensity of untreated control + 2SD (N=2, n=22).*

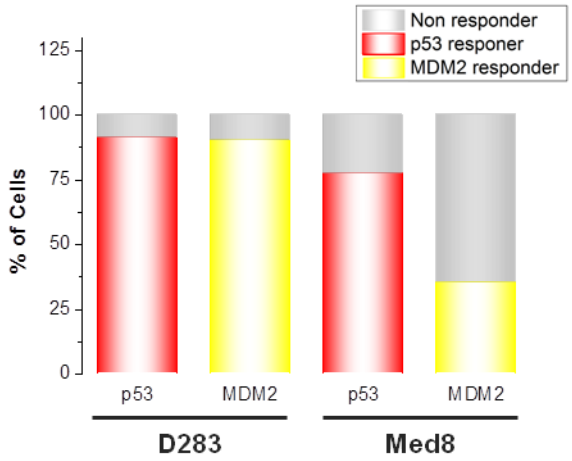

Figure 3.6 Live measurement of p53 and MDM2 activation. *A stack column showing the percentage of MB cells with or without p53 or MDM2 expression above threshold level upon etoposide treatment. Threshold was calculated as average intensity of untreated control + 2SD (see material and methods 2.7.3.1). D283 cells (N=2, n=33); Med8 cells (N=2, n=22)*

3.2.3 Bypassing p53 activation

In section 3.2.2.3, our results support that etoposide-induced cell death is correlated with the cell ability to induce p53 activation. To overcome chemoresistance due to impaired p53 activation, we hypothesised that downstream p53 target genes could constitute potential drug targets, which would then bypass the need for p53 activation.

As described in chapter one, p53 has a broad genetic program of target genes involved in DNA repair, cell cycle arrest and apoptosis (chapter 1.7). Therefore, we anticipated that targeting individual downstream candidates might not be enough to induce a significant cell death response. For this reason, we focused on a p53-dependent miRNA, a non coding RNA, which can itself regulate hundreds of downstream targets (Bartel, 2004, Cai *et al.*, 2009). Single miRNA can alter the expression of hundreds of proteins, and have been suggested as potential powerful targets for cancer treatment. One well described p53 miRNA targets is miR-34a (Raver-Shapira *et al.*, 2007).

3.2.3.1 Induction of miR-34a by etoposide

We investigated the expression of miR-34a upon etoposide treatment in MB cell lines. MB cells were treated with etoposide [20µM] for up to 24 hours and miR-34a levels were assessed by qPCR. miR-34a mRNA levels were increased by ~2.5 fold after 7 hours and ~12 fold by 24 hours of etoposide in D283 cells (**Figure 3.7A**). The kinetics of miR-34a transcription induced by etoposide was correlated with the up-regulation of p53 transcriptional activity measured by MDM2 as observed in **Figure 3.3**. In Med1 cells, miR-34a induction was also increased by ~2 fold up to 24 hours of etoposide treatment (**Figure 3.7B**). We did not observe any induction of miR-34a transcription upon etoposide treatment in Med8 cells (**Figure 3.7C**).

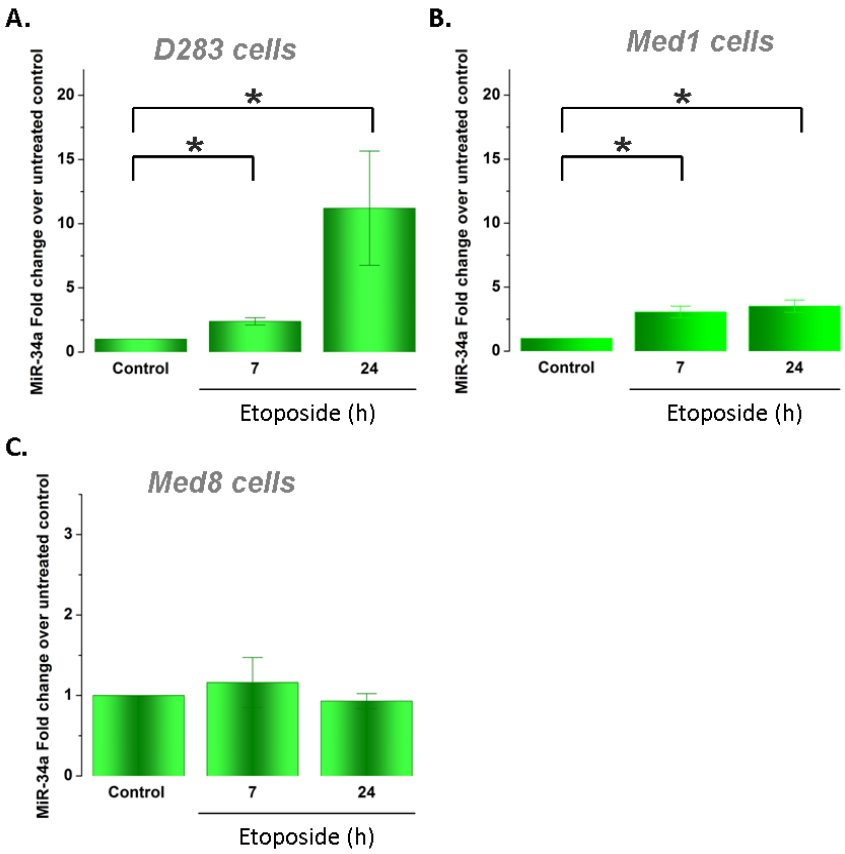

Figure 3.7 miR-34 induction upon etoposide treatment. *MB cells were treated with etoposide [20µM] for indicated time points. The transcription of miR-34a and MDM2 was assessed by qPCR.* ***(A)*** *D283 cells* ***(B)*** *Med1 cells* ***(C)*** *Med8 cells. Fold changes were normalised to cyclophilin A and the untreated control. Data shown are the mean ± S.E.M of three independent experiments. Kruskal-Wallis ANOVA test was performed (*indicates p<0.05).*

3.2.3.2 Etoposide-induced miR-34a is p53 dependent

We then sought to confirm the role of p53 in etoposide-induced miR-34a levels in D283 cells. Cells were transfected either with siRNA directed to silence p53 expression or with a non-specific scrambled siRNA control for 48 hours. The levels of miR-34a were assessed by qPCR post transfection and etoposide [20µM] treatment or no treatment for comparison (**Figure 3.8**).

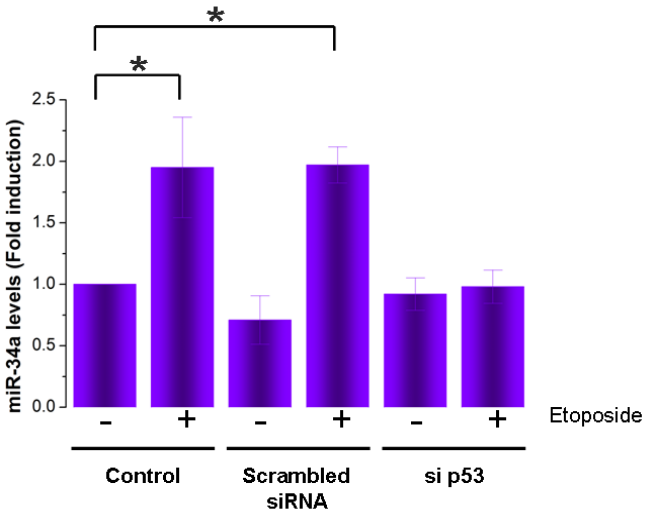

Figure 3.8 Etoposide-induced miR-34a transcription is p53 dependent. *D283 cells were transfected for 48 hours with siRNA directed to p53 or non-specific siRNA as a negative control before a 7 hour treatment with etoposide [20µM]. The transcription of miR-34a was assessed by qPCR, data were normalised to cycA and untreated control. Data shown are the mean ± S.E.M of three independent experiments. Kruskal-Wallis ANOVA test was performed (*indicates p<0.05).*

The transfection itself (scrambled siRNA or sip53) without etoposide treatment, did not alter the level of miR-34a transcript. In non-transfected D283 cells or cells transfected with a scrambled siRNA, a two fold increase in miR-34a level was observed upon etoposide treatment as previously shown in **Figure 3.7**. However, no induction of miR-34a was measured in the presence of sip53. These data show that etoposide-induced miR-34a transcription is inhibited by p53 knockdown, confirming that in D283 cells, etoposide-dependent induction of miR-34a is p53 dependent. These data confirm the essential role of p53 in miR-34a regulation and further explains the lack of miR-34a transcription in Med8 cells where p53 function is impaired.

3.2.3.3 Functional role of miR-34a

Independent studies have shown that miR-34a exhibits tumour suppression functions, targeting the expression of pro-survival and oncogenes genes such as SIRT1, E2F3, MYCN, Notch1, c-Met, Bcl2 (Li *et al.*, 2009, Yamakuchi *et al.*, 2008, Bommer *et al.*, 2007). In particular, SIRT1 is one of the most validated targets of miR-34a. It is a pro-survival protein and plays a protective role towards cellular oxidative stress and DNA damage by deacetylating transcription factors including p53 (Yamakuchi and Lowenstein, 2009, Deng *et al.*, 2007, Kwon and Ott, 2008). SIRT1 therefore downregulates p53 transcriptional activation, thus mediating cell survival during cellular stress through inhibition of apoptosis (Luo *et al.*, 2001, Vaziri *et al.*, 2001). In this respect, in cells with intact p53, etoposide induction of p53 may up-regulate miR-34a and repress SIRT1 as part of its signalling cascade, hence forming a positive feedback loop for p53 activity (**Figure 3.9**). Moreover, SIRT1 can deacetylate other proteins (e.g. Forkhead Box protein (FOXO), Retinoblastoma protein (Rb), BAX and E2F1), involved in cell cycle arrest and apoptosis, therefore SIRT1 inhibition have a potential to reduce cell growth independently of p53 (**Figure 3.9**) (Ford *et al.*, 2005, Wong and Weber, 2007).

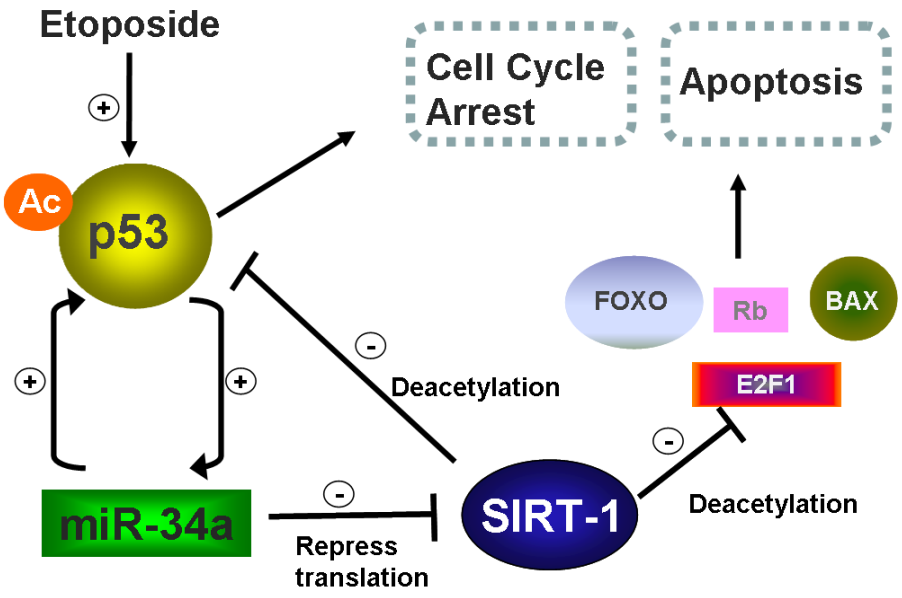

Figure 3.9 Schematic diagram of p53-miR-34a positive feedback loop. *p53 induces miR-34a which represses SIRT1 expression. Reduction of SIRT1 increases p53 acetylation and downstream activation. SIRT1 also deacetylates E2F1; Rb; BAX and FOXO, altering their cell cycle arrest and apoptotic functions.*

We first investigated the ability of etoposide-induced miR-34a to regulate SIRT1 expression. SIRT1 levels were measured by both western blot and qPCR. **Figure 3.10** shows that SIRT1 mRNA levels decreased concomitantly with miR-34a increase following etoposide treatment. After 24 hours of etoposide stimulation, miR-34a levels have increased ~5 fold whilst SIRT1 mRNA levels have decreased by ~4 fold (**Figure 3.10A**). SIRT1 protein levels clearly decreased after 7 hours of etoposide treatment (**Figure 3.10B**). By 24 hours, SIRT1 band intensity on western blot decreased by 80% compared to untreated control. This was also confirmed by immunocytofluorescence detection of SIRT1 (**Figure 3.10C**). These results suggest that etoposide-induced miR-34a is functional and is associated with down regulation of SIRT1 expression at both mRNA and protein levels.

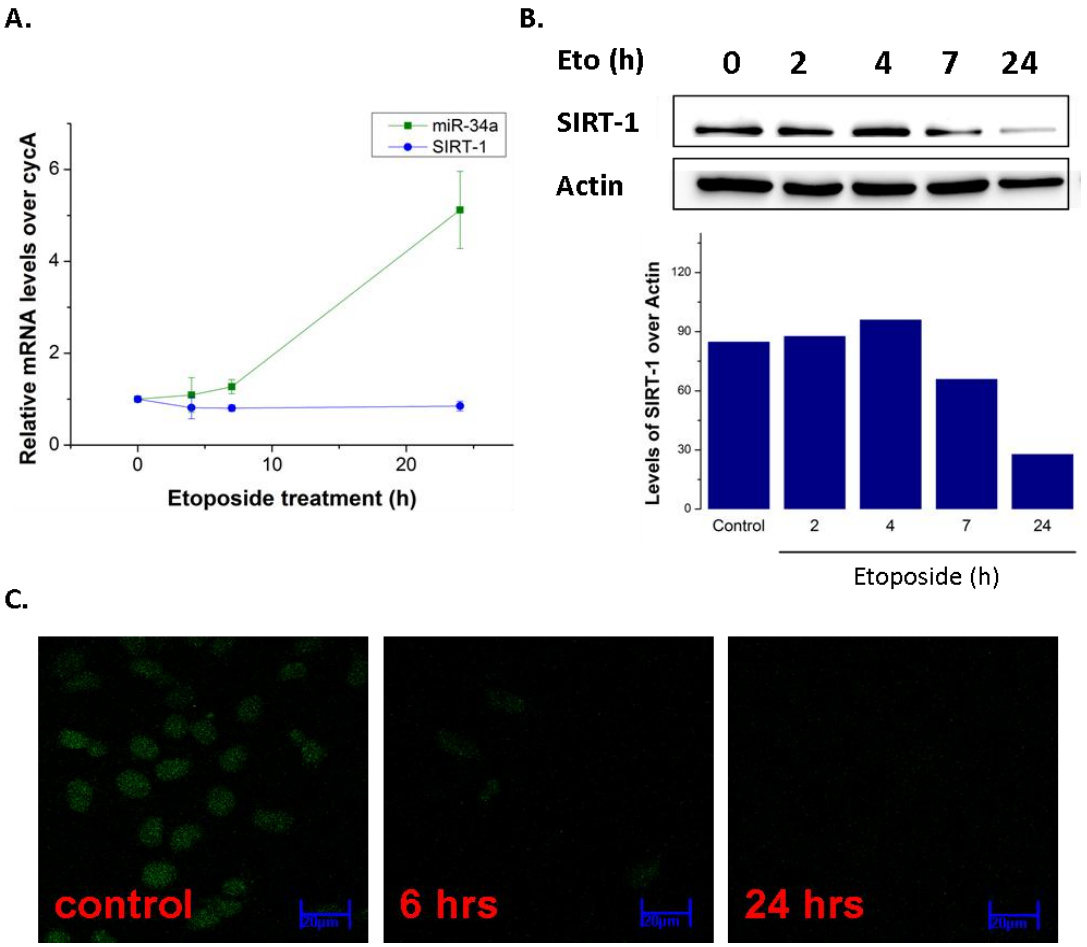

Figure 3.10 Decrease in SIRT1 levels upon etoposide treatment. *D283 cells were treated with etoposide [20μM] for indicated time points.* ***(A)*** *SIRT1 mRNA levels were measured by qPCR (N=2, error bars here are SD of the 2 experiments).* ***(B)*** *Western Blot with SIRT1 antibody normalised to the house keeping protein actin, this blot is a representative of four independent experiments.* ***(C)*** *Immunocytofluorescene with SIRT1 antibody after etoposide treatment at indicated time point, this image is a representative of three independent experiments.*

3.2.3.4 The effect of SIRT1 inhibitors on cell number

In order to better assess the importance of SIRT1 decrease for triggering MB apoptosis, we sought to inhibit SIRT1 directly. There are several inhibitors known to inhibit the family of SIRT1 proteins such as nicotinamide, EX527 and sirtinol (Ota *et al.*, 2006, Peck *et al.*). D283 and Med8 cells were treated with nicotinamide [25mM to 100mM] for a 48 hours time course and cell viability was measured by MTS (Audrito *et al.*, 2011, Bitterman *et al.*, 2002, Aoyagi and Archer, 2008). In D283 cells, nicotinamide was very potent at 50mM and 100mM, with respectively only ~25% and ~5% of viable cell at 48 hours (**Figure 3.11A**). These results were comparable to etoposide toxicity (10% of viable cells at 48 hours; **Figure 3.1**). More importantly and interestingly, nicotinamide was able to induce cell death in Med8, which was resistant to etoposide. We observed almost no viable cells by 48 hours with 50 or 100mM nicotinamide (**Figure 3.11B**) compared to the ~70% cell viability with 48 hours etoposide treatment observed by *Meley et al.* (Meley *et al.*, 2010). Nicotinamide [50mM] can effectively induce cell death in both p53 WT and p53 mutated cell lines (**Figure 3.11C**). This finding was also reported by *Audrito et al*., where 50mM of nicotinamide induce apoptosis in chronic lymphocytic leukemia cells *in vitro* (Audrito *et al.*, 2011). However, it has to be noted that the concentration of 50mM nicotinamide required to induce cell death is higher than what would be possible to obtain in a physiological setting. The dosage of nicotinamide used in neck and head cancer patients without severe side effect is 60mg/kg, measuring at ~0.8mM peak plasma concentration (Bussink *et al.*, 2002), which is 60 times lower than the *in vitro* dose needed to observe an effect.

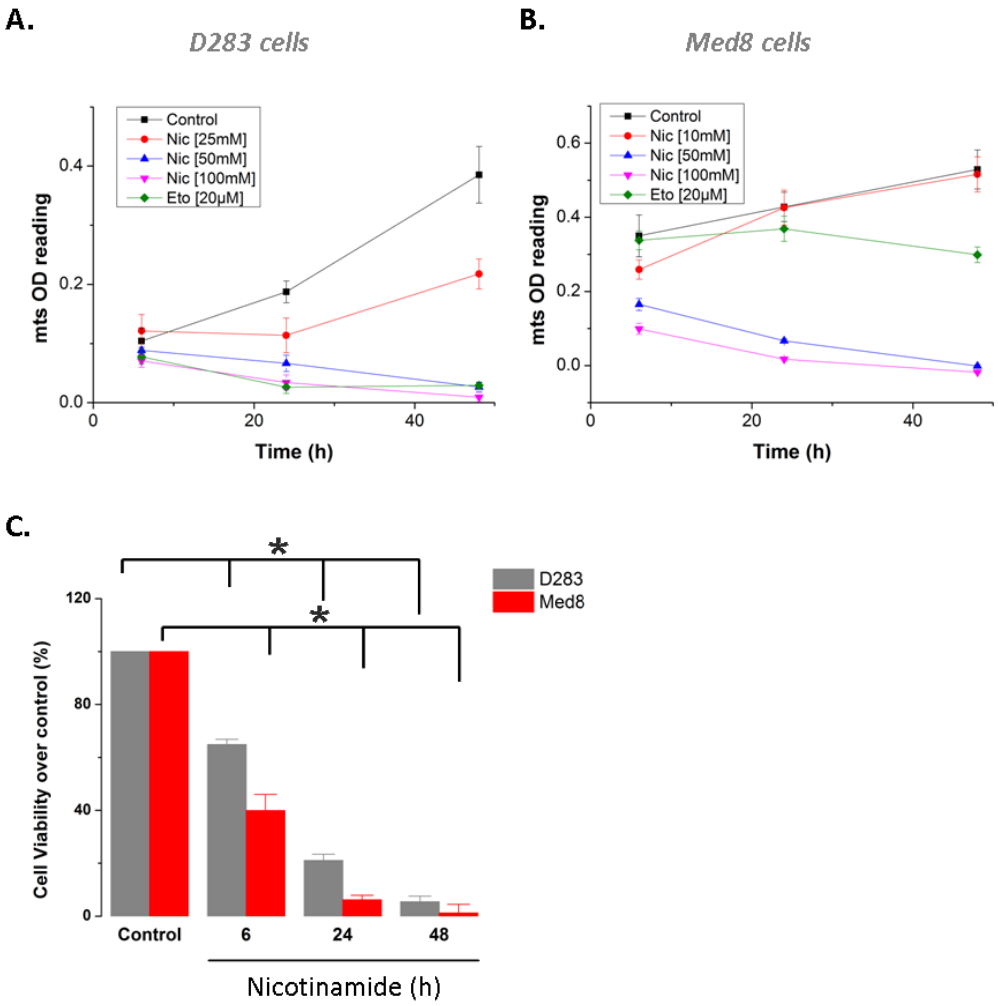

Figure 3.11 Cell viability assay of MB cell lines treated with nicotinamide. ***(A)*** *D283 cells* ***(B)*** *Med8 cells were treated with nicotinamide (Nic) for 6, 24 or 48 hours, concentration as indicated (n=1, error bars shown are SD of 6 replicates).* ***(C)*** *MB cell lines treated with nicotinamide [100mM] at indicated time points. The percentage of cell viability was measured by MTS assay over the untreated control. Data shown are the mean ± S.E.M of three independent experiments. One-way ANOVA followed by Bonferroni test was performed (* indicates p<0.05).*

We subsequently investigated the effects of other SIRT1 inhibitors, EX527 and sirtinol. A dose dependent response was observed for EX527 in both D283 and Med8 cells. In D283 cells, cell viability of ~70% and ~45% was observed with 48 hours of EX527 [50µM] or [100µM] treatment respectively (**Figure 3.12A**). Whilst for Med8 cells, viability remained ~100% and ~70% at these concentrations (**Figure 3.12B**). In D283 cells treated with sirtinol, cell viability remained relatively high at ~55% and ~58% with [50µM] or [100µM] sirtinol for

48 hours. These results demonstrated that the use of EX527 and sirtinol was not comparable to etoposide in terms of their cell death induction property.

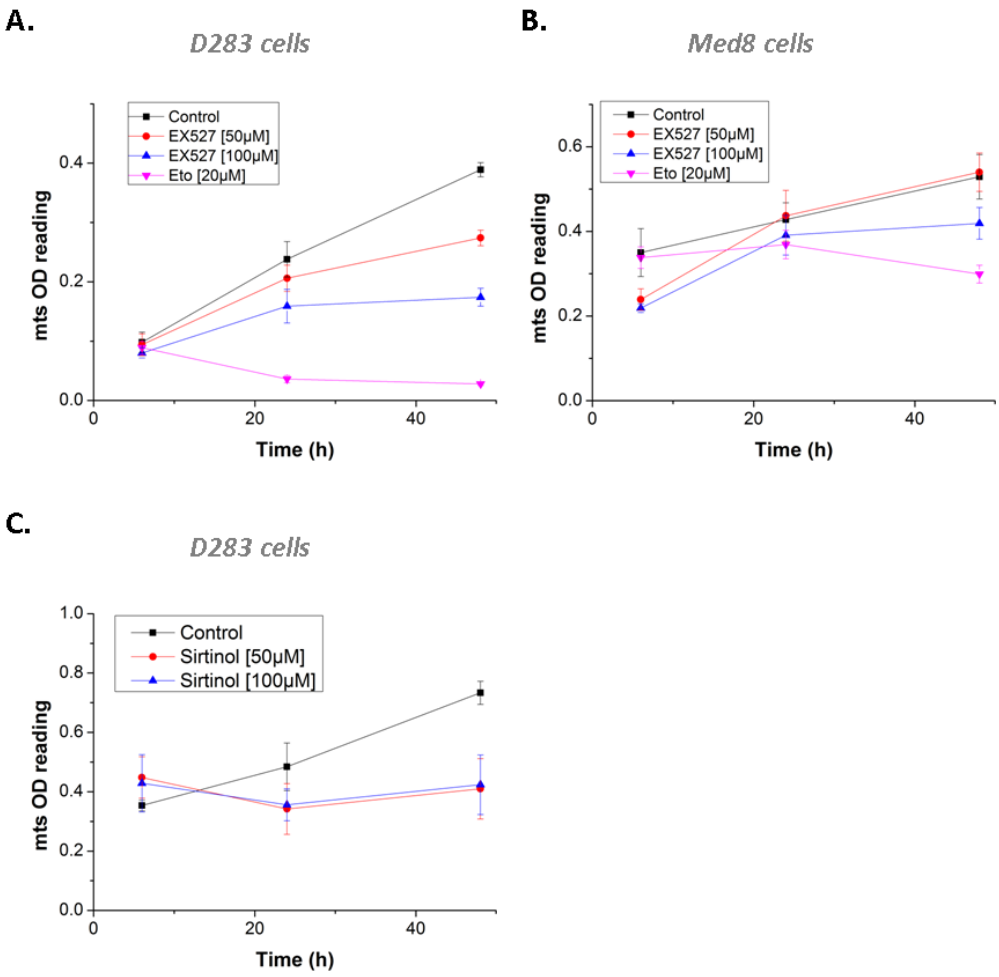

Figure 3.12 Cell Viability assay of MB cell lines treated with SIRT1 inhibitors. ***(A)*** *D283 cells.* ***(B)*** *Med8 cells were treated with EX527 for 6, 24 or 48 hours, at indicated concentrations.* ***(C)*** *D283 cell line treated with sirtinol [50μM] and [100μM] for 6, 24 or 48 hours (n=1, error bars shown are SD of 6 replicates).*

Taken together for all SIRT1 inhibitors tested, only with the use of nicotinamide at high concentrations induced a strong cytotoxic effect in both D283 and Med8 cells. The use of sirtinol and EX525 did not induce apoptosis and would not make a suitable MB drug. Therefore, instead of targeting this one single target, we next investigated the potential of using miR-34a itself as a cell death inducer.

3.2.3.5 The effect of miR-34a on cell number

A synthetic miR-34a mimic (Dharmacon, UK) was used to potentially induce cell death in MB cells. Control experiments were first performed to test the delivery and expression efficiency of miR-34a mimic. The delivery of miR-34a mimic oligonucleotides was tested by transfection alongside a fluorescently labelled (Dy547) mimic transfection control. Images show that all cells were stained positive with Dy547, suggesting a ~100% delivery (**Figure 3.13**). The level of transfected miR-34a was also measured by qPCR, ~250 fold increase of miR-34a was detected compared to non transfected or negative transfection control (**Figure 3.14**).

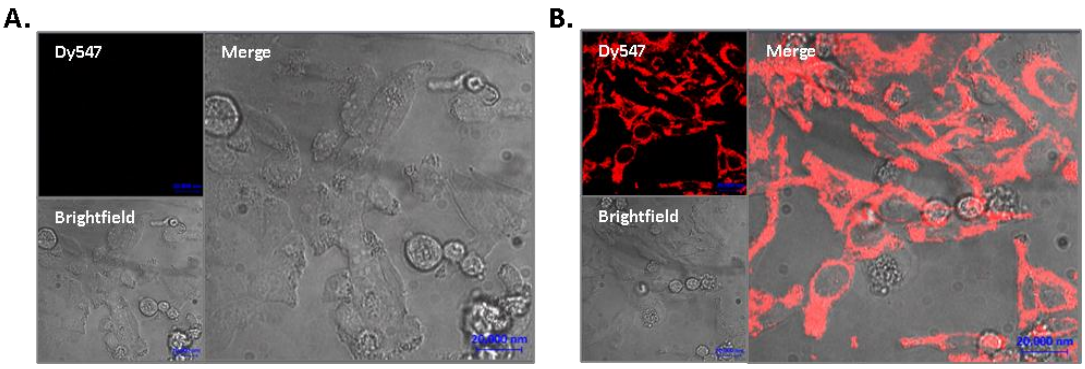

Figure 3.13 Validation of synthetic miR-34a transfection delivery. *D283 cells were* ***(A)*** *Not transfected* ***(B)*** *Transfected with miR-34a mimic [50nM] and negative control Dy527 [50nM] for 72 hours. Samples were fixed by immunocytofluorescence protocol and Imaged on LSM710, (n=2).*

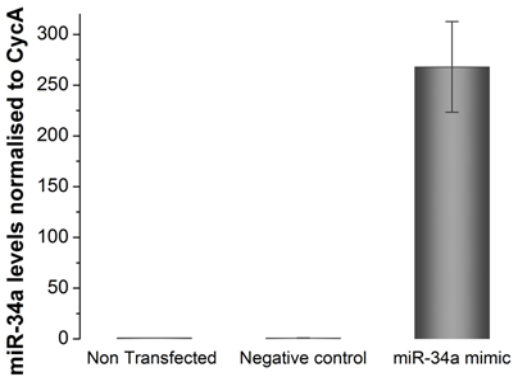

Figure 3.14 Validation of synthetic miR-34a transfection levels. *MB cells were transfected with miR-34a mimic [100nM] or non specific negative control [100nM] for 72 hours. The level of miR-34a was measured by qPCR normalised to cycA housekeeping gene, (n=1, errors shown here are SD of 3 replicates).*

The effect of miR-34a on cell viability was assessed 72 hours post transfection. The effects of miR-34a mimic transfection on cell viability were measured by MTS in both p53 WT (D283) and p53 mutated cells (Med8). We observed that 80% of D283 cells and 67% of Med8 cells were viable upon miR-34a transfection (**Figure 3.15**). The number of viable cells in D283 cells is higher than what was obtained with the SIRT1 inhibitors, EX527 [100µM] and sirtinol [100µM], where ~70 % of cells were viable after 24 hours treatment (**Figure 3.10**). The cytotoxicity effect of miR-34a mimic is minimal compared to etoposide treatment in D283 cell line (**Figure 3.1**).

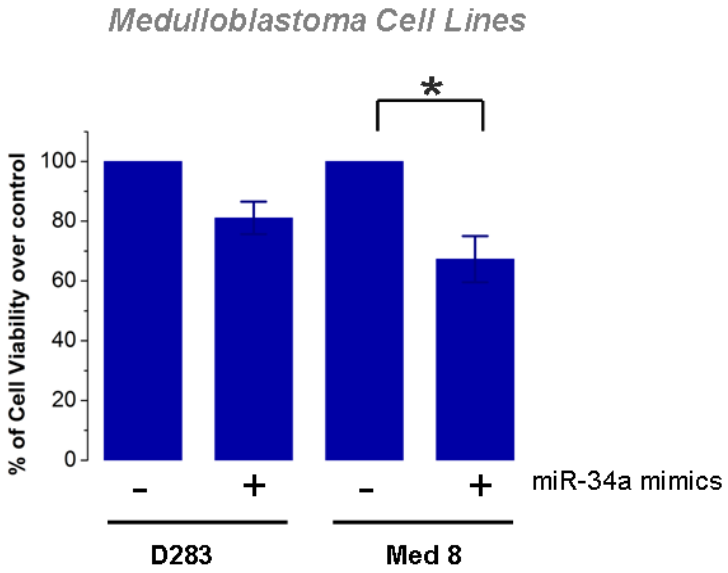

Figure 3.15 miR-34a mimic reduce cell numbers in p53 WT and p53 mutated MB cell line. *D283 (p53 WT) and Med8 (p53-mut) cells were transfected with miR-34a mimics [100nM] and expressed for 72 hours before MTS assay. Percentage (%) of cell viability were normalised over transfection control. Data shown are the mean ± S.E.M of four independent experiments. One-way ANOVA followed by Bonferroni test was performed (*indicates p<0.05).*

Interestingly, miR-34a mimics also reduce cell proliferation in the resistant Med8 cells. The effect of miR-34a mimics on viable cell number in this cell line is more pronounced than etoposide [20µM] or EX527 [100µM] which had no effect and a reduction of ~20% of viable cell number respectively after 24 hours of treatment ((Meley *et al.*, 2010), (**Figure 3.12**), compared to the a reduction of 33% in viable cell number when treated with miR-34a mimic (**Figure 3.16**). The ability of miR-34a mimics to reduce cell proliferation in Med8, a p53 mutated cell line, indicates that miR-34a introduction can indeed bypass p53 upstream activation and be used as a target for MB treatment.

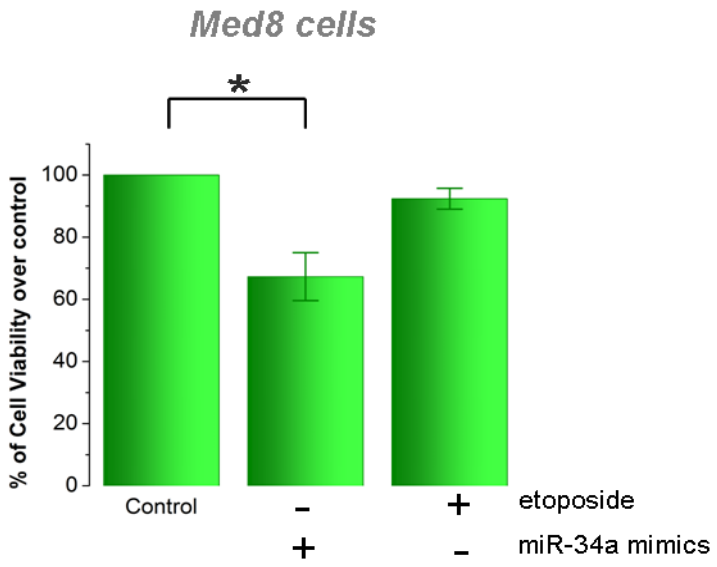

Figure 3.16 The effect of miR-34a mimic and etoposide in p53 mutated Med8 cells. *Med8 cells were transfected with miR-34a mimics [100nM] and expressed for 72 hours or treated with etoposide [20μM] for 24 hours before MTS assay. Percentage (%) of cell viability were normalised over transfection control. Data shown are the mean ± S.E.M of four independent experiments. One-way ANOVA followed by Bonferroni test was performed (*indicates p<0.05).*

3.2.4 Role of miR-34a in other brain tumours

We next investigated the potential of miR-34a in inducing cell death in other brain tumours, such as Glioblastoma (GBM). The use of a miR-34a mimic to induce cell death in p53 WT cell line (U87) and in a p53-mutated cell line (T98G) was tested. We observed a 10% reduction in U87 cell number and 18% in T98G cell number upon miR-34a transfection (**Figure 3.17**). These results demonstrated that the effect of miR-34a induction is not restricted to MB and it is also observed in GBM. However, the potential use of miR-34a to induce cell death in GBM is limited.

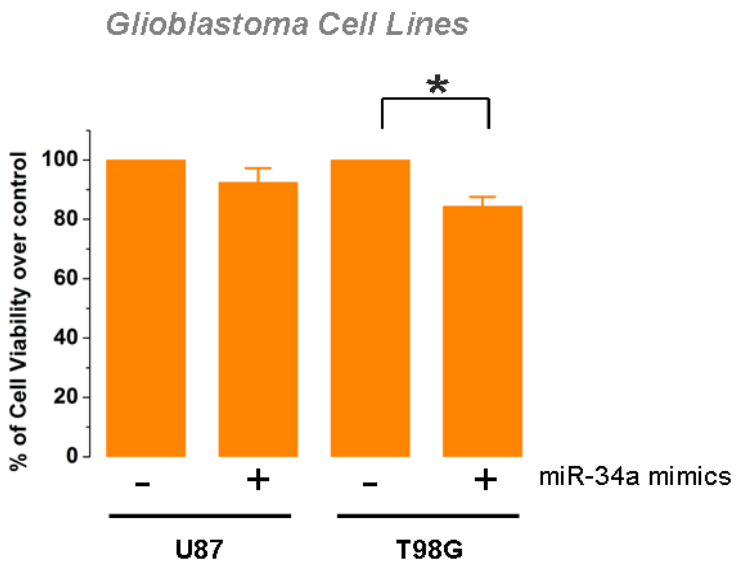

Figure 3.17 Effect of miR-34a mimics induce in p53 WT and p53 mutated GBM cell line. *U87 (p53 WT) and T98G (p53-mut) cells were transfected with miR-34a mimics [100nM] and expressed for 72 hours prior to MTS assay. Percentage (%) of cell viability was normalised over transfection control. Data shown are the mean ± S.E.M of three (T98G) and four (U87) independent experiments. One-way ANOVA followed by Bonferroni test was performed (*indicates p<0.05).*

3.3 Chapter 3 Discussion

3.3.1 p53 status and chemoresistance

It is well established that the loss of WT p53 is associated with many human cancers, including those in the brain (Levine *et al.*, 1991, Hollstein *et al.*, 1991, Frankel *et al.*, 1992). Generally, in most cancers, p53 itself is not a critical marker for chemoresistance, but nevertheless many studies have supported evidence that successive chemotherapeutic treatments require a functional p53 response (Lowe *et al.*, 1993, Lowe *et al.*, 1994, Wattel *et al.*, 1994, Gasco and Crook, 2003). This is true for many cancer models including breast cancer, gliomas and GBM (Gjerset *et al.*, 1995, Trepel *et al.*, 1998, Hermisson *et al.*, 2006, Jin *et al.*, 2010). In breast cancer, *TP53* mutation is associated with resistance to anthracyclines and mitoycin (Knappskog and Lonning, 2012). In glioma cells, mutant p53 are resistant to temozolomide (Roos *et al.*, 2007) and in GBM, knockout of WT p53 with siRNA prevented chloroquine-induced cell death (Kim, E. L. *et al.*, 2010).

In brain tumours such as gliomas and GBMs, WT p53 is not always associated with better chemotherapeutic response and treatment outcome can be dependent on the choice of drug used (Batista *et al.*, 2007, Roos *et al.*, 2007). *Roos et al.* have demonstrated that p53 mutated GBM cells confer resistance to methylating drugs such as temozolomide (Roos *et al.*, 2007), but the reverse effect was observed using carmustine (BCNU), where p53 mutated cells are more sensitive to treatment (Batista *et al.*, 2007). Similarly, the negative association of p53 WT expression and poor chemotherapy response has been observed in other models too, such as breast, colon and head & neck cancer (Fan *et al.*, 1995, Parsels *et al.*, 1997, Brachman *et al.*, 1993). Thus it is rather important to understand the relationship between p53 status in a particular tumour type and its response to treatment to enable the best chemotherapeutic choice.

Currently, the association of p53 mutation, chemosensitivity and treatment outcome in MB is understudied (Tabori *et al.*, 2010, Woodburn *et al.*, 2001, Meley *et al.*, 2010). A sequencing study performed by *Tabori et al.* has shown that *TP53* mutation was found in 8/49 (15%) of MB patients samples (Tabori *et al.*, 2010). Furthermore, patients with p53 mutated tumours had a shorter average recurrence time of 10 months compared to 14 months in non mutated tumour and the 5-year survival rate was 0% compared to 74% in p53 WT tumours (Tabori *et al.*, 2010). The author concluded that the overall poor survival of patients with *TP53*-mutated tumours is contributed by the resistance to treatment

(Tabori *et al.*, 2010). Here, we have also confirmed that MB cell lines do exhibit altered sensitivities to chemotherapeutic drugs and that drug resistance observed was correlated with the cells p53 status. This is in agreement with previous studies by *Meley et al.* (Meley *et al.*, 2010). Therefore, it is necessary to be able to activate apoptosis via an alternative route or bypass p53 upstream activation in resistant MB cell lines.

3.3.2 Inhibition of a pro survival gene, SIRT1

SIRT1 is a deacetylase that removes the acetyl group from p53, thus reducing its target activation. We have demonstrated in the presence of etoposide, activated p53 induce miR-34a expression, and subsequently down regulates SIRT1. This agrees with the current literature where p53, miR-34a and SIRT1 forms a positive feedback loop (Yamakuchi *et al.*, 2008, Yamakuchi and Lowenstein, 2009). The effect of this signalling is evident in several other cancers such as colon cancer, as it is shown that an increase of miR-34a leads to a reduction of SIRT1, resulting in an increased level of acetylated p53. Consequently, an increase of p53 proapoptotic target genes such as PUMA was detected (Yamakuchi and Lowenstein, 2009).

We have used nicotinamide, EX527 and sirtinol SIRT1 inhibitors to confirm the role of SIRT1 inhibition in cell death induction in our model. The use of EX527 has asserted minimal effect on cell viability at relatively high concentrations and that sirtinol failed to induce cell death in D283 p53 WT cell line. This finding is similar to that of *Solomon et al.* where they found that EX527 has no effect on cell viability even though they measured a decreased SIRT1 deacetylate activity in epithelial cells (Solomon *et al.*, 2006). These compounds have been demonstrated to be active at these concentrations because they increased p53 acetylation, but it seems that p53 acetylation at lysine 382 might not be sufficient to activate a pro-apoptotic p53 response.

The effect of nicotinamide at high concentration [50mM] in inducing cell death is in line with other findings, where SIRT1 inhibition can trigger apoptosis (Peck *et al.*, 2010, Audrito *et al.*, 2011). Interestingly, apoptosis was observed in both p53 WT and p53 mutated cells, suggesting that the p53 activated-apoptosis can be bypassed. It is speculated that nicotinamide-induced cell death is caused by mechanisms independent of p53. For example, treatment of [50mM] nicotinamide for 24 hours has been demonstrated to inhibit poly (ADP-ribose) polymerase which can lead to cell cycle arrest and apoptosis (Saldeen *et*

al., 2003). However, with the high concentrations needed in vitro to induce sufficient cell death, this limits the potential of using this SIRT1 inhibitor in clinic.

3.3.3 Introduction of miR-34a

MiR-34a expression has been reported to be associated with drug sensitivity in several models including MB (Fujita *et al.*, 2008, Zenz *et al.*, 2009, Weeraratne *et al.*, 2011). *Weeraratne et al.* have observed that primary MB baring functional p53 expressed significant higher levels of miR-34a and that it was positively correlated with sensitivity of these cell lines to chemotherapeutic drugs. Several studies have highlighted the importance of loss of miR-34a in tumourgenesis and the potential use of miR-34a in altering tumour cells fate, but via different mechanisms. For example, *Li et al.* and *Guessous et al.* have found that pre-miR-34a levels are lower in GBM compared to normal tissues or in mutated p53 than p53 WT tumours. They further demonstrated that miR-34a levels negatively correlated to c-Met (Met proto-oncogene) expression, and that transfection with miR-34a in both GBM or MB cell lines downregulated c-Met expression and inhibited cell proliferation and survival (Li *et al.*, 2009, Guessous *et al.*, 2010); *Welch et al.* have demonstrated that miR-34a directly targets E2F3, reducing its protein level and preventing cell cycle progression (Welch *et al.*, 2007). In a gastric cancer model, *Ji et al*. have shown that restoration of miR-34a with mimic molecules impaired cell growth, increased caspase-3 activation and sensitised cells to treatment (Ji *et al.*, 2008). These results demonstrate how the use of one miRNA can alter cell fate. In our hands, we have also observed that direct introduction of a miR-34a mimic was able to reduce viable cell numbers in both MB and GBM. Although these results confirm that we can directly alter MB cell viability, the effect of miR-34a-induced cell death is limited and may not translate well into pre-clinical or clinical models.

Chapter 4: Hypoxia-induced Chemoresistance

4.1 Introduction

Brain tumours such as MB are typically present as solid tumours. Tumour cells can experience varied levels of oxygen and nutrient supply dependent on the cells' proximity to the nearest blood vessels. Cells located at the centre of the mass, away from the vessels, are often deprived of appropriate oxygen supply causing hypoxic regions within the tumour mass (chapter 1.2.2).

Hypoxia is commonly associated with resistance to chemotherapy and radiotherapy either through a direct effect on a drug's efficiency or through alterations of intracellular signals (Sullivan *et al.*, 2008, Brown, 1999). Firstly, the efficiency of drug delivery relies on the presence of a well vascularised structure. Secondly, a hypoxic environment might affect the drug's mechanism of action if oxygen is required for the drug function, thus hindering drug's cytotoxicity (chapter 1.5.2.5) (Hicks *et al.*, 2004, Koch, 1993, Teicher, 1994). Lastly, hypoxia can activate signalling pathways, which can consequently lead to activation of genes involved in drug resistance (Cosse *et al.*, 2007, Flamant *et al.*, 2010, Sermeus *et al.*, 2008).

However, there are discrepancies on the length and severity of hypoxia required to induce drug resistance and this appears to be dependent on cell type. We hence sought to investigate the effects of altered duration of hypoxia and how it affects MB drug sensitivity.

Moreover, the crosstalk between hypoxia, HIF and p53, and their involvement in apoptosis in hypoxia is unclear. Since we have previously demonstrated the importance of a fully functional p53 pathway for etoposide-induced cell death (chapter 3), here we aim to investigate if hypoxia affects the DNA damage induced by etoposide and if the subsequent p53 activation is altered. We have selected the D283 cell line to test our hypothesis as this cell line is sensitive to etoposide and we have demonstrated in this cell line, etoposide-induced p53 activation.

Objectives:

1. To investigate etoposide-induced death of D283 cells in hypoxia
2. To measure DNA damage induced by etoposide in normoxic and hypoxic conditions
3. To measure etoposide-induced p53 activation in hypoxia in comparison to normoxic conditions.

4.2 Results

4.2.1 Effects of Hypoxia on Cell Fate

Oxygen plays an important role in many cellular processes such as cell fate, cell migration and cellular energy expenditure. Under hypoxic conditions, a cell may switch the focus of its energy expenditure to maintain homeostasis, altering the rate of cell cycle progression. As chemotherapeutic drugs commonly target rapidly dividing cells, treatment may become ineffective during a slowed cell cycle. Therefore, it was necessary to initially determine cell viability and proliferation rate in hypoxic conditions. To investigate the effects of hypoxia on cell growth and cell cycle, D283 cells were cultured and monitored under hypoxic conditions for a prolonged period of 5 days. Given that physio-pathological O_2 concentrations in brain tumours are around 1% or below (chapter 1.3). We have used 1% O_2 for our 'hypoxic condition', with 'normoxic' referring to the atmospheric 21% O_2 for studies in this chapter.

4.2.1.1 Growth Analysis of D283 cells in hypoxia

D283 cells cultured under normoxia or hypoxia were visualised by light microscopy to provide an indication of cell morphology and a rough assessment of cell growth and viability (**Figure 4.1**). We saw no observable differences of cell density in hypoxia compared to normoxia up to 72 hours. However, at 96 and 120 hours incubation, cell density of the hypoxic cells appeared to be more sparse than those in normoxia, suggesting a potential slower cell proliferation rate or an increase in cell death due to hypoxia.

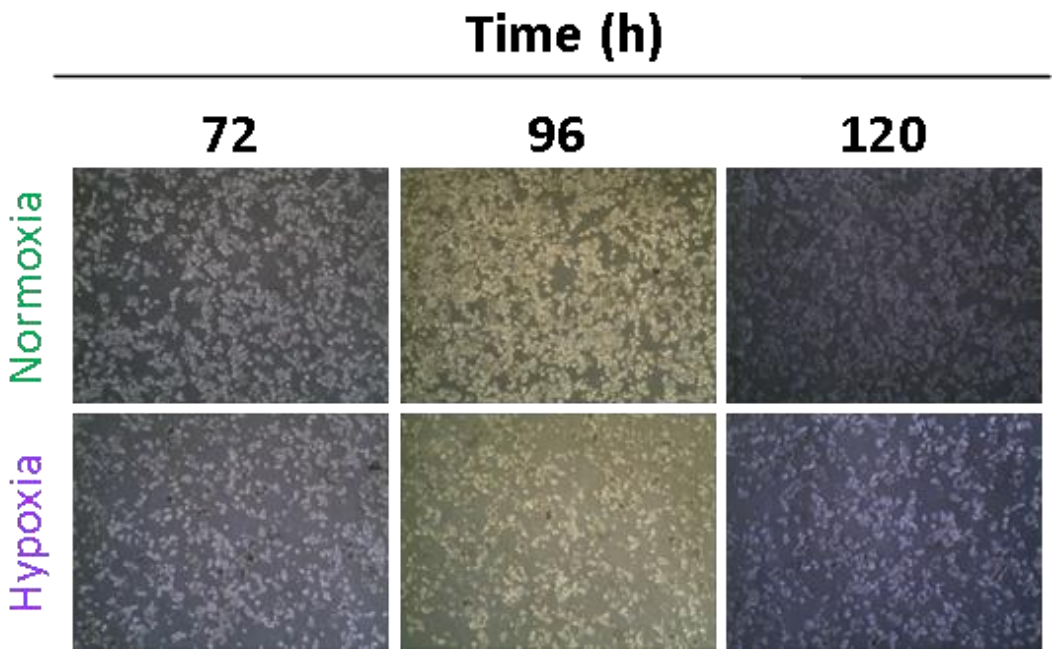

Figure 4.1 Brightfield pictures of D283 cells in normoxia and hypoxia. *0.25x10^6 cells/ml of D283 cells were plated in 3 ml medium and incubated in normoxia or hypoxia (1% O_2) for indicated periods. Bright field images were captured on a Zeiss Axiovert 25 light microscope attached to a GXCAM-3 with a 20x objective.*

To accurately determine the rate of cell growth in normoxia and hypoxia, we performed a cell count using a Beckman Coulter cell counter. In agreement with the microscopy images, the population of cells counted was higher in normoxia than cells in hypoxia (**Figure 4.2A**), with 2.6x10^6 cells/ml at 96 hours in normoxia and only 1.6x10^{6}cells/ml in hypoxia. We further determined cell viability in these two conditions using the ViaCount cell viability assay (chapter 2.9.2). After 5 days of incubation in normoxia, 75% of cells were viable; this value was reduced to ~40% for cells incubated in hypoxia. This result demonstrates that chronic hypoxia incubation induces some cell death in D283 cells (**Figure 4.2B**).

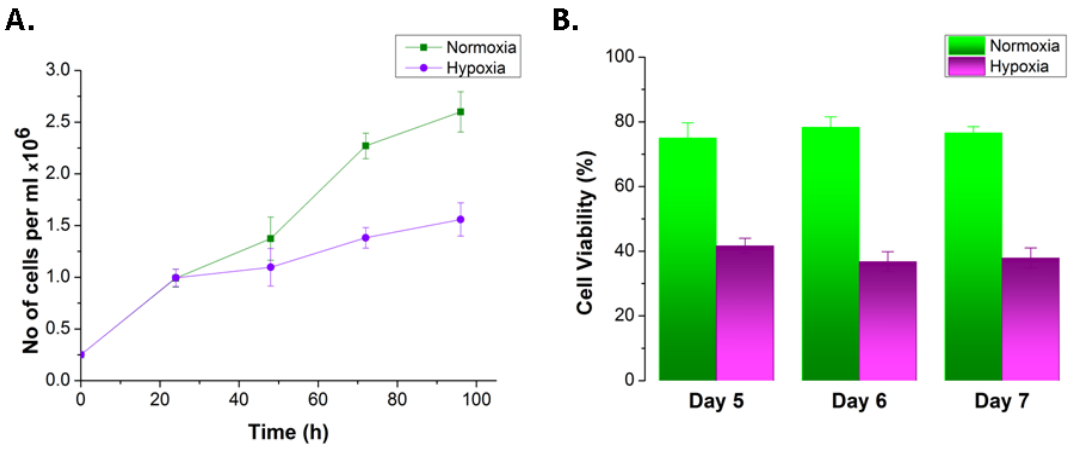

Figure 4.2 Cell counts of D283 cells in hypoxia. *Cells cultured under normoxic or hypoxic (1% O_2) condition were counted at indicated time points.* ***(A)*** *The graph shows the number of cells in normoxia and hypoxia over a 96 hours time course.* ***(B)*** *Viable cell count of D283 cells measured by ViaCount assay. Data shown are the mean ± S.E.M of three independent experiments.*

4.2.1.2 Cell Cycle profile of D283 cells in hypoxia

Cell cycle distribution profiles for D283 cells were obtained from measuring the intensity of Propidium Iodide (P.I) incorporation using flow cytometry. The plot shown in **Figure 4.3** is a typical plot, showing the size (forward scatter) and granularity, which are granular materials inside the cells (side scatter) of the analysed cell. The use of PI is ideal for cell cycle profiling as PI can intercalate into double stranded DNA and hence the quantity of PI staining is directly proportional to the amount of DNA material present within the cells. Cells in G0/G1 phase contain one copy of DNA and will therefore have 1xintensity of PI staining. Cells in G2/M phase will have two copies of DNA and therefore will have 2x intensity of PI staining, twice that of the cells in G0/G1 (**Figure 4.3B**). The amount of DNA material for cells undergoing DNA synthesis (cells in S phase) is between the one of G1 and G2, depending on the stage of DNA replication process. The markers for each of the cell cycle phase were manually placed on the cell cycle profile graph and this gating remained the same for each sample (**Figure 4.3**).

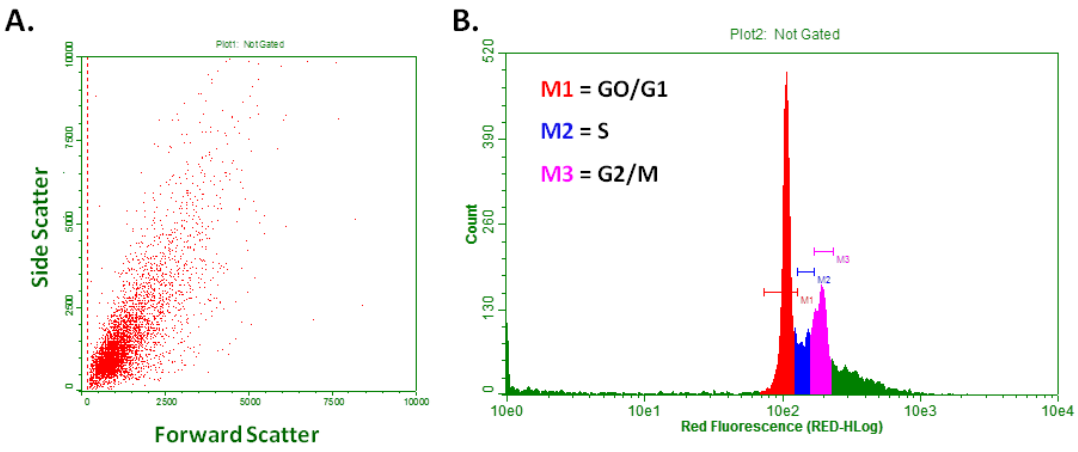

Figure 4.3 GUAVA Express Pro analysis. ***(A)*** *A Scatter graph showing the size and granularity of cells.* ***(B)*** *A cell cycle profile graph demonstrating the different phases of cell cycle stage, the first peak (red) in the graph represents cells in G0/G1 phase and the second peak (purple) represents cells in G2/M phase. The blue portion in between the two peaks represents cells in S phase. The green portion is likely to be cells that are clumped together or cells which have polyploidy, therefore this section of the graph was disregarded in the analysis.*

The cell cycle profile of D283 cells cultured in normoxia or hypoxia were obtained every 24 hours up to 96 hours (**Figure 4.4A**). We found that the cell cycle distribution of both hypoxic and normoxic cells remained similar throughout the time course. At any given time points (24-96 hours), we measured ~45% of cells in G0/G1 phase, ~10% of cells in S phase and ~20% in G2/M phase in both conditions (**Figure 4.4A**). Altogether our results suggest that chronic hypoxia does not arrest the cell cycle and that the decreased proliferation is more likely attributable to the increased cell death. This also suggests that the cells, which survive in hypoxia continue cycling and it is this remaining population of cell, which is likely to be the most resistant to cell death and the hardest to kill in the context of a tumour. Therefore we have focused on how this remaining population of surviving cells in chronic hypoxia responded to the chemotherapeutic agent etoposide.

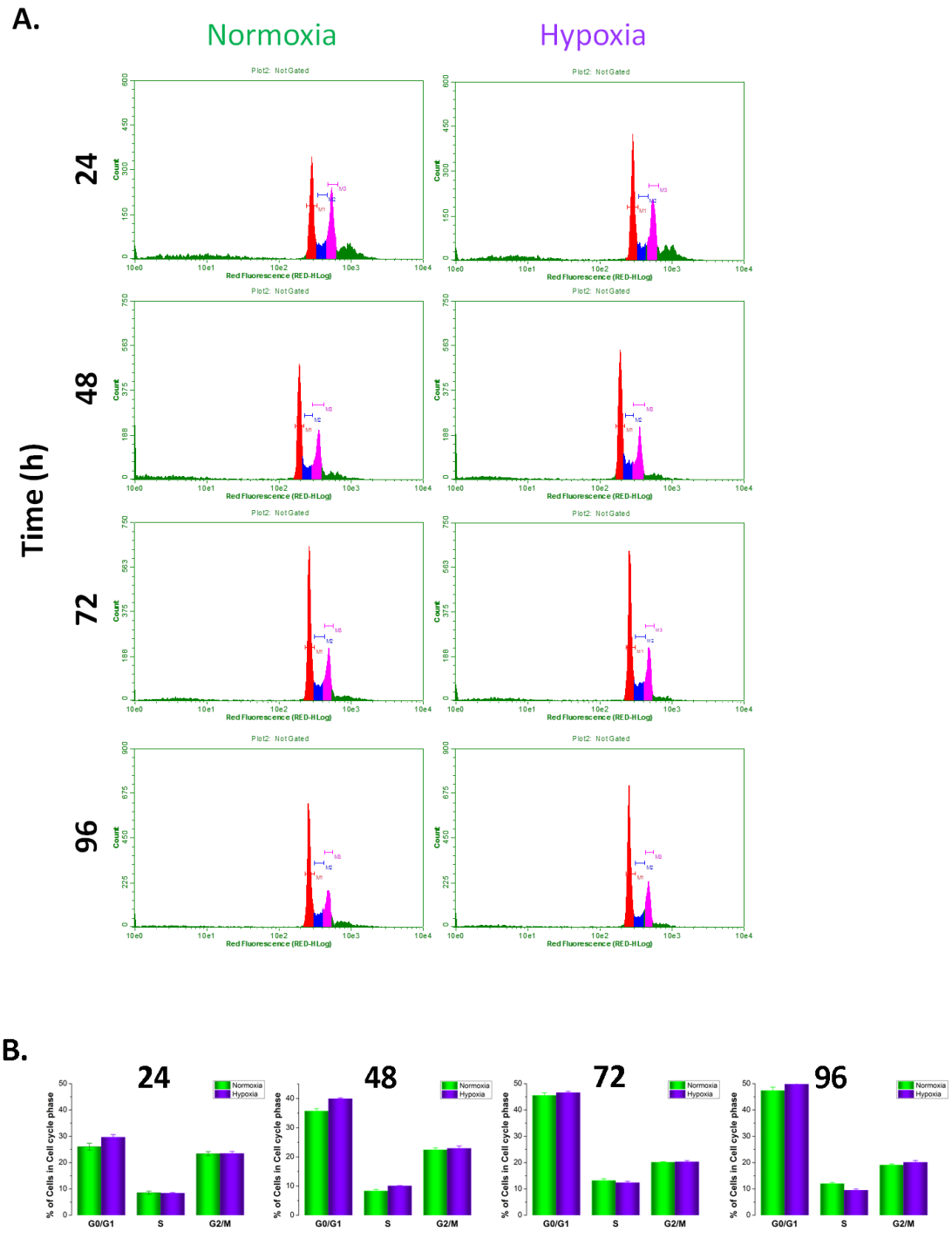

Figure 4.4 Cell cycle profile of D283 cells in hypoxia. ***(A)*** *Cell cycle profiles obtained from flow cytometry. D283 cells were cultured in normoxia or hypoxia (1% O_2) for indicated times.* ***(B)*** *Cell cycle profile quantification showing percentage of cells in each cell cycle phase. This is a representative of three independent experiments, error bars shown are experimental errors of 2 replicates.*

4.2.2 Effect of hypoxia on response to chemotherapy

The exact mechanism of hypoxia-induced chemoresistance remains unclear, it seems to be cell type dependent (Cosse *et al.*, 2007) and varies depending on the length and degree of hypoxic exposure (Hussein *et al.*, 2006, Cosse *et al.*, 2007, Sullivan *et al.*, 2008). It has been reported that hypoxia is able to prevent etoposide-induced cell death in several tumours such as neuroblastoma, breast cancer and prostatic cancer (Hussein *et al.*, 2006, Sullivan and Graham, 2009). *Cosse et al*. and *Sermeus et al*. have observed drug resistance in various cell lines after 16 hours of 1% hypoxic incubation. However, *Hussein et al.* found that exposure to hypoxia of up to 16 hours had little effect on drug induced apoptosis in neuroblastoma cell lines, whereas long exposure up to 1 week decreased drug-induced apoptosis. Whilst *Sullivan et al*. have demonstrated that breast cancer cell lines incubated at 0.2% hypoxia for 24 hours were sufficient enough to cause etoposide resistance (Sullivan *et al.*, 2008). Given the variation in these findings, the effects of hypoxia induced chemoresistance needed to be clarified in our cellular model.

In this chapter, where cells have been incubated in hypoxia, any subsequent treatment was also performed in hypoxic conditions, in order to avoid any effect of re-oxygenation during the drug treatment.

4.2.2.1 Sensitivity of Etoposide treatment in hypoxia

We investigated the effect of hypoxia on etoposide-induced cell death in D283 cells. The effect of short term hypoxia (24 hours pre-exposure) and chronic hypoxia (5 days pre-exposure) on etoposide-induced cell death was tested using MTS assay. We observed ~90% of cell death after 48 hours of etoposide treatment in cells cultured in normoxia or short term hypoxia. Strikingly, the same etoposide treatment in chronic hypoxic cells resulted in only 43% of cell death (**Figure 4.5**).

It has to be noted that the MTS assay does not directly measure cell survival but rather the cellular mitochondrial activity. The MTS reagent is a tetrazolium compound which can be chemically reduced by cells into formazan. The reduction of MTS is carried out by a dehydrogenase enzyme, which is only found in metabolically active cells. Usually, the production of formazan (measured by its absorbance at 492nm) indicates the proportional number of viable cells. However, under low oxygen levels, it is possible that the mitochondrial activity is altered, without affecting cell survival and therefore the MTS reaction might be wrongly interpreted.

To ensure that the MTS experiment is a reliable viability assay in hypoxia, we repeated this experiment with a different viability assay (ViaCount) based on using two differential permeable DNA binding dyes, one staining nucleated cells and one staining only dying cells. The results obtained from the ViaCount assay showed a similar trend compared to the one obtained from the MTS assay (**Figure 4.5A**). However, the actual percentage of viable cells obtained from ViaCount was higher than the values obtained from MTS assay in both normoxic and hypoxic conditions. This can be explained by the fact that one method is based on measuring metabolic activity (MTS) and one is dependent on the integrity of plasma membrane (ViaCount), thus can resulted in a varied kinetic of measurements. Considered together, these results clearly show that D283 cells incubated in chronic hypoxic conditions are more resistant to etoposide treatment compared to cells cultured in normoxia or in short term hypoxia, where no significant changes were observed.

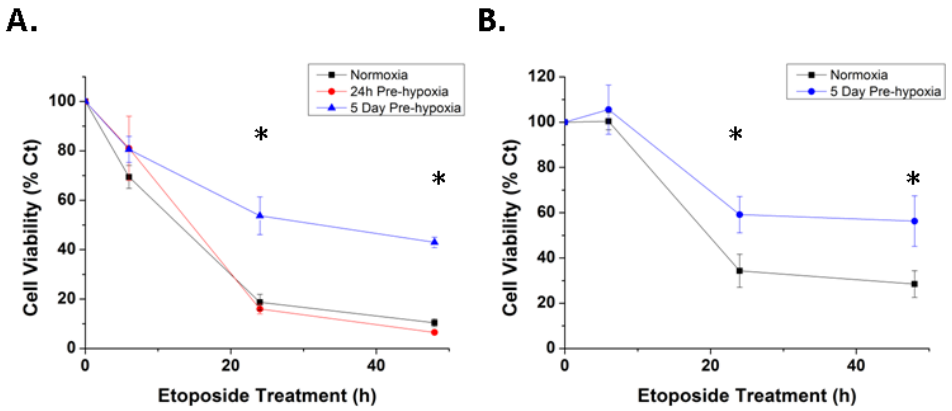

Figure 4.5 Chronic hypoxia increases etoposide resistance in D283 Cells. *D283 cells were pre-incubated in 1% O_2 for 5 days (blue line), 24 hours (red line) or left in normoxia 21% O_2 (black line). Cells were treated with etoposide [20 µM] for the indicated time. Cell survival was assessed using **(A)** MTS assay **(B)** ViaCount assay. Results are expressed as % of cell survival relative to the untreated control. Data shown are the mean ± S.E.M of three independent experiments (N>3). One-Way ANOVA followed by a Bonferroni test was performed (* indicates $p < 0.05$).*

4.2.2.2 Etoposide-induced G2/M accumulation

Etoposide primarily acts on proliferating cells during S phase, by inducing double strand breaks (DSBs), hence inducing p53-mediated cell cycle arrest and, accumulation in G2/M phase. We investigated whether chronic hypoxia would affect etoposide-induced cell cycle arrest using flow cytometry. Given that the regular etoposide dosage of [20µM] induces a high level of cell death, the cells were treated with a lower dose of etoposide [1µM] to allow the monitoring of the cell cycle distribution after 30 hours of treatment.

When normoxic cells were treated with etoposide [1µM] for 30 hours, we observed an increase of cells from 30% to 60% in the G2/M phase. (**Figure 4.6A**). In contrast, the proportion of cells accumulating at the G2/M phase in chronic hypoxia was only ~40%, implying that hypoxia reduces the ability of etoposide to induce a G2/M arrest (**Figure 4.6B**).

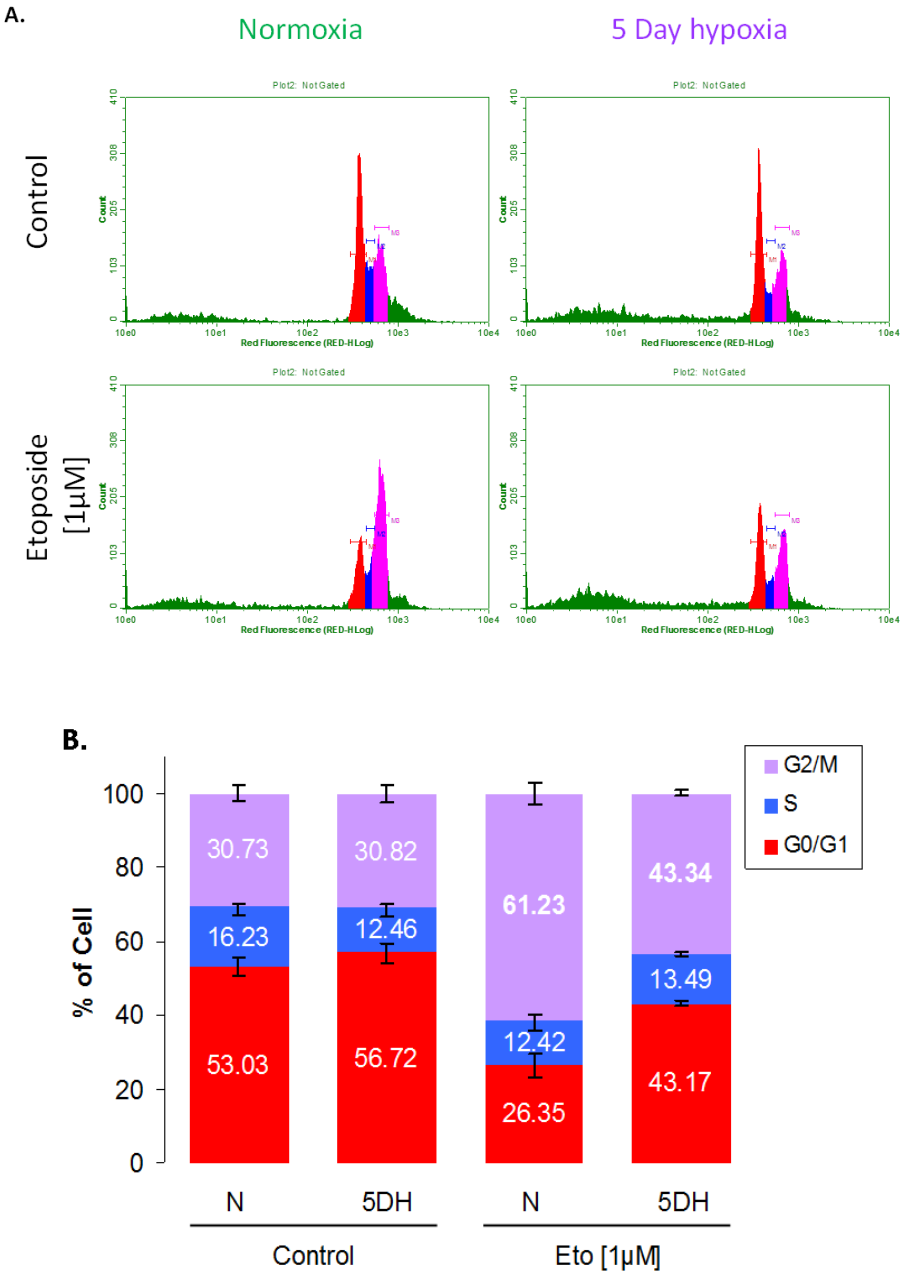

Figure 4.6 Reduction of etoposide-induced G2/M arrest in chronic hypoxia. *Cells were incubated in normoxia or 5 days hypoxia and treated with etoposide [1µM] for 30 hours.* ***(A)*** *Cell cycle profile obtained from the Guava software, this is a representative of 3 independent experiments.* ***(B)*** *Quantitative data showing the percentage of cells in each phase, value is calculated by dividing the number of cells in each phase by the total number of cells for that sample. Data shown are the mean ± S.E.M of three independent experiments.*

4.2.3 Validating etoposide drug action in hypoxia

We next tested if the reduction of etoposide effects on cell death and cell cycle arrest in chronic hypoxia was due to a loss of its activity at low oxygen level, such as previously reported for the drug tirapazamine (Hicks *et al.*, 2004, Koch, 1993, Teicher, 1994). For this, the first physical effect of etoposide on triggering DNA breaks was measured using the comet assay. Comet assay is a single cell gel electrophoresis method, whereby DNA damage can be visualised as a 'comet tail'. When DNA nicks and breaks occur, the DNA integrity is compromised and the chromosomes become less compacted. Such DNA will therefore migrate slower when an electrophoretic field is applied, hence creating a 'tail'. Whereas undamaged DNA migrates as an intact unit within the gel matrix appearing as a circular shape (**Figure 4.7**).

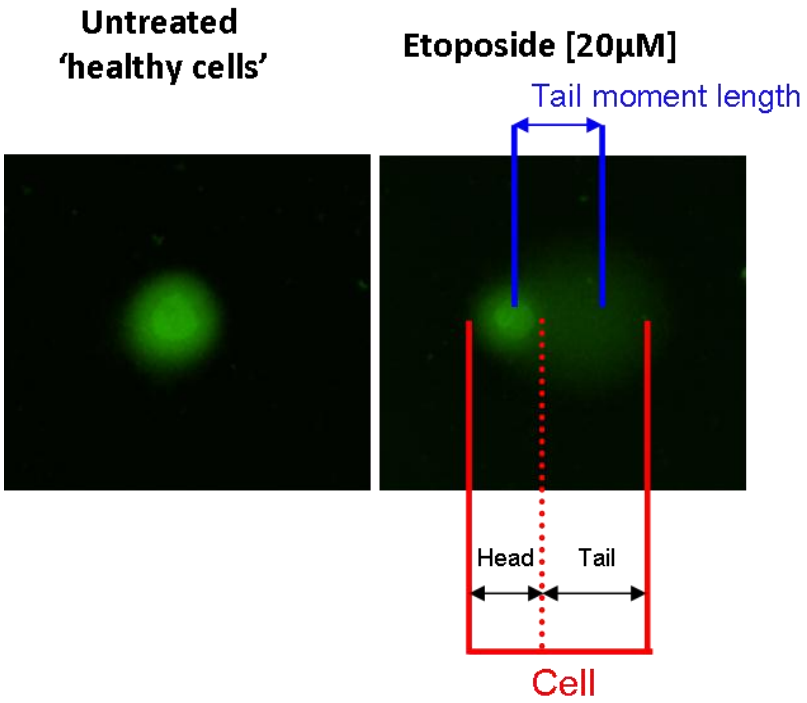

***Figure 4.7* An example of Comet assay**. *Untreated D283 cell shows an intact circular DNA stain. Etoposide treated cells present as a 'comet'. The whole cells including the head and tail are marked in red, the tail moment length are marked in blue.*

Typically, the amount of DNA damage measured using a Comet assay is expressed as the 'Olive Tail Moment' (Cell Biolabs, Inc, comet assay manual). This takes into account the intensity of the DNA within the head/ tail region and the length of the comet tail. The method of calculation is described in **Figure 4.8**. Apart from the degree of DNA damage, the length of the comet tail is also governed by the duration of electrophoresis.

$$\text{Tail DNA \%} = \frac{\text{Tail DNA Intensity}}{\text{DNA Intensity}} \times 100$$

$$\text{Olive Tail moment} = \text{Tail DNA \%} \times \text{Tail moment length}$$

Figure 4.8 Calculation methods for 'Olive Tail moment'. *Cells Biolabs, Inc. (http://www.cellbiolabs.com/sites/default/files/STA-350-comet-assay-kit.)*

4.2.3.1 Visualising DNA breaks induced by etoposide in normoxia and hypoxia

A comet assay was performed on normoxic and chronic hypoxic cells in the presence or absence (control) of etoposide. The physical properties of the comet were measured (**Figure 4.9**) and later used for Olive tail moment calculations. These properties includes **(A)** Head size **(B)** Head intensity **(C)** Tail size **(D)** Tail intensity and **(E)** Tail moment. The measurement of comet head size and head intensity indicates intact DNA, while the latter 3 measurements indicate the degree of fragmented DNA. In the absence of etoposide treatment, we have observed no change in any of these properties between normoxic and hypoxic samples, indicating hypoxia itself do not induce DNA damage. Upon etoposide treatment, we also detected no significant difference of any comet measurements between normoxic and chronic hypoxic cells, at any time points (**Figure 4.9A to F**).

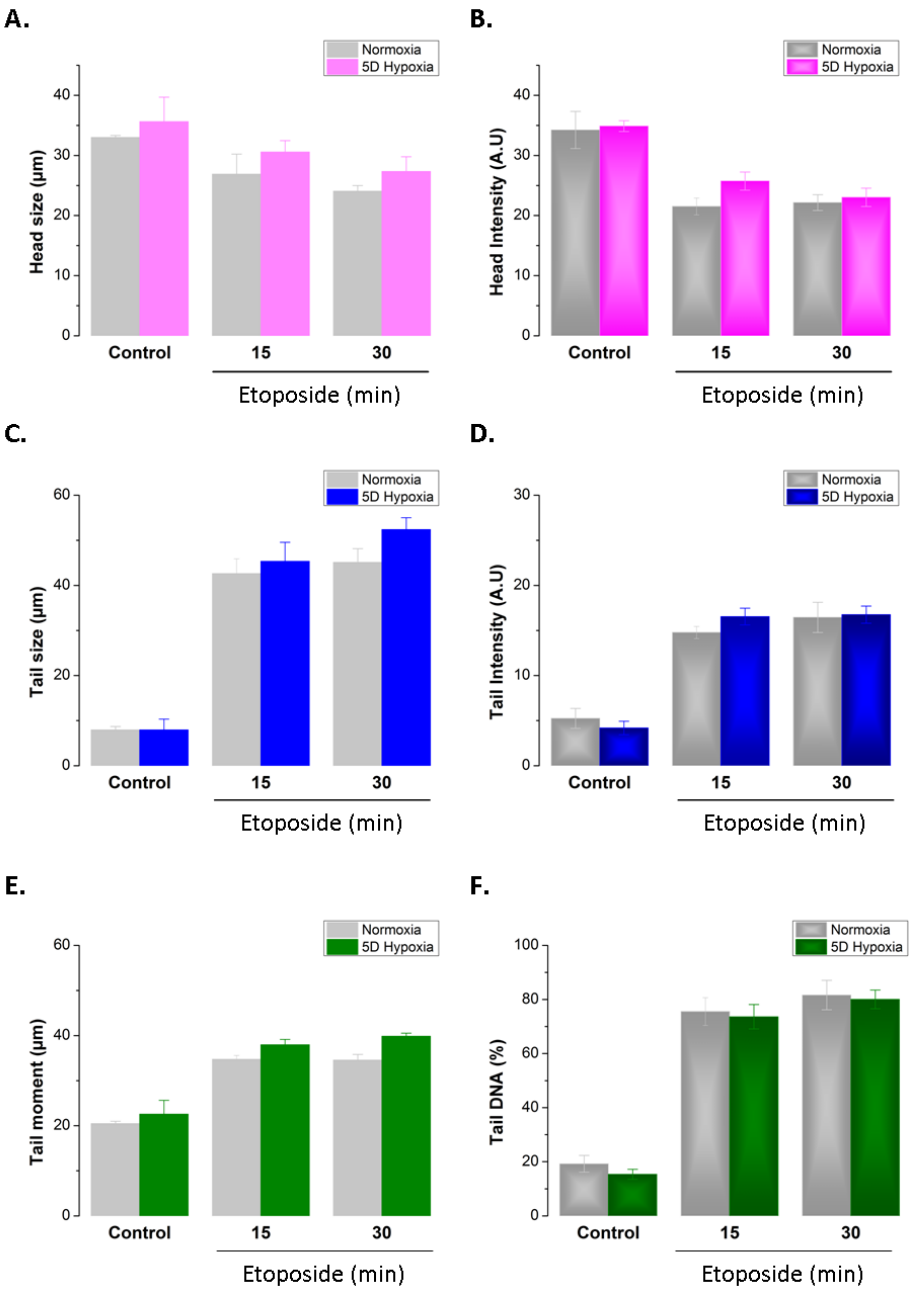

Figure 4.9 Summary of Comet assay measurements. *D283 cells were pre-incubated in 1% O_2 for 5 days or left in 21% O_2 prior to etoposide [20µM] treatment for indicated durations. Graphs shown are* ***(A)*** *Head size* ***(B)*** *Head intensity, which indicated intact DNA* ***(C)*** *Tail size* ***(D)*** *Tail intensity* ***(E)*** *Tail moment* ***(F)*** *Tail DNA % which indicates fragmented DNA. Data shown are the mean ± S.E.M of three independent experiments (n >100cells).*

Using the raw measurements of the comet's properties (**Figure 4.9**), we were able to further quantify the data and calculate the Olive tail moments (**Figure 4.8**), as used conventionally for comet assay analysis (chapter 4.2.3). In the untreated control sample, Olive tail moments were similar in both conditions. After 15 minutes of etoposide treatment, Olive Tail moment of ~3000(A.U) was measured in both normoxia and chronic

hypoxia. After 30 minutes, the Olive tail moment remain similar at ~3400 and ~3000 respectively (**Figure 4.10**). Furthermore, the size of the comet tails reached maximum length of ~45µm and ~52µm for normoxic and chronic hypoxic conditions respectively (P>0.05) after 30 minutes of etoposide treatment. These results indicate that hypoxia on its own, does not induce any DNA damage and that etoposide can effectively create physical DNA damage even in chronic hypoxia.

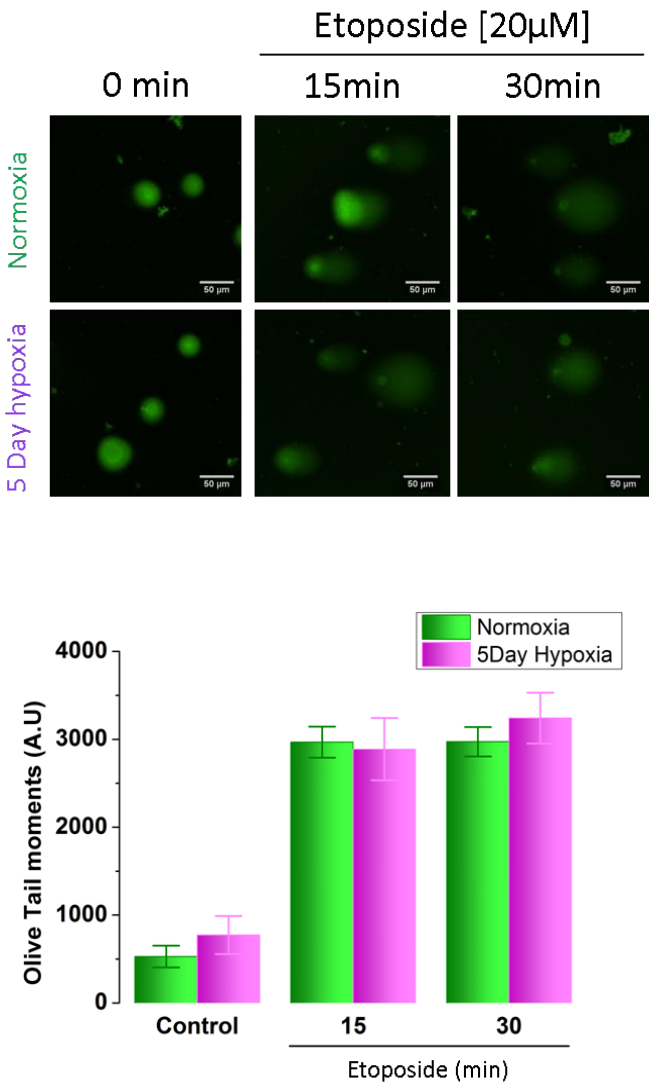

Figure 4.10 **Etoposide induces DNA damage in both normoxia and hypoxia.** *D283 cells were pre-incubated in 1% O_2 for 5 days (green bar) or left in 21%O_2 normoxia (pink bar) prior to etoposide [20µM] treatment for indicated durations. Comet assays were performed following manufacturer's protocol. Percentages of Olive tail moment were calculated. Data shown are the mean ± S.E.M of three independent experiments (n >100cells). One-way ANOVA followed by Bonferroni test was performed (* indicates p<0.05).*

4.2.4 Effect of chronic hypoxia on p53 signalling pathway

We have established from comet assay experiments that etoposide can efficiently induce DSBs in normoxic or chronic hypoxic cells. Therefore the differences of chemosensitivity observed in **Figure 4.5** cannot be due to a lack of efficacy of etoposide. In the previous chapter, we saw the importance of functional p53 pathway for etoposide-induced apoptosis. Moreover, many studies have reported effects of hypoxia on cell death/ cell survival through regulation of the p53 pathway where several studies have demonstrated the stabilisation and accumulation of p53 protein (An *et al.*, 1998, Greijer and van der Wall, 2004, Koumenis *et al.*, 2001) but with no direct evidence of downstream p53 activity. We therefore investigated the degree of p53 basal levels and activity as well as activation upon etoposide in chronic hypoxia.

4.2.4.1 Etoposide-induced p53 transcriptional activity in hypoxia

As a readout of p53 activity, the mRNA levels of three well known p53 target genes, MDM2, PUMA and p21 were measured by qPCR. We first examined the effect of hypoxia only on the basal levels of these target genes in normoxia and upon hypoxic incubation. There were no changes on the basal levels of all three target genes after either 1 day or 5 day hypoxia, suggesting that hypoxia itself do not alter the basal p53 activity (**Figure 4.11**).

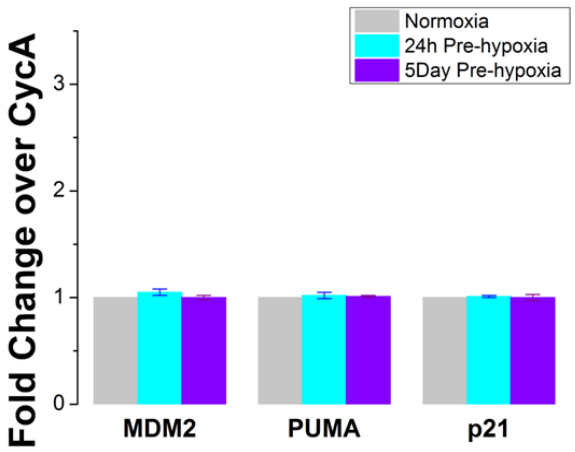

Figure 4.11 Basal levels of p53 targets genes in hypoxia. *p53 target genes of untreated samples were assessed by qPCR. D283 cells were incubated in 1% O_2 for 24 hours or 5 days, or left in normoxia (21% O_2). The level of MDM2, PUMA and p21 were normalised to the normoxic samples. Data shown are the mean ± S.E.M of three independent experiments.*

Upon etoposide treatment, we observed a strong induction of MDM2, PUMA and p21 mRNA levels in normoxic conditions, with a ~32, ~5 and ~26 fold increase respectively (***Figure 4.12***). The same induction of target genes was observed in cells pre-exposed to 24hr hypoxia before etoposide treatment. The fold changes observed in PUMA were similar to that of normoxic cells, but MDM2 and p21 expression were respectively ~60% and ~50% less than in normoxia. These data suggest that after 1 day of hypoxic incubation, the cells already show reduced p53 activation by etoposide. Moreover, in cells pre-exposed to 5 days hypoxia, the mRNA level induction of all three target genes was significantly reduced. MDM2 and PUMA level were only increased 3 times upon stimulation (compared to 32 and 5 times in normoxia), and no increase could be detected for p21. This strong reduction in etoposide-induced p53 transcriptional activity is likely to contribute to the resistance to cell death as well as to the absence of cell cycle arrest upon etoposide treatment, which were observed in chronic hypoxia (**Figure 4.4**).

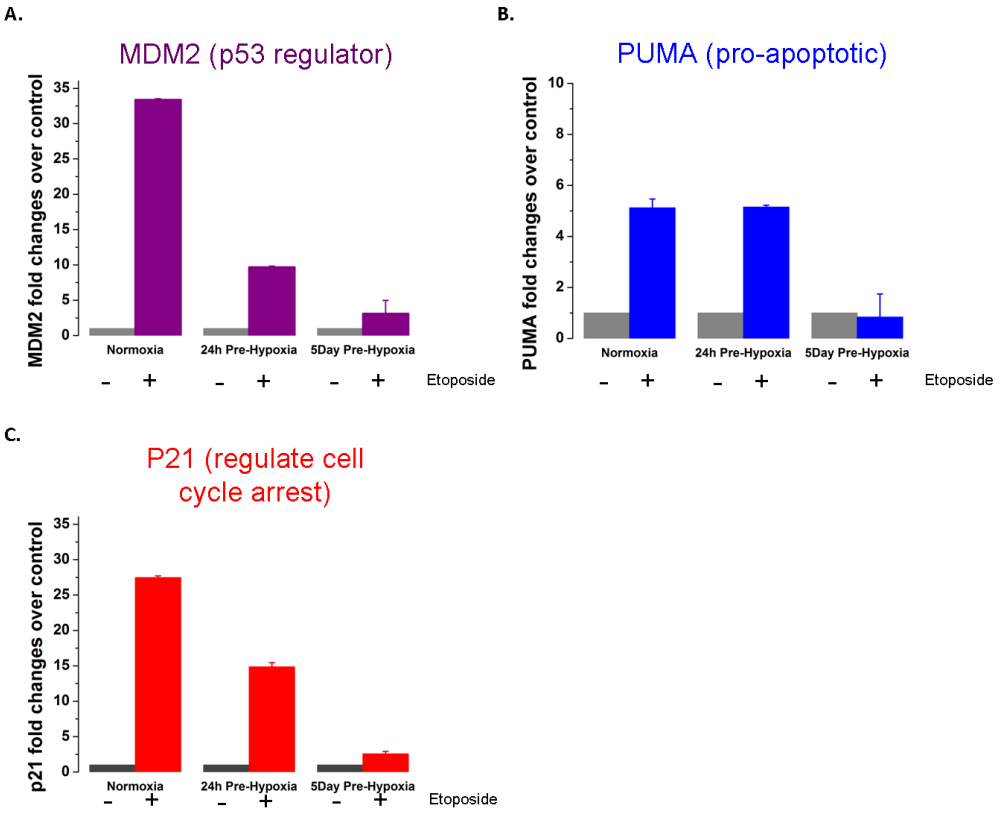

Figure 4.12 Etoposide-induced p53 transcriptional activity is reduced by chronic hypoxia*. Three p53 target genes* ***(A)*** *MDM2* ***(B)*** *PUMA* ***(C)*** *p21were assessed by qPCR in D283 cells treated with etoposide [20μM] for 7 hours. Cells were incubated in 1% O_2 5 days or left in normoxia (21% O_2), prior to and during etoposide treatment. The levels of MDM2, p21 and PUMA were normalised with the house-keeping gene cyclophilin A and over untreated control. These data are representative of three independent experiments, error bars here are SD of a single experiment.*

4.2.4.2 Etoposide-induced p53 phosphorylation in chronic hypoxia

To understand why there is a reduction of p53 activity in chronic hypoxia, we focused on the p53 protein. We measured p53 total protein levels and its phosphorylated form (p53-serine15), a marker of active p53 (Craig *et al.*, 1999, Sakaguchi *et al.*, 1998, Schon *et al.*, 2002) in both normoxia and chronic hypoxia following etoposide treatment. Firstly, in untreated control, both p53 and p53-serine15 levels were similar in normoxia and chronic hypoxia. Upon etoposide treatment, in normoxic conditions, p53 total protein levels increased transiently with a peak after 4 hours of treatment, (**Figure 4.13**). In chronic hypoxia, however, the p53 total protein accumulation was slower with a maximum protein stabilisation only reached by 7 hours. Furthermore, the p53 protein levels were lower than in normoxic conditions (**Figure 4.13**). To assess the ability of etoposide to induce serine15 phosphorylation, the level of phosphorylated form were measured and normalised to the total p53 levels (**Figure 4.13**). In normoxia, the level of serine15 induced by etoposide was ~4 fold higher compared to chronic hypoxia at 4 hours treatment. These data suggest that both etoposide-induced total p53 expression and the level of phosphorylated p53 were reduced in cells exposed to chronic low oxygen environment, explaining the reduction of p53 transactivation observed in **Figure *4.12***.

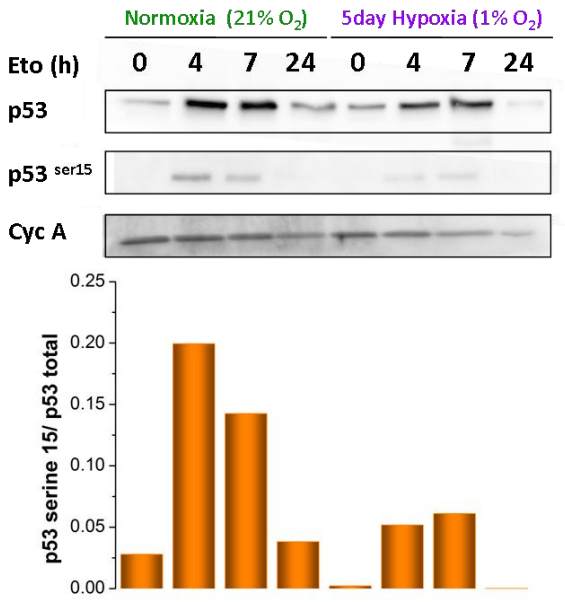

Figure 4.13 **Etoposide-induced p53 protein levels are reduced in chronic hypoxia.** *D283 cells were incubated in normoxia (21% O_2) or pre-incubated in hypoxia (1% O_2) for 5 days and treated with etoposide [20μM] for the indicated time points. Total p53 and phosphorylated p53 serine15 levels were assessed by western blot. Quantification of the band intensity is measured by AQM software and p53 serine 15 is normalised over the p53 total. This blot is a representative of three repeated experiments.*

4.2.5 Bridging DNA damage to p53 activation

We have so far demonstrated that etoposide can cause physical DNA damage and that p53 activity, although not completely abolished, is strongly reduced in chronic hypoxia. The observed reduction of p53 accumulation, phosphorylation and transcriptional activity is likely to be due to an impaired signalling upstream of p53 activation (**Figure 4.14**).

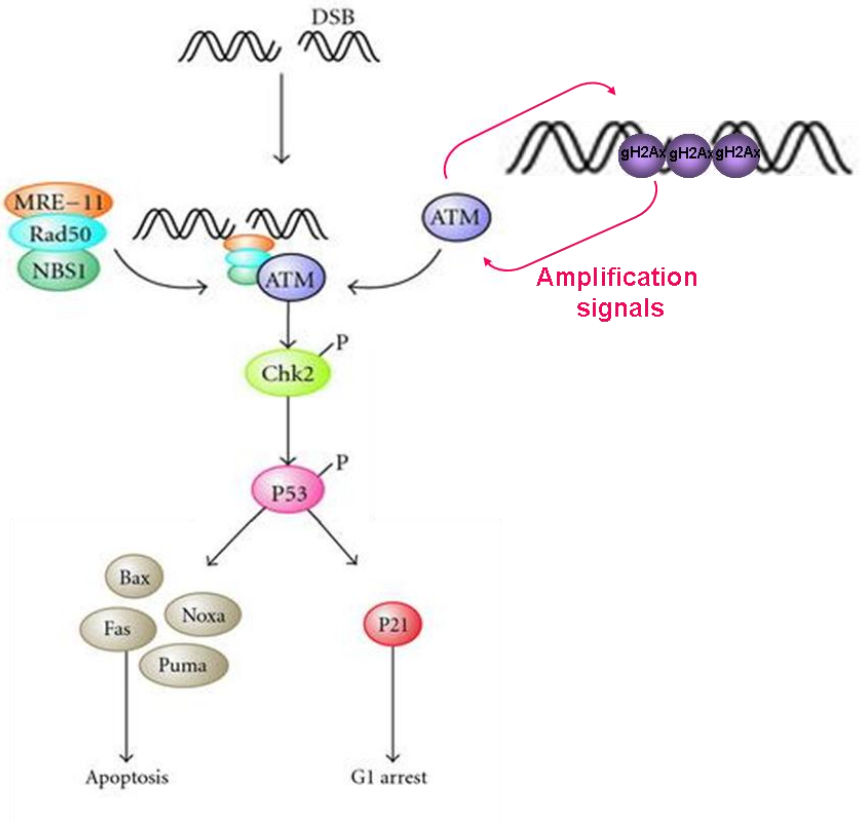

Figure 4.14 From DNA damage to p53 activation. *DSBs are sensed by the MRN complex (Mre11/Rad50/NBS1 or nibrin) which activates ATM, in turn phosphorylating Chk2 and H2AX. ATM and γH2AX form a positive feedback loop which amplify DSB signals and mediates p53 response. Activated p53 transactivate apoptotic targets or induce cell cycle arrest through, for example, p21 induction. Diagram adapted from www.hindawi.com/journals/ijcb/2010/214074/fig3.*

Upon etoposide treatment, DNA damage sensors, namely the MRN complex, are recruited to the breakage site, rapidly activating effector proteins such as ATM (Horejsi *et al.*, 2004, Costanzo *et al.*, 2004). ATM kinases phosphorylate targets including Chk2 (a p53 activating kinase) and a histone variant called H2AX (Stiff *et al.*, 2004). In turn, γH2AX (H2AX-serine139) can itself phosphorylate ATM, hence forming a positive regulatory loop. The interplay of these DNA damage proteins acts as an important signal amplifier to provoke responses such as p53 activation (chapter 1.6.1.2 and 1.7.2.2).

4.2.5.1 ATM activities in chronic hypoxia

Due to the interaction between ATM and H2AX, with H2AX phosphorylated within minutes of DSB damage, γH2AX makes a suitable candidate as a DSB marker and a reporter for ATM activity and DNA repair signal amplification. Moreover, the detection of γH2AX has been extensively reported in the literature as a measurement of DSBs. Immunocytofluorescence was used to measure the intensity of γH2AX staining after etoposide treatment of normoxic and chronic hypoxic cells. In untreated conditions, little γH2AX staining was visible in both normoxic and hypoxic conditions. This was used as the background threshold for measuring γH2AX intensity in treated samples.

In normoxia, a steady increase of γH2AX level was observed as quickly as 15 minutes after etoposide treatment with a steady increase up to 120 minutes, then reaching a plateau up to 360 minutes. The intensity has increased to ~4 fold by 30 minutes and ~10 fold by 360 minutes. In hypoxic cells, γH2AX level increased up to ~3 fold in 30 minutes but the maximum fold change was only ~6 fold at 360 minutes post treatment (**Figure 4.15**). These results indicate that in chronic hypoxia, initial ATM activation remains functionally similar to that of normoxia. However, by 120 and 360 minutes, the reduction of γH2AX staining suggests a lower amplification signal, which can explain the previously observed reduction of p53 activation by etoposide (**Figure 4.12** & **Figure 4.13**).

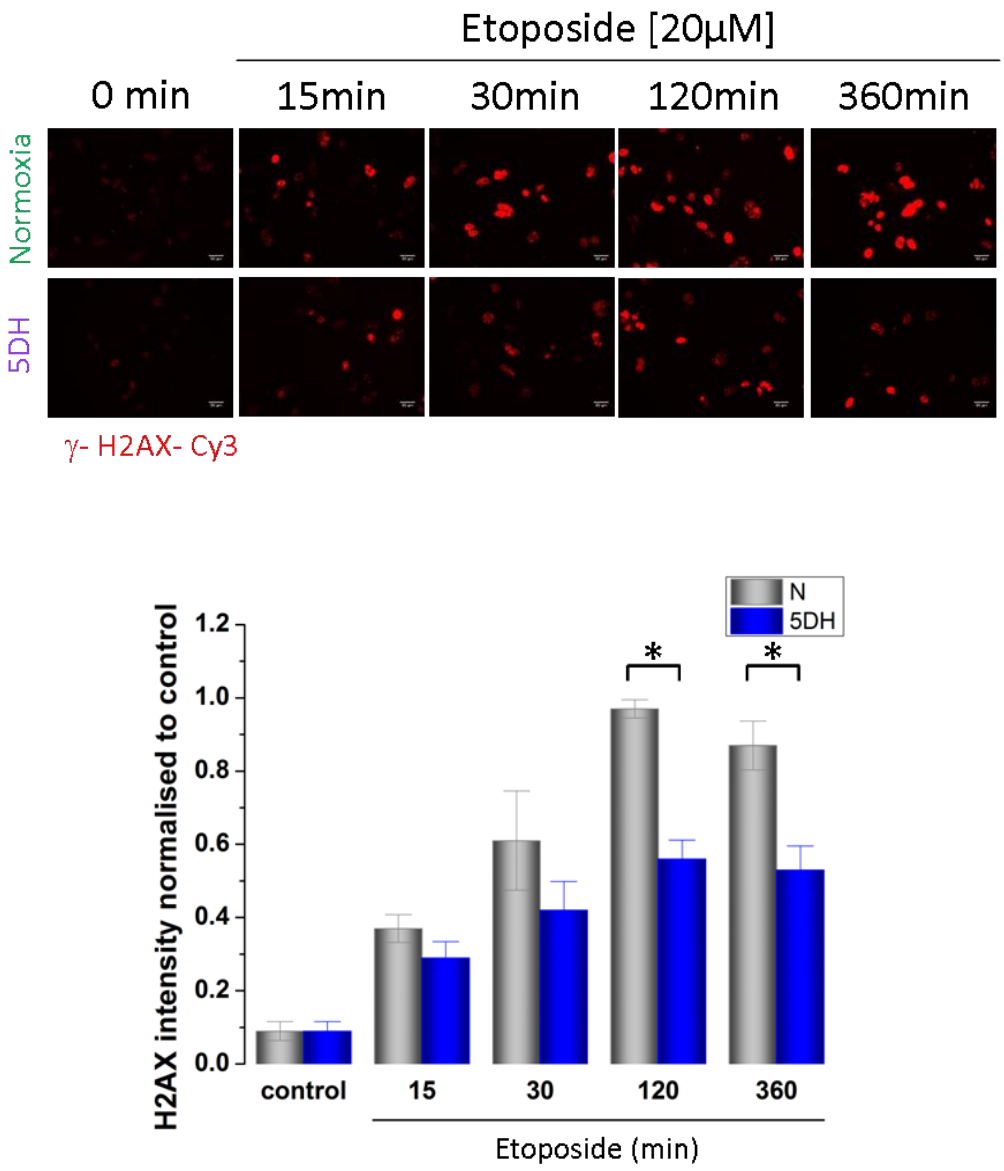

Figure 4.15 DNA damaging sensing is reduced in hypoxia. *D283 cells were pre-incubated in 1% O_2 for 5 days or left in 21% O_2 normoxia prior to etoposide treatment for indicated durations. D283 cells were stained with γH2AX and Cy3 antibodies and fluorescence intensity was quantified for individual cells. Data shown are the mean ± S.E.M of three independent experiments (n >350 cells). One-way ANOVA followed by Bonferroni test was performed (* indicates p<0.05).*

4.2.6 Role of hypoxia on p53 activation in other brain tumours

To test if the reduction of p53 activation in hypoxia was also true in other brain tumours, we examined p53 protein levels and activity in a p53 WT GBM cell line, U87, in normoxia and chronic hypoxia (4 days hypoxic exposure).

4.2.6.1 Etoposide-induced p53 expression in Glioblastoma

The basal total p53 and p53 serine15 levels in U87 were similar in both oxygen conditions (**Figure 4.16**). As observed in D283 cells, the levels of p53 serine15 phosphorylation over p53 total level after etoposide treatment were lower compared to normoxia at 4 hours etoposide treatment (**Figure 4.16**). These data demonstrate that etoposide-induced p53 expression and p53 phosphorylation is also reduced and slowed in a GBM cell line in chronic hypoxia (**Figure 4.16**), validating our previous observation with MB cells.

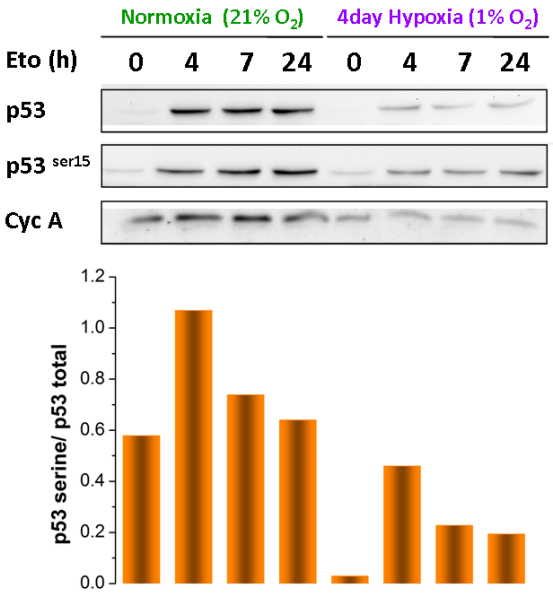

Figure 4.16 Etoposide-induced p53 protein levels are also reduced in chronic hypoxic U87 cells. *U87 cells were incubated in normoxia (21% O_2) or pre-incubated in hypoxia (1% O_2) for 4 days and treated with etoposide [20 µM] for the indicated time points. Total p53 and phosphorylated p53 serine15 levels were assessed by western blot. Quantification of the band intensity is measured by AQM software and p53 serine 15 is normalised over the p53 total. This blot is a representative of three repeated experiments.*

4.2.6.2 Etoposide-induced p53 activity in Glioblastoma

We next looked at the p53 transcriptional activity in hypoxic GBM cells following etoposide treatment. As previously in MB cells, the mRNA levels of MDM2, p21 and PUMA were measured by qPCR following 24 hours of etoposide activation in normoxic or chronic hypoxic conditions (**Figure 4.17**). The level of induction of all three target genes was higher in normoxic cells than chronic hypoxic cells after etoposide stimulation. The fold induction for MDM2, PUMA and p21 was 12, 14 and 10 respectively in normoxia compared to 6, 2 and 4 in hypoxia. These results are similar to the ones obtained for D283 cells (**Figure 4.12**), and further support the conclusion that chronic hypoxia reduces p53 transactivation.

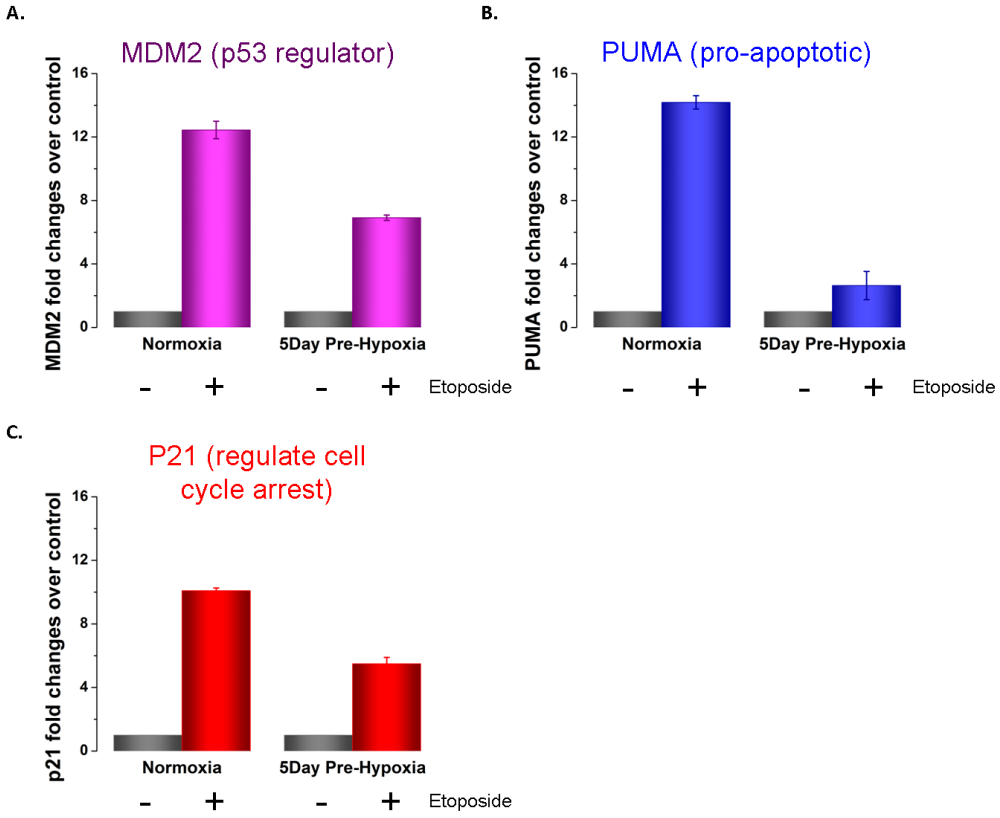

Figure 4.17 Etoposide-induced p53 transcriptional activity is reduced in chronic hypoxia in U87 GB cells. *Three p53 target genes* ***(A)*** *MDM* ***(B)*** *PUMA* ***(C)*** *p21were assessed by qPCR in U87 cells treated with etoposide [20µM] for 7 hours. Prior to etoposide treatment, cells were incubated in 1% O_2 for 4 days or left in normoxia (21% O_2). The levels of MDM2, p21 and PUMA were normalised with the house-keeping gene cyclophilin A and over untreated control. These data are representative of three experiments.*

4.2.6.3 Chemosensitivity of U87 cells in hypoxia

We further aimed to confirm in U87 cells, that the reduced p53 activation by etoposide in hypoxia was also correlated with a decreased sensitivity to treatment. U87 cells were treated with different concentrations of etoposide ranging from [20µM] to [100µM] for 24 hours, and cell viability was measured using the MTS assay (**Figure 4.18**). U87 cells were relatively resistant to etoposide compared to D283 cells, showing 60% cell viability after 24 hours of treatment at high concentrations of etoposide [100µM]. This resistance to treatment was even higher for cells incubated in chronic hypoxia with a cell viability of 90% (**Figure 4.18**). These results demonstrate that the previous observation made in D283 MB cells is also valid in GBM cells.

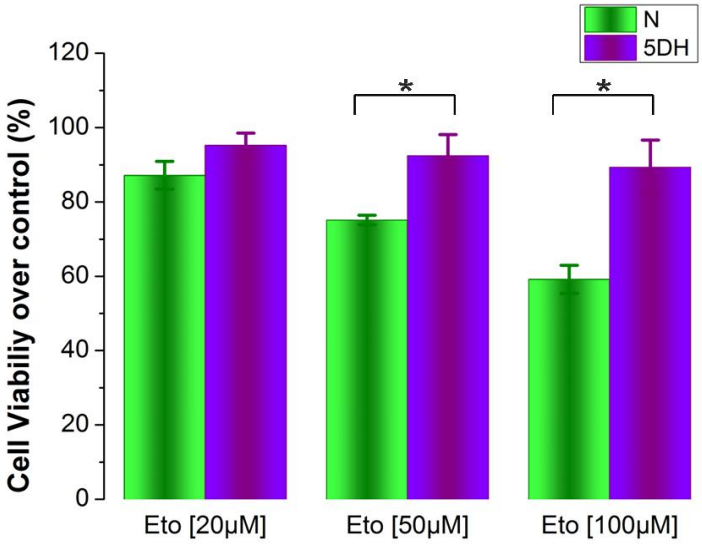

Figure 4.18 Chronic hypoxia-induced etoposide resistance in U87 cells. *U87 cells were treated with [20µM], [50µM] or [100µM] Etoposide for a 24 hours.* ***(A)*** *Normoxia* ***(B)*** *5 Day hypoxia. The percentage of cell viability was measured by MTS assay over the untreated control. Data shown are the mean ± S.E.M of three independent experiments. One-way ANOVA followed by Bonferroni test was performed (* indicates p<0.05).*

4.3 Chapter 4 Discussion

4.3.1 Hypoxia duration and acquired chemoresistance

Hypoxia is strongly associated with tumour progression, invasiveness and metastasis (chapter 1.2.2). Although the role of hypoxia contributing to chemoresistance has been documented in some cancers, the length of hypoxia required and the mechanism of resistance acquisition were not consistent in the literature, partly due to differences in experimental settings.

Hypoxia-induced chemotherapy resistance has been demonstrated by several groups, such as the studies of *Flamant et al*., *Sermeus et al*. and *Cosse et al*. (Flamant *et al.*, 2010, Cosse *et al.*, 2007, Sermeus *et al.*, 2008). *Flamant et al*. have shown that hypoxia protects breast cancer cells (MDA-MB231) against paclitaxel-induced apoptosis (Flamant *et al.*, 2010); in both *Sermeus et al.* and *Cosse et al.* reports, a Hepatocellular carcinoma (HCC) HepG2 cell line became more resistant to etoposide, after 1% hypoxic incubation during 16 hours (Cosse *et al.*, 2007, Sermeus *et al.*, 2008). In our hands, we have observed the dampening of etoposide-induced cell death in hypoxia, with it requiring a much longer time frame. We observed that etoposide-induced cell death is only reduced after 5 days of hypoxia in D283 MB and U87 GBM cells but not acute hypoxia (24 hours). These findings are similar to those of *Hussein et al.* where they have demonstrated that in neuroblastoma cell lines, 16 hours of 1% hypoxic incubation did not have any effect on etoposide- or viscristine-induced cell death while a longer exposure of up to 7 days promoted hypoxia-induced resistance (Hussein *et al.*, 2006).

Despite several reports supporting a cell death resistance role of hypoxia, this is not true for all cellular models. In an extensive study performed by *Sermeus et al*., 7 cell lines and their response to 5 different drug treatments in hypoxia were investigated. Agreeing with their previous studies, some cell lines gained resistance but some other cell lines such as lung carcinoma (A549) showed increased sensitivity with certain drugs (e.g. etoposide) whilst other drugs (e.g. cisplatin) had no effect on cell death when exposed to hypoxia (Cosse *et al.*, 2007, Sermeus *et al.*, 2012). Similarly, MCF-7 cells became more sensitive to treatment under the same treatment condition of 1% O_2 for 16 hours (Cosse *et al.*, 2007). These results reaffirm that hypoxia-induced resistance is cell line dependent. This difference has been experienced in our own laboratory, where neuroblastoma cell lines (SK-N-AS, SHEP, IMR32) did not exhibit any acquired resistance to etoposide nor doxorubicin upon chronic

hypoxia incubation (Heyward, unpublished observations). We have proposed a theory in the next chapter which might predict the effects of hypoxia on drug resistance based on the expression of a DNA break sensing protein, nibrin (chapter 5.2.7 and 5.2.8).

4.3.2 The relationship of hypoxia and p53

The effect of hypoxia on p53 expression levels and activity remain unclear, and this is once again dependent on the severity and length of hypoxic exposure as well as the cell type studied. It is generally agreed that 'mild hypoxia' does not influence p53 protein levels, as we have observed, (Pan *et al.*, 2004, Wenger *et al.*, 1998), while severe hypoxia, anoxia, and hypoxic mimics up-regulate p53 expression. For example, cobalt chloride ($CoCl_2$), a PHD inhibitor, which mimics a similar effect to severe hypoxia was able to stabilise p53 protein expression in breast cancer cells (An *et al.*, 1998). This was similar to the *Archison et al.* report, where they observed that colorectal carcinoma (HCT116) cells incubated in anoxia (0.1%) showed stabilisation of p53 (Achison and Hupp, 2003).

In addition to p53 stabilisation in hypoxia, several reports have suggested that hypoxia-induced p53 leads to p53 dependent apoptosis, but again these studies are performed in relatively low oxygen concentration between 0.001% to 0.02% or with $CoCl_2$ (Graeber *et al.*, 1994, Blagosklonny *et al.*, 1998). However, our data are in direct contrast to this. We saw that under 1% chronic hypoxia, a relatively mild hypoxic condition, p53 protein levels were not significantly changed and, if any effect, it was rather a reduction than an induction of p53. Moreover, p53 activation by etoposide was also dampened in these conditions. Our results therefore suggest that chronic hypoxia-induced chemoresistance might be partly due to the impairment of p53 activation. The finding that hypoxia reduces p53 activity, is supported by similar work of *Cosse et al.,* where they have observed that HepG2 cells expressed a lower level of p53 in hypoxia, a reduction of p53 binding activity and a decrease in etoposide-induced apoptosis (Cosse *et al.*, 2007). From another study, *Archsion et al.* have further demonstrated that hypoxia-induced p53-dependent apoptosis is indeed dependent on the hypoxic level. In their study, anoxia increased p53 induced apoptosis, whilst 1% hypoxia inhibited p53 serine15 and 392 phosphorylation upon 5-FU (florouracil) treatment, leading to attenuation of cell death (Achison and Hupp, 2003).

It must also be noted that hypoxia or other stress-induced p53 expression can often occur without DNA damage and therefore might result in a different classical p53 downstream outcome even upon protein stabilisation (Nitta *et al.*, 1997, Giaccia and Kastan, 1998, Williams *et al.*, 1999, Liu and Chen, 2006). Whilst in most cases p53 induction is followed by transcriptional activation and apoptotic response, in some cases, stabilisation of p53 does not lead to p53 transactivation or apoptosis (Koumenis *et al.*, 2001). This effect is illustrated in a study by *Ashcroft et al*, who used a hypoxic mimic drug (deferoxamine mesylate) to induce p53, and were only able to detect phosphorylation at serine15 but not serine20. In addition, all three tumour cell lines (breast, colon and osteosarcoma) that they have tested failed to induce classical p53 targets such as p21 and MDM2 (Ashcroft *et al.*, 1999).

Furthermore, there are indications that hypoxia-induced p53 can actually lead to transcriptional repression by formation of a repression complex with the corepressor molecule mSin31 (Murphy *et al.*, 1999, Hassig *et al.*, 1998, Koumenis *et al.*, 2001, Hammond and Giaccia, 2005). However, the role of p53 repression in hypoxic condition remains relatively unexplored.

4.3.3 ATM activation and p53 induced apoptosis

ATM is one of the key components, which is activated in response to DNA damage. It phosphorylates proteins involved in cell cycle, DNA repair and apoptosis (chapter 1.6). There is evidence that shows the loss of ATM is correlated to sensitivity to chemotherapy treatment (Shiloh *et al.*, 1983, Barlow *et al.*, 1996), but contrasting results have been reported (Haidar *et al.*, 2000, Ripolles *et al.*, 2006, Austen *et al.*, 2007). Its functional importance in achieving good treatment response has been demonstrated in primary cell lines obtained from ataxia telangiectasia (A-T) patients or from ATM knockout mice. In these cases, the absence of ATM render the cells hypersensitive to both ionizing radiation and DSB inducing agents (Shiloh *et al.*, 1983, Barlow *et al.*, 1996, Chun and Gatti, 2004). These findings are also supported by a study on primary (GBM) tumours where high ATM expression correlates to increased radioresistance (Tribius *et al.*, 2001). Since then, development of ATM inhibitors and their use as cancer chemotherapeutic agents has been investigated and indeed shown some promising results, but only in certain cell types (Golding *et al.*, 2012, Korwek *et al.*, 2012).

Controversially, in several studies on chronic lymphocytic leukemia (CLL) patients, the loss of ATM is associated with poor response to irradiation, resistance to chlorambucil and cyclophosphamide plus reduced patient survival (Haidar *et al.*, 2000, Ripolles *et al.*, 2006, Austen *et al.*, 2007). In another study using human T cells, ATM inhibitors actually render the cells more resistant to etoposide (Korwek *et al.*, 2012). It is not surprising to see these contrasting results as ATM kinase have many targets which are involved in different cellular pathways. It is largely unknown the exact mechanisms which dictate the action of ATM downstream response and the final outcome of cell cycle arrest, repair or apoptotic response remain elusive.

Recent studies have demonstrated that ATM alone is not sufficient to predict the outcome of treatment response but it is dependent on both the upstream and downstream of this pathway. In particular, the p53 functional status plays a role in the success of ATM inhibition in chemosensitisation (Jiang *et al.*, 2009, Knappskog *et al.*, 2012, Biddlestone-Thorpe *et al.*, 2013). *Jiang et al.* is one of the first reports to have speculated this dependency. They found that p53 WT cells became more resistant to treatment when ATM activity was inhibited and that p53 dependent apoptotic response was prevented by ATM inhibition (Jiang *et al.*, 2009). Additionally, *Jiang et al.* have also demonstrated that p53 deficient cell lines show the reverse results upon ATM inhibition (Jiang *et al.*, 2009).

More recent studies in breast cancer models have further demonstrated the importance of ATM expression in treatment response and clinical outcome prediction (Knappskog *et al.*, 2012). Generally, in this setting, breast cancer containing *TP53* and or *CHK2* mutations are more resistant to treatment and patients have poorer outcome. However, *Knappskog et al.* have observed that a group of patients, without any *TP53* and or *CHK2* mutations, also displayed poor treatment response and progressive disease (Knappskog *et al.*, 2012, Chrisanthar *et al.*, 2008, Geisler *et al.*, 2001). On further examination, they have revealed that 12/18 patient in this group expressed a lower than median level of ATM at a transcription level (Knappskog *et al.*, 2012). Thus, even if cells carry a p53 WT genotype, a low expression of ATM effectively renders the chemotherapeutic response similar to that of *TP53* and or *CHK2* mutated cells. As with our own findings, reduction of ATM activity (measured by γH2AX) is associated with resistance in a p53 WT cell line under chronic hypoxia. Altogether, this demonstrates a role of the whole ATM-Chk2-p53 signalling cascade in chemoresistance. It is therefore advisable to consider ATM expression as well as p53 status as a prognostic indicator in treatment response.

4.3.4 The effect of hypoxia on cancer cell biology

Due to the genetic heterogeneous nature of tumours, hypoxia can affect cells within a population differently. Some cells will undergo apoptosis due to the severe conditions, while others will promote survival though activation of genes needed for adaptation or cells can be naturally more resilient (Attolini and Michor, 2009, Diaz *et al.*, 2012, Wenger, 2002). Cells which are unable to adapt will die, as we have witnessed with our model that hypoxia itself triggers some cell death. However, the cells which are either well adapted or with a malfunctioned cell death pathway will be favoured. Thus this selection can be both a spontaneous event, i.e. naturally selecting cells which carried mutations with a 'growth advantage', or by adaptation response which will have a long lasting effect (Pisco *et al.*, 2013). Additionally, the tumour oxygenation is also heterogeneous. Cells across a tumour may be differently oxygenated, creating differing severities of hypoxia. This may promote heterogeneity within the population of cells, which in turn promotes enough variance to increase the tumour survival rate against chemotherapy. Hence, hypoxia can ultimately select for the more resistant, transformed population. Under chronic hypoxia, the cellular biology of the tumour cells is undoubtedly altered and other targets/ pathways are likely to contribute to the chemoresistance. We therefore need to monitor global changes in the overall gene expression in hypoxia to further investigate the mechanisms of chronic hypoxia-induced resistance.

Chapter 5: Gene Expression in Hypoxia Associated with Drug Resistance

5.1 Introduction

We have demonstrated in the previous chapter that a chronic hypoxic environment is associated with poor response to etoposide treatment, whereas, acute hypoxia does not alter etoposide effects. However, it is possible that other mechanisms other than reduction of p53 activation could contribute to chemoresistance in chronic hypoxia. There is for example, evidence of hypoxia-induced chemoresistance by expression of multidrug resistance genes (Comerford *et al.*, 2002, Liu, L. L. *et al.*, 2008).

Expression of multidrug resistance genes has been observed in many cancer types, correlating to chemotherapy resistance and poor prognosis. Three of the ATP binding cassette (ABC) transporter families, ABCB/C/G (i.e. MDR1/ MRP1/ ABCG1), have been associated with drug resistance. In particular, MDR1 association with drug resistance has been shown in gastric, breast and liver cancers (Liu, L. L. *et al.*, 2008, Li *et al.*, 2006, Zhu *et al.*, 2005, Sasabe *et al.*, 2007, Volk *et al.*, 2002). Expression of MDR1 and MRP1 have also been observed in neuronal tumours including neuroblastoma, high grade glioma and GBM cell lines (Loscher and Potschka, 2005, Hermann and Bassetti, 2007, Hussein *et al.*, 2006, Chen, L. *et al.*, 2009, Feun *et al.*, 1994, Matsumoto *et al.*, 1990, Abe *et al.*, 1994, Nardinocchi *et al.*, 2009, Cordon-Cardo *et al.*, 1989, Schinkel, 1999, Sun *et al.*, 2003), but there are currently few reports on ABC transporters expression in MB (Chou *et al.*, 1995). The *Chou et al.* study is the only report in MB, where they found that the expression of MDR1 was correlated to poor patient outcome (Chou *et al.*, 1995). However, in another report, a gene expression study on chemoresistant MB cell lines showed no significant expression of MDR1 (Bacolod *et al.*, 2008). Moreover, the expression of these genes in chronic hypoxia remains controversial.

To better evaluate the implications of hypoxia on drug resistance genes and other genes that could be responsible for the lack of sensitivity to etoposide, we have carried out a global gene expression study by microarray analysis to allow an efficient search for a range of genes. We first focused on multidrug resistance gene family, as well as other potential genes, which might also be associated with drug resistance. Additionally, the two classical DSBs pathway, Homologous End Joining Recombination (NHEJ) and Homologous recombination (HR), were investigated to deduce whether the DNA damage sensing machinery is altered by chronic hypoxia as hypothesised in chapter 4. An unbiased analysis of the micro-array data is presented chapter 6.

Objectives:

1. To investigate the regulation of HIF in long term hypoxia

2. To examine the expression of multidrug resistance genes in chronic hypoxia

3. To investigate, in the micro-array data, potential gene expression related to drug resistance

4. To specifically analyse the changes in the expression of genes involved in DNA repair and p53 signalling during chronic hypoxia

5.2 Results

5.2.1 HIF signalling in chronic hypoxia

HIF-1α is the major transcription factor playing a crucial role under low oxygen tensions. It is well known that HIF-1α expression increases rapidly under hypoxia and accumulates to a peak level within 4 to 7 hours in most cell lines (Wang *et al.*, 1995, Stiehl *et al.*, 2006). In some cell lines such as Hep3B (hepatocellular carcinoma), HEK293 and HeLa cells, after accumulation, HIF-1α expression returns close to basal levels by 16-24 hours (Wang *et al.*, 1995, Stiehl *et al.*, 2006, Bagnall, 2013). It has been reported that HIF-1α can directly transcribe many downstream targets, including ones involving drug resistance such as MDR1 (Comerford *et al.*, 2002). However, there are inconsistencies in the literature as to whether hypoxia-induced chemoresistance is directly dependent on HIF (Chen, J. *et al.*, 2009, Nardinocchi *et al.*, 2009, Song *et al.*, 2006, Hussein *et al.*, 2006). Moreover, most published studies only look at a relatively short hypoxic time course. HIF expression and its target gene expression are less well studied over chronic hypoxia. Here, we will first investigate the expression of HIF-1α and the expression of well known HIF target genes in a long hypoxic time course. Secondly, we will investigate whether chronic hypoxia-induced resistance is contributed by the induction of multidrug resistance genes and other genes potentially involved in the drug resistance mechanism.

5.2.1.1 HIF-1α expression in chronic hypoxia

We measured HIF-1α protein expression over a long hypoxic time course of 96 hours (**Figure 5.1**). We observed an accumulation of HIF-1α protein within the first 2 to 7 hours of hypoxic incubation, with maximum band intensity at 7 hours. This level returned to basal normoxic levels by 24 hours. The HIF-1α expression observed during the first 24 hours was similar to that previously observed in our laboratory in HeLa cells (Bagnall, 2013), by *Wang & Jiang et al.* and by *Stiehl & Wirthner et al.* (Wang *et al.*, 1995, Stiehl *et al.*, 2006, Bagnall, 2013). Interestingly, we also measured secondary peaks of HIF-1α accumulation at later time points, with peaks at 40, 64 and 78 hours (**Figure 5.1**). These latter HIF-1α peaks were not previously observed as most experiments are performed under 48 hours and they were not measured at a high resolution time points, thus missing the subsequent HIF-1α peaks.

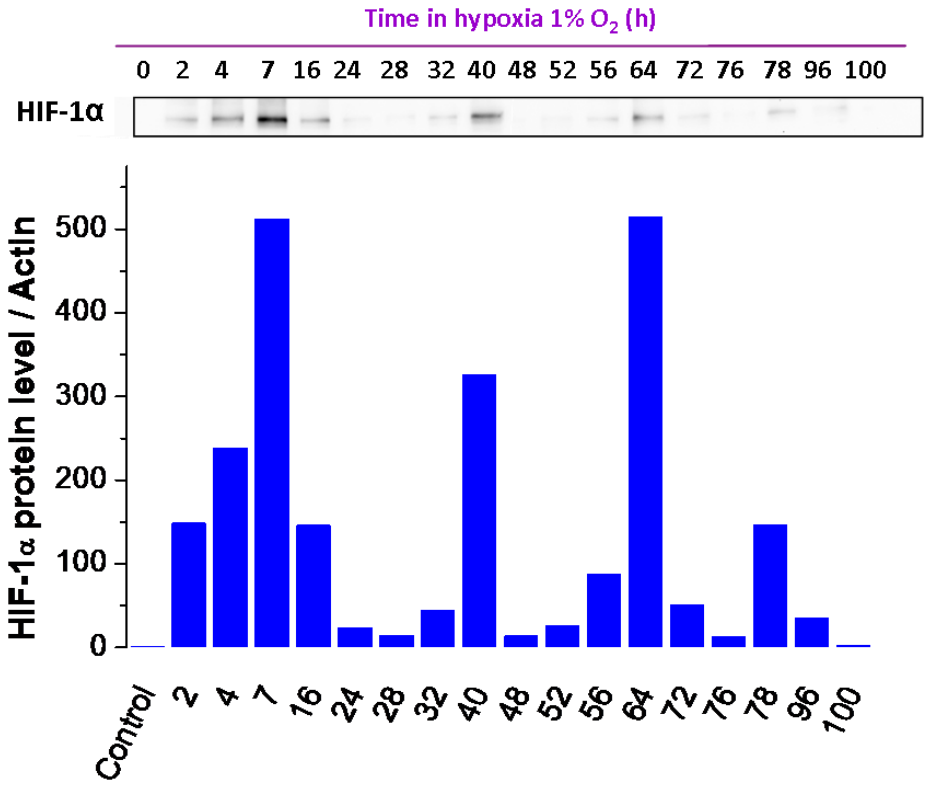

Figure 5.1 Chronic hypoxia induced HIF-1α protein accumulation at different time points. *D283 medulloblastoma cells were incubated in normoxia (21% O_2) as a control or at indicated time points in hypoxia (1% O_2). HIF-1α protein levels were assessed by western blotting. Quantification of the band intensity was measured by AQM software. This blot is a representative of two independent experiments.*

5.2.1.2 HIF-1α target genes expression in chronic hypoxia

We examined whether the continued HIF-1α expression in chronic hypoxia translates to long term transcriptional activity and its possible involvement in activating genes involved in drug resistance. Three classical well described HIF-1α targets: PHD2, EPO and VEGF and a specific target of interest: MDR1 (Elvidge *et al.*, 2006) were measured by qPCR. As expected, the classical target PHD2 was increased ~16 fold after 7 hours of hypoxic incubation and returned to basal level by 24 hours (**Figure 5.2A**). A secondary and a third peak of PHD was also observed at 32 hours and 64 hours. Interestingly for EPO, mRNA was only increased by ~3 fold after 4 hours of hypoxic exposure, yet a 50 fold induction was observed after 24 hours and this remained relatively high at later time points (**Figure 5.2B**). Similarly, VEGF was upregulated by 4 hours but a stronger induction was observed after 24 hours of hypoxic exposure (**Figure 5.2C**). These results suggest that HIF-1α remains transcriptionally active over a long hypoxic time course, however we cannot exclude additional HIF-independent mechanisms.

The multidrug resistance gene MDR1 was found to be upregulated in some studies (section 5.1), suggesting that MDR1 could be responsible for the observed chemoresistance in hypoxia. However, in our model, we did not detect any alterations of MDR1 mRNA levels at either early or late time points (**Figure 5.2D**). This suggests that other mechanisms or genes are involved in hypoxia-induced etoposide resistance. The expression and involvement of other multidrug resistance genes are shown in section 5.2.3 and 5.2.4.

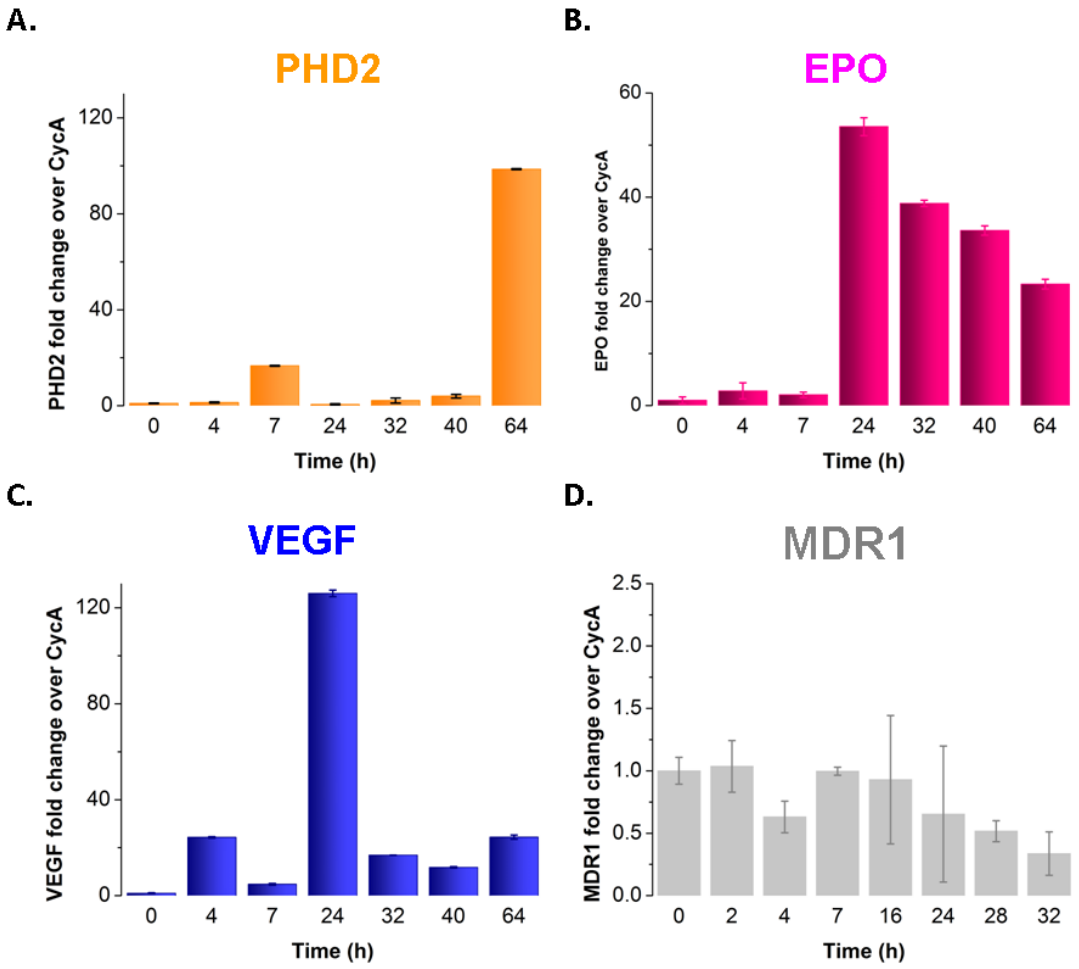

Figure 5.2 HIF-1α downstream target activation in hypoxia. *HIF-1α target genes,* ***(A)*** *PHD2* ***(B)*** *EPO and* ***(C)*** *VEGF* ***(D)*** *MDR1 were assessed using qPCR after exposure in hypoxia (1% O_2) at indicated time point. The levels of mRNA were normalised with the house-keeping gene cyclophilin A and the untreated control. This is from one single experiment, error bars here are technical SD of 1 experiment.*

5.2.2 Microarray Gene Expression study

There are approximately 20000 to 25000 genes within the human genome (Stein, 2004), making it a notorious and potentially a biased task to manually select for and perform individual qPCR on genes which might be involved in chemoresistance. Hence, we used microarray analysis to allow an efficient view of chemoresistance gene expression under chronic hypoxia. We performed a hypoxic time course (up to 96 hours), and microarray data were analysed manually (chapter 2.6.3).

We observed that, at all time points taken together, over 6124 transcripts were significantly up- or down-regulated under hypoxia and ~39,000 transcripts were not regulated by hypoxia (

Figure 5.3). As one gene can have more than one transcript, this corresponds to 4303 significantly regulated and 23, 611 non-regulated genes.

Significantly expressed/repressed Transcripts	**6124**
Non-significantly expressed/repressed Transcripts	38,910

Figure 5.3 Number of significantly and non-significantly expressed/ repressed transcripts. *Transcripts are said to be 'significant' if they meet the criteria of: the ANOVA p value for all 3 probes is ≤0.01 or the ANOVA p value for 2 out of 3 probes is ≤0.000 and that minimum fold change is greater than 2 at any given time points (Methods section Table 2.16).*

5.2.3 Expression of multidrug drug resistance genes

Although ABC transporter have been observed in hypoxic brain tumour, for example, *Chen et al.* have reported that hypoxia-induced resistance to both doxorubicin and etoposide treatment in human glioma cells is via HIF-1α is dependent upregulation of MDR1 (Chen, L. *et al.*, 2009), in the context of MB, the role of ABC transporters in hypoxia is unclear. Also, considered that MRP1 and ABCG1 transporters are also associated with resistant in other tumours (section 5.1), there are few studies of their expression in MB and their roles in MB remain elusive. We will therefore investigate the expression patterns of these ABC transporters in our hypoxic model.

We searched for each of the drug resistance genes mentioned above in our microarray 'significant expressed transcript list' (**Figure 5.3**) to investigate whether they were expressed in hypoxia at any time points (**Table 5.1** and **Figure 5.4**). From our data, there is no significant induction or reduction of any of these efflux transporters, suggesting that hypoxia-induced chemoresistance is not due to the expression of these transporters.

Gene	Protein	Expressed/ Repressed (Y/N)
MDR1/ABCB1	Multidrug resistance gene/ P-glycoprotein 1	N
MRP1/ ABCC1	Multidrug resistance-associated protein 1	N
ABCG1/ BCRP	breast cancer resistance protein	N

Table 5.1 ABC transporter genes. *A table of ABC transporters, showing whether they are expressed or repressed in the hypoxia microarray data.*

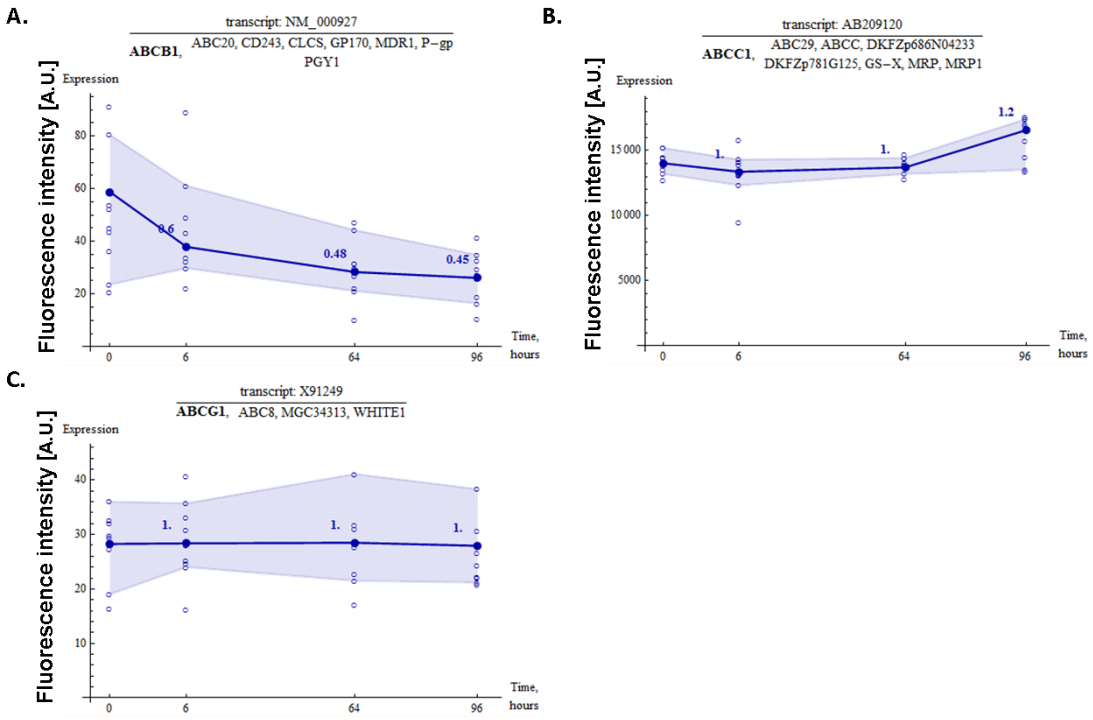

Figure 5.4 Expression plots of MDR1, MRP1 and ABCG1. *The expression plots of* ***(A)*** *MDR1* ***(B)*** *MRP1* ***(C)*** *ABCG1 in hypoxia. The filled circle and dark blue line shows the average expression plot of the transcript. The open circle shows the data point for each individual probe. The shaded blue area shows the range of data variation and the number above the point indicate the fold change normalised to basal ratio (chapter 2.6.3).*

5.2.4 Expression of hypoxia-induced drug resistance genes

Currently, besides the ABC transporters, little is known about other mechanisms of hypoxia-induced drug resistance. However, there has been some evidence that hypoxia is involved in the expression of other genes, which interfere with drug sensitivity. Attention has been turned to the following gene lists in **Table 5.2**, as they are candidates, which have been demonstrated to be expressed in hypoxic levels similar to our study and found to be associated with chemoresistance (Tong *et al.*, 2013, Chen, J. *et al.*, 2009, Zou *et al.*, 2013, Flamant *et al.*, 2012). These genes includes Notch-1, WD repeat and SOCS box (WSB-1), Transmembrane protein 45A (TMEM45A), Carbonic Anhydrase IX (CAIX/ CA9), and Pim-1 kinase (PIM-1).

Gene	Description	Expressed/ Repressed (Y/N)	Reference
Notch-1	Notch homolog 1	**Y, Repressed**	(Zou *et al.*, 2013)
WSB-1	WD repeat and SOCS box	N	(Tong *et al.*, 2013)
TMEM45A	Transmembrane protein 45A	**Y, Expressed**	(Flamant *et al.*, 2012)
CAIX/ CA9	Carbonic Anhydrase IX	**Y, Expressed**	(Tan *et al.*, 2009)
PIM-1	Pim-1 kinase	N	(Chen, J. *et al.*, 2009)

Table 5.2 Known hypoxia-induced chemoresistance related genes. *Table showing Gene names, their description and whether they are expressed or repressed in our microarray data.*

Notch-1

Notch-1 expression has been shown to play a role in malignancy in different cancer types by promoting invasion, metastasis and correlated with chemoresistance (Roy *et al.*, 2007, Sahlgren *et al.*, 2008, Nefedova *et al.*, 2004, Nefedova *et al.*, 2008). Several lines of evidence show that hypoxia can mediate Notch-1 activity (Chen *et al.*, 2010, Sahlgren *et al.*, 2008, Zou *et al.*, 2013).

WSB-1

WSB-1 encodes for an ubiquitin ligase, which complexes with other proteins to mediate target gene degradation (Choi *et al.*, 2008). It has been demonstrated that WSB-1 accumulates in hypoxia (1%) in a hypoxic dependent manner in HepG2 cells.

TMEM45A

TMEM45A is a transmembrane protein without clear defined function, however, its expression is found to be upregulated by hypoxia (1%) in a HIF dependent manner in breast cancer cells. Furthermore, the silencing of this gene renders the cells resistant to paclitaxel and etoposide in HepG2 cell (Flamant *et al.*, 2012).

CAIX

In a highly metabolic active tumour, CO_2 and lactic acid builds up due to the increase rate of glycolysis (Raghunand *et al.*, 2003, Gatenby and Gillies, 2004). It is often observed that in hypoxic tumours of many cancer types, CAIX is overexpressed. CAIX is a transmembrane protein located on the extracellular membrane, it is an enzyme which catalyses the

hydration of carbon dioxide to bicarbonate and hydrogen ions. This process increases extracellular acidification (Swietach *et al.*, 2008) and it is associated with resistance to slightly basic drug (McCarty and Whitaker, 2010, Staab *et al.*, 2007, Supuran and Scozzafava, 2000, Said *et al.*, 2013). CAIX expression is HIF dependent and its expression is correlated to tumour progression and poor drug response in several cancer models including GBM and breast cancer (Hui *et al.*, 2002, Chia *et al.*, 2001, Tan *et al.*, 2009, Lou *et al.*, 2011, Wykoff *et al.*, 2000a, Said *et al.*, 2007).

PIM-1

PIM-1 is a serine/threonine kinase phosphorylating genes such as p21 and BAD, thus asserting regulatory roles in cell cycle and apoptosis (Selten *et al.*, 1986, Wang *et al.*, 2002, Aho *et al.*, 2004). In a study performed by *Chen et al.* (Chen, J. *et al.*, 2009), they found that PIM-1 is upregulated in hypoxia in a HIF independent manner, and that PIM-1 expression is associated with cisplatin resistance in pancreatic cell lines under 1 % hypoxic incubation (48h) (Chen, J. *et al.*, 2009).

The set of genes described above were searched individually in our microarray expressed transcript list. We saw no significant expression of *WSB-1* or *PIM-1* which was reported to be upregulated in Hepatoma cell line and pancreatic cell line respectively (**Figure 5.5**) (Tong *et al.*, 2013, Chen, J. *et al.*, 2009). For *Notch-1*, we saw a slight decrease at 64 hours and only a mild increase of ~1.5 fold at 96 hours hypoxia (**Figure 5.5C**).

In agreement with other findings, we did observe an induction of both *TMEM45A* and *CAIX* in hypoxia (**Figure 5.5D & E**) (Flamant *et al.*, 2012, Isa *et al.*, 2006, Tan *et al.*, 2009). *TMEM45A* expression increased continuously for the duration of hypoxic incubation up to 4.5 fold by 64 hours (**Figure 5.5C**). While *CAIX* expression was highest in acute hypoxia (~6 fold) yet its levels remained above ~2.5 fold in chronic hypoxia (**Figure 5.5D**). To conclude, although these results might contribute to the observed resistance in hypoxia, further validation is required.

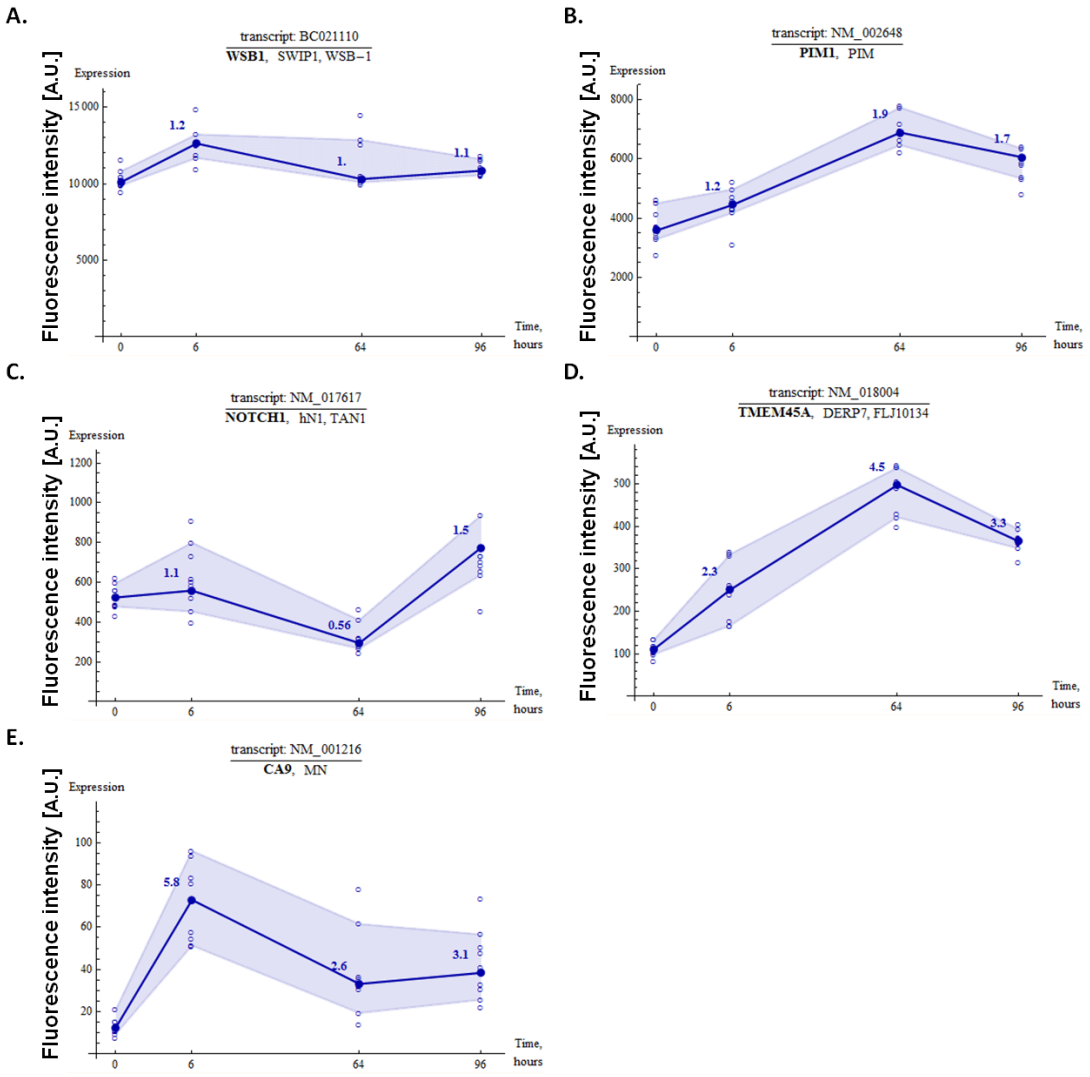

Figure 5.5 Expression plots of WSB-1, PIM-1, Notch1, TMEM45A, CAIX / CA9 transcripts. ***(A)*** *WSB-1* ***(B)*** *PIM-1* ***(C)*** *Notch1* ***(D)*** *TMEM45A* ***(E)*** *CAIX/ CA9 expression plot in chronic hypoxia from our microarray data. The filled circle and dark blue line shows the average expression plot of the transcript. The open circle shows the data point for each individual probe. The shaded blue area shows the range of data variation and the number above the point indicate the fold change normalised to basal ratio (chapter 2.6.3).*

5.2.5 Significantly expressed genes

The gene expression of hypoxic response from the microarray data were further analysed for a global overview. In the next section, only significantly expressed transcripts obtained from **Figure 5.3** were used.

5.2.5.1 Producing heat map clustergrams

Clustergrams are one of the standard ways for visualising microarray results; it is a heat map with dendrograms showing the hierarchical clustering of data. The default MATLAB setting normalise the data over the mean transcript data set, a red colour represents a value above mean, black equals the mean and green represents values below mean. Using MATLAB default clustergram function, a clustergram of the list of significantly regulated genes was produced (**Figure 5.6**).

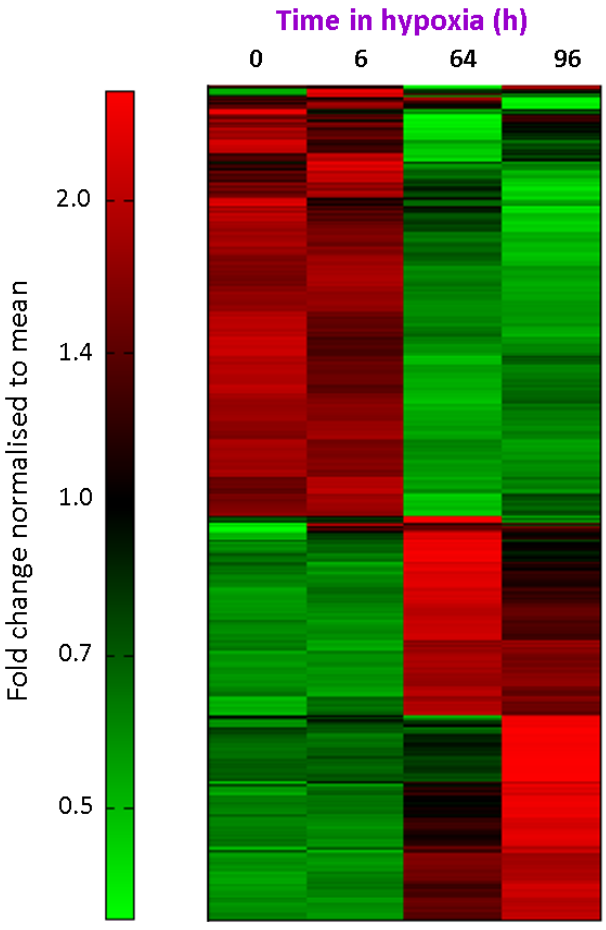

Figure 5.6 A default MATLAB clustergram. *A heatmap of the clustered data result (without dendrogram) showing all significantly upregulated (red) and down regulated (green) transcripts normalised to mean of each data set.*

5.2.5.2 Optimising heatmap clustergrams

From a biological point of view, clustergrams resulted above can be difficult to interpret for two reasons. Firstly, the data are normalised over the mean of the data set, therefore it does not provide a clear visual indication of the relationship of gene expression in hypoxia compared to normoxia, which is what we were aiming to measure. This was resolved by manually dividing the data to normoxic control (T0) as well as suppressing the automatic normalisation function in MATLAB clutergram code (see Appendix 1.2). This enabled us to generate a clustergram where the values (and in terms of colour representation on the clustergram) relative to T0 control (**Figure 5.8**).

Secondly, the default MATLAB method of normalising generates data with a weak separation of fold changes. For example, a two-fold decrease and a three-fold decrease would result in a value of 0.5 and 0.3 respectively. On a linear scale, the number of '0.3' and '0.5' lies relatively close together even though we are examining a two and three fold change. These data will therefore give a low resolution of separation, yielding a non symmetrical scale and making it visually less satisfactory (**Figure 5.7A**). Therefore, the data were log 2 transformed to produce a more symmetrical scale (**Figure 5.7B & C**).

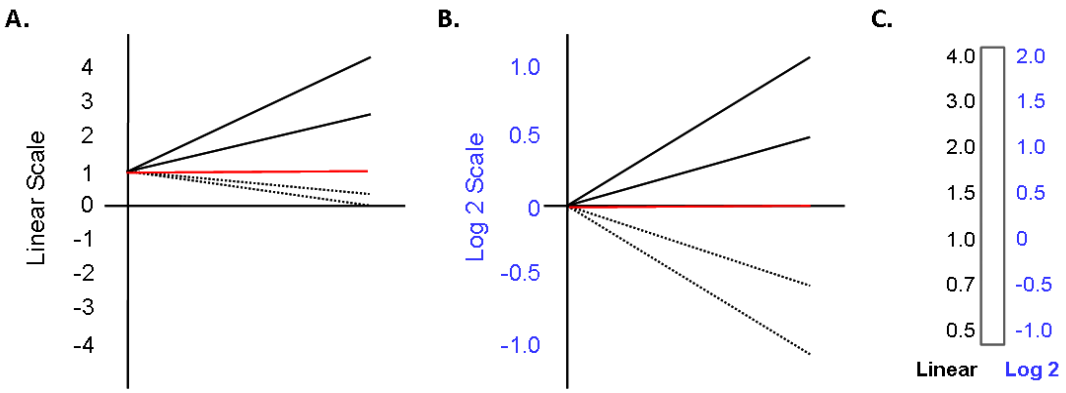

Figure 5.7 A schematic diagram demonstrating the relationship of a linear scale versus a Log2 scale. ***(A)*** *Results as visualised on a Linear scale.* ***(B)*** *Results as visualised on a Log2 scale. Upregulated (black line), Downregulated (dotted line) and control (red line)* ***(C)*** *Conversion of linear to log2 scale.*

Clustergram were reproduced after normalisation to control T0 and transforming the data on a Log2 scale (**Figure 5.8**). We observed very little changes in expression at 6 hours hypoxia (indicated by black colour and lack of red and green). However at 64 and 96 hours, many transcripts were upregulated or downregulated (indicated by red or green colour) (**Figure 5.8**). These results demonstrated that at acute hypoxic time points, there is little differential gene expression compared to longer hypoxic incubation.

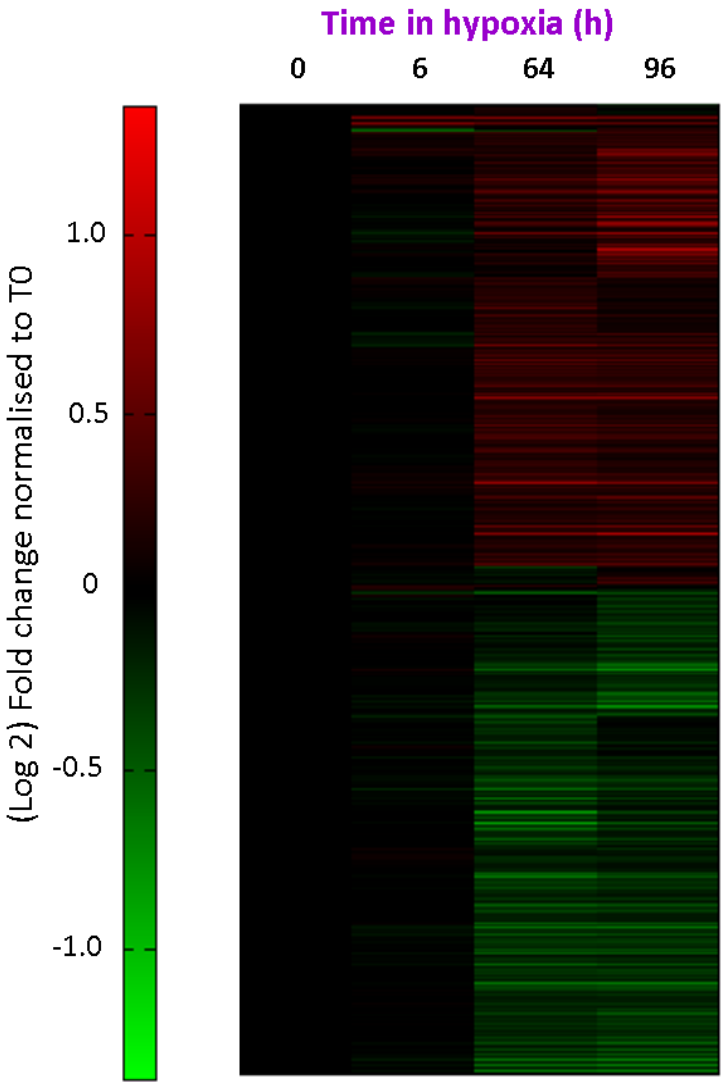

Figure 5.8. Gene expression profile of D283 cells in hypoxia. *D283 cells were incubated in 1% O_2 for 0, 6, 64 or 96 hours. A microarray heatmap of the clustered data result showing all significantly upregulated (green) and down regulated (red) genes normalised to control.*

5.2.6 Expression of p53 and DNA damage genes in chronic hypoxia

We previously described the dampening of p53 activation by etoposide in chronic hypoxia (chapter 4). Using the microarray data, we further examined whether hypoxia affects the expression pattern of p53 signalling pathway components, which could explain the altered p53 activation.

Here, we have used the microarray raw data to generate heat map clustergrams of specific pathways of interest. The raw expression data containing all transcripts from the microarray array were used, therefore the results presented bear no statistical significance (otherwise indicated). The purpose of this analysis was to allow an easier visualisation of the expression of a whole group of genes, rather than separately studying individual expression plots.

5.2.6.1 p53 pathway analysis

The p53 pathway gene list was obtained from KEGG online database (Kanehisa and Goto, 2000, Kanehisa *et al.*, 2012), and their corresponding transcripts IDs were extracted using MATLAB (see Appendix 1.3 for MATLAB codes). This list was matched with the significantly 'expressed transcript lists' (**Figure 5.3**) manually and only the significantly expressed data were selected to produce a readable heatmap clustergram (**Figure 5.9**).

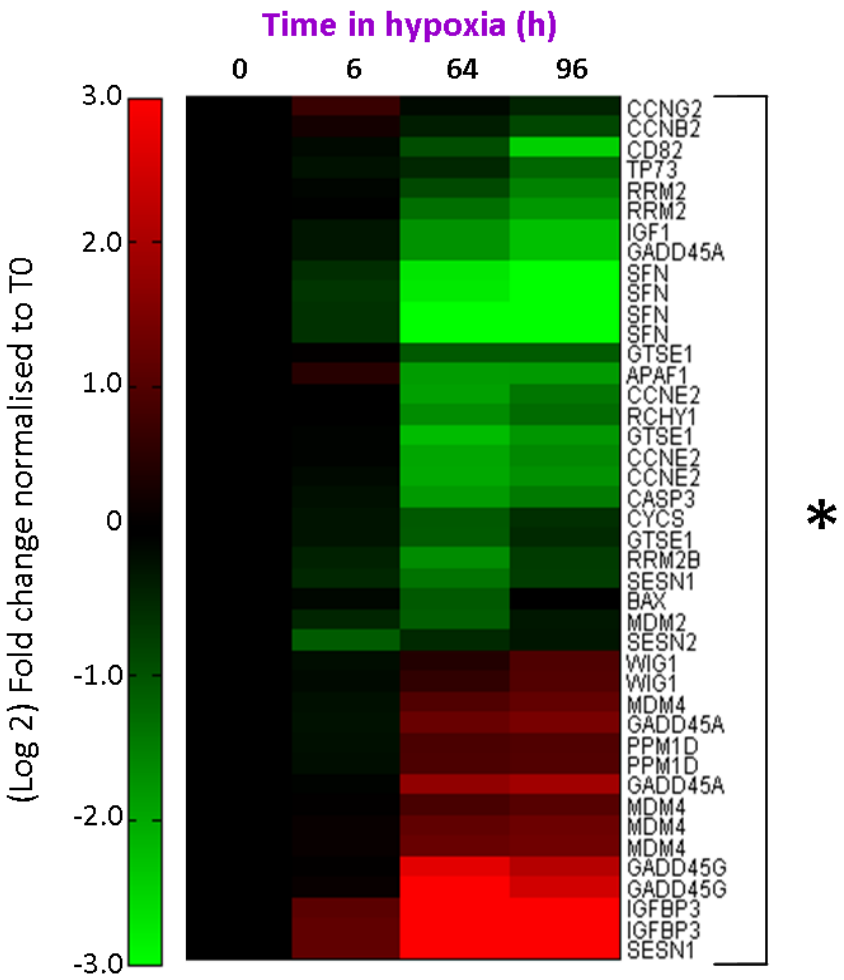

Figure 5.9 Gene expression profile of significantly expressed p53 pathway transcripts in hypoxia. *A heatmap of selected p53 pathway gene lists showing upregulated transcripts (red) and downregulated genes (green) normalised to control (black), *significantly expressed or repressed.*

All 4 transcripts belonging to the *MDM4* gene were expressed up to 2.5 fold (**Figure 5.9**). MDM4 protein is structurally similar to MDM2, it also contains a p53 binding domain and interacts with p53 (Shvarts *et al.*, 1996). However, unlike MDM2, MDM4 does not target p53 for protein degradation but instead regulates p53 transcriptional activity (Toledo *et al.*, 2006). Upon MDM4 binding to p53 N terminal domain, MDM4 inhibits p53 transactivation, thus suppressing p53 mediated apoptotic functions (Francoz *et al.*, 2006, Toledo *et al.*, 2006). Additionally, both transcripts of the *PPM1D* (protein phosphatase, 1D) were also increased by 2 fold (**Figure 5.9**). PPM1D is p53-inducible and it belongs to the serine/threonine phosphatase family (Fiscella *et al.*, 1997, Takekawa *et al.*, 2000). PPM1D is a negative regulator of p38 MAP kinase (MAPK), inhibiting its function by

dephosphorylating p38 at Thr180, and in turn reduces p53 phosphorylation, thus decreasing p53-activated apoptosis (Bulavin *et al.*, 1999, Takekawa *et al.*, 2000). Moreover, PPMID also dephosphorylates both Chk 1 and p53 directly, upon dephosphorylation of both Chk1 and p53, p53 activity is inhibited. Altogether, with the upregulation of both *MDM4* and *PPM1D* mRNA level, this suggests that p53 transactivation might be dampened in chronic hypoxia as observed in chapter 4.

Moreover, there were 21 genes which were significantly downregulated, these included several apoptotic genes: *APAF1* (apoptotic peptidase activating factor 1), *CASP3* (apoptosis-related cysteine peptidase) and *BAX* (**Figure 5.9**). We observed from our clustergram that *APAF1* was reduced by ~3 fold at chronic hypoxia (**Figure 5.9**). *CASP3* transcript was also reduced by ~3 fold in chronic hypoxic incubation. CASP3 is a member of the caspase cascade family, activating caspases 6 and 7 and playing a role in executing apoptosis (Porter and Janicke, 1999, Wang and Lenardo, 2000). Taken together, the induction of negative p53 regulators and a decrease of pro-apoptotic genes in chronic hypoxia might have an implication on resistance to cell death.

5.2.6.2 DSB repair pathways

In chapter 4, we have also observed a reduction in ATM activity and hypothesised that this might contribute to the reduce p53 activation. Here, we investigated further upstream of p53 and probed whether DNA damage sensing is altered in chronic hypoxia.

The list of genes involved in both NHEJ and HR were exported from KEGG online database (Kanehisa and Goto, 2000, Kanehisa *et al.*, 2012). Firstly the gene lists were converted to their corresponding transcripts IDs using MATLAB (see Appendix 1.3 for MATLAB codes). Secondly, the transcripts IDs and their corresponding expression data were used to produce a heatmap clustergram for both the NHEJ (**Figure 5.10**) and HR pathway (**Figure 5.11**).

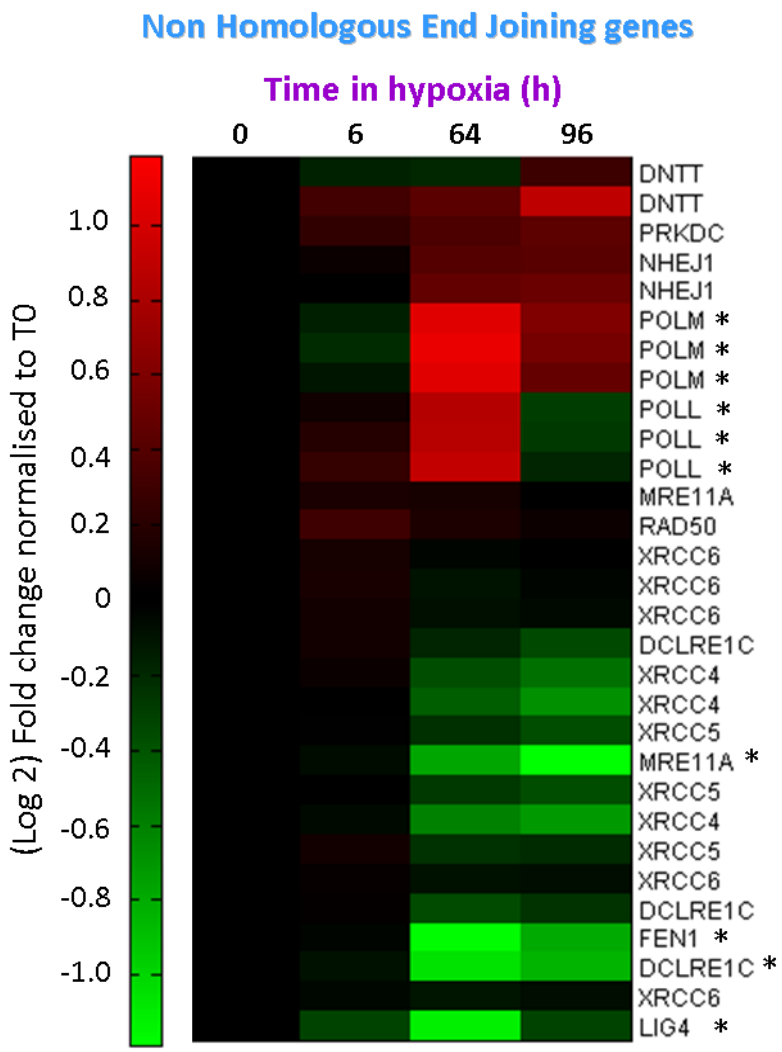

Figure 5.10 Gene expression profile of NHEJ gene transcripts in hypoxia. *A heatmap of NHEJ pathway gene lists showing upregulated transcripts (red) and downregulated genes (green) normalised to control (black),*significantly expressed*

The initial recognition of DSBs in the NHEJ pathway is by Ku70/Ku80 (XRCC6/XRCC5) (chapter 1.6.1.1). The transcripts belonging to these genes were not regulated (**Figure 5.10**), suggesting that DNA sensing by this pathway might not be affected by hypoxia. This supports our finding in chapter 4 where we demonstrated that initial detection of physical DNA damage was not affected by hypoxia. However, there is a reduction of transcripts belonging to other NHEJ key components. One transcript of each of the following genes was down regulated: *DCLRE1C* (Artemis), *FEN1* (flap structure-specific endonuclease 1) and *LIG4* (DNA ligase IV) (**Figure 5.10**) (chapter 1.6.1.1). Artemis and *Fen1* transcripts are both

reduced by ~2 fold at 64 and 96 hours hypoxic time point. *LIG4* is reduced by 2 fold at 64 hours but it was only reduced by 1.2 fold at 96 hours. Both FEN1 and Artemis function as an endonuclease, involved in the end processing and trimming of damaged DNA (chapter 1.6.1.1), while LIG4 is involved in the ligation step of NHEJ repair (Koch *et al.*, 2004) (chapter 1.6.1.1). Although we have observed reduction of some NHEJ repair gene transcripts, not all transcripts of the same gene showed the same expression trend (e.g. GADD45A, SENS1). This could be due to both biological and or technical reasons. Firstly, the probes may target different transcript splice variants of the same gene, thus if the mRNA expression levels of the splice variants differ, this will be reflected in our data. Secondly, the probe set definitions used in the microarray might be inaccurate, or lack specificity and require an update. As our knowledge of accurately mapping genes and transcript improve, an updated probe set will minimise technical errors. Therefore, due to the different expression pattern observed for some of these transcripts, it is not possible to make a firm conclusion of whether chronic hypoxia affects the actual protein expression levels or the functionality of these NHEJ pathway components.

On investigation of the HR pathway, the clustergram showed that only one candidate was significantly upregulated (**Figure 5.11**), the RAD51L1 (RAD51 homolog 2) transcripts, a gene coding for a protein belonging to the RAD51 family (Rice *et al.*, 1997). For downregulated transcripts, we observed that several of the HR repair genes were reduced in chronic hypoxia (**Figure 5.11**), including *BRCA2*. BRCA2 is known to play an important role in maintaining genomic integrity and its mutation leads to susceptibility to breast cancer development (King *et al.*, 2003, Venkitaraman, 2002, Meyn, 1997, Tutt *et al.*, 1999). Molecularly, the role of BRCA2 is to directly interact with RAD51, controlling and meditating RAD51 catalytic activity in aiding strand exchange during HR response (Wong *et al.*, 1997, Marmorstein *et al.*, 1998, Shinohara *et al.*, 1992) (chapter 1.6.1.2).

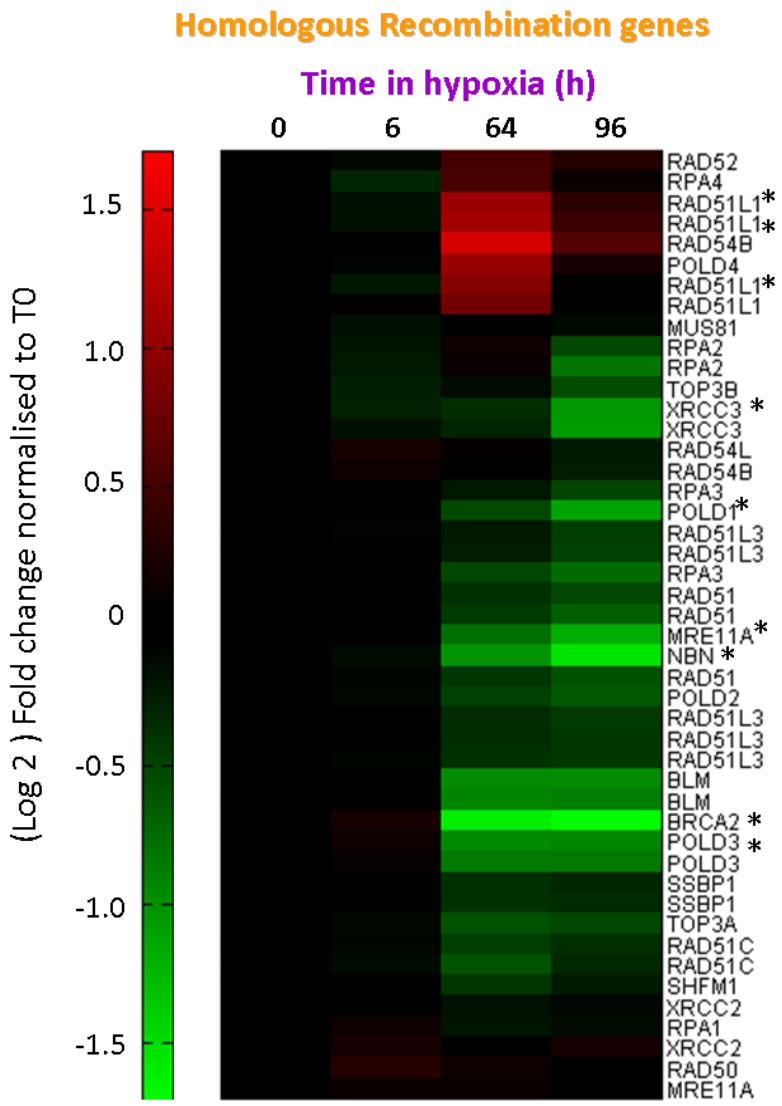

Figure 5.11 Gene expression profile of HR pathway gene transcripts in hypoxia. *A heatmap of HR pathway gene lists showing upregulated transcripts (red) and downregulated genes (green) normalised to control (black), *significantly expressed.*

We further focused on the down regulation on one of the MRN complex components, NBN. As described in chapter 1.6.1.2, NBN plays a key role in ATM activation and signal amplification of the DNA damage response (Cerosaletti and Concannon, 2004, Cerosaletti *et al.*, 2006), reduction of this can explain the dampened p53 response observed in chapter 4.2.4.1 and 4.2.4.2. We therefore hypothesised that this reduction in NBN mRNA levels might be responsible for reduced p53 activation and have further investigated the role of NBN expression in our model.

5.2.7 Microarray target validation

5.2.7.1 Target gene validation by qRT-PCR

The microarray data showed that the NBN mRNA level decreased by 50% after 64 hours of hypoxia and this was further reduced to 30% by 96 hours (**Figure 5.12A**). To validate this result, NBN mRNA levels upon hypoxic exposure were measured by qRT-PCR (**Figure 5.12B**). We have found that the qRT-PCR results were similar to the ones of the microarray. NBN mRNA levels were reduced to 50% at 48 and 64 hours hypoxic incubation. This was further reduced to ~20% by 96 hours hypoxia (**Figure 5.12B**). These results confirmed the decrease of NBN mRNA levels in chronic hypoxia.

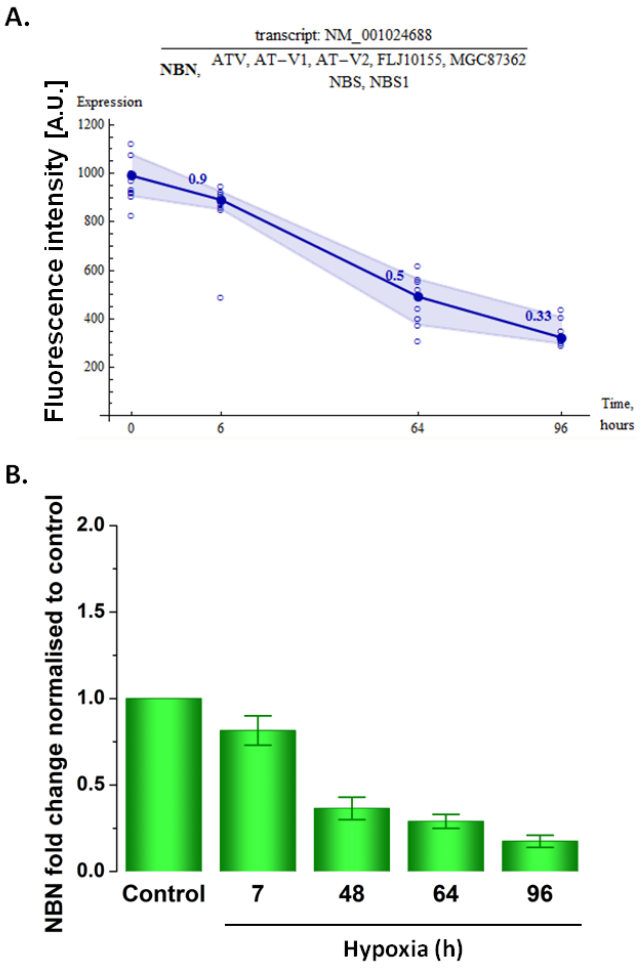

Figure 5.12 Nibrin mRNA levels in chronic hypoxia. *D283 cells were incubated in 1% O_2 in hypoxia as indicated. The transcription of NBN was assessed by* ***(A)*** *microarray. The filled circle and dark blue line shows the average expression plot of the transcript. The open circle shows the data point for each individual probe. The shaded blue area shows the range of data variation and the number above the point indicate the fold change normalised to basal ratio (chapter 2.6.3)* ***(B)*** *qPCR. Nibrin levels measured by qPCR were normalised to T0 and cycA housekeeping gene. Data shown are ± S.E.M of two independent experiments.*

5.2.7.2 Nibrin protein levels in hypoxia

To confirm whether the reduced NBN mRNA translates to a reduction in protein levels, we measured NBN protein expression by western blot. We observed that NBN protein levels were reduced by ~50 % by 64 and 96 hours hypoxia (**Figure 5.13**). These results were comparable to the NBN mRNA levels measured by qPCR (**Figure 5.12B**), supporting the idea that nibrin expression is decreased in chronic hypoxia.

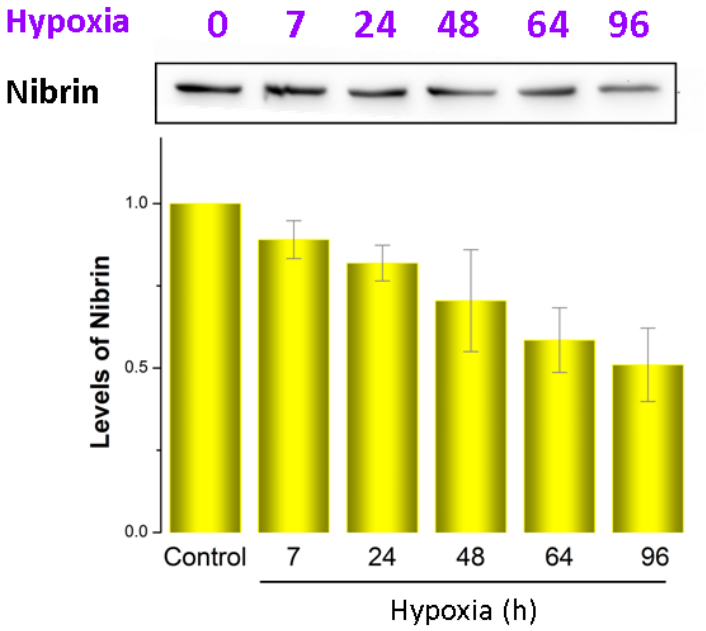

Figure 5.13 Nibrin expression in hypoxia. *D283 cells were pre-incubated in 1% O_2 in hypoxia as indicated. NBN protein levels were assessed by western blot. Western bands shown are representative of three independent experiments. Quantifications of data are ± S.E.M of three independent experiments normalised to control.*

5.2.8 Role of nibrin in other cell lines

We have demonstrated that NBN expression is reduced in chronic hypoxia at both the transcript and protein level in MB. We wanted to further investigate if this is a common event in other brain tumours and how these changes could be correlated with drug resistance. We examined NBN protein levels in the U87 GB cell line (in which we observed a reduction in p53 transactivation by etoposide in hypoxia as well as increased resistance) and a neuroblastoma cell line, SK-N-AS. *In the following section the work on SK-N-AS cell line was performed by another lab member Dr Catherine Heyward.*

The cell lines were incubated for duration of up to 5 days of hypoxia. Similar to D283 cells, the NBN protein levels in U87 cells were reduced by 50% and 30% at 3 and 5 days of hypoxia respectively (**Figure 4.16**) and this was correlated with an increase in resistance to etoposide (Figure 4.18) (**Figure 5.15A**). However, for the neuroblastoma cell line, no significant difference in nibrin levels were measured up to 5 days of hypoxic incubation (**Figure 5.14B**). Interestingly, we have observed no changes in chemosensitivity for this cell line up to 48 hours of etoposide [20µM] treatment (**Figure 5.15B**). These data suggest that the presence of changes in NBN mRNA expression in hypoxia might be correlated to the acquired drug resistance.

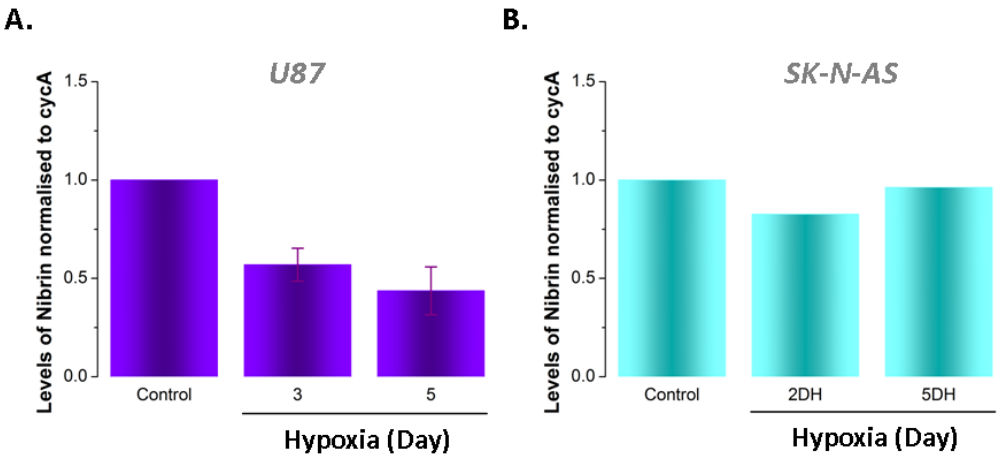

Figure 5.14 Nibrin mRNA levels in other brain tumour cell lines in hypoxia. ***(A)*** *U87 (GB)* ***(B)*** *SK-N-AS (neuroblastoma) cell lines were incubated in normoxia or 1% O_2 in hypoxia, treatment as indicated. The transcription of NBN was assessed by qPCR. Nibrin levels were normalised to T0 and cyclophilin housekeeping gene. Data shown are ± S.E.M of four independent experiments for U87. Data for SK-N-AS is from one experiment.*

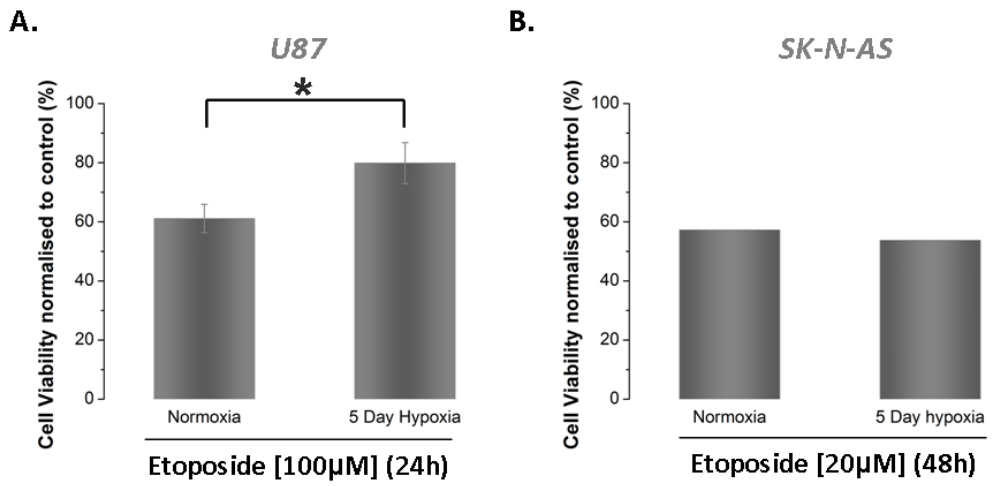

Figure 5.15 Cell viability assay of U87 and SK-N-AS cells chronic in hypoxia. ***(A)*** *U87 (GB)* ***(B)*** *SK-N-AS (neuroblastoma) cell lines were incubated in normoxia or 1% O_2 (hypoxia), treatment as indicated. The percentage of cell viability was measured by MTS assay (for U87)/ MTT assay (for SK-N-AS) over the untreated control. Data shown for U87 are the mean ± S.E.M of three independent experiments. One-way ANOVA followed by Bonferroni test was performed (* indicates p<0.05). Data for SK-N-AS is from one experiment.*

5.3 Chapter 5 Discussion

5.3.1 HIF kinetics

We have observed a transient HIF expression peak at an early hypoxic time point agreeing with other studies (section 5.1.2). The resolution of HIF-1α is due to its negative feedback system with PHDs enzymes being up-regulated by HIF (Berra *et al.*, 2003, Henze *et al.*, 2010, Minamishima *et al.*, 2009, Stiehl *et al.*, 2006). Other regulatory mechanisms involving miRNA expression have also been suggested (Bruning *et al.*, 2011), *Bruning et al.* have shown that HIF-1α expression is also under a negative feedback regulation by a miRNA (miR-155), controlling HIF-1α expression at the mRNA level (Bruning *et al.*, 2011).

Interestingly, we observed a secondary and third peak at later hypoxic time points, which, to our knowledge have never been previously reported. We have also demonstrated that this late HIF-1α accumulation is associated with long lasting transcription of specific HIF target genes such as VEGF and EPO. *Kamat et al.* studied HIF-1α expression and functions under long term but using very mild hypoxia (15%) in human epithelial cells (Kamat *et al.*, 2007). They showed that HIF-1α protein is still detectable after 14 days of hypoxic incubation, but they did not have any other time point over the 14 days (Kamat *et al.*, 2007). They showed that this induction was not due to an increase in HIF-1α transcription. Additionally, HIF targets such as VEGF, GLUT-1 were also measured on both the protein and mRNA levels, suggesting that HIF-1α might still be functionally active after a very long period (Kamat *et al.*, 2007). In another study with neuroblastoma cells, the authors investigated HIF-1α expression in a gradual decrease of oxygen concentration from 5% to 1% during a 72 hours time course and compared it to an acute (24 hours) 1% hypoxia (Lin *et al.*, 2011). They have found that acute hypoxia induced a strong HIF protein expression but only barely detectable HIF-1α levels were measured for the gradual decrease oxygen levels. Upregulation of VEGF transcription was measured under these conditions (Lin *et al.*, 2011). Although the settings of both of these studies are different to ours, these results provide evidence that HIF signalling is capable of remaining 'active' in chronic hypoxia and potentially playing long lasting roles in cellular signalling during prolonged low oxygen conditions.

5.3.2 Hypoxia-induced chemoresistance genes

Hypoxia acquired chemoresistance in tumours has been shown to be correlated with HIF-1α induced multidrug resistance genes in a wide range of cancer, including breast, gastric, liver, lung and brain (Doublier *et al.*, 2012, Liu, L. L. *et al.*, 2008, Zhu *et al.*, 2005, Xia *et al.*, 2004, Brown *et al.*, 2006, Hao *et al.*, 2008, Chen, L. *et al.*, 2009). Several reports have addressed the direct evidence of HIF-1α and MDR1 expression. One of the earliest studies performed by *Comerford et al.* showed that epithelial cells incubated in hypoxia (2.5%) induced a 2 fold induction of MDR1 at 6 hours and a 7 fold increase by 18 hours. They also showed that MDR1 induction is via HIF-1α binding to *MDR1* gene and subsequent MDR1 expression was correlated to the drug resistance observed (Comerford *et al.*, 2002). This direct relationship of HIF-1α inducing a multidrug resistance gene was also reported by *Doublier et al.* (Doublier *et al.*, 2012). They demonstrated an induction of HIF-1α expression in MCF-7 breast cancer cells cultured in 3% hypoxia for 24 hours, associated with HIF-1α binding to the *MDR1* promoter. This was again linked to doxorubicin resistance (Doublier *et al.*, 2012). In another study, resistance to doxorubicin-induced apoptosis was observed in GBM cells and this was associated with HIF-1α induced MDR1 expression (Nardinocchi *et al.*, 2009).

In other studies where oxygen concentrations used were closer to our own study, *Liu et al.* have also demonstrated that HIF-1α induces both MDR1 and MRP expression under 1% O_2 for as short as 8 hours, in gastric cancer cell line (Liu, L. L. *et al.*, 2008). This hypoxia-induced MDR1 can be prevented by siRNA HIF-1α knockdown. Furthermore, overexpression of HIF-1α increased viscritine resistance, while knockdown increased cells sensitivity to drug treatment (Liu, L. L. *et al.*, 2008). Similarly, *Li et al.* have shown that breast cancer cell lines incubated in 1% hypoxia for 12 hours displayed resistance to methotrexate (Li *et al.*, 2006). Moreover, cell lines with a HIF-1α knockdown by shRNA had shown a reduction of MDR1 expression in a time dependent manner, once again demonstrating MDR1 dependency on HIF-1α. This was further correlated to increased sensitivity to drug treatment (Li *et al.*, 2006). However, in our hands with MB where we have incubated the cells at 1% hypoxia for duration of 96 hours, we did not observe regulated expression of MDR1, MRP1 or ABCG1 in acute or chronic hypoxic time points. Our findings are supported by other reports where the authors have observed hypoxia-induced resistance, but no expression of multidrug resistance genes (Jogi *et al.*, 2004, Liang, 1996). In one case, *Jogi et al.* has measured a decrease in MDR1 expression in their microarray study, where a neuroblastoma cell line was incubated in hypoxia 1% for 72 hours (Jogi *et*

al., 2004). Interestingly, another study by *Liang et al.* demonstrated that glioma cell lines in hypoxia (0.001% O_2) for 24 hours followed by 12 hours reoxygenation, became more resistant to BCNU and cisplain, without increased expression of MDR1 or MRP1 (Liang, 1996). Taken together, although some reports have demonstrated the association and correlation of HIF-1α, MDR1 and chemoresistance, this is clearly not a general mechanism.

Several studies suggest that there are alternative mechanisms for increased drug resistance in hypoxia. One proposed explanation is that HIF-1α can mediate resistance via apoptosis inhibition by altering expression of proapoptotic and anti-apoptotic genes. *Erler et al.* has demonstrated hypoxia down regulates Bid, Bax in a HIF-1α dependent manner and this is associated with hypoxia-induced drug resistance in colon carcinoma (Erler *et al.*, 2004). Similarly, *Sermeus et al.* have shown that hypoxia inhibits the upregulation of Bax and Bak (Sermeus *et al.*, 2008, Sermeus *et al.*, 2012). Additionally, HIF-1α dependent Notch expression increases pro-survival gene expression (Bcl-2 & Bcl-xL) (Zou *et al.*, 2013). Moreover, in some cases, inactivation of HIF-1α did not sensitise cancer cells to drug treatments, thus challenging the direct role of HIF-1α in chemoresistance (Hussein *et al.*, 2006).

5.3.3 DNA repair in hypoxia

DSBs are repaired by NHEJ and HR pathways, defects and inhibition of these mechanisms have been linked to genomic instability and tumourgenesis (Thompson and Schild, 2001, Stark *et al.*, 2004, Bertrand *et al.*, 2003). The effect of hypoxia on these responses is not well studied. We have observed from our data that some genes belonging to the HR pathway are regulated in chronic hypoxia. The regulation of NHEJ related genes in hypoxia is less conclusive in both our own observations and studies perform by others. There is only one study, which suggests that NHEJ is upregulated in hypoxia. *Um et al.* has shown that acute (4 hours) hypoxia of 1% O_2 increases Ku70 and Ku80 expression in hepatoma cells (Um *et al.*, 2004). Yet, in another study, incubation in 0.2% O_2 up to 72 hours has shown no change in protein expression of essential NHEJ genes (Meng *et al.*, 2005).

On the other hand, the expressions of HR genes in hypoxia has been better documented. It is generally agreed that HR gene expression is reduced in chronic hypoxia. *Meng et al.* have shown that in prostate cancer cells treated in 0.02% O_2 for 72 hours, both the mRNA synthesis and protein levels of several HR genes including *RAD51*, *BRCA1* and *BRCA2* were

downregulated (Meng *et al.*, 2005). The regulation of HR gene transcription in hypoxia is suggested to be through the alteration of transcription regulators and/or repressors (Iwanaga *et al.*, 2004, Bindra *et al.*, 2005). For example, it has been demonstrated that the reduction of Rad51 is due to a switch of E2F transcriptional activation to repression (Iwanaga *et al.*, 2004). The idea of translational repression as the base of decreased HR protein expression is also supported by other models (Chan *et al.*, 2008, Wouters *et al.*, 2004).

How these changes affect the actual repair and downstream pathway is not well characterised and it is important to consider the protein expression as well as to perform functionality studies beyond gene expression levels to make any further conclusion.

5.3.4 Role of nibrin and p53

Currently, the majority of studies on DNA repair and chemotherapeutic response are performed under normoxic or anoxic conditions. It is generally agreed that cancer cells with a functional repair response are less sensitive to treatment in particular to ionization radiation (Abbott *et al.*, 1998, Takata *et al.*, 1998, Mahaney *et al.*, 2009). The consensus is that DSBs induced by DNA damaging agents are repaired more effectively, allowing the cells to continue to proliferate post repair. For example, mutations in both or either two of the HR component, BRCA1 and BRCA2 (Powell and Kachnic, 2003) accounts not only for breast cancer susceptibility (Peto *et al.*, 1999) but also increased sensitivity to cancer treatment such as mitomycin (Moynahan *et al.*, 2001, Bhattacharyya *et al.*, 2000, Bartz *et al.*, 2006, Treszezamsky *et al.*, 2007). There is one study, which demonstrated that chronic hypoxia-induced HR defective cells were more sensitive to ionization radiation, to drugs such as cisplatin and mitomycin C (Chan *et al.*, 2008). These studies are in contrast to our results where we have observed a reduction in expression of some of the HR components, namely NBN and MRE11, but an increase in resistance.

NBN is an important protein which plays an essential part of the HR pathway (Tauchi *et al.*, 2002). NBN's role is to activate ATM and recruit ATM to break sites. Moreover, NBN and ATM phosphorylate each other, together amplifying downstream signals including p53 (Gatei *et al.*, 2000). Hence we proposed the idea that a reduction of NBN and ATM expression might reduce p53 activation (chapter 4). Although NBN is not generally directly listed as part of the p53 pathway, it is clear that NBN is upstream of p53 and that there are

links between these two components. There is evidence which also suggest that NBN mutations are directly associated with *TP53* gene inactivation (Huang *et al.*, 2008). It is considered that *TP53* gene mutation is a secondary effect of *NBN* mutations. The evidence came from a MB tumour sample from a patient, which was assessed for genetic mutation, only a *NBN* mutation was found. When a second biopsy sample was taken from the same patient 2 years later, the screening showed additional new mutations which included *TP53* (Huang *et al.*, 2008), suggesting that *NBN* mutations might drive genomic instability. However, the definite role of NBN on p53 will have to be ascertained in the future by knockdown and expression experiments.

5.3.5 Prognostic value of nibrin

In MB, therapy responses due to NBN mutation is not understood but there are two case studies, which showed that MB patients with Nijmegen Breakage Syndrome (NBS) are more sensitive to radiotherapy (Bakhshi *et al.*, 2003, Kraakman-van der Zwet *et al.*, 1999). In other cancers, *Eich et al.* have demonstrated that human lymphoblastoid cells and human fibroblasts derived from NBS patients were more sensitive to methylating cancer drugs (Eich *et al.*, 2010). These results are in contrast to our hypothesis, but we have to be cautious with direct comparison to NBS cancer patients. As in the case of NBS, NBN is mutated and non-functional, while in our case, NBN is reduced in level of expression only.

Currently, the exact correlations of NBN expression and treatment outcome have shown contradictory results. In some cancer models, overexpression of NBN is associated with more aggressive cancer types and poor prognosis (Yang, M. H. *et al.*, 2006, Ehlers and Harbour, 2005, Le Scodan *et al.*, 2010). These observations concluded that cancer cells are more proficient in recognising DNA damage, increase DNA repair and thus become resistant to treatment. Conversely, other clinical studies revealed that expression of NBN or an intact MRE11 complex is essential for good treatment outcome (Kuo *et al.*, 2012, Soderlund *et al.*, 2007, Gao *et al.*, 2008, Choudhury *et al.*, 2010). These later studies support our own and can be explained by the downregulation of NBN or MRE11 components, which reduces the cells ability to recognise DNA damage thus failing to induce cell cycle arrest and apoptosis. The discrepency of these studies can be due to different cell types, where basal levels of these components are not the same; cancer cell samples obtained at different stage of the disease; the definition of overexpression; and importantly how these measurements are obtained. For example, *Yang et al.* took the staining measurement of

NBN abundance in both the cytoplasm and nucleus (Yang, M. H. *et al.*, 2006), whilst others only took nuclear intensity into account (Soderlund *et al.*, 2007). Here, we have demonstrated that higher nibrin expression were correlated with better chemosensitivity response in the different brain tumour types. We therefore propose that it might be possible to use NBN expression as a prognostic marker for brain tumour response to drug.

Chapter 6: Global Gene Expression in Acute and Chronic Hypoxia

6.1 Introduction

Following the biased examination of drug resistance genes in attempt to explain the observed etoposide resistance of MB cells in chronic hypoxia, we took a more general approach to analyse the microarray data for a global gene expression overview.

Although there are other studies of gene expression profiles in hypoxia, these are either comparing the severity of hypoxia or only performed after relatively short hypoxic exposure, i.e. generally 18-24h (Ragel *et al.*, 2007, Wykoff *et al.*, 2000b, Koong *et al.*, 2000). Gene expression profiling of chronic hypoxia is under explored and currently there are no reports on MB. To better evaluate, the broad implications of hypoxia on cells in hypoxia, we have decided to analyse the global changes in gene expression by biological functional analysis.

The aim of this chapter is to investigate the global cellular response to hypoxic exposure and to especially focus on genes and pathways potentially contributing to tumourgenesis in MB.

Aims:

1. To carry out genome-wide investigation of acute and chronic hypoxia induced genes in D283 cells

2. To perform biological pathway analysis and achieve a global perspective of the effect of acute and chronic hypoxia on MB cells

3. To perform upstream analysis of chronic hypoxia on MB cells

6.2 Results

6.2.1 Microarray further analysis

In an earlier chapter (4.2.2.1), we observed that hypoxia-induced resistance required chronic hypoxia. Here, we further explore gene expression under acute and chronic hypoxic conditions to elucidate the implication of chronic hypoxia on MB cells.

6.2.1.1 Profile Clustering by hypoxic time points

A 'Profile search' function was added to the MATLAB code to allow us to obtain an output list of expressed transcripts at a particular time point, which can be used for further functional analysis. Profile clustering was achieved by adding a simple 'binary code' within our microarray analysis coding. The output search profile was then grouped by each or a combination of time points to allow better visualisation of genes up- or down- regulated during a given time frame.

The ordering (left to right) of the binary codes corresponds to the hypoxic time points 0, 6, 64 and 96 hours. In the binary code, it is set to be '1', '0' or '-1', where '1' means the data have met the criteria of ≥two fold upregulation; '0' means criteria not met; and '-1' means data met criteria of ≥two fold downregulation. Some possible binary code combinations are illustrated in **Figure 6.1**. As we are interested to differentiate between the gene expressions in acute and chronic hypoxia, we have manually altered the MATLAB binary codes between each run to generate transcript lists up- and down-regulated at early and late hypoxic time points.

A.

Time (h)	0	6	64	96
Profile search	[0,	0,	0,	0]
	[0,	1,	0,	0]
	[0,	0,	1,	0]
	[0,	0,	0,	1]
	[0,	1,	1,	0]
	[0,	0,	1,	1]
	[0,	1,	0,	1]
	[0,	1,	1,	1]

B.

Time (h)	0	6	64	96
Profile search	[0,	0,	0,	0]
	[0,	-1,	0,	0]
	[0,	0,	-1,	0]
	[0,	0,	0,	-1]
	[0,	-1,	-1,	0]
	[0,	0,	-1,	-1]
	[0,	-1,	0,	-1]
	[0,	-1,	-1,	-1]

Figure 6.1 Binary combination for Profile searches. *Hypoxic time points are across the top row of the table. Rows underneath are some possible binary combinations for a given profile search.* ***(A)*** *Upregulated transcripts. For example, first line are transcripts, which are not expressed in hypoxia (**Figure 5.3**); second line for transcripts upregulated at 6 hours only; third line for transcripts upregulated at 64 hours only.* ***(B)*** *Downregulated transcripts. For example, second line for transcripts downregulated at 6 hours only; third line for transcripts down regulated at 64 hours only and fifth line for transcripts downregulated at both 64 and 96 hours hypoxia.*

Taking into account that a gene can have more than one transcript, we have here condensed the output transcript lists by grouping them into their corresponding gene names. The gene lists resulting from of all the profiles analysed were used to produce Venn diagrams for both up/down regulated genes (**Figure 6.2**). We first examined genes, which were expressed at a single time point and at that time point only. We observed an upregulation of 28 genes at 6 hours hypoxia only, the expression of these genes returned to a non-significant expression level for the remaining duration of the hypoxic time course. At 64 hours, 401 genes were upregulated, these genes were not regulated before or after this time point. Lastly, there were 625 genes which were upregulated at the 96 hours hypoxic time point but they are not expressed at 6 or 64 hours (**Figure 6.2A**). For the hypoxia repressed genes at each individual time point, there were 4 genes which were downregulated at 6 hours, 590 genes at 64 hours only and 551 genes at 96 hours (**Figure 6.2B**).

When we analysed genes expressed at 2 different time points, interestingly, the highest number of genes regulated was seen at the joint time points of 64 and 96 hours, where

~900 genes were upregulated and over ~1000 genes were downregulated at both of these times (**Figure 6.2**). Of note, the total number of genes which were upregulated at 96 hours will therefore be the combination value of 625 genes (upregulated at T96) plus 927 genes (upregulated at T64& 96). These results demonstrate that chronic hypoxia has a larger influence in genetic expression than acute hypoxia and this is likely to affect the cellular response of cells cultured under these conditions.

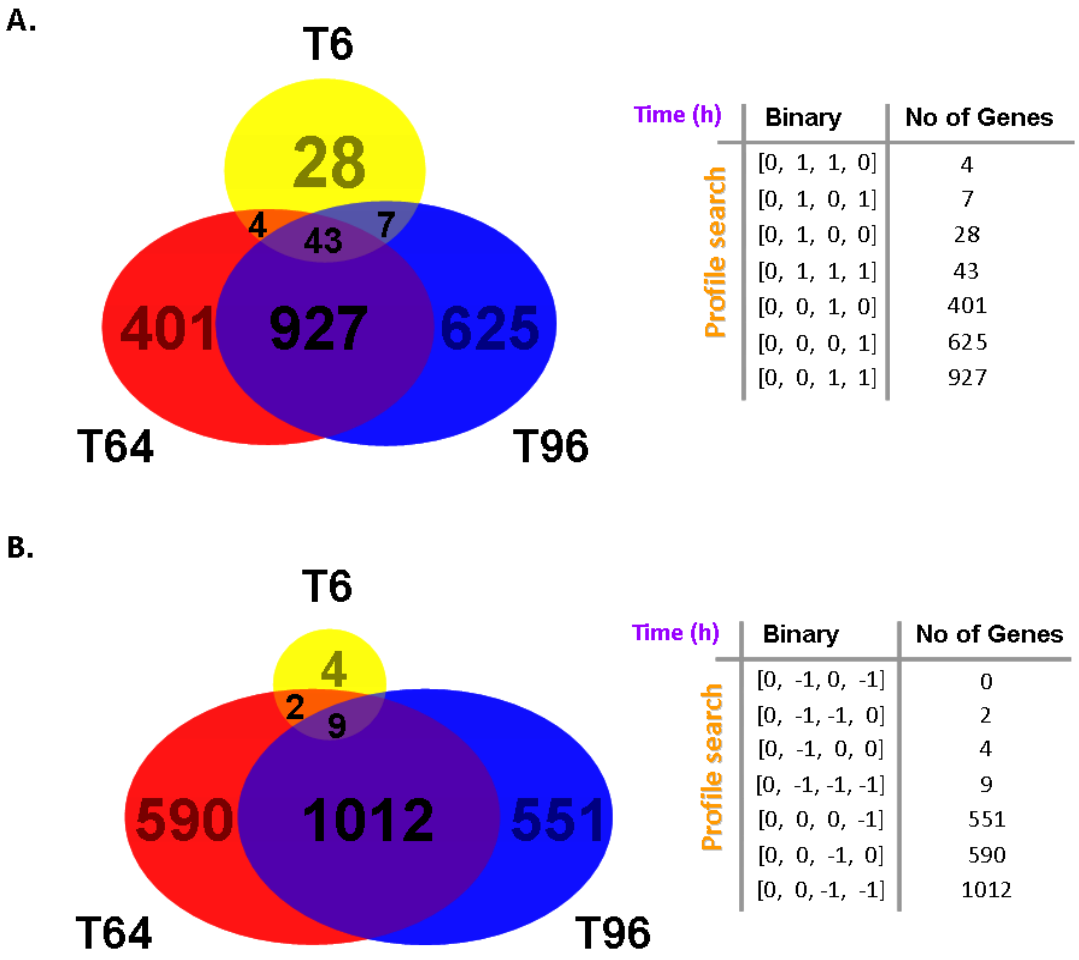

Time (h)	Binary	No of Genes
Profile search	[0, 1, 1, 0]	4
	[0, 1, 0, 1]	7
	[0, 1, 0, 0]	28
	[0, 1, 1, 1]	43
	[0, 0, 1, 0]	401
	[0, 0, 0, 1]	625
	[0, 0, 1, 1]	927

Time (h)	Binary	No of Genes
Profile search	[0, -1, 0, -1]	0
	[0, -1, -1, 0]	2
	[0, -1, 0, 0]	4
	[0, -1, -1, -1]	9
	[0, 0, 0, -1]	551
	[0, 0, -1, 0]	590
	[0, 0, -1, -1]	1012

Figure 6.2 Venn diagram showing up/down regulated genes at each hypoxic time point. *D283 cells were incubated in 1% O_2 for 0, 6, 64 or 96 hours. Data were analysed using MATLAB binary code profile search functions.* ***(A)*** *Upregulated genes. For examples, 28 genes are upregulated at 6 hours only; 401 genes are upregulated at 64 hours only; and 927 genes are upregulated at combined time point of 64 and 96 hours* ***(B)*** *Downregulated transcripts. For examples, 4 genes are downregulated at 6 hours only; 590 genes are downregulated at 64 hours only; and 1012 genes are downregulated at combined time point of 64 and 96 hours.*

6.2.1.2 Grouping by expression pattern using k-means clustering

We have demonstrated that the clustering by hypoxic time points results in a large list of genes which are expressed or repressed in chronic hypoxia. In order to resolve this further into smaller clusters, we took the pattern of expression profile into account and performed clustering using another method. This allowed us to better deduce whether there is a correlation between a groups of genes with similar expression dynamics in relation to their biological functions. The significantly expressed transcripts were clustered by their expression pattern using a method called *k*-means clustering. *k*-means is a partition method based on actual observations, treating data as an object belonging to a location in space. The data (observations) are separated into *k* number of cluster using an iterative algorithm. Initially, *k* means are computationally generated within the data domain, ideally placing the means as far away from each other as possible. Then each observation (objects) in the data are associated with the nearest *k* mean thus partitioning into the defined number of *k* clusters. After the initial *k* clusters partitioning, a new mean is calculated for each of the cluster, this will be the centroid of all the objects within that cluster. The process of associating each object with the nearest *k* means and recalculating new *k* cluster centroid is repeated till the sum of distances of every object within one cluster to the centroid is minimised. The final *k* clusters would then be produced when the algorithm has converged, producing the most possible well-separated compacted clusters.

We have utilised MATLB built in *K*-means function, "kmeans" algorithm to run a 16 partition clustering using the default settings with the exceptions of parameters listed in **Table 6.1**.

Parameter	Value	Description
'replicates'	*15*	Number of times to repeat the clustering, each with a new set of cluster centroid position
'display'	*final*	Level of display output

Table 6.1 Alterations to k-means clustering parameters. *The number of replicates is set to '15', this increase in repeated clustering ensures a good separation of all the transcripts with similar expression patterns. The display is set as final, meaning that only the final output of the clustering analysis is exported.*

The 16 *k*-means clusters generated are shown in (**Figure 6.3**). Each cluster display the expression plot of each of the transcripts grouped to that cluster due to mean normalisation. Although some of the expression trends look similar between clusters, the data actually fall on different scales. For example, to look at upregulated transcripts in hypoxia, candidates from both cluster 8 and 14 should be considered.

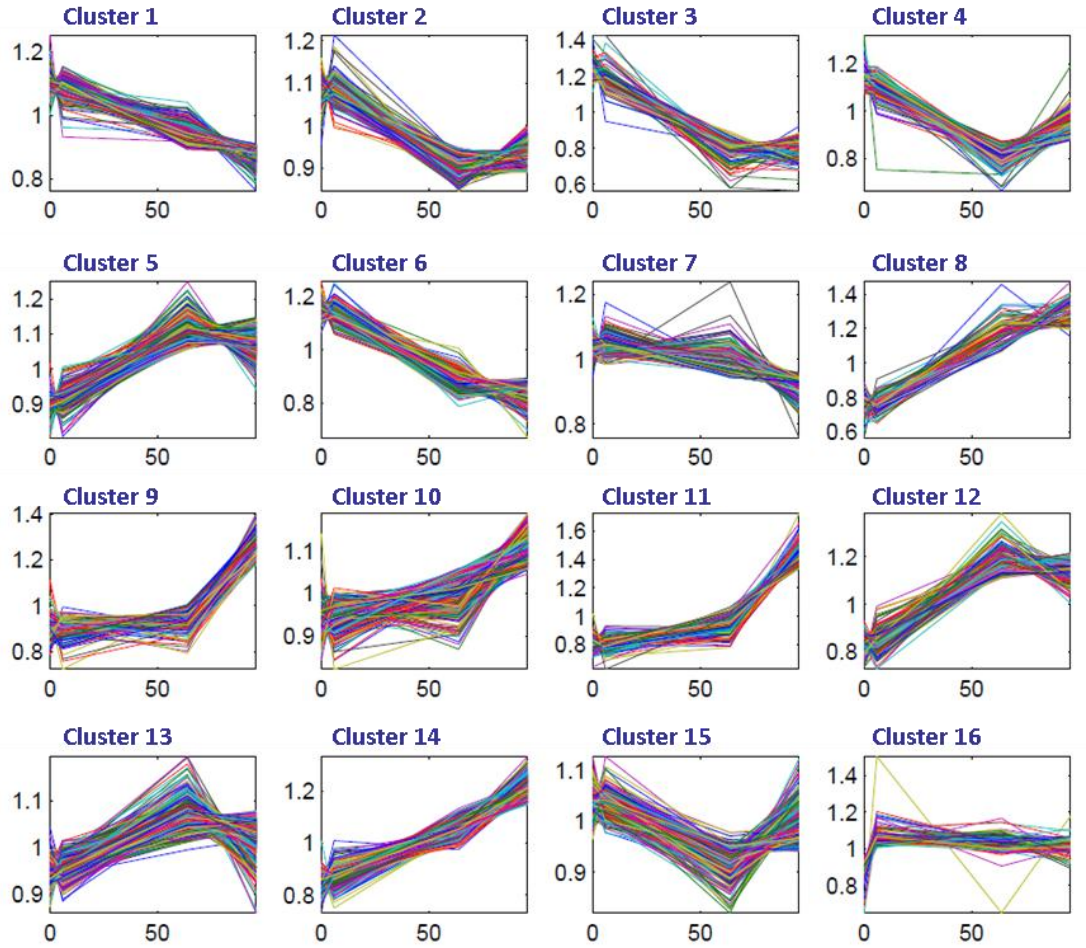

Figure 6.3 MATLAB k-mean clustering output. *Significantly expressed transcripts are clustered into one of sixteen clusters. Transcripts with similar expression pattern and level of expression in hypoxia are grouped together in the same cluster.*

6.2.2 Biological analysis of acute and chronic hypoxia gene expression

The genes clustered by time points or by *k*means described resulted in large lists of transcripts, which necessitated further classification to deduce meaningful biological significance. Using the expression data clustered by time points, functional analysis were carried out with Ingenuity Pathway analysis (IPA) software. The basis of IPA analysis software relies on the utilisation of a database (IPA Knowledge Base) generated from published literature to predict biological functions. Due to limited access of IPA software and time constraints, the clustered results from *k*means were not used for further analysis. Here, we compared the effect of acute (T6) and chronic (combined T64 and T96) hypoxia on biological functions.

6.2.2.1 Network and canonical pathway analysis in acute hypoxia

The IPA Network analysis uses an algorithm to connect the interaction between genes within our data set, however this interaction is linked without functional directions. Nevertheless, highly-interconnected networks are accepted to represent a more trusted genuine biological interaction. We have first used this analysis function to deduce the connection between the molecular networks of regulated genes in acute hypoxia. Noticeably, the network diagram indicated several connections involving HIF-1α and related genes (**Figure 6.4**). HIF-1α is connected to *EGLN3* and *PFKFB3* (6-phosphofructo-2-kinase/fructose-2, 6-biphosphatase 3). This is as expected as both of these are HIF-1α downstream targets (Obach *et al.*, 2004). Additionally, we can see a connection between *PLOD2* (procollagen-lysine) and *PPP1R3B* (protein phosphatase 1, regulatory subunit 3B) to HIF-1α through links with *NEDD9* (neural precursor cell expressed). *NEDD9* is a HIF-1α regulated gene which mediates cell migration (Kim, S. H. *et al.*, 2010). Moreover, we saw that 7 other genes in our data are interlinked in this network, meaning altogether, ~30% of our upregulated genes in acute hypoxia are able to show an interconnection with HIF-1α, providing confidence that the cells displayed a clear hypoxic response.

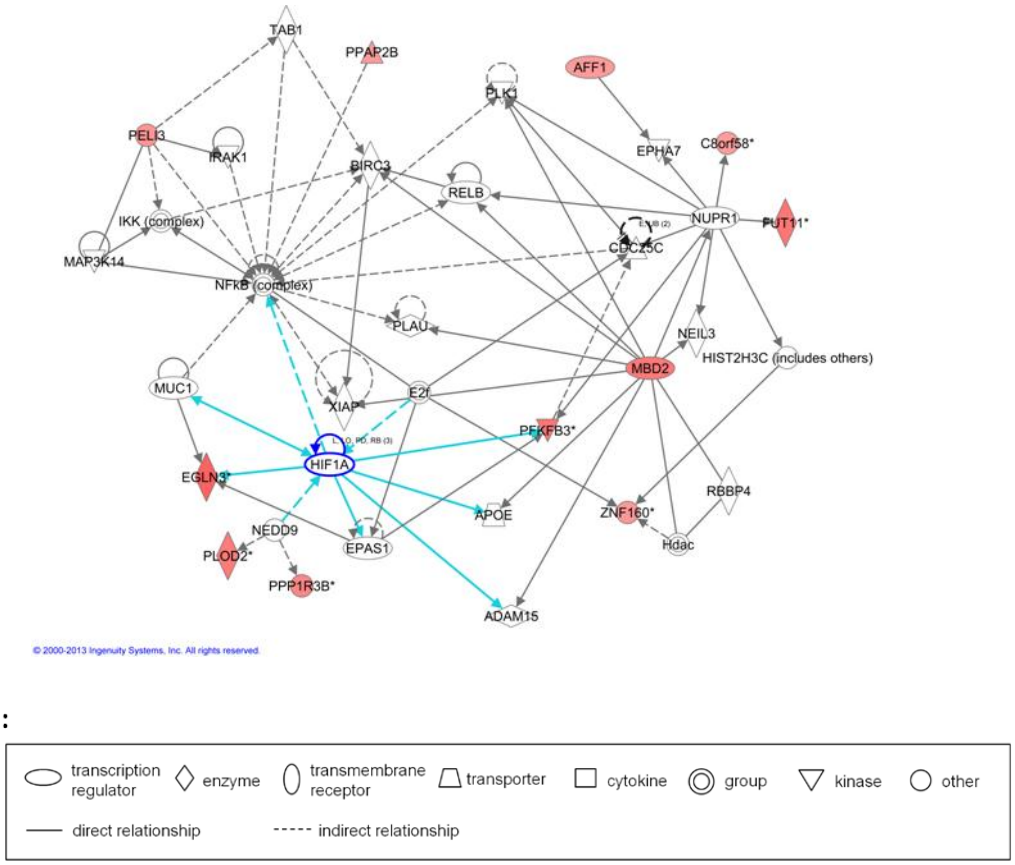

Figure 6.4 Network connection of upregulated genes in acute hypoxia. *IPA network analysis linking the genes interaction in our acute hypoxia expression data. The connections with HIF-1α are highlighted in light blue demonstrating a direct connection with two of its target genes, EGLN3 and PFKFB3. Genes highlighted in red are upregulated in our data at 6 hours hypoxia.*

We next examined the canonical pathways which are affected in acute hypoxia. IPA Canonical pathways are pre-generated based on literature before our results were input. Upregulated gene list in acute hypoxia was uploaded and compared to these known pathways in IPA. Statistical analyses are performed by IPA using Fisher's Exact p-value methods (chapter 2.6.3.4). The number of genes expressed in our data is calculated over the total number of genes involved in that pathway and expressed as a 'Ratio'. For acute hypoxia, the predicted involvement of canonical pathways includes HIF-1α signalling, DNA methylation & transcription repression signalling, AMPK (AMP-activated protein kinase) and ILK (integrin-linked kinase) signalling (**Figure 6.5**). The only result which was above statistical threshold was DNA methylation and transcription repression. However, the higher p-value and low ratio can be due to smaller number of genes involved in DNA methylation and transcription repression signalling. Vice versa, larger numbers of genes

are involved with the other pathways will thus give a higher p-value and or low ratio. We must also be aware that a low p-value or value above the threshold does not mean that the pathway is the most affected, it is only an indication that it is less likely to happen by chance. In terms of HIF-1α signalling and current knowledge, we do expect this pathway to be affected positively by hypoxia even though the p-value fell below 0.05. However, based on these results and analysis, we cannot accurately comment on whether the other pathways are regulated in acute hypoxia without further investigation.

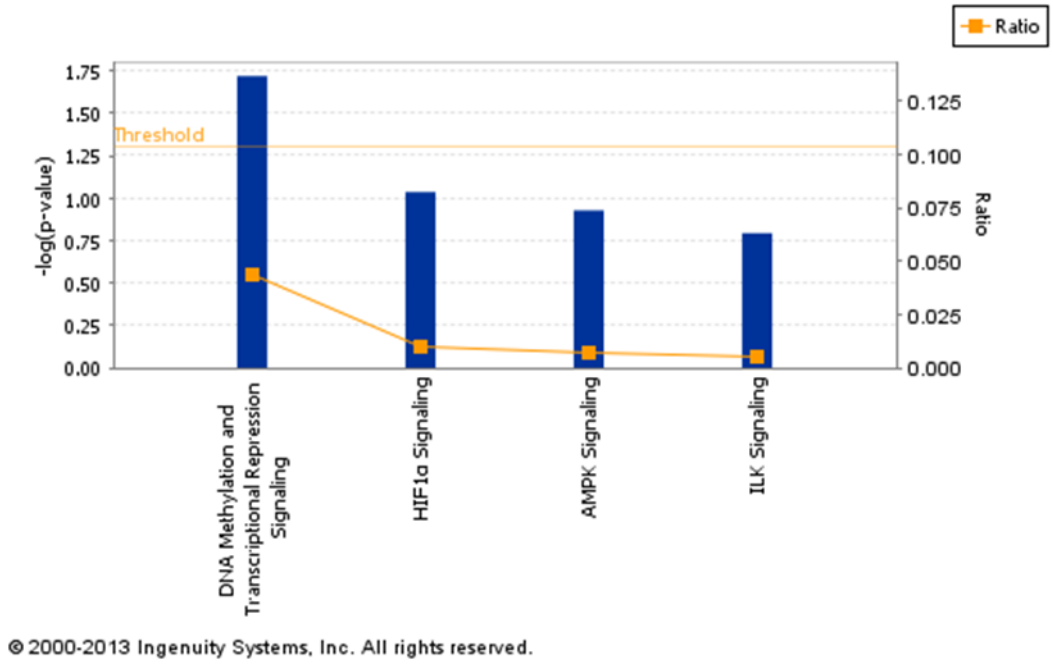

Figure 6.5 IPA Canonical Pathway analysis of acute hypoxia. *Canonical pathway hits associated with our expression data set at 6 hours hypoxia. The p-value is calculated using Fisher's extract methods, the threshold is preset at p<0.05. NOTE: IPA automatically uses the minus log p-value instead of the p-value on the y-axis for a better represented scale bar purposes. The Ratio represents the number of genes in our expression data over the total number of genes found to be involved in that pathway.*

6.2.2.2 Upstream transcription factor analysis in acute hypoxia

We further searched for upstream transcription factors which might be activated or inhibited in acute hypoxia using IPA Regulators prediction function. IPA listed HIF-1α, EPAS1 (HIF-2α) and NURP1 (nuclear protein, transcriptional regulator, 1) and their downstream targets (**Table 6.2**). Although they did not receive a prediction activation state by the software, it still provides clear indication that in acute hypoxia, the main transcription factors involved are the HIF family.

Transcription regulators	p-value	Target genes in data	Predicted activation state
EPAS1 (HIF-2A)	2.03E-03	EGLN3,PFKFB3	N/A
NUPR1	2.08E-02	C8orf58,FUT11,PFKFB3	N/A
HIF-1A	1.20E-02	EGLN3,PFKFB3	N/A

Table 6.2 IPA transcription regulators analysis in acute hypoxia. *A table showing transcription factor involved in acute hypoxia and their target gene. p-value is obtained using Fisher's Extact method.*

6.2.2.3 Canonical pathway analysis for chronic hypoxia

Using the expressed/ repressed data at 64 and 96 hours of hypoxia, IPA Canonical Pathway analysis resulted in an extensive list of pathways associated with the gene expression at this combined time point. A selected section of the results with the highest p-values are displayed in **Figure 6.6**. The pathway which is the most significantly above threshold is the human embryonic stem cells (hESCs) pluripotency, other highly predicted pathways include PI3K/AKT kinase signalling, p70S6K signalling, Wnt/β-catenin signalling and MIF regulation of innate immunity pathway. Each all these pathway, a gene ratio of 0.10 to 0.15 was observed.

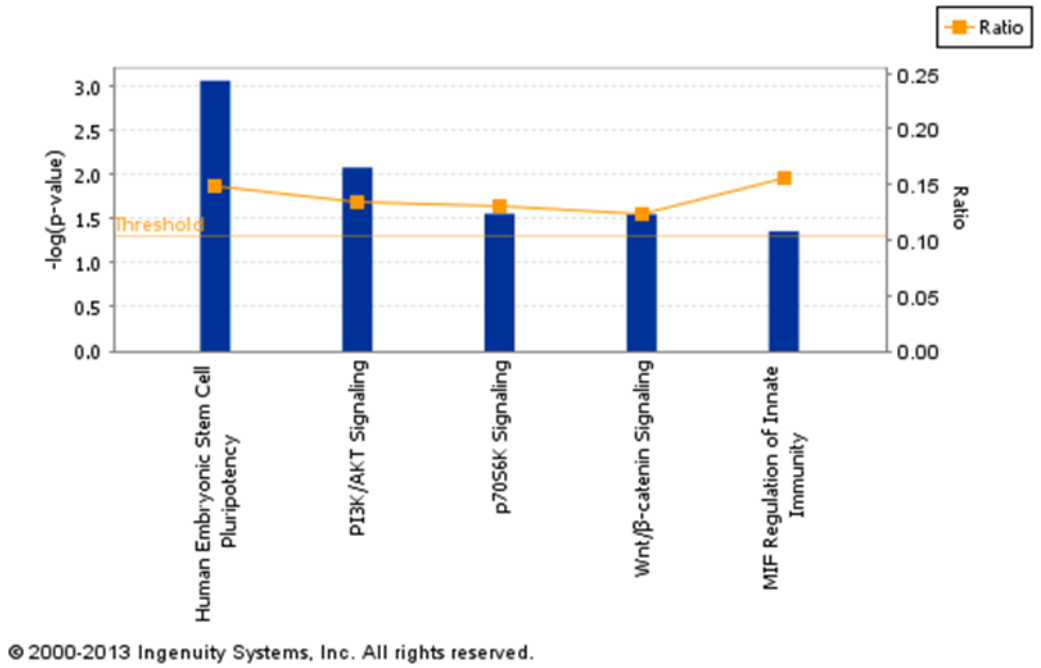

Figure 6.6 IPA Canonical Pathway analysis of selected signalling pathway hits in chronic hypoxia. *Canonical pathway hits associated with our expression data in chronic hypoxia. The p-value is calculated using Fisher's extract methods, the threshold is preset at p<0.05. NOTE: IPA automatically uses the minus log p-value instead of the p-value on the y-axis for a better represented scale bar purposes. The Ratio represents the number of genes in our expression data over the total number of genes found to be involved in that pathway.*

We focused in more detail on the hESCs signalling pathway as this pathway plays a key role in cells dedifferentiating into a more stem cells like phenotype. It has been previously shown that hypoxia is associated with hESCs pluripotency in other models and often linked to tumourgenesis (Keith and Simon, 2007, Covello *et al.*, 2006, Hill *et al.*, 2009, Forristal *et al.*, 2010). We saw that several components implicated in hESCs pluripotency are regulated in chronic hypoxia, including the downregulation of SMAD family components, upregulation of BMP (bone morphogenetic proteins) and EDG (endothelial differentiation gene) (**Figure 6.7**). However, we do not have strong evidence of how these molecules will contribute to the activation of pluripotency pathway as inhibitory signals are also observed upstream in the signalling. However, a major transcription regulator relating to stem cells pluripotency, Oct-4 (Loh *et al.*, 2006, Chambers, 2004, Niwa *et al.*, 2000), is upregulated by 2.4 fold (**Figure 6.7, lower**). As Oct-4 overexpression regulates ESC pluripotency, this provides an indication that the cells have may an increased potential to be more stem-like in chronic hypoxia.

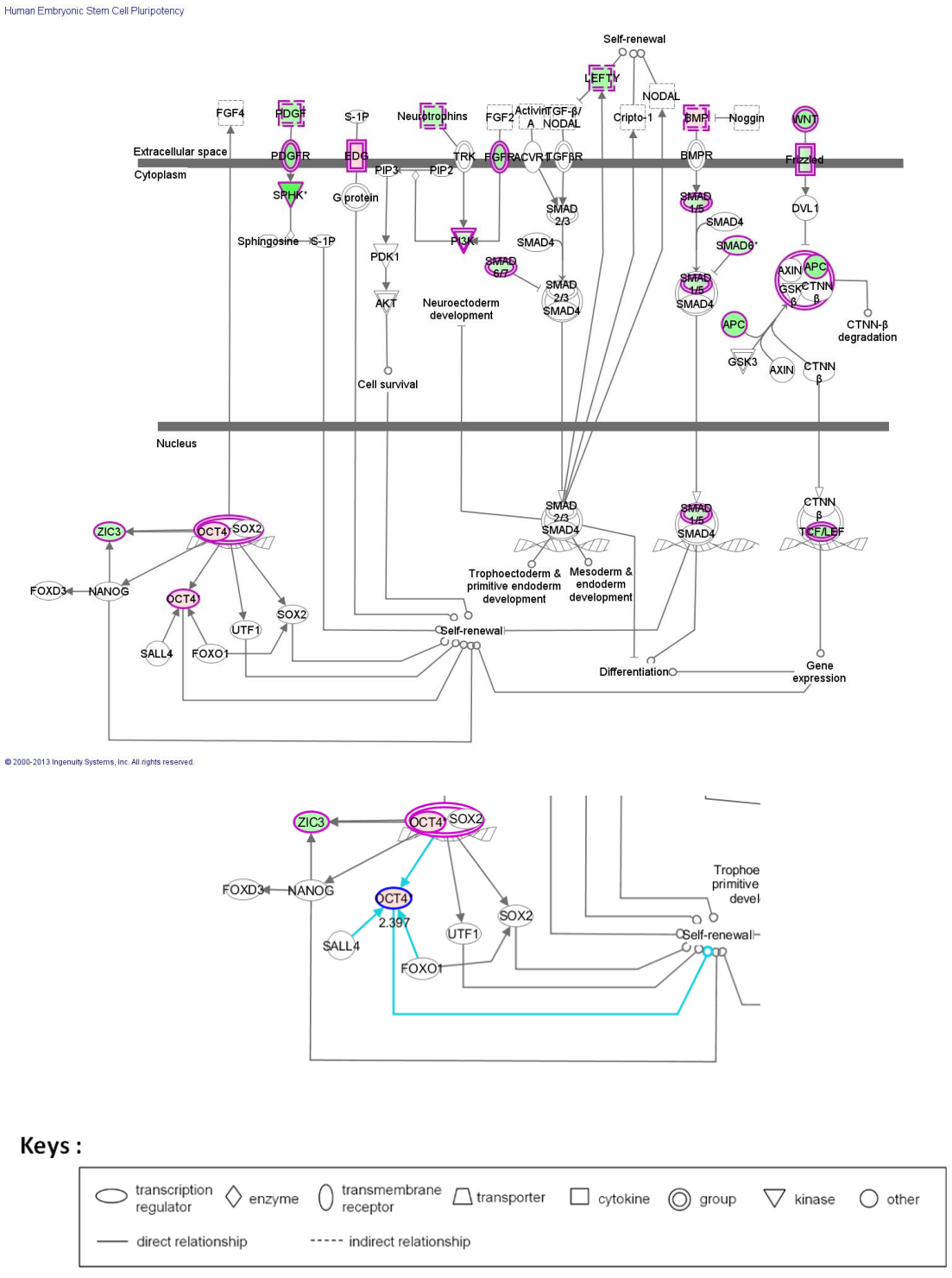

Figure 6.7 Human embryonic stem cells pluripotency (hESC) pathway obtained from IPA. (Upper) *A component pathway of the hESC highlighting genes which are regulated (highlighted in purple) in chronic hypoxia. Expressed genes are shaded in red, repressed genes are shaded in green.* ***(Lower)*** *A zoom-in of the OCT-4 gene, showing a 2.4 fold upregulation.*

We next focused on the Wnt signalling pathway, due to its implication with MB development (chapter 1.5.1.4). Wnt signalling is involved in normal embryonic development, activation is via Wnt-protein ligand binding to the frizzled family of receptors. The binding of these proteins allow a cascade of signal transduction which ultimately prevent the degradation of β-catenin and aid its transport into the cell nucleus. In the nucleus, β-catenin activates transcription factors which induce cellular responses such as cell growth and cell migration. Here, we observed that a majority of the Wnt signalling components are regulated in chronic hypoxia, but yet again the global direction of pathway inhibition or activation is not clear (**Figure 6.8**). However, we did observe that a couple of downstream effectors components are upregulated, such that of Oct-4, as mentioned earlier and the C-Jun proto-oncogene. C-Jun has a key biological role in cell proliferation and embryonic morphogenesis (Johnson *et al.*, 1993, Hilberg *et al.*, 1993, Schreiber *et al.*, 1999, Johnson *et al.*, 1996). The activation of C-Jun has also been implicated with tumourgenesis (Black *et al.*, 1994, Black *et al.*, 1991, Bos *et al.*, 1990, Dunn *et al.*, 2002). Altogether, it appears that chronic hypoxia directs the cells to a more stem cell like phenotypes, potentially contributing to tumourgenesis.

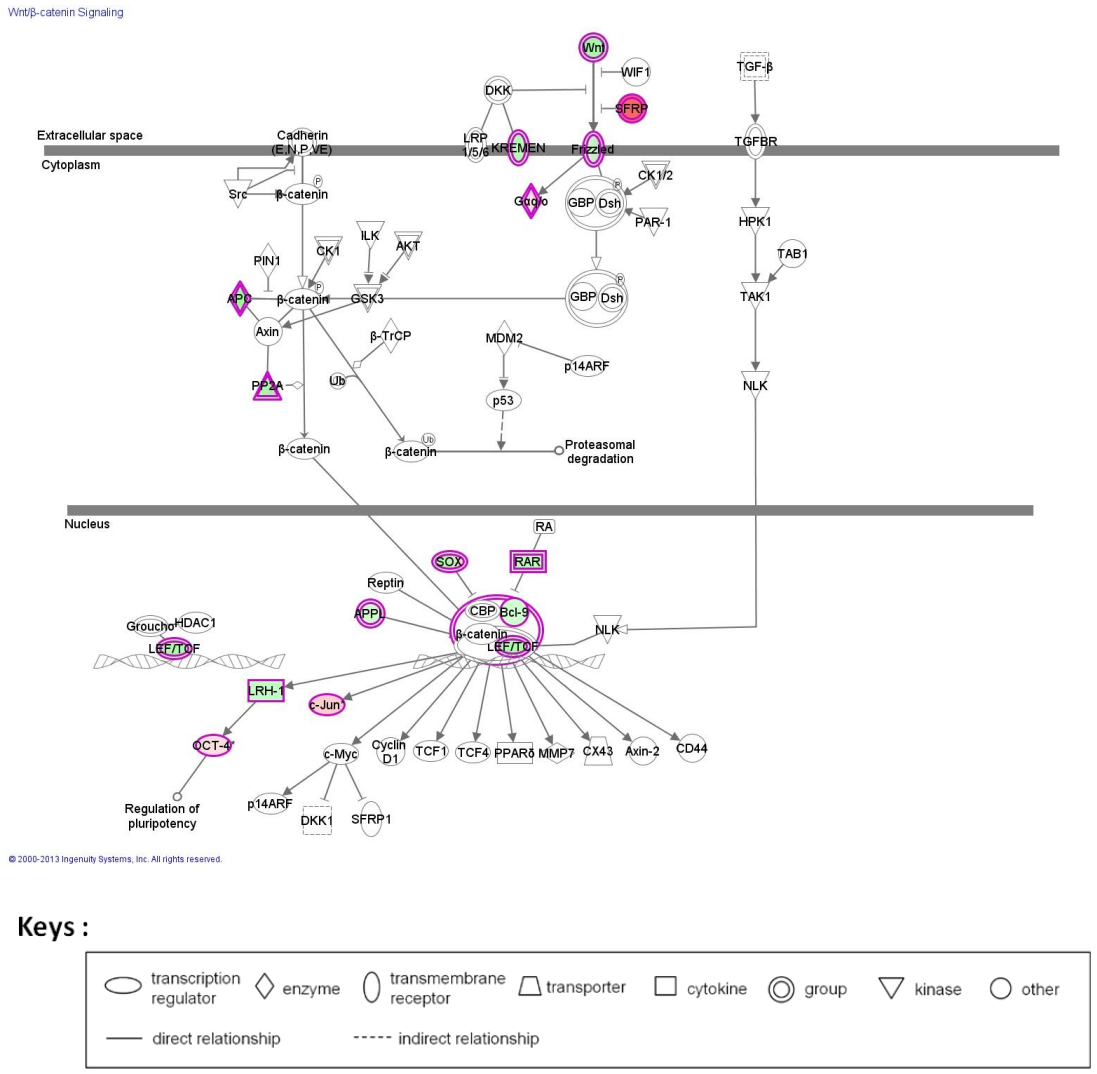

Keys :

Figure 6.8 Wnt signalling pathway obtained from IPA. *A component pathway of the Wnt signalling pathway, highlighting the genes which are regulated (highlighted in purple) in chronic hypoxia. Expressed genes are shaded in red, repressed genes are shaded in green.*

Lastly, we will discuss on the P13K/Akt pathway (see Appendix 1.4 for pathway). Changes in cellular metabolism are one of the major characteristics detected in cells when exposed to hypoxic insults (chapter 1.2.2). This is also reflected in the canonical analysis where we saw that P13K/Akt was regulated in chronic hypoxia. The PI3K (phosphatidylinositol 3 kinase)/AKT signalling is a complex pathway which plays a central role in transduction of cytokines and growth factors signals and is important for insulin signalling and glucose metabolism. Akt is a key mediator involved in cell survival through inhibition of apoptotic regulators (Osaki *et al.*, 2004). Here, we observed that some of the P13K/Akt signalling components are affected in chronic hypoxia but again, the global direction of pathway

inhibition or activation is not clear. However, it is reasonable to consider that, during chronic hypoxia, cellular energy consumption is regulated through this pathway.

6.2.2.4 Upstream transcription factor analysis in chronic hypoxia

In chronic hypoxia (combined 64 and 96 hours time point), several transcription factors are predicted to be regulated (**Table 6.3**). Using comparison analysis, where both the expressed and repressed gene lists were uploaded into IPA, the top hits were *NURP1*, *SPDEF* (SAM pointed domain containing Ets transcription factor) being activated and *ERG* (ETS belated gene) being inhibited. The upregulation of *NURP1* found in our data can be due to stress, as NURP1 is primarily a stress sensor found to be upregulated by high temperature or change in culturing medium (Garcia-Montero *et al.*, 2001, Jiang *et al.*, 1999). The function of NURP1 appears to be both pro- and antiapoptotic (Su *et al.*, 2001, Vasseur *et al.*, 2002, Carracedo *et al.*, 2006, Ree *et al.*, 1999), thus it is difficult to determine what impact of this transcription factor has on cells in chronic hypoxia. Both SPDEG and ERG belongs to the ETS transcription factor family of proteins, with a diverse role in biological processes including cellular differentiation, cell cycle, apoptosis and angiogenesis (Sharrocks, 2001). SPDEF is positively associated with tumours and was found to be upregulated in breast, prostate and lung cancers (Feldman *et al.*, 2003, Sood *et al.*, 2007), contributing to cells migration and invasion (Feldman *et al.*, 2003, Osisami and Keller, 2013, Turner *et al.*, 2008). The predicted activation of SPDEF in chronic hypoxia suggests that MB might similarly undergo a more tumourgenesis state. ERG is found to be overexpressed in several cancer types, indicating an oncogenic function but the molecular mechanisms of this ERG transcription factor are unclear (Baldus *et al.*, 2006, Metzeler *et al.*, 2009, Li *et al.*, 2012). Moreover, we have found that ERG is down-regulated in our data, thus its contribution to increased tumourgenesis in our model is unlikely.

Transcription regulators	p-value	Number of Genes	Predicted activation state
NUPR1	5.42E-10	79	Activated
SPDEF	1.58E-03	12	Activated
*ZNF217***	2.06E-02	8	Activated
*EZH2**	2.10E-02	7	Activated
ERG	1.83E-02	17	Inhibited

Table 6.3 IPA transcription regulators analysis in chronic hypoxia. *A table showing transcription factor involved in combined expressed and repressed gene list in chronic hypoxia of (predicted from *expressed gene list, ** repressed gene list only) and number of target genes involved. The p-value is obtained using Fisher's Extact method.*

When the expressed and repressed data were analysed separately, two other transcription factors were found to be regulated. IPA predicted that both *ZNF217* (zinc finger protein 217) and *EZH2* (enhancer of zeste homologue 2) are activated. However, these transcription factors were not predicted to be regulated when the expressed and repressed gene list were analysed together. This is due to contradictory results or the up- and downregulated gene lists, thus giving a low prediction score (**Figure 6.9**). Nevertheless, we looked more closely at these findings as both of these transcription factors are potential interesting targets. Both EZH2 and ZNF217 are transcription repressors. EZH2 catalyzes trimethylation of histone 3, while ZNF217 binds to promoters of target genes and primarily acts as a transcription repressor (Cao *et al.*, 2002, Tsang and Cheng, 2011, Cowger *et al.*, 2007, Banck *et al.*, 2009). The upregulation of these genes may suggest that transcription might be repressed in chronic hypoxia.

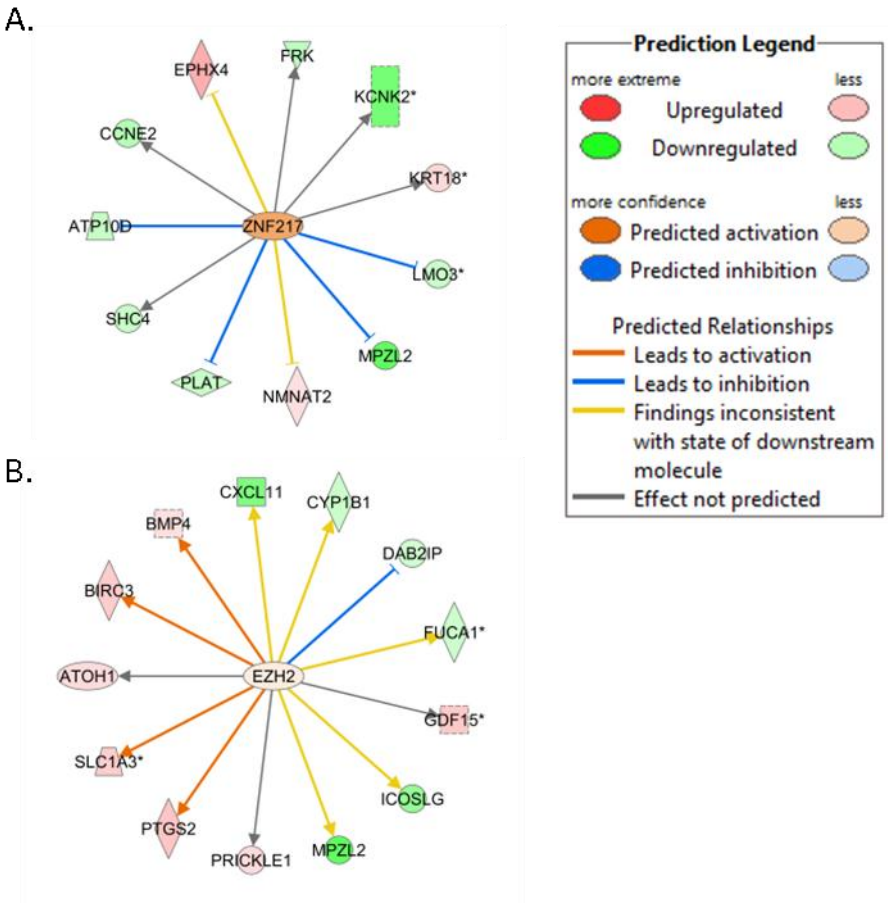

Figure 6.9 Network display of transcription factors interactions obtained from IPA. *Prediction of activated transcription factor* ***(A) ZNF217 (B) EZH2*** *and their relationship with downstream targets found in chronic hypoxia*

6.3 Chapter 6 Discussion

6.3.1 A global view of microarray analysis

In this chapter we have carried out a global gene expression profiling of MB cells in hypoxia, primarily focused on the differential gene expression between early and late hypoxic time points. We found that there was little change in genetic expression in acute compared to chronic hypoxia.

There are currently no other global gene expression studies of MB in any length of hypoxic duration, only one microarray of another brain tumour, GBM in 1% hypoxia for 24 hours (Ragel *et al.*, 2007). However, there was minimal overlap in our data, likely due to the different experimental conditions. *Ragel et al.* has primarily only examined HIF targets and stress response genes. Similar to our finding, upregulatioin of *VEGF*, *IGFBP3* (insulin-like growth factor binding protein 3) and *CAIX* were detected. However, the upregulation of stress response genes found by *Ragel et al.* was not observed in our data at any time point. It is possible that the expression of these genes might have been missed in the 6 hour time point and that, at later time points, cells under stress were already dead. Moreover, it must be noted that under hypoxic incubation, we would expect genes involved in the glycolytic pathway to be altered. Perhaps surprisingly, the regulation of this pathway was not highlighted in our analysis in either acute (T6) or chronic hypoxia (T64 and T96). However, on manual searches for several key enzymes which promote a transition of oxidative to glycolytic metabolism (Semenza, 2012b, Kim *et al.*, 2006, Papandreou *et al.*, 2006, Zhang *et al.*, 2008), we found that enzymes such as *PDK1* (pyruvate dehydrogenase kinase 1) and *BNIP3* expression are in fact up-regulated throughout the hypoxic incubation. Thus when we compared acute versus chronic hypoxia, this result and potentially other results could be missed as they do not fall in the acute or chronic group but in a 'continuously expressed in hypoxia' group.

It will therefore be useful in the near future, to compare some of the gene clusters obtained from (**Figure 6.3**), examining the genes with differential expression dynamics. For example, to compare group of genes only expressed at the later time point and the ones which were increased gradually over hypoxia. This will provide an insight to the cellular response in relation to the time frame of hypoxic exposure, giving us the finer details of how cells as a population behave in hypoxia. To further implement our current microarray results, network integration approaches could be useful. This method first uses metabolic

interactions from published databases to construct an integrated network. Then using differential values of gene expressions data between different microarrays (e.g chemoresistance versus chemo sensitive), pathway are scored. *For example, Chao et al.* used this method and identified chemoresistance-associated pathways using ovarian and lung models (Chao *et al.*, 2011). They identified a high score of several pathways including Wnt and P13K/Akt signalling and suggested that these pathways play a role in tumourgenesis in their cancer model as with our own finding (Chao *et al.*, 2011, Gatcliffe *et al.*, 2008). In the future, similar studies should be performed using different brain tumour cell lines, to help further predict key pathways and genes which are involved in resistance.

6.3.1.1 Signalling pathways affected by chronic hypoxia

This study confirms that hypoxia has a major effect in cellular gene expression as found by others (Rocha, 2007, Kenneth and Rocha, 2008). These changes are likely the cause of helping the cells to adapt to the reduced oxygen level. Besides the acute HIF regulation, hypoxia can affect many other cellular pathways as described in the result of section 6.2.2.3. IPA analysis has predicted that the most regulated pathways in chronic hypoxia are those involved in cellular energy metabolism, stem cells pluripotency and the developmental Wnt signalling pathway.

- P13K/Akt pathways are of major importance in regulating many cellular processes including glucose signalling and insulin metabolism (Fruman *et al.*, 1998, Osaki *et al.*, 2004, Lawlor and Alessi, 2001). Amplification of Akt is frequent in cancers (including GBM) (Staal, 1987, Knobbe and Reifenberger, 2003) and its activation is known to promote cell growth and treatment resistance (Testa and Bellacosa, 2001, Vivanco and Sawyers, 2002, Vara *et al.*, 2004, Franke *et al.*, 1997). The activation of this pathway is correlated with the loss of tumour suppressor *PTEN*, which generally inhibits Akt (Hartmann *et al.*, 2006, Carnero *et al.*, 2008).

- One interesting pathway regulated in hypoxic MB is the Wnt signalling, as mis-regulation of this pathway is associated with MB (chapter 1.4.1.2). Mutations in the Wnt pathway accounts for 25% of all MB (Northcott *et al.*, 2011, Clifford *et al.*, 2006, Ellison *et al.*, 2005, Fattet *et al.*, 2009). In normal embryonic growth, Wnt/β-catenin plays an important role in neuronal stem cell proliferation and

contributes to cerebellum development (Thomas and Capecchi, 1990). However, the continuous activation of Wnt signalling can thus lead to dysregulated cell proliferation and MB development. As found by independent studies, MB is associated with activation mutation of β-catenin gene (*CTNBN1*) (Thompson *et al.*, 2006, Kool *et al.*, 2008, Parsons *et al.*, 2011, Northcott *et al.*, 2011) or inactivation of β-catenin inhibitory molecules such as APC and Axin (Eberhart, 2003, Huang *et al.*, 2000, Baeza *et al.*, 2003). Although we did not observe a direct upregulation of Wnt or its downstream targets, changes of several Wnt components and reduction of APC was measured, thus chronic hypoxia might potentially alter this pathway and contribute to MB development.

- *Oct-4*/ *Sox* and *NANOG* where induced in hypoxia and these are the major transcription factors involved in the process of cancer cells dedifferentiating into a more stem-like phenotype (Nichols *et al.*, 1998, Boiani and Scholer, 2005, Ponti *et al.*, 2005, Wen *et al.*, 2010, Ji and Zheng, 2010). The implication of stem cells and tumourgenesis is witnessed in brain tumours including MB (Hemmati *et al.*, 2003, Bao *et al.*, 2006, Beier *et al.*, 2007, Hambardzumyan *et al.*, 2008). For example, detection of neural stem cells markers CD15 and CD133 have been found in both MB models and MB tumours (Hemmati *et al.*, 2003, Read *et al.*, 2009, Annabi *et al.*, 2008, Gowda *et al.*, 2012). *Gowda et al.* had found that 42 of 60 MB tumour samples were CD133+ and that 37/60 were CD15+ and that the expression of both these markers are associated with worst outcome (Gowda *et al.*, 2012). Other examples of stem cell marker expression in MB such as SOX2 and SOX9, has also been found to be associated with poorer clinical outcome (Sutter *et al.*, 2010). Furthermore, *Shutter et al.* demonstrated that Nanog activation in human cerebellar stem cells resulted in MB development in a mouse model (Sutter *et al.*, 2010). These studies and findings of our own suggest that chronic hypoxia might have an involvement of activating pathways involved in MB dedifferentiation, thus driving the cells into a more stem-like and progressive tumour phenotype.

Altogether, the alteration of these signalling pathways all point towards MB development, hence indicating a potential role of hypoxia in MB, not only in drug resistance but also in driving tumour progression.

6.3.1.2 Transcription factor regulation in chronic hypoxic conditions: and the role of ZNF217 and EZH2 transcription repressor

IPA analysis has revealed and predicted the activation and inhibition of several transcription factors in chronic hypoxia. Of interest, we focused on the two transcriptional regulators, ZNF217 and EZH2. ZNF217 is a Krüppel-like zinc-finger protein found to be amplified in several tumour types and relates to poor survival (Kallioniemi *et al.*, 1994, Nonet *et al.*, 2001, Li *et al.*, 2007, Mao *et al.*, 2011). ZNF217 primarily acts as a transcription repressor by interacting with co-repressors and histone modifying proteins within the nucleus.

High expression of ZNF217 is associated with poor prognosis in breast cancer (Sun, G. *et al.*, 2008, Krig *et al.*, 2010, Quinlan *et al.*, 2007, Vendrell *et al.*, 2012). *Vendrell et al.* have demonstrated that overexpression of ZNF217 in breast cancer cell lines stimulated cells migration, invasion and that it promoted EMT in human mammary epithelial cells (Vendrell *et al.*, 2012). In breast cancer, ZNF217 expression have also been found to be associated with chemoresistance (Huang *et al.*, 2005, Thollet *et al.*, 2010). For example, *Thollet et al.* have demonstrated that overexpression of ZNF217 in a breast cancer cell line conferred resistance to paclitaxel and that siRNA inhibition of ZNF217 re-sensitised the cells to treatment (Thollet *et al.*, 2010).

In a GBM study, ZNF217 is associated with aggressive tumour behaviour and poor prognosis, it is amplified in 32% of GBM and it is overexpressed in 71.2% of GBM's patients. (Mao *et al.*, 2011). Expression of ZNF217 is higher in Glioma stem cells than non-GSC and siRNA knockdown of ZNF217 in GSC inhibited cell growth and promote differentiation. *Mao et al.* have also reported that ZNF217 expression is dependent on both HIF-1α and HIF-2α, as both GSCs and GBM cell lines incubated in hypoxia show upregulation of ZNF217 and hypoxia-induced ZNF217 is inhibited upon HIF knockdown by siRNA (Mao *et al.*, 2011). These studies support our prediction that ZNF217 could potentially be upregulated in chronic hypoxia and that ZNF217 might contribute to chemoresistance and also to the dedifferentiation phenotype observed. However, there are currently no reports of ZNF217 and its implication in MB, thus the role of ZNF217 in MB remains an interesting target to be studied in the near future.

EZH2 is the active catalytic subunit part of the Polycomb repressive complex 2 (PRC2) which function to methylate lysine 27 on histone 3. It is responsible for chromatin compaction and thus acts as a transcriptional repressor (Cao *et al.*, 2002, Tsang and Cheng, 2011, Margueron and Reinberg, 2011). EZH2 is also associated with tumourgenesis, poor clinical

prognosis and drug resistance in prostate, breast and ovarian cancer (Bachmann *et al.*, 2006, Rizzo *et al.*, 2011). Moreover, EZH2 have been demonstrated to be involved in tumour stem cell maintenance in GBM (Suva *et al.*, 2009, Crea *et al.*, 2012). Interestingly, EZH2 was predicted to be activated in our data and that EZH2 has been reported to be associated with group 3 and group 4 MB. Recently, a study performed by *Alimova et al.* has shown that inhibition of EZH2 by RNAi suppresses MB cell growth and reduces tumour sphere formation (Crea *et al.*, 2012). Similar to ZNF217, we once again speculate the potential role of EZH2 in MB and that both these transcription factors might drive a more aggressive, chemoresistance, and stem cell phenotype in chronic hypoxia.

6.3.1.3 Limitations of microarray

The genomic studies we have performed have yielded vast amounts of genetic expression data. Besides from correctly filtering out genuine changes of gene expression that have occurred in hypoxia, interpretation of the results remained challenging. Although the sophisticated software IPA has provided us with a good platform for an overview of biological functions affected in chronic hypoxia, these are after all bioinformatic predictions which rely on known published literature. Thus, the upmost limitation of this software is the availability of known information. Thus say, if knowledge on a certain pathway has not been established yet, this information will be missed out in the analysis. So although IPA can calculate statistical p-value and ratio of predicted results, output results should be interpreted carefully dependent on how well known a pathway is. Moreover, IPA cannot provide a clear indication of which pathway is the most regulated as low p-value does not equate to 'most affected'. Also, because there are many genes involved in any given pathway, it is likely that for a pathway some genes will drive both up and down regulation, as found with some of our results. It is therefore difficult to get a clear picture of the final outcome of the pathway. To deduce a clear meaning of a predicted affected pathway, a more focused investigation is required. Moreover, the apparent contradicting regulation of a given signalling pathways, might be caused by cell heterogeneity, hence a single cell analysis approach could help to provide a clearer mechanism.

Chapter 7: General Discussion

7.1 Project overview

The purpose of this study was to investigate how brain tumour cells respond to chemotherapeutic treatment and how this was affected by their genomic status (p53) and their hypoxic microenvironment. The aim of this work was to gain a better understanding of the molecular mechanisms contributing to chemoresistance in order to improve current therapeutic strategies for MB treatment.

We have confirmed that (1) MB and GBM cell lines exhibit altered sensitivities to chemotherapeutic drugs and that drug resistance observed was associated with the cells' ability to transactivate p53; (2) MB p53 WT cells became more resistant to etoposide treatment in chronic but not acute hypoxic incubation; (3) Hypoxia-induced resistance is not caused by the expression of multidrug resistance transporters in our model but, at least in part, is due to a reduction in DNA damage sensing mechanisms; (4) Chronic hypoxia triggered a substantial effect on global genetic expression, affecting many biological functions of tumour cells.

7.1.1 The significance of p53 in MB

In general, most cancer types with p53 mutations are found to be more prone to tumourgenesis, this is due to the lack of cell cycle arrest control and apoptotic response in the presence of DNA damage which may have been inflicted upon the cells. In terms of association of *TP53* mutations and worst survival, it is clear in some cancers such as breast, liver and head & neck (Olivier *et al.*, 2006, Robles and Harris, 2010, Erber *et al.*, 1998).

For MB, accumulating studies have revealed the association of *TP53* mutation and bad prognosis in patients (Tabori *et al.*, 2010, Zhukova *et al.*, 2013). In particular, it is found that the *TP53* status in Shh group MB is of high predictive outcome (Northcott *et al.*, 2012) . *TP53* mutations in this group have extremely poor survival and a worse outcome compared to Shh/ WT tumours (Zhukova *et al.*, 2013). A whole-genome-sequencing-based analysis has further revealed that Shh group patients with *TP53* germline mutations are linked to chromosome rearrangement (chromothripsis). *Raush et al.* found that in 10 out of 10 tumour samples tested, where the cells carried a loss of *TP53* or heterozygosity mutation, there were occurrences of chromothripsis. Whilst, in the twenty two p53 WT samples examined, none displayed unusual chromosomal arrangement (Rausch *et al.*, 2012).

When investigating *TP53* mutations, caution must be taken due to the nature of p53 mutations. Unlike other gene mutations, *TP53* mutations tend not to result in a loss of protein expression but rather a mutated protein. Mutated p53 protein can be functionally active, asserting a dominant negative effect on WT protein or gain of function (GOF) (chapter 1.7.3). For example, in breast and colon cancer, p53 GOF down-regulated miR-223 can lead to treatment resistance (Masciarelli *et al.*, 2013). The method of p53 detection must be able to differentiate between WT and mutated protein, otherwise a malfunctioning p53 protein can be wrongly labelled as a p53 WT tumour. Evaluation of p53 status by sequencing is the best detection method for somatic mutations. Moreover, WT protein can still be functionally prohibited, for example TopBP1 (Topoisomerase IIβ binding protein) can interact with the p53 DNA binding domain and inhibit its promoter binding activity leading to repression of p53 transactivation (Liu *et al.*, 2009). Thus when determining MB p53 status, it is also important to access the protein activity, yet this can be more complicated at a large scale for diagnosis or stratification purposes.

7.1.2 The global cellular effect of hypoxia

There are surprisingly few reports of MB experiments performed in hypoxia compared to other solid brain tumours. Although there is no direct study that measures hypoxia markers in MB, it has been shown that MB arises from stem cells (Fan and Eberhart, 2008) and that hypoxia is a classic feature of the stem cell niche (Mohyeldin *et al.*, 2010). Stem cell arisen MB is further associated with HIF dependent Notch activation which maintains MB in an undifferentiated state (Pistollato *et al.*, 2010, Manoranjan *et al.*, 2012, Fan *et al.*, 2006). These studies demonstrate that the characteristics of MB are similar to other hypoxic brain tumours such as GBM (Collingridge *et al.*, 1999, Rampling *et al.*, 1994, Evans *et al.*, 2004). Therefore, our work reflects the necessity and importance of taking hypoxia into account when studying these tumours.

The mechanism behind the control of gene transcription under prolonged hypoxia could be due to changes in the DNA chromatin structure. Beside DNA organisation, histones are involved in transcriptional activity and epigenetic control of transcription factors via post translation modifications (Berger, 2002, Felsenfeld and Groudine, 2003). It has been shown that in hypoxia, certain gene promoters (e.g. VEGF) display an increase in trimethylation of histone3 at lysine4, which corresponds to an active transcription state (Shilatifard, 2006,

Johnson *et al.*, 2008). Moreover, it is speculated that other mechanisms, such as miRNA can have a role in the regulation of gene expression in hypoxia.

It will also be essential to see how the transcriptomic data would translate to the proteome as protein translation could be slowed down or inhibited in hypoxia (Bi *et al.*, 2005, Koritzinsky *et al.*, 2005, Liu *et al.*, 2006, Uniacke *et al.*, 2012). Thus transcriptomic data does not always reflect the protein levels and does not provide any information on their activity. Therefore a future proteomic approach would help further elucidate the role of hypoxia in MB.

7.1.3 Future perspective for MB treatment

Despite the fact that treatments for MB have improved in the recent years, cancer reoccurrence seen in children is as high as 40% (Faria, 2013). Importantly, due to the nature of tumour location and the high incidence of MB in young children, treatment choices are frequently limited to drugs. Yet, treatment causes significant long term side effects leaving survivors with lifelong disabilities. Therefore, there is a need for a better, more specific treatment for MB patients to improve their outcome.

Recently, classification of MB, tumour subgroup and their genetic status has provided a step-change in the understanding of MB behaviour clinically. With the advances in genetic screening, the large genetic variations of these tumours have been revealed, with different mutations linked to key biological pathways. This demonstrates that MB is a heterogeneous tumour and explains why histopathologically identical tumours have a different response to treatments and different clinical outcomes.

7.1.3.1 Targeted therapy

The idea of cancer targeted therapy is based on using compounds and inhibitors, which interfere and block a specific signalling pathway. In the past few years, development of specifically targeted anticancer drugs for MB has generated lots of hope and excitement. However, due to acquired resistance, the only targetable group with good results so far is the Shh subgroup. Using SHH inhibitors such as GDC-0449 and NVP-LDE225, promising results were obtained in reducing tumour growth (LoRusso *et al.*, 2011, Buonamici *et al.*, 2010). GDC-0449 inhibitors have been tested in phase II clinical trials (LoRusso *et al.*, 2011). For the other subgroups, a deeper understanding and development of target therapy is still

required, especially for Group 3 patients, which only have 20-30% survival rate (Cho *et al.*, 2011). Group 3 tumours are the most aggressive with high reoccurrence and metastasis rate. Hence, they tend to be treated with a higher treatment dose, resulting in an increased toxicity and morbidity.

There are other more general cancer targeted therapies developed to target pathways such as growth signal transduction, gene expression and angiogenesis. For example, cancer cell proliferation can be blocked by using compounds such as pertuzumab, docetaxel, gefitinib and erlotinib which target EGFR and HER-2 growth factors (Baselga *et al.*, 2012, Geoerger *et al.*, 2011, Pollack *et al.*, 2011). These compounds are being used to treat metastatic breast cancer and small-cell lung cancer (Tan *et al.*, 2004, Fukuoka *et al.*, 2003, Shepherd *et al.*, 2005). Inhibitors such as sorafenib and bevacizumab (Ichihara *et al.*, 2011) have been developed to block angiogenesis. Some promising results with compounds such as gefitinib and sorafenib in MB cell lines have been shown and this could be useful for future MB treatment (Meco *et al.*, 2009, Yang *et al.*, 2008, Blechacz *et al.*, 2009).

7.1.4 Moving towards *in vivo* study

The work in this project is based on using cultured cell lines as a model for MB. Although the results provided a good bases on how chemoresistance arises, results obtained with cell lines and their actual responses in patient might differ (Baguley and Marshall, 2004). Testing on cultured tissue gives concerns of its true representation of original tumour and unfortunately, primary MB tumour cells are difficult to grow (Romer and Curran, 2005). Moreover, culture cells might hinder the true characteristic of the disease *in vivo, as in vitro* work neglects many physiological factors that a complex biological system might experience. The use of mouse models can provide information on how MB is initiated, progresses and metastasises (Read *et al.*, 2009). Furthermore, using an *in vivo* model to study chemotherapeutic response would provide a more accurate tumour response closer to human cancer. The testing of these new targets *in vivo* is therefore necessary and more experiments are now being performed with mouse models (Romer and Curran, 2005, Lee *et al.*, 2012).

7.1.5 Final Remarks

The increase in our understanding of cancer cell biology has allowed discovery of novel targets, drugs and biomarkers, hence therapeutic approaches have better efficiency.

The major concern clinicians still face are the insensitivity to drug treatment and the relapse associated with acquired resistance to particular molecular targets. In theory, knowing the MB subgroup and genetics could provide a clearer direction for surgeons and oncologists to treat the patients in a more specific, personalised regime. However, the practicalities of sequencing methods for individual patients are not available due to cost issues. Moreover, knowing the cancer genetics would still not take into account the large tumour heterogeneity (some subpopulations of cells bearing different mutations), nor the important role of tumour microenvironment such as hypoxia as we have shown, and also the interaction with stromal cells. Efforts in the development of drugs which target different pathways or by using combination therapy would therefore be advantageous to tackle the tumour heterogeneity, the role of the microenvironment and avoid relapse. Finally, based on our observations we propose that the activity and levels of DNA damage sensing and repair machinery proteins (such as nibrin) should be taken into consideration for defining the therapeutic strategy and might also be useful indicators to predict treatment outcome.

Our work provided a general principle of the relationship between hypoxia and chemosensitivity in MB and this can be translated for other closely related tumours such as GBM for future investigations.

References

Abbott, D. W., Freeman, M. L. and Holt, J. T. (1998). Double-strand break repair deficiency and radiation sensitivity in BRCA2 mutant cancer cells. *J Natl Cancer Inst* **13**, 978-85.

Abe, T., Hasegawa, S., Taniguchi, K., Yokomizo, A., Kuwano, T., Ono, M., Mori, T., Hori, S., Kohno, K. and Kuwano, M. (1994). Possible involvement of multidrug-resistance-associated protein (MRP) gene expression in spontaneous drug resistance to vincristine, etoposide and adriamycin in human glioma cells. *Int J Cancer* **6**, 860-4.

Achison, M. and Hupp, T. R. (2003). Hypoxia attenuates the p53 response to cellular damage. *Oncogene* **22**, 3431-40.

Adesina, A. M., Nguyen, Y., Mehta, V., Takei, H., Stangeby, P., Crabtree, S., Chintagumpala, M. and Gumerlock, M. K. (2007). FOXG1 dysregulation is a frequent event in medulloblastoma. *J Neurooncol* **2**, 111-22.

Agnihotri, S., Gajadhar, A. S., Ternamian, C., Gorlia, T., Diefes, K. L., Mischel, P. S., Kelly, J., McGown, G., Thorncroft, M., Carlson, B. L., Sarkaria, J. N., Margison, G. P., Aldape, K., Hawkins, C., Hegi, M. and Guha, A. (2012). Alkylpurine-DNA-N-glycosylase confers resistance to temozolomide in xenograft models of glioblastoma multiforme and is associated with poor survival in patients. *J Clin Invest* **1**, 253-66.

Aho, T. L. T., Sandholm, J., Peltola, K. J., Mankonen, H. P., Lilly, M. and Koskinen, P. J. (2004). Pim-1 kinase promotes inactivation of the pro-apoptotic bad protein by phosphorylating it on the Ser(112) gatekeeper site. *Febs Letters* **1-3**, 43-49.

Alibes, A., Yankilevich, P., Canada, A. and Diaz-Uriarte, R. (2007). IDconverter and IDClight: Conversion and annotation of gene and protein IDs. *Bmc Bioinformatics*

Almeida, K. H. and Sobol, R. W. (2007). A unified view of base excision repair: Lesion-dependent protein complexes regulated by post-translational modification. *DNA Repair* **6**, 695-711.

Altaba, A. R. I., Palma, V. and Dahmane, N. (2002). Hedgehog-Gli signalling and the growth of the brain. *Nature Reviews Neuroscience* **1**, 24-33.

Altaner, C. (2008). Glioblastoma and stem cells. *Neoplasma* **5**, 369-74.

An, W. G., Kanekal, M., Simon, M. C., Maltepe, E., Blagosklonny, M. V. and Neckers, L. M. (1998). Stabilization of wild-type p53 by hypoxia-inducible factor 1alpha. *Nature* **6674**, 405-8.

Annabi, B., Rojas-Sutterlin, S., Laflamme, C., Lachambre, M. P., Rolland, Y., Sartelet, H. and Beliveau, R. (2008). Tumor environment dictates medulloblastoma cancer stem cell expression and invasive phenotype. *Molecular Cancer Research* **6**, 907-916.

Aoyagi, S. and Archer, T. K. (2008). Nicotinamide uncouples hormone-dependent chromatin remodeling from transcription complex assembly. *Mol Cell Biol* **1**, 30-39.

Appella, E. and Anderson, C. W. (2001). Post-translational modifications and activation of p53 by genotoxic stresses. *Eur J Biochem* **10**, 2764-72.

Arany, Z., Huang, L. E., Eckner, R., Bhattacharya, S., Jiang, C., Goldberg, M. A., Bunn, H. F. and Livingston, D. M. (1996). An essential role for p300/CBP in the cellular response to hypoxia. *Proceedings of the National Academy of Sciences of the United States of America* **23**, 12969-12973.

Ashcroft, M., Kubbutat, M. H. G. and Vousden, K. H. (1999). Regulation of p53 function and stability by phosphorylation. *Molecular and Cellular Biology* **3**, 1751-1758.

Attolini, C. S. O. and Michor, F. (2009). Evolutionary Theory of Cancer. *Year in Evolutionary Biology 2009* 23-51.

Audrito, V., Vaisitti, T., Rossi, D., Gottardi, D., D'Arena, G., Laurenti, L., Gaidano, G., Malavasi, F. and Deaglio, S. (2011). Nicotinamide Blocks Proliferation and Induces Apoptosis of Chronic Lymphocytic Leukemia Cells through Activation of the p53/miR-34a/SIRT1 Tumor Suppressor Network. *Cancer Research* **13**, 4473-4483.

Austen, B., Skowronska, A., Baker, C., Powell, J. E., Gardiner, A., Oscier, D., Majid, A., Dyer, M., Siebert, R., Taylor, A. M., Moss, P. A. and Stankovic, T. (2007). Mutation status of the residual ATM allele is an important determinant of the cellular response to chemotherapy and survival in patients with chronic lymphocytic leukemia containing an 11q deletion. *Journal of Clinical Oncology* **34**, 5448-5457.

Azad, M. B., Chen, Y., Henson, E. S., Cizeau, J., McMillan-Ward, E., Israels, S. J. and Gibson, S. B. (2008). Hypoxia induces autophagic cell death in apoptosis-competent cells through a mechanism involving BNIP3. *Autophagy* **2**, 195-204.

Bachmann, I. M., Halvorsen, O. J., Collett, K., Stefansson, I. M., Straume, O., Haukaas, S. A., Salvesen, H. B., Otte, A. P. and Akslen, L. A. (2006). EZH2 expression is associated with high proliferation rate and aggressive tumor subgroups in cutaneous melanoma and cancers of the endometrium, prostate, and breast. *Journal of Clinical Oncology* **2**, 268-273.

Bacolod, M. D., Lin, S. M., Johnson, S. P., Bullock, N. S., Colvin, M., Bigner, D. D. and Friedman, H. S. (2008). The gene expression profiles of medulloblastoma cell lines resistant to preactivated cyclophosphamide. *Current Cancer Drug Targets* **3**, 172-179.

Bacolod, M. D., Fehdrau, R., Johnson, S. P., Bullock, N. S., Bigner, D. D., Colvin, M. and Friedman, H. S. (2009). BCNU-sequestration by metallothioneins may contribute to resistance in a medulloblastoma cell line. *Cancer Chemother Pharmacol* **4**, 753-758.

Baeriswyl, V. and Christofori, G. (2009). The angiogenic switch in carcinogenesis. *Seminars in Cancer Biology* **5**, 329-337.

Baeza, N., Weller, M., Yonekawa, Y., Kleihues, P. and Ohgaki, H. (2003). PTEN methylation and expression in glioblastomas. *Acta Neuropathol* **5**, 479-485.

Bagnall, J. L., J.; Taylor, S.; Spiller, D.G.; White, M.R.H.; Sharkey, K.J.; Bearon, R.N.; See, V. (2013). Tight control of Hypoxia Inducible Factor (HIF)-alpha transient dynamics is essential for cell survival in hypoxia. *Journal of Biological Chemistry*

Baguley, B. C. and Marshall, E. S. (2004). In vitro modelling of human tumour behaviour in drug discovery programmes. *European Journal of Cancer* **6**, 794-801.

Baker, S. J., Fearon, E. R., Nigro, J. M., Hamilton, S. R., Preisinger, A. C., Jessup, J. M., vanTuinen, P., Ledbetter, D. H., Barker, D. F., Nakamura, Y., White, R. and Vogelstein, B. (1989). Chromosome 17 deletions and p53 gene mutations in colorectal carcinomas. *Science* **4901**, 217-21.

Bakhshi, S., Cerosaletti, K. M., Concannon, P., Bawle, E. V., Fontanesi, J., Gatti, R. A. and Bhambhani, K. (2003). Medulloblastoma with adverse reaction to radiation therapy in Nijmegen breakage syndrome. *Journal of Pediatric Hematology Oncology* **3**, 248-251.

Baldus, C. D., Burmeister, T., Martus, P., Schwartz, S., Goekbuget, N., Bloomfield, C. D., Hoelzer, D., Thiel, E. and Hofmann, W. K. (2006). High expression of the ETS transcription

factor ERG predicts adverse outcome in acute T-lymphoblastic leukemia in adults. *Journal of Clinical Oncology* **29**, 4714-4720.

Banck, M. S., Li, S., Nishio, H., Wang, C., Beutler, A. S. and Walsh, M. J. (2009). The ZNF217 oncogene is a candidate organizer of repressive histone modifiers. *Epigenetics* **2**, 100-106.

Bao, S. D., Wu, Q. L., McLendon, R. E., Hao, Y. L., Shi, Q., Hjelmeland, A. B., Dewhirst, M. W., Bigner, D. D. and Rich, J. N. (2006). Glioma stem cells promote radioresistance by preferential activation of the DNA damage response. *Nature* **7120**, 756-760.

Bar-Or, R. L., Maya, R., Segel, L. A., Alon, U., Levine, A. J. and Oren, M. (2000). Generation of oscillations by the p53-Mdm2 feedback loop: A theoretical and experimental study. *Proceedings of the National Academy of Sciences of the United States of America* **21**, 11250-11255.

Bar, E. E., Lin, A., Mahairaki, V., Matsui, W. and Eberhart, C. G. (2010). Hypoxia increases the expression of stem-cell markers and promotes clonogenicity in glioblastoma neurospheres. *Am J Pathol* **3**, 1491-502.

Barel, D., Avigad, S., Mor, C., Fogel, M., Cohen, I. J. and Zaizov, R. (1998). A novel germ-line mutation in the noncoding region of the p53 gene in a Li-Fraumeni family. *Cancer Genetics and Cytogenetics* **1**, 1-6.

Barlow, C., Hirotsune, S., Paylor, R., Liyanage, M., Eckhaus, M., Collins, F., Shiloh, Y., Crawley, J. N., Ried, T., Tagle, D. and WynshawBoris, A. (1996). Atm-deficient mice: A paradigm of ataxia telangiectasia. *Cell* **1**, 159-171.

Barnhart, K., Coutifaris, C. and Esposito, M. (2001). The pharmacology of methotrexate. *Expert Opin Pharmacother* **3**, 409-17.

Barrallo-Gimeno, A. and Nieto, M. A. (2005). The Snail genes as inducers of cell movement and survival: implications in development and cancer. *Development* **14**, 3151-3161.

Bartel, D. P. (2004). MicroRNAs: genomics, biogenesis, mechanism, and function. *Cell* **2**, 281-97.

Bartz, S. R., Zhang, Z., Burchard, J., Imakura, M., Martin, M., Palmieri, A., Needham, R., Guo, J., Gordon, M., Chung, N., Warrener, P., Jackson, A. L., Carleton, M., Oatley, M., Locco, L., Santini, F., Smith, T., Kunapuli, P., Ferrer, M., Strulovici, B., Friend, S. H. and Linsley, P. S. (2006). Small interfering RNA screens reveal enhanced cisplatin cytotoxicity in tumor cells having both BRCA network and TP53 disruptions. *Molecular and Cellular Biology* **24**, 9377-9386.

Baselga, J., Cortes, J., Kim, S. B., Im, S. A., Hegg, R., Im, Y. H., Roman, L., Pedrini, J. L., Pienkowski, T., Knott, A., Clark, E., Benyunes, M. C., Ross, G., Swain, S. M. and Grp, C. S. (2012). Pertuzumab plus Trastuzumab plus Docetaxel for Metastatic Breast Cancer. *New England Journal of Medicine* **2**, 109-119.

Batista, L. F. Z., Roos, W. P., Christmann, M., Menck, C. F. M. and Kaina, B. (2007). Differential sensitivity of malignant glioma cells to methylating and chloroethylating anticancer drugs: p53 determines the switch by regulating xpc, ddb2, and DNA double-strand breaks. *Cancer Research* **24**, 11886-11895.

Behrens, J. (1993). The Role of Cell-Adhesion Molecules in Cancer Invasion and Metastasis. *Breast Cancer Research and Treatment* **3**, 175-184.

Beier, D., Hau, P., Proescholdt, M., Lohmeier, A., Wischhusen, J., Oefner, P. J., Aigner, L., Brawanski, A., Bogdahn, U. and Beier, C. P. (2007). CD133(+) and CD133(-) glioblastoma-

derived cancer stem cells show differential growth characteristics and molecular profiles. *Cancer Research* **9**, 4010-4015.

Benita, Y., Kikuchi, H., Smith, A. D., Zhang, M. Q., Chung, D. C. and Xavier, R. J. (2009). An integrative genomics approach identifies Hypoxia Inducible Factor-1 (HIF-1)-target genes that form the core response to hypoxia. *Nucleic Acids Research* **14**, 4587-602.

Bennett, W. P., Hussain, S. P., Vahakangas, K. H., Khan, M. A., Shields, P. G. and Harris, C. C. (1999). Molecular epidemiology of human cancer risk: Gene-environment interactions and p53 mutation spectrum in human lung cancer. *Journal of Pathology* **1**, 8-18.

Berger, S. L. (2002). Histone modifications in transcriptional regulation. *Current Opinion in Genetics & Development* **2**, 142-148.

Berkovich, E., Monnat, R. J. and Kastan, M. B. (2007). Roles of ATM and NBS1 in chromatin structure modulation and DNA double-strand break repair. *Nature Cell Biology* **6**, 683-U137.

Berra, E., Benizri, E., Ginouves, A., Volmat, V., Roux, D. and Pouyssegur, J. (2003). HIF prolyl-hydroxylase 2 is the key oxygen sensor setting low steady-state levels of HIF-1 alpha in normoxia. *Embo Journal* **16**, 4082-4090.

Bertrand, P., Lambert, S., Joubert, C. and Lopez, B. S. (2003). Overexpression of mammalian Rad51 does not stimulate tumorigenesis while a dominant-negative Rad51 affects centrosome fragmentation, ploidy and stimulates tumorigenesis, in p53-defective CHO cells. *Oncogene* **48**, 7587-7592.

Berx, G. and van Roy, F. (2009). Involvement of Members of the Cadherin Superfamily in Cancer. *Cold Spring Harbor Perspectives in Biology* **6**,

Bhattacharyya, A., Ear, U. S., Koller, B. H., Weichselbaum, R. R. and Bishop, D. K. (2000). The breast cancer susceptibility gene BRCA1 is required for subnuclear assembly of Rad51 and survival following treatment with the DNA cross-linking agent cisplatin. *Journal of Biological Chemistry* **31**, 23899-23903.

Bi, M. X., Naczki, C., Koritzinsky, M., Fels, D., Blais, J., Hu, N. P., Harding, H., Novoa, I., Varia, M., Raleigh, J., Scheuner, D., Kaufman, R. J., Bell, J., Ron, D., Wouters, B. G. and Koumenis, C. (2005). ER stress-regulated translation increases tolerance to extreme hypoxia and promotes tumor growth. *Embo Journal* **19**, 3470-3481.

Biddlestone-Thorpe, L., Sajjad, M., Rosenberg, E., Beckta, J. M., Valerie, N. C. K., Tokarz, M., Adams, B. R., Wagner, A. F., Khalil, A., Gilfor, D., Golding, S. E., Deb, S., Temesi, D. G., Lau, A., O'Connor, M. J., Choe, K. S., Parada, L. F., Lim, S. K., Mukhopadhyay, N. D. and Valerie, K. (2013). ATM Kinase Inhibition Preferentially Sensitizes p53-Mutant Glioma to Ionizing Radiation. *Clinical Cancer Research* **12**, 3189-3200.

Bindra, R. S., Gibson, S. L., Meng, A., Westermark, U., Jasin, M., Pierce, A. J., Bristow, R. G., Classon, M. K. and Glazer, P. M. (2005). Hypoxia-induced down-regulation of BRCA1 expression by E2Fs. *Cancer Research* **24**, 11597-11604.

Birner, P., Gatterbauer, B., Oberhuber, G., Schindl, M., Rossler, K., Prodinger, A., Budka, H. and Hainfellner, J. A. (2001). Expression of hypoxia-inducible factor-1 alpha in oligodendrogliomas - Its impact on prognosis and on neoangiogenesis. *Cancer* **1**, 165-171.

Bitterman, K. J., Anderson, R. M., Cohen, H. Y., Latorre-Esteves, M. and Sinclair, D. A. (2002). Inhibition of silencing and accelerated aging by nicotinamide, a putative negative regulator of yeast sir2 and human SIRT1. *J Biol Chem* **47**, 45099-107.

Black, E. J., Street, A. J. and Gillespie, D. A. F. (1991). Protein Phosphatase 2a Reverses Phosphorylation of C-Jun Specified by the Delta Domain Invitro - Correlation with

Oncogenic Activation and Deregulated Transactivation Activity of V-Jun. *Oncogene* **11**, 1949-1958.

Black, E. J., Catling, A. D., Woodgett, J. R., Kilbey, A. and Gillespie, D. A. F. (1994). Transcriptional Activation by the V-Jun Oncoprotein Is Independent of Positive Regulatory Phosphorylation. *Oncogene* **8**, 2363-2368.

Blagosklonny, M. V., An, W. G., Romanova, L. Y., Trepel, J., Fojo, T. and Neckers, L. (1998). p53 inhibits hypoxia-inducible factor-stimulated transcription. *J Biol Chem* **20**, 11995-8.

Blechacz, B. R. A., Smoot, R. L., Bronk, S. F., Werneburg, N. W., Sirica, A. E. and Gores, G. J. (2009). Sorafenib Inhibits Signal Transducer and Activator of Transcription-3 Signaling in Cholangiocarcinoma Cells by Activating the Phosphatase Shatterproof 2. *Hepatology* **6**, 1861-1870.

Bobola, M. S., Silber, J. R., Ellenbogen, R. G., Geyer, J. R., Blank, A. and Goff, R. D. (2005). O-6-methylguanine-DNA methyltransferase, O-6-benzylguanine, and resistance to clinical alkylators in pediatric primary brain tumor cell lines. *Clinical Cancer Research* **7**, 2747-2755.

Bockhorn, M., Jain, R. K. and Munn, L. L. (2007). Active versus passive mechanisms in metastasis: do cancer cells crawl into vessels, or are they pushed? *Lancet Oncology* **5**, 444-448.

Bogdanova, N., Feshchenko, S., Schurmann, P., Waltes, R., Wieland, B., Hillemanns, P., Rogov, Y. I., Dammann, O., Bremer, M., Karstens, J. H., Sohn, C., Varon, R. and Dork, T. (2008). Nijmegen BREAKAGE SYNDROME mutations and risk of breast cancer. *International Journal of Cancer* **4**, 802-806.

Bohnsack, M. T., Czaplinski, K. and Gorlich, D. (2004). Exportin 5 is a RanGTP-dependent dsRNA-binding protein that mediates nuclear export of pre-miRNAs. *Rna-a Publication of the Rna Society* **2**, 185-191.

Boiani, M. and Scholer, H. R. (2005). Regulatory networks in embryo-derived pluripotent stem cells. *Nature Reviews Molecular Cell Biology* **11**, 872-884.

Bolstad, B. M., Irizarry, R. A., Astrand, M. and Speed, T. P. (2003). A comparison of normalization methods for high density oligonucleotide array data based on variance and bias. *Bioinformatics* **2**, 185-193.

Bommer, G. T., Gerin, I., Feng, Y., Kaczorowski, A. J., Kuick, R., Love, R. E., Zhai, Y., Giordano, T. J., Qin, Z. S., Moore, B. B., MacDougald, O. A., Cho, K. R. and Fearon, E. R. (2007). p53-mediated activation of miRNA34 candidate tumor-suppressor genes. *Curr Biol* **15**, 1298-307.

Bos, T. J., Monteclaro, F. S., Mitsunobu, F., Ball, A. R., Chang, C. H. W., Nishimura, T. and Vogt, P. K. (1990). Efficient Transformation of Chicken-Embryo Fibroblasts by C-Jun Requires Structural Modification in Coding and Noncoding Sequences. *Genes & Development* **10**, 1677-1687.

Bossi, G., Marampon, F., Maor-Aloni, R., Zani, B., Rotter, V., Oren, M., Strano, S., Blandino, G. and Sacchi, A. (2008). Conditional RNA interference in vivo to study mutant p53 oncogenic gain of function on tumor malignancy. *Cell Cycle* **12**, 1870-1879.

Brachman, D. G., Beckett, M., Graves, D., Haraf, D., Vokes, E. and Weichselbaum, R. R. (1993). P53 Mutation Does Not Correlate with Radiosensitivity in 24 Head and Neck-Cancer Cell-Lines. *Cancer Research* **16**, 3667-3669.

Brennan, C., Momota, H., Hambardzumyan, D., Ozawa, T., Tandon, A., Pedraza, A. and Holland, E. (2009). Glioblastoma subclasses can be defined by activity among signal transduction pathways and associated genomic alterations. *PLoS One* **11**, e7752.

Broniscer, A., Chintagumpala, M., Fouladi, M., Krasin, M. J., Kocak, M., Bowers, D. C., Iacono, L. C., Merchant, T. E., Stewart, C. F., Houghton, P. J., Kun, L. E., Ledet, D. and Gajjar, A. (2006). Temozolomide after radiotherapy for newly diagnosed high-grade glioma and unfavorable low-grade glioma in children. *J Neurooncol* **3**, 313-9.

Brosh, R. and Rotter, V. (2009). When mutants gain new powers: news from the mutant p53 field. *Nature Reviews Cancer* **10**, 701-713.

Brown, J. M. (1999). The hypoxic cell: a target for selective cancer therapy--eighteenth Bruce F. Cain Memorial Award lecture. *Cancer Res* **23**, 5863-70.

Brown, L. M., Cowen, R. L., Debray, C., Eustace, A., Erler, J. T., Sheppard, F. C. D., Parker, C. A., Stratford, I. J. and Williams, K. J. (2006). Reversing hypoxic cell chemoresistance in vitro using genetic and small molecule approaches targeting hypoxia inducible factor-1. *Molecular Pharmacology* **2**, 411-418.

Bruick, R. K. (2003). Oxygen sensing in the hypoxic response pathway: regulation of the hypoxia-inducible transcription factor. *Genes & Development* **21**, 2614-2623.

Bruning, U., Cerone, L., Neufeld, Z., Fitzpatrick, S. F., Cheong, A., Scholz, C. C., Simpson, D. A., Leonard, M. O., Tambuwala, M. M., Cummins, E. P. and Taylor, C. T. (2011). MicroRNA-155 Promotes Resolution of Hypoxia-Inducible Factor 1 alpha Activity during Prolonged Hypoxia. *Molecular and Cellular Biology* **19**, 4087-4096.

Bulavin, D. V., Saito, S., Hollander, M. C., Sakaguchi, K., Anderson, C. W., Appella, E. and Fornace, A. J., Jr. (1999). Phosphorylation of human p53 by p38 kinase coordinates N-terminal phosphorylation and apoptosis in response to UV radiation. *Embo Journal* **23**, 6845-54.

Buonamici, S., Williams, J., Morrissey, M., Wang, A. L., Guo, R. B., Vattay, A., Hsiao, K., Yuan, J., Green, J., Ospina, B., Yu, Q. Y., Ostrom, L., Fordjour, P., Anderson, D. L., Monahan, J. E., Kelleher, J. F., Peukert, S., Pan, S. F., Wu, X., Maira, S. M., Garcia-Echeverria, C., Briggs, K. J., Watkins, D. N., Yao, Y. M., Lengauer, C., Warmuth, M., Sellers, W. R. and Dorsch, M. (2010). Interfering with Resistance to Smoothened Antagonists by Inhibition of the PI3K Pathway in Medulloblastoma. *Science Translational Medicine* **51**,

Buscemi, G., Perego, P., Carenini, N., Nakanishi, M., Chessa, L., Chen, J. J., Khanna, K. and Delia, D. (2004). Activation of ATM and Chk2 kinases in relation to the amount of DNA strand breaks. *Oncogene* **46**, 7691-7700.

Bussink, J., Stratford, M. R. L., van der Kogel, A. J., Folkes, L. K. and Kaanders, J. H. A. M. (2002). Pharmacology and toxicity of nicotinamide combined with domperidone during fractionated radiotherapy. *Radiotherapy and Oncology* **3**, 285-291.

Cai, Y., Yu, X., Hu, S. and Yu, J. (2009). A brief review on the mechanisms of miRNA regulation. *Genomics Proteomics Bioinformatics* **4**, 147-54.

Calin, G. A., Ferracin, M., Cimmino, A., Di Leva, G., Shimizu, M., Wojcik, S. E., Iorio, M. V., Visone, R., Sever, N. I., Fabbri, M., Iuliano, R., Palumbo, T., Pichiorri, F., Roldo, C., Garzon, R., Sevignani, C., Rassenti, L., Alder, H., Volinia, S., Liu, C. G., Kipps, T. J., Negrini, M. and Croce, C. M. (2005). A MicroRNA signature associated with prognosis and progression in chronic lymphocytic leukemia. *New England Journal of Medicine* **17**, 1793-1801.

Calin, G. A. and Croce, C. M. (2006). MicroRNA signatures in human cancers. *Nature Reviews Cancer* **11**, 857-866.

Camps, C., Buffa, F. M., Colella, S., Moore, J., Sotiriou, C., Sheldon, H., Harris, A. L., Gleadle, J. M. and Ragoussis, J. (2008). hsa-miR-210 is induced by hypoxia and is an independent prognostic factor in breast cancer. *Clinical Cancer Research* **5**, 1340-1348.

Cao, R., Wang, L. J., Wang, H. B., Xia, L., Erdjument-Bromage, H., Tempst, P., Jones, R. S. and Zhang, Y. (2002). Role of histone H3 lysine 27 methylation in polycomb-group silencing. *Science* **5595**, 1039-1043.

Carnero, A., Blanco-Aparicio, C., Renner, O., Link, W. and Leal, J. F. M. (2008). The PTEN/PI3K/AKT signalling pathway in cancer, therapeutic implications. *Current Cancer Drug Targets* **3**, 187-198.

Carracedo, A., Lorente, M., Egia, A., Blazquez, C., Garcia, S., Giroux, V., Malicet, C., Villuendas, R., Gironella, M., Gonzalez-Feria, L., Piris, M. A., Iovanna, J. L., Guzman, M. and Velasco, G. (2006). The stress-regulated protein p8 mediates cannabinoid-induced apoptosis of tumor cells. *Cancer Cell* **4**, 301-312.

Carreau, A., El Hafny-Rahbi, B., Matejuk, A., Grillon, C. and Kieda, C. (2011). Why is the partial oxygen pressure of human tissues a crucial parameter? Small molecules and hypoxia. *J Cell Mol Med* **6**, 1239-53.

Cavallaro, U. and Christofori, G. (2004). Cell adhesion and signalling by cadherins and Ig-CAMs in cancer. *Nature Reviews Cancer* **2**, 118-132.

Cerosaletti, K. and Concannon, P. (2004). Independent roles for nibrin and Mre11-Rad50 in the activation and function of Atm. *Journal of Biological Chemistry* **37**, 38813-9.

Cerosaletti, K., Wright, J. and Concannon, P. (2006). Active role for nibrin in the kinetics of atm activation. *Molecular and Cellular Biology* **5**, 1691-9.

Chambers, I. (2004). The molecular basis of pluripotency in mouse embryonic stem cells. *Cloning and Stem Cells* **4**, 386-391.

Chan, K. T. and Lung, M. L. (2004). Mutant p53 expression enhances drug resistance in a hepatocellular carcinoma cell line. *Cancer Chemother Pharmacol* **6**, 519-26.

Chan, N., Koritzinsky, M., Zhao, H., Bindra, R., Glazer, P. M., Powell, S., Belmaaza, A., Wouters, B. and Bristow, R. G. (2008). Chronic hypoxia decreases synthesis of homologous recombination proteins to offset chemoresistance and radioresistance. *Cancer Research* **2**, 605-614.

Chang, T. C., Wentzel, E. A., Kent, O. A., Ramachandran, K., Mullendore, M., Lee, K. H., Feldmann, G., Yamakuchi, M., Ferlito, M., Lowenstein, C. J., Arking, D. E., Beer, M. A., Maitra, A. and Mendell, J. T. (2007). Transactivation of miR-34a by p53 broadly influences gene expression and promotes apoptosis. *Mol Cell* **5**, 745-52.

Chao, S. Y., Chiang, J. H., Huang, A. M. and Chang, W. S. (2011). An integrative approach to identifying cancer chemoresistance-associated pathways. *Bmc Medical Genomics*

Chen, J., Kobayashi, M., Darmanin, S., Qiao, Y., Gully, C., Zhao, R., Yeung, S. C. and Lee, M. H. (2009). Pim-1 plays a pivotal role in hypoxia-induced chemoresistance. *Oncogene* **28**, 2581-92.

Chen, J., Imanaka, N., Chen, J. and Griffin, J. D. (2010). Hypoxia potentiates Notch signaling in breast cancer leading to decreased E-cadherin expression and increased cell migration and invasion. *British Journal of Cancer* **2**, 351-360.

Chen, J., Guo, K. and Kastan, M. B. (2012). Interactions of nucleolin and ribosomal protein L26 (RPL26) in translational control of human p53 mRNA. *Journal of Biological Chemistry* **20**, 16467-76.

Chen, J. D., Lin, J. Y. and Levine, A. J. (1995). Regulation of Transcription Functions of the P53 Tumor-Suppressor by the Mdm-2 Oncogene. *Molecular Medicine* **2**, 142-152.

Chen, L., Feng, P. M., Li, S. F., Long, D., Cheng, J. Q., Lu, Y. R. and Zhou, D. (2009). Effect of Hypoxia-inducible Factor-1 alpha Silencing on the Sensitivity of Human Brain Glioma Cells to Doxorubicin and Etoposide. *Neurochemical Research* **5**, 984-990.

Chen, M. J., Shimada, T., Moulton, A. D., Cline, A., Humphries, R. K., Maizel, J. and Nienhuis, A. W. (1984). The functional human dihydrofolate reductase gene. *Journal of Biological Chemistry* **6**, 3933-43.

Chen, Z., Lai, T. C., Jan, Y. H., Lin, F. M., Wang, W. C., Xiao, H., Wang, Y. T., Sun, W., Cui, X. P., Li, Y. S., Fang, T., Zhao, H. W., Padmanabhan, C., Sun, R. B., Wang, D. L., Jin, H. L., Chau, G. Y., Huang, H. D., Hsiao, M. and Shyy, J. Y. J. (2013). Hypoxia-responsive miRNAs target argonaute 1 to promote angiogenesis. *Journal of Clinical Investigation* **3**, 1057-1067.

Chendrimada, T. P., Gregory, R. I., Kumaraswamy, E., Norman, J., Cooch, N., Nishikura, K. and Shiekhattar, R. (2005). TRBP recruits the Dicer complex to Ago2 for microRNA processing and gene silencing. *Nature* **7051**, 740-744.

Cheng, Y. H., Tao, Y., Black, I. B. and DiCicco-Bloom, E. (2001). A single peripheral injection of basic fibroblast growth factor (bFGF) stimulates granule cell production and increases cerebellar growth in newborn rats. *Journal of Neurobiology* **3**, 220-229.

Chia, S. K., Wykoff, C. C., Watson, P. H., Han, C., Leek, R. D., Pastorek, J., Gatter, K. C., Ratcliffe, P. and Harris, A. L. (2001). Prognostic significance of a novel hypoxia-regulated marker, carbonic anhydrase IX, in invasive breast carcinoma. *Journal of Clinical Oncology* **16**, 3660-3668.

Chin, K. V., Ueda, K., Pastan, I. and Gottesman, M. M. (1992). Modulation of activity of the promoter of the human MDR1 gene by Ras and p53. *Science* **5043**, 459-62.

Cho, W. C. S. (2007). OncomiRs: the discovery and progress of microRNAs in cancers. *Molecular Cancer*

Cho, Y. J., Tsherniak, A., Tamayo, P., Santagata, S., Ligon, A., Greulich, H., Berhoukim, R., Amani, V., Goumnerova, L., Eberhart, C. G., Lau, C. C., Olson, J. M., Gilbertson, R. J., Gajjar, A., Delattre, O., Kool, M., Ligon, K., Meyerson, M., Mesirov, J. P. and Pomeroy, S. L. (2011). Integrative Genomic Analysis of Medulloblastoma Identifies a Molecular Subgroup That Drives Poor Clinical Outcome. *Journal of Clinical Oncology* **11**, 1424-1430.

Choi, D. W., Seo, Y. M., Kim, E. A., Sung, K. S., Ahn, J. W., Park, S. J., Lee, S. R. and Choi, C. Y. (2008). Ubiquitination and degradation of homeodomain-interacting protein kinase 2 by WD40 repeat/SOCS box protein WSB-1. *Journal of Biological Chemistry* **8**, 4682-4689.

Chou, P. M., ReyesMugica, M., Barquin, N., Yasuda, T., Tan, X. D. and Tomita, T. (1995). Multidrug resistance gene expression in childhood medulloblastoma: Correlation with clinical outcome and DNA ploidy in 29 patients. *Pediatric Neurosurgery* **6**, 283-291.

Choudhury, A., Nelson, L. D., Teo, M. T. W., Chilka, S., Bhattarai, S., Johnston, C. F., Elliott, F., Lowery, J., Taylor, C. F., Churchman, M., Bentley, J., Knowles, M. A., Harnden, P., Bristow, R. G., Bishop, D. T. and Kiltie, A. E. (2010). MRE11 Expression Is Predictive of Cause-Specific Survival following Radical Radiotherapy for Muscle-Invasive Bladder Cancer. *Cancer Research* **18**, 7017-7026.

Chrisanthar, R., Knappskog, S., Lokkevik, E., Anker, G., Ostenstad, B., Lundgren, S., Berge, E. O., Risberg, T., Mjaaland, I., Maehle, L., Engebretsen, L. F., Lillehaug, J. R. and Lonning, P. E. (2008). CHEK2 Mutations Affecting Kinase Activity Together With Mutations in TP53

Indicate a Functional Pathway Associated with Resistance to Epirubicin in Primary Breast Cancer. *Plos One* **8**,

Christofori, G. and Semb, H. (1999). The role of the cell-adhesion molecule E-cadherin as a tumour-suppressor gene. *Trends in Biochemical Sciences* **2**, 73-76.

Chun, H. H. and Gatti, R. A. (2004). Ataxia-telangiectasia, an evolving phenotype. *DNA Repair* **8-9**, 1187-1196.

Cimmino, A., Calin, G. A., Fabbri, M., Iorio, M. V., Ferracin, M., Shimizu, M., Wojcik, S. E., Aqeilan, R. I., Zupo, S., Dono, M., Rassenti, L., Alder, H., Volinia, S., Liu, C. G., Kipps, T. J., Negrini, M. and Croce, C. M. (2005). miR-15 and miR-16 induce apoptosis by targeting BCL2. *Proc Natl Acad Sci U S A* **39**, 13944-9.

Ciruna, B. and Rossant, J. (2001). FGF signaling regulates mesoderm cell fate specification and morphogenetic movement at the primitive streak. *Developmental Cell* **1**, 37-49.

Clifford, S. C., Lusher, M. E., Lindsey, J. C., Langdon, J. A., Gilbertson, R. J., Straughton, D. and Ellison, D. W. (2006). Wnt/Wingless pathway activation and chromosome 6 loss characterize a distinct molecular sub-group of medulloblastomas associated with a favorable prognosis. *Cell Cycle* **22**, 2666-70.

Collingridge, D. R., Piepmeier, J. M., Rockwell, S. and Knisely, J. P. S. (1999). Polarographic measurements of oxygen tension in human glioma and surrounding peritumoural brain tissue. *Radiotherapy and Oncology* **2**, 127-131.

Comerford, K. M., Wallace, T. J., Karhausen, J., Louis, N. A., Montalto, M. C. and Colgan, S. P. (2002). Hypoxia-inducible factor-1-dependent regulation of the multidrug resistance (MDR1) gene. *Cancer Res* **12**, 3387-94.

Connolly, D. T., Heuvelman, D. M., Nelson, R., Olander, J. V., Eppley, B. L., Delfino, J. J., Siegel, N. R., Leimgruber, R. M. and Feder, J. (1989). Tumor Vascular-Permeability Factor Stimulates Endothelial-Cell Growth and Angiogenesis. *Journal of Clinical Investigation* **5**, 1470-1478.

Cordon-Cardo, C., O'Brien, J. P., Casals, D., Rittman-Grauer, L., Biedler, J. L., Melamed, M. R. and Bertino, J. R. (1989). Multidrug-resistance gene (P-glycoprotein) is expressed by endothelial cells at blood-brain barrier sites. *Proc Natl Acad Sci U S A* **2**, 695-8.

Cosse, J. P., Sermeus, A., Vannuvel, K., Ninane, N., Raes, M. and Michiels, C. (2007). Differential effects of hypoxia on etoposide-induced apoptosis according to the cancer cell lines. *Mol Cancer* 61.

Costanzo, V., Paull, T., Gottesman, M. and Gautier, J. (2004). Mre11 assembles linear DNA fragments into DNA damage signaling complexes. *Plos Biology* **6**, 876-876.

Covello, K. L., Kehler, J., Yu, H. W., Gordan, J. D., Arsham, A. M., Hu, C. J., Labosky, P. A., Simon, M. C. and Keith, B. (2006). HIF-2 alpha regulates Oct-4: effects of hypoxia on stem cell function, embryonic development, and tumor growth. *Genes & Development* **5**, 557-570.

Cowger, J. J. M., Zhao, Q., Isovic, M. and Torchia, J. (2007). Biochemical characterization of the zinc-finger protein 217 transcriptional repressor complex: identification of a ZNF217 consensus recognition sequence. *Oncogene* **23**, 3378-3386.

Craig, A. L., Burch, L., Vojtesek, B., Mikutowska, J., Thompson, A. and Hupp, T. R. (1999). Novel phosphorylation sites of human tumour suppressor protein p53 at Ser(20) and Thr(18) that disrupt the binding of mdm2 (mouse double minute 2) protein are modified in human cancers. *Biochemical Journal* 133-141.

Crea, F., Fornaro, L., Paolicchi, E., Masi, G., Frumento, P., Loupakis, F., Salvatore, L., Cremolini, C., Schirripa, M., Graziano, F., Ronzoni, M., Ricci, V., Farrar, W. L., Falcone, A. and Danesi, R. (2012). An EZH2 polymorphism is associated with clinical outcome in metastatic colorectal cancer patients. *Ann Oncol* **5**, 1207-13.

Dahmen, R. P., Koch, A., Denkhaus, D., Tonn, J. C., Sorensen, N., Berthold, F., Behrens, J., Birchmeier, W., Wiestler, O. D. and Pietsch, T. (2001). Deletions of AXIN1, a component of the WNT/wingless pathway, in sporadic medulloblastomas. *Cancer Research* **19**, 7039-7043.

Dai, C. and Gu, W. (2010). p53 post-translational modification: deregulated in tumorigenesis. *Trends in Molecular Medicine* **11**, 528-536.

Deb, S., Jackson, C. T., Subler, M. A. and Martin, D. W. (1992). Modulation of cellular and viral promoters by mutant human p53 proteins found in tumor cells. *Journal of Virology* **10**, 6164-70.

Deng, X. Q., Chen, L. L. and Li, N. X. (2007). The expression of SIRT1 in nonalcoholic fatty liver disease induced by high-fat diet in rats. *Liver Int* **5**, 708-15.

Dewhirst, M. W., Cao, Y. and Moeller, B. (2008). Cycling hypoxia and free radicals regulate angiogenesis and radiotherapy response. *Nature Reviews Cancer* **6**, 425-437.

Di Como, C. J. and Prives, C. (1998). Human tumor-derived p53 proteins exhibit binding site selectivity and temperature sensitivity for transactivation in a yeast-based assay. *Oncogene* **19**, 2527-2539.

Diaz, L. A., Williams, R. T., Wu, J., Kinde, I., Hecht, J. R., Berlin, J., Allen, B., Bozic, I., Reiter, J. G., Nowak, M. A., Kinzler, K. W., Oliner, K. S. and Vogelstein, B. (2012). The molecular evolution of acquired resistance to targeted EGFR blockade in colorectal cancers. *Nature* **7404**, 537-540.

Diedrich, U., Lucius, J., Baron, E., Behnke, J., Pabst, B. and Zoll, B. (1995). Distribution of Epidermal Growth-Factor Receptor Gene Amplification in Brain-Tumors and Correlation to Prognosis. *Journal of Neurology* **10**, 683-688.

Dirks, P. B. (2001). Glioma migration: clues from the biology of neural progenitor cells and embryonic CNS cell migration. *Journal of Neuro-Oncology* **2**, 203-212.

Dirks, P. B. (2008). Brain tumor stem cells: Bringing order to the chaos of brain cancer. *Journal of Clinical Oncology* **17**, 2916-2924.

Distel, L., Neubauer, S., Varon, R., Holter, W. and Grabenbauer, G. (2003). Fatal toxicity following radio- and chemotherapy of medulloblastoma in a child with unrecognized Nijmegen breakage syndrome. *Medical and Pediatric Oncology* **1**, 44-48.

Dong, Q., Johnson, S. P., Colvin, O. M., Bullock, N., Kilborn, C., Runyon, G., Sullivan, D. M., Easton, J., Bigner, D. D., Nahta, R., Marks, J., Modrich, P. and Friedman, H. S. (1999). Multiple DNA repair mechanisms and alkylator resistance in the human medulloblastoma cell line D-283 Med (4-HCR). *Cancer Chemotherapy and Pharmacology* **1**, 73-79.

Doublier, S., Belisario, D. C., Polimeni, M., Annaratone, L., Riganti, C., Allia, E., Ghigo, D., Bosia, A. and Sapino, A. (2012). HIF-1 activation induces doxorubicin resistance in MCF7 3-D spheroids via P-glycoprotein expression: a potential model of the chemoresistance of invasive micropapillary carcinoma of the breast. *Bmc Cancer*

Dunn, C., Wiltshire, C., MacLaren, A. and Gillespie, D. A. F. (2002). Molecular mechanism and biological functions of c-Jun N-terminal kinase signalling via the c-Jun transcription factor. *Cellular Signalling* **7**, 585-593.

Dunwoodie, S. L. (2009). The Role of Hypoxia in Development of the Mammalian Embryo. *Developmental Cell* **6**, 755-773.

Dvorak, H. F., Nagy, J. A. and Dvorak, A. M. (1991). Structure of Solid Tumors and Their Vasculature - Implications for Therapy with Monoclonal-Antibodies. *Cancer Cells-a Monthly Review* **3**, 77-85.

Eastman, A. (1987). The Formation, Isolation and Characterization of DNA Adducts Produced by Anticancer Platinum Complexes. *Pharmacology & Therapeutics* **2**, 155-166.

Eberhart, C. G. (2003). Medulloblastoma in mice lacking p53 and PARP - A roads lead to Gli. *American Journal of Pathology* **1**, 7-10.

Ebi, H., Matsuo, K., Sugito, N., Suzuki, M., Osada, H., Tajima, K., Ueda, R. and Takahashi, T. (2007). Novel NBS1 heterozygous germ line mutation causing MRE11-binding domain loss predisposes to common types of cancer. *Cancer Research* **23**, 11158-11165.

Ehlers, J. P. and Harbour, J. W. (2005). NBS1 expression as a prognostic marker in uveal melanoma. *Clinical Cancer Research* **5**, 1849-1853.

Eich, M., Roos, W. P., Dianov, G. L., Digweed, M. and Kaina, B. (2010). Nijmegen Breakage Syndrome Protein (NBN) Causes Resistance to Methylating Anticancer Drugs Such as Temozolomide. *Molecular Pharmacology* **5**, 943-951.

Ekstrand, A. J., James, C. D., Cavenee, W. K., Seliger, B., Pettersson, R. F. and Collins, V. P. (1991). Genes for Epidermal Growth-Factor Receptor, Transforming Growth Factor-Alpha, and Epidermal Growth-Factor and Their Expression in Human Gliomas Invivo. *Cancer Res* **8**, 2164-2172.

Eliyahu, D., Raz, A., Gruss, P., Givol, D. and Oren, M. (1984). Participation of p53 cellular tumour antigen in transformation of normal embryonic cells. *Nature* **5995**, 646-9.

Ellison, D., Dalton, J., Brat, D., Perry, A., Yong, W. and Kocak, M. (2011). Molecular Subgroups In Medulloblastoma. *Journal of Neuropathology and Experimental Neurology* **6**, 526-526.

Ellison, D. W., Onilude, O. E., Lindsey, J. C., Lusher, M. E., Weston, C. L., Taylor, R. E., Pearson, A. D., Clifford, S. C. and United Kingdom Children's Cancer Study Group Brain Tumour, C. (2005). beta-Catenin status predicts a favorable outcome in childhood medulloblastoma: the United Kingdom Children's Cancer Study Group Brain Tumour Committee. *Journal of Clinical Oncology* **31**, 7951-7.

Ellison, D. W., Dalton, J., Kocak, M., Nicholson, S. L., Fraga, C., Neale, G., Kenney, A. M., Brat, D. J., Perry, A., Yong, W. H., Taylor, R. E., Bailey, S., Clifford, S. C. and Gilbertson, R. J. (2011). Medulloblastoma: clinicopathological correlates of SHH, WNT, and non-SHH/WNT molecular subgroups. *Acta Neuropathol* **3**, 381-396.

Elvidge, G. P., Glenny, L., Appelhoff, R. J., Ratcliffe, P. J., Ragoussis, J. and Gleadle, J. M. (2006). Concordant regulation of gene expression by hypoxia and 2-oxoglutarate-dependent dioxygenase inhibition: the role of HIF-1alpha, HIF-2alpha, and other pathways. *J Biol Chem* **22**, 15215-26.

Erber, R., Conradt, C., Homann, N., Enders, C., Finckh, M., Dietz, A., Weidauer, H. and Bosch, F. X. (1998). TP53 DNA contact mutations are selectively associated with allelic loss and have a strong clinical impact in head and neck cancer. *Oncogene* **13**, 1671-1679.

Erler, J. T., Cawthorne, C. J., Williams, K. J., Koritzinsky, M., Wouters, B. G., Wilson, C., Miller, C., Demonacos, C., Stratford, I. J. and Dive, C. (2004). Hypoxia-mediated down-

regulation of Bid and Bax in tumors occurs via hypoxia-inducible factor 1-dependent and -independent mechanisms and contributes to drug resistance. *Mol Cell Biol* **7**, 2875-89.

Evans, S. M., Judy, K. D., Dunphy, I., Jenkins, W. T., Nelson, P. T., Collins, R., Wileyto, E. P., Jenkins, K., Hahn, S. M., Stevens, C. W., Judkins, A. R., Phillips, P., Geoerger, B. and Koch, C. J. (2004). Comparative measurements of hypoxia in human brain tumors using needle electrodes and EF5 binding. *Cancer Research* **5**, 1886-1892.

Fan, S. J., Smith, M. L., Rivet, D. J., Duba, D., Zhan, Q. M., Kohn, K. W., Fornace, A. J. and Oconnor, P. M. (1995). Disruption of P53 Function Sensitizes Breast-Cancer Mcf-7 Cells to Cisplatin and Pentoxifylline. *Cancer Research* **8**, 1649-1654.

Fan, X., Matsui, W., Khaki, L., Stearns, D., Chun, J., Li, Y. M. and Eberhart, C. G. (2006). Notch pathway inhibition depletes stem-like cells and blocks engraftment in embryonal brain tumors. *Neuro-Oncology* **4**, 396-396.

Fan, X. and Eberhart, C. G. (2008). Medulloblastoma stem cells. *Journal of Clinical Oncology* **17**, 2821-2827.

Faria, C. C. S., C.A.; Rutka, J.T. (2013). New Molecular Targets and Treatments for Pediatric Brain Tumors.

Fattet, S., Haberler, C., Legoix, P., Varlet, P., Lellouch-Tubiana, A., Lair, S., Manie, E., Raquin, M. A., Bours, D., Carpentier, S., Barillot, E., Grill, J., Doz, F., Puget, S., Janoueix-Lerosey, I. and Delattre, O. (2009). Beta-catenin status in paediatric medulloblastomas: correlation of immunohistochemical expression with mutational status, genetic profiles, and clinical characteristics. *Journal of Pathology* **1**, 86-94.

Feldman, R. J., Sementchenko, V. I., Gayed, M., Fraig, M. M. and Watson, D. K. (2003). Pdef expression in human breast cancer is correlated with invasive potential and altered gene expression. *Cancer Research* **15**, 4626-4631.

Felsenfeld, G. and Groudine, M. (2003). Controlling the double helix. *Nature* **6921**, 448-453.

Ferretti, E., De Smaele, E., Po, A., Di Marcotullio, L., Tosi, E., Espinola, M. S., Di Rocco, C., Riccardi, R., Giangaspero, F., Farcomeni, A., Nofroni, I., Laneve, P., Gioia, U., Caffarelli, E., Bozzoni, I., Screpanti, I. and Gulino, A. (2009). MicroRNA profiling in human medulloblastoma. *Int J Cancer* **3**, 568-77.

Feun, L. G., Savaraj, N. and Landy, H. J. (1994). Drug resistance in brain tumors. *J Neurooncol* **2**, 165-76.

Filippo, J. S., Sung, P. and Klein, H. (2008). Mechanism of eukaryotic homologous recombination. *Annual Review of Biochemistry* 229-257.

Finlay, C. A., Hinds, P. W. and Levine, A. J. (1989). The p53 proto-oncogene can act as a suppressor of transformation. *Cell* **7**, 1083-93.

Fiscella, M., Zhang, H., Fan, S., Sakaguchi, K., Shen, S., Mercer, W. E., Vande Woude, G. F., O'Connor, P. M. and Appella, E. (1997). Wip1, a novel human protein phosphatase that is induced in response to ionizing radiation in a p53-dependent manner. *Proc Natl Acad Sci U S A* **12**, 6048-53.

Fisher, R. A. (1922). On the interpretation of x(2) from contingency tables, and the calculation of P. *Journal of the Royal Statistical Society* 87-94.

Flamant, L., Notte, A., Ninane, N., Raes, M. and Michiels, C. (2010). Anti-apoptotic role of HIF-1 and AP-1 in paclitaxel exposed breast cancer cells under hypoxia. *Molecular Cancer*

Flamant, L., Roegiers, E., Pierre, M., Hayez, A., Sterpin, C., De Backer, O., Arnould, T., Poumay, Y. and Michiels, C. (2012). TMEM45A is essential for hypoxia-induced chemoresistance in breast and liver cancer cells. *Bmc Cancer*

Folkman, J., Hahnfeldt, P. and Hlatky, L. (2000). Cancer: looking outside the genome. *Nature Reviews Molecular Cell Biology* **1**, 76-79.

Ford, J., Jiang, M. and Milner, J. (2005). Cancer-specific functions of SIRT1 enable human epithelial cancer cell growth and survival. *Cancer Research* **22**, 10457-10463.

Forment, J. V., Kaidi, A. and Jackson, S. P. (2012). Chromothripsis and cancer: causes and consequences of chromosome shattering. *Nature Reviews Cancer* **10**, 663-670.

Forristal, C. E., Wright, K. L., Hanley, N. A., Oreffo, R. O. C. and Houghton, F. D. (2010). Hypoxia inducible factors regulate pluripotency and proliferation in human embryonic stem cells cultured at reduced oxygen tensions. *Reproduction* **1**, 85-97.

Forsythe, J. A., Jiang, B. H., Iyer, N. V., Agani, F., Leung, S. W., Koos, R. D. and Semenza, G. L. (1996). Activation of vascular endothelial growth factor gene transcription by hypoxia-inducible factor 1. *Molecular and Cellular Biology* **9**, 4604-4613.

Francoz, S., Froment, P., Bogaerts, S., De Clercq, S., Maetens, M., Doumont, G., Bellefroid, E. and Marine, J. C. (2006). Mdm4 and Mdm2 cooperate to inhibit p53 activity in proliferating and quiescent cells in vivo. *Proceedings of the National Academy of Sciences of the United States of America* **9**, 3232-3237.

Frange, P., Alapetite, C., Gaboriaud, G., Bours, D., Zucker, J. M., Zerah, M., Brisse, H., Chevignard, M., Mosseri, V., Bouffet, E. and Doz, F. (2009). From childhood to adulthood: long-term outcome of medulloblastoma patients. The Institut Curie experience (1980-2000). *J Neurooncol* **2**, 271-9.

Franke, T. F., Kaplan, D. R. and Cantley, L. C. (1997). PI3K: Downstream AKTion blocks apoptosis. *Cell* **4**, 435-437.

Frankel, R. H., Bayona, W., Koslow, M. and Newcomb, E. W. (1992). P53 Mutations in Human-Malignant Gliomas - Comparison of Loss of Heterozygosity with Mutation Frequency. *Cancer Research* **6**, 1427-1433.

Freed-Pastor, W. A. and Prives, C. (2012). Mutant p53: one name, many proteins. *Genes & Development* **12**, 1268-1286.

Friedman, H. S., Colvin, O. M., Kaufmann, S. H., Ludeman, S. M., Bullock, N., Bigner, D. D. and Griffith, O. W. (1992). Cyclophosphamide Resistance in Medulloblastoma. *Cancer Research* **19**, 5373-5378.

Fruman, D. A., Meyers, R. E. and Cantley, L. C. (1998). Phosphoinositide kinases. *Annual Review of Biochemistry* 481-507.

Fujita, Y., Kojima, K., Hamada, N., Ohhashi, R., Akao, Y., Nozawa, Y., Deguchi, T. and Ito, M. (2008). Effects of miR-34a on cell growth and chemoresistance in prostate cancer PC3 cells. *Biochem Biophys Res Commun* **1**, 114-9.

Fukuoka, M., Yano, S., Giaccone, G., Tamura, T., Nakagawa, K., Douillard, J. Y., Nishiwaki, Y., Vansteenkiste, J., Kudoh, S., Rischin, D., Eek, R., Horai, T., Noda, K., Takata, I., Smit, E., Averbuch, S., Macleod, A., Feyereislova, A., Dong, R. P. and Baselga, J. (2003). Multi-institutional randomized phase II trial of gefitinib for previously treated patients with advanced non-small-cell lung cancer. *Journal of Clinical Oncology* **12**, 2237-2246.

Furnari, F. B., Fenton, T., Bachoo, R. M., Mukasa, A., Stommel, J. M., Stegh, A., Hahn, W. C., Ligon, K. L., Louis, D. N., Brennan, C., Chin, L., DePinho, R. A. and Cavenee, W. K. (2007).

Malignant astrocytic glioma: genetics, biology, and paths to treatment. *Genes Dev* **21**, 2683-710.

Gaiddon, C., Lokshin, M., Ahn, J., Zhang, T. and Prives, C. (2001). A subset of tumor-derived mutant forms of p53 down-regulate p63 and p73 through a direct interaction with the p53 core domain. *Molecular and Cellular Biology* **5**, 1874-1887.

Gao, J. F., Zhang, H., Arbman, G. and Sun, X. F. (2008). RAD50/MRE11/NBS1 proteins in relation to tumour development and prognosis in patients with microsatellite stable colorectal cancer. *Histology and Histopathology* **12**, 1495-1502.

Garcia-Montero, A., Vasseur, S., Mallo, G. V., Soubeyran, P., Dagorn, J. C. and Iovanna, J. L. (2001). Expression of the stress-induced p8 mRNA is transiently activated after culture medium change. *European Journal of Cell Biology* **11**, 720-725.

Garzia, L., Andolfo, I., Cusanelli, E., Marino, N., Petrosino, G., De Martino, D., Esposito, V., Galeone, A., Navas, L., Esposito, S., Gargiulo, S., Fattet, S., Donofrio, V., Cinalli, G., Brunetti, A., Del Vecchio, L., Northcott, P. A., Delattre, O., Taylor, M. D., Iolascon, A. and Zollo, M. (2009). MicroRNA-199b-5p Impairs Cancer Stem Cells through Negative Regulation of HES1 in Medulloblastoma. *PLoS One* **3**,

Gasco, M. and Crook, T. (2003). p53 family members and chemoresistance in cancer: what we know and what we need to know. *Drug Resistance Updates* **6**, 323-328.

Gatcliffe, T. A., Monk, B. J., Planutis, K. and Holcombe, R. F. (2008). Wnt signaling in ovarian tumorigenesis. *International Journal of Gynecological Cancer* **5**, 954-962.

Gatei, M., Young, D., Cerosaletti, K. M., Desai-Mehta, A., Spring, K., Kozlov, S., Lavin, M. F., Gatti, R. A., Concannon, P. and Khanna, K. (2000). ATM-dependent phosphorylation of nibrin in response to radiation exposure. *Nat Genet* **1**, 115-9.

Gatenby, R. A. and Gillies, R. J. (2004). Why do cancers have high aerobic glycolysis? *Nature Reviews Cancer* **11**, 891-899.

Gatti, L. and Zunino, F. (2005). Overview of tumor cell chemoresistance mechanisms. *Methods Mol Med* 127-48.

Gee, H. E., Camps, C., Buffa, F. M., Patiar, S., Winter, S. C., Betts, G., Homer, J., Corbridge, R., Cox, G., West, C. M. L., Ragoussis, J. and Harris, A. L. (2010). hsa-mir-210 Is a Marker of Tumor Hypoxia and a Prognostic Factor in Head and Neck Cancer. *Cancer* **9**, 2148-2158.

Geisler, S., Lonning, P. E., Aas, T., Johnsen, H., Fluge, O., Haugen, D. F., Lillehaug, J. R., Akslen, L. A. and Borresen-Dale, A. L. (2001). Influence of TP53 gene alterations and c-erbB-2 expression on the response to treatment with doxorubicin in locally advanced breast cancer. *Cancer Research* **6**, 2505-2512.

Geoerger, B., Hargrave, D., Thomas, F., Ndiaye, A., Frappaz, D., Andreiuolo, F., Varlet, P., Aerts, I., Riccardi, R., Jaspan, T., Chatelut, E., Le Deley, M. C., Paoletti, X., Saint-Rose, C., Leblond, P., Morland, B., Gentet, J. C., Meresse, V., Vassal, G. and Ca, I. I. T. C. (2011). Innovative Therapies for Children with Cancer pediatric phase I study of erlotinib in brainstem glioma and relapsing/refractory brain tumors. *Neuro-Oncology* **1**, 109-118.

Geva-Zatorsky, N., Rosenfeld, N., Itzkovitz, S., Milo, R., Sigal, A., Dekel, E., Yarnitzky, T., Liron, Y., Polak, P., Lahav, G. and Alon, U. (2006). Oscillations and variability in the p53 system. *Molecular Systems Biology*

Ghosh, G., Subramanian, I. V., Adhikari, N., Zhang, X. X., Joshi, H. P., Basi, D., Chandrashekhar, Y. S., Hall, J. L., Roy, S., Zeng, Y. and Ramakrishnan, S. (2010). Hypoxia-

induced microRNA-424 expression in human endothelial cells regulates HIF-alpha isoforms and promotes angiogenesis. *Journal of Clinical Investigation* **11**, 4141-4154.

Giaccia, A. J. and Kastan, M. B. (1998). The complexity of p53 modulation: emerging patterns from divergent signals. *Genes & Development* **19**, 2973-2983.

Giampieri, S., Manning, C., Hooper, S., Jones, L., Hill, C. S. and Sahai, E. (2009). Localized and reversible TGF beta signalling switches breast cancer cells from cohesive to single cell motility. *Nature Cell Biology* **11**, 1287-U49.

Gilbertson, R., Wickramasinghe, C., Hernan, R., Balaji, V., Hunt, D., Jones-Wallace, D., Crolla, J., Perry, R., Lunec, J., Pearson, A. and Ellison, D. (2001). Clinical and molecular stratification of disease risk in medulloblastoma. *British Journal of Cancer* **5**, 705-712.

Gilbertson, R. J. (2004). Medulloblastoma: signalling a change in treatment. *Lancet Oncol* **4**, 209-18.

Gjerset, R. A., Turla, S. T., Sobol, R. E., Scalise, J. J., Mercola, D., Collins, H. and Hopkins, P. J. (1995). Use of wild-type p53 to achieve complete treatment sensitization of tumor cells expressing endogenous mutant p53. *Molecular Carcinogenesis* **4**, 275-285.

Goldberg, E., Nemudry, A., Boldyrev, V. and Schollhorn, R. (1998). Model for anomalous transport of oxygen in nonstoichiometric perovskites 1. General formulation of the problem. *Solid State Ionics* **3-4**, 223-233.

Golding, S. E., Rosenberg, E., Adams, B. R., Wignarajah, S., Beckta, J. M., O'Connor, M. J. and Valerie, K. (2012). Dynamic inhibition of ATM kinase provides a strategy for glioblastoma multiforme radiosensitization and growth control. *Cell Cycle* **6**, 1167-1173.

Gottesman, M. M., Fojo, T. and Bates, S. E. (2002). Multidrug resistance in cancer: Role of ATP-dependent transporters. *Nature Reviews Cancer* **1**, 48-58.

Gowda, K. K., Gupta, K., Kapoor, R. and Vasishta, R. K. (2012). Nuclear expression of beta-catenin and stem cell markers as potential prognostic indicators in medulloblastoma. *Neurology India* **5**, 487-494.

Graeber, T. G., Peterson, J. F., Tsai, M., Monica, K., Fornace, A. J. and Giaccia, A. J. (1994). Hypoxia Induces Accumulation of P53 Protein, but Activation of a G(1)-Phase Checkpoint by Low-Oxygen Conditions Is Independent of P53 Status. *Molecular and Cellular Biology* **9**, 6264-6277.

Greijer, A. E. and van der Wall, E. (2004). The role of hypoxia inducible factor 1 (HIF-1) in hypoxia induced apoptosis. *J Clin Pathol* **10**, 1009-14.

Gu, Y. Z., Moran, S. M., Hogenesch, J. B., Wartman, L. and Bradfield, C. A. (1998). Molecular characterization and chromosomal localization of a third alpha-class hypoxia inducible factor subunit, HIF3 alpha. *Gene Expression* **3**, 205-213.

Guessous, F., Li, Y. Q. and Abounader, R. (2008). Signaling Pathways in Medulloblastoma. *Journal of Cellular Physiology* **3**, 577-583.

Guessous, F., Zhang, Y., Kofman, A., Catania, A., Li, Y., Schiff, D., Purow, B. and Abounader, R. (2010). microRNA-34a is tumor suppressive in brain tumors and glioma stem cells. *Cell Cycle* **6**, 1031-6.

Guo, K., Searfoss, G., Krolikowski, D., Pagnoni, M., Franks, C., Clark, K., Yu, K. T., Jaye, M. and Ivashchenko, Y. (2001). Hypoxia induces the expression of the pro-apoptotic gene BNIP3. *Cell Death Differ* **4**, 367-76.

Gurtner, A., Starace, G., Norelli, G., Piaggio, G., Sacchi, A. and Bossi, G. (2010). Mutant p53-induced up-regulation of mitogen-activated protein kinase kinase 3 contributes to gain of function. *Journal of Biological Chemistry* **19**, 14160-9.

Gustafsson, M. V., Zheng, X. W., Pereira, T., Gradin, K., Jin, S. B., Lundkvist, J., Ruas, J. L., Poellinger, L., Lendahl, U. and Bondesson, M. (2005). Hypoxia requires Notch signaling to maintain the undifferentiated cell state. *Developmental Cell* **5**, 617-628.

Haidar, M. A., Kantarjian, H., Manshouri, T., Chang, C. Y., O'Brien, S., Freireich, E., Keating, M. and Albitar, M. (2000). ATM gene deletion in patients with adult acute lymphoblastic leukemia. *Cancer* **5**, 1057-1062.

Hama, S., Matsuura, S., Tauchi, H., Sawada, J., Kato, C., Yamasaki, F., Yoshioka, H., Sugiyama, K., Arita, K., Kurisu, K., Kamada, N., Heike, Y. and Komatsu, K. (2000). Absence of mutations in the NBS1 gene in B-cell malignant lymphoma patients. *Anticancer Research* **3B**, 1897-1900.

Hambardzumyan, D., Becher, O. J., Rosenblum, M. K., Pandolfi, P. P., Manova-Todorova, K. and Holland, E. C. (2008). PI3K pathway regulates survival of cancer stem cells residing in the perivascular niche following radiation in medulloblastoma in vivo. *Genes & Development* **4**, 436-448.

Hammond, E. M. and Giaccia, A. J. (2005). The role of p53 in hypoxia-induced apoptosis. *Biochem Biophys Res Commun* **3**, 718-25.

Hammond, S. M., Bernstein, E., Beach, D. and Hannon, G. J. (2000). An RNA-directed nuclease mediates post-transcriptional gene silencing in Drosophila cells. *Nature* **6775**, 293-6.

Hamstra, D. A., Bhojani, M. S., Griffin, L. B., Laxman, B., Ross, B. D. and Rehemtulla, A. (2006). Real-time evaluation of p53 oscillatory behavior in vivo using bioluminescent imaging. *Cancer Research* **15**, 7482-7489.

Hanahan, D. and Folkman, J. (1996). Patterns and emerging mechanisms of the angiogenic switch during tumorigenesis. *Cell* **3**, 353-364.

Hanahan, D. and Weinberg, R. A. (2000). The hallmarks of cancer. *Cell* **1**, 57-70.

Hanahan, D. and Weinberg, R. A. (2011). Hallmarks of Cancer: The Next Generation. *Cell* **5**, 646-674.

Hao, J., Song, X., Song, B., Liu, Y., Wei, L., Wang, X. and Yu, J. (2008). Effects of lentivirus-mediated HIF-1 alpha knockdown on hypoxia-related cisplatin resistance and their dependence on p53 status in fibrosarcoma cells. *Cancer Gene Therapy* **7**, 449-455.

Hargrave, D. R. and Zacharoulis, S. (2007). Pediatric CNS tumors: current treatment and future directions. *Expert Rev Neurother* **8**, 1029-42.

Harris, S. L. and Levine, A. J. (2005). The p53 pathway: positive and negative feedback loops. *Oncogene* **17**, 2899-908.

Hartlerode, A. J. and Scully, R. (2009). Mechanisms of double-strand break repair in somatic mammalian cells. *Biochemical Journal* 157-168.

Hartmann, W., Digon-Sontgerath, B., Koch, A., Waha, A., Endl, E., Dani, I., Denkhaus, D., Goodyer, C. G., Sorensen, N., Wiestler, O. D. and Pietsch, T. (2006). Phosphatidylinositol 3 '-kinase/AKT signaling is activated in medulloblastoma cell proliferation and is associated with reduced expression of PTEN. *Clinical Cancer Research* **10**, 3019-3027.

Hassig, C. A., Tong, J. K., Fleischer, T. C., Owa, T., Grable, P. G., Ayer, D. E. and Schreiber, S. L. (1998). A role for histone deacetylase activity in HDAC1-mediated transcriptional repression. *Proc Natl Acad Sci U S A* **7**, 3519-24.

Haupt, Y., Maya, R., Kazaz, A. and Oren, M. (1997). Mdm2 promotes the rapid degradation of p53. *Nature* **6630**, 296-9.

He, X. Y., He, L. and Hannon, G. J. (2007). The guardian's little helper: MicroRNAs in the p53 tumor suppressor network. *Cancer Research* **23**, 11099-11101.

Hemmati, H. D., Nakano, I., Lazareff, J. A., Masterman-Smith, M., Geschwind, D. H., Bronner-Fraser, M. and Kornblum, H. I. (2003). Cancerous stem cells can arise from pediatric brain tumors. *Proceedings of the National Academy of Sciences of the United States of America* **25**, 15178-15183.

Henze, A. T., Riedel, J., Diem, T., Wenner, J., Flamme, I., Pouyseggur, J., Plate, K. H. and Acker, T. (2010). Prolyl Hydroxylases 2 and 3 Act in Gliomas as Protective Negative Feedback Regulators of Hypoxia-Inducible Factors. *Cancer Research* **1**, 357-366.

Hermann, D. M. and Bassetti, C. L. (2007). Implications of ATP-binding cassette transporters for brain pharmacotherapies. *Trends in Pharmacological Sciences* **3**, 128-134.

Hermisson, M., Klumpp, A., Wick, W., Wischhusen, J., Nagel, G., Roos, W., Kaina, B. and Weller, M. (2006). O-6-methylguanine DNA methyltransferase and p53 status predict temozolomide sensitivity in human malignant glioma cells. *Journal of Neurochemistry* **3**, 766-776.

Hicklin, D. J. and Ellis, L. M. (2005). Role of the vascular endothelial growth factor pathway in tumor growth and angiogenesis. *Journal of Clinical Oncology* **5**, 1011-1027.

Hicks, K. O., Siim, B. G., Pruijn, F. B. and Wilson, W. R. (2004). Oxygen dependence of the metabolic activation and cytotoxicity of tirapazamine: implications for extravascular transport and activity in tumors. *Radiat Res* **6**, 656-66.

Hilberg, F., Aguzzi, A., Howells, N. and Wagner, E. F. (1993). C-Jun Is Essential for Normal Mouse Development and Hepatogenesis (Vol 365, Pg 179, 1993). *Nature* **6453**, 368-368.

Hill, R. P., Marie-Egyptienne, D. T. and Hedley, D. W. (2009). Cancer Stem Cells, Hypoxia and Metastasis. *Seminars in Radiation Oncology* **2**, 106-111.

Hitomi, K., Iwai, S. and Tainer, J. A. (2007). The intricate structural chemistry of base excision repair machinery: Implications for DNA damage recognition, removal, and repair. *DNA Repair* **4**, 410-428.

Hoffmann, A., Levchenko, A., Scott, M. L. and Baltimore, D. (2002). The I kappa B-NF-kappa B signaling module: Temporal control and selective gene activation. *Science* **5596**, 1241-1245.

Hollstein, M., Sidransky, D., Vogelstein, B. and Harris, C. C. (1991). P53 Mutations in Human Cancers. *Science* **5015**, 49-53.

Honda, R., Tanaka, H. and Yasuda, H. (1997). Oncoprotein MDM2 is a ubiquitin ligase E3 for tumor suppressor p53. *FEBS Lett* **1**, 25-7.

Hood, J. D. and Cheresh, D. A. (2002). Role of integrins in cell invasion and migration. *Nature Reviews Cancer* **2**, 91-+.

Horejsi, Z., Falck, J., Bakkenist, C. J., Kastan, M. B., Lukas, J. and Bartek, J. (2004). Distinct functional domains of Nbs1 modulate the timing and magnitude of ATM activation after low doses of ionizing radiation. *Oncogene* **17**, 3122-3127.

Hsu, P. P. and Sabatini, D. M. (2008). Cancer cell metabolism: Warburg and beyond. *Cell* **5**, 703-707.

Hu, Y. L., DeLay, M., Jahangiri, A., Molinaro, A. M., Rose, S. D., Carbonell, W. S. and Aghi, M. K. (2012). Hypoxia-induced autophagy promotes tumor cell survival and adaptation to antiangiogenic treatment in glioblastoma. *Cancer Res* **7**, 1773-83.

Huang, E., Strother, D. R., Davis, Q. G., Chiu, J. K., Lu, H. H., Carpenter, L. S., Mai, W. Y., Chintagumpala, M. M., South, M., Grant, W. H., Butler, E. B. and Woo, S. Y. (2002). Intensity-modulated radiation therapy for pediatric medulloblastoma: Early report on the reduction of ototoxicity. *International Journal of Radiation Oncology Biology Physics* **3**, 599-605.

Huang, G. Q., Krig, S., Kowbel, D., Xu, H. M., Hyun, B., Volik, S., Feuerstein, B., Mills, G. B., Stokoe, D., Yaswen, P. and Collins, C. (2005). ZNF217 suppresses cell death associated with chemotherapy and telomere dysfunction. *Human Molecular Genetics* **21**, 3219-3225.

Huang, H. T., Mahler-Araujo, B. M., Sankila, A., Chimelli, L., Yonekawa, Y., Kleihues, P. and Ohgaki, H. (2000). APC mutations in sporadic medulloblastomas. *American Journal of Pathology* **2**, 433-437.

Huang, J., Grotzer, M. A., Watanabe, T., Hewer, E., Pietsch, T., Rutkowski, S. and Ohgaki, H. (2008). Mutations in the Nijmegen breakage syndrome gene in medulloblastomas. *Clinical Cancer Research* **13**, 4053-4058.

Huang, X., Ding, L. H., Bennewith, K. L., Tong, R. T., Welford, S. M., Ang, K. K., Story, M., Le, Q. T. and Giaccia, A. J. (2009). Hypoxia-Inducible mir-210 Regulates Normoxic Gene Expression Involved in Tumor Initiation. *Molecular Cell* **6**, 856-867.

Huang, Z., Cheng, L., Guryanova, O. A., Wu, Q. and Bao, S. (2010). Cancer stem cells in glioblastoma--molecular signaling and therapeutic targeting. *Protein Cell* **7**, 638-55.

Hui, E. P., Chan, A. T. C., Pezzella, F., Turley, H., To, K. F., Poon, T. C. W., Zee, B., Mo, F., Teo, P. M. L., Huang, D. P., Gatter, K. C., Johnson, P. J. and Harris, A. L. (2002). Coexpression of hypoxia-inducible factors 1 alpha and 2 alpha, carbonic anhydrase IX, and vascular endothelial growth factor in nasopharyngeal carcinoma and relationship to survival. *Clinical Cancer Research* **8**, 2595-2604.

Hulten, L. M., Olson, F. J., Aberg, H., Carlsson, J., Karlstrom, L., Boren, J., Fagerberg, B. and Wiklund, O. (2010). 15-Lipoxygenase-2 is expressed in macrophages in human carotid plaques and regulated by hypoxia-inducible factor-1 alpha. *European Journal of Clinical Investigation* **1**, 11-17.

Hussein, D., Estlin, E. J., Dive, C. and Makin, G. W. (2006). Chronic hypoxia promotes hypoxia-inducible factor-1alpha-dependent resistance to etoposide and vincristine in neuroblastoma cells. *Mol Cancer Ther* **9**, 2241-50.

Hutvagner, G., McLachlan, J., Pasquinelli, A. E., Balint, E., Tuschl, T. and Zamore, P. D. (2001). A cellular function for the RNA-interference enzyme Dicer in the maturation of the let-7 small temporal RNA. *Science* **5531**, 834-8.

Ichihara, E., Kiura, K. and Tanimoto, M. (2011). Targeting Angiogenesis in Cancer Therapy. *Acta Medica Okayama* **6**, 353-362.

Irizarry, R. A., Bolstad, B. M., Collin, F., Cope, L. M., Hobbs, B. and Speed, T. P. (2003a). Summaries of affymetrix GeneChip probe level data. *Nucleic Acids Research* **4**,

Irizarry, R. A., Hobbs, B., Collin, F., Beazer-Barclay, Y. D., Antonellis, K. J., Scherf, U. and Speed, T. P. (2003b). Exploration, normalization, and summaries of high density oligonucleotide array probe level data. *Biostatistics* **2**, 249-264.

Isa, A. Y., Ward, T. H., West, C. M. L., Slevin, N. J. and Homer, J. J. (2006). Hypoxia in head and neck cancer. *British Journal of Radiology* **946**, 791-798.

Issa, A., Le, T. X., Shoushtari, A. N., Shields, J. D. and Swartz, M. A. (2009). Vascular Endothelial Growth Factor-C and C-C Chemokine Receptor 7 in Tumor Cell-Lymphatic Cross-talk Promote Invasive Phenotype. *Cancer Research* **1**, 349-357.

Iwanaga, R., Komori, H. and Ohtani, K. (2004). Differential regulation of expression of the mammalian DNA repair genes by growth stimulation. *Oncogene* **53**, 8581-8590.

Iyer, N. V., Kotch, L. E., Agani, F., Leung, S. W., Laughner, E., Wenger, R. H., Gassmann, M., Gearhart, J. D., Lawler, A. M., Yu, A. Y. and Semenza, G. L. (1998). Cellular and developmental control of O-2 homeostasis by hypoxia-inducible factor 1 alpha. *Genes & Development* **2**, 149-162.

Jackson, S. P. and Bartek, J. (2009). The DNA-damage response in human biology and disease. *Nature* **7267**, 1071-1078.

Jacobs, A. L. and Schar, P. (2012). DNA glycosylases: in DNA repair and beyond. *Chromosoma* **1**, 1-20.

Jenkins, J. R., Rudge, K. and Currie, G. A. (1984). Cellular immortalization by a cDNA clone encoding the transformation-associated phosphoprotein p53. *Nature* **5995**, 651-4.

Jezek, P., Plecita-Hlavata, L., Smolkova, K. and Rossignol, R. (2010). Distinctions and similarities of cell bioenergetics and the role of mitochondria in hypoxia, cancer, and embryonic development. *Int J Biochem Cell Biol* **5**, 604-22.

Ji, J. and Zheng, P. S. (2010). Expression of Sox2 in human cervical carcinogenesis. *Human Pathology* **10**, 1438-1447.

Ji, Q., Hao, X., Meng, Y., Zhang, M., Desano, J., Fan, D. and Xu, L. (2008). Restoration of tumor suppressor miR-34 inhibits human p53-mutant gastric cancer tumorspheres. *BMC Cancer* 266.

Jiang, B. H., Rue, E., Wang, G. L., Roe, R. and Semenza, G. L. (1996). Dimerization, DNA binding, and transactivation properties of hypoxia-inducible factor 1. *Journal of Biological Chemistry* **30**, 17771-17778.

Jiang, H., Reinhardt, H. C., Bartkova, J., Tommiska, J., Blomqvist, C., Nevanlinna, H., Bartek, J., Yaffe, M. B. and Hemann, M. T. (2009). The combined status of ATM and p53 link tumor development with therapeutic response. *Genes Dev* **16**, 1895-909.

Jiang, Y. F., Vaccaro, M. I., Fiedler, F., Calvo, E. L. and Iovanna, J. L. (1999). Lipopolysaccharides induce p8 mRNA expression in vivo and in vitro. *Biochemical and Biophysical Research Communications* **3**, 686-690.

Jin, G. L., Cook, S., Cui, B., Chen, W. C., Keir, S. T., Killela, P., Di, C. H., Payne, C. A., Gregory, S. G., McLendon, R., Bigner, D. D. and Yan, H. (2010). HDMX regulates p53 activity and confers chemoresistance to 3-Bis(2-chloroethyl)-1-nitrosourea. *Neuro-Oncology* **9**, 956-966.

Jogi, A., Vallon-Christersson, J., Holmquist, L., Axelson, H., Borg, A. and Pahlman, S. (2004). Human neuroblastoma cells exposed to hypoxia: induction of genes associated with growth, survival, and aggressive behavior. *Experimental Cell Research* **2**, 469-487.

Johnson, A. B., Denko, N. and Barton, M. C. (2008). Hypoxia induces a novel signature of chromatin modifications and global repression of transcription. *Mutation Research-Fundamental and Molecular Mechanisms of Mutagenesis* **1-2**, 174-179.

Johnson, R., Spiegelman, B., Hanahan, D. and Wisdom, R. (1996). Cellular transformation and malignancy induced by ras require c-jun. *Molecular and Cellular Biology* **8**, 4504-4511.

Johnson, R. S., Vanlingen, B., Papaioannou, V. E. and Spiegelman, B. M. (1993). A Null Mutation at the C-Jun Locus Causes Embryonic Lethality and Retarded Cell-Growth in Culture. *Genes & Development* **7B**, 1309-1317.

Jones, R. G. and Thompson, C. B. (2009). Tumor suppressors and cell metabolism: a recipe for cancer growth. *Genes Dev* **5**, 537-548.

Jowsey, P., Morrice, N. A., Hastie, C. J., McLauchlan, H., Toth, R. and Rouse, J. (2007). Characterisation of the sites of DNA damage-induced 53BP1 phosphorylation catalysed by ATM and ATR. *DNA Repair* **10**, 1536-1544.

Joyce, J. A. and Pollard, J. W. (2009). Microenvironmental regulation of metastasis. *Nature Reviews Cancer* **4**, 239-252.

Kallioniemi, A., Kallioniemi, O. P., Piper, J., Tanner, M., Stokke, T., Chen, L., Smith, H. S., Pinkel, D., Gray, J. W. and Waldman, F. M. (1994). Detection and Mapping of Amplified DNA-Sequences in Breast-Cancer by Comparative Genomic Hybridization. *Proceedings of the National Academy of Sciences of the United States of America* **6**, 2156-2160.

Kamat, C. D., Thorpe, J. E., Shenoy, S. S., Ceriello, A., Green, D. E., Warnke, L. A. and Ihnat, M. A. (2007). A long-term "memory" of HIF induction in response to chronic mild decreased oxygen after oxygen normalization. *BMC Cardiovasc Disord* 4.

Kanehisa, M. and Goto, S. (2000). KEGG: kyoto encyclopedia of genes and genomes. *Nucleic Acids Research* **1**, 27-30.

Kanehisa, M., Goto, S., Sato, Y., Furumichi, M. and Tanabe, M. (2012). KEGG for integration and interpretation of large-scale molecular data sets. *Nucleic Acids Research* **Database issue**, D109-14.

Kaur, B., Khwaja, F. W., Severson, E. A., Matheny, S. L., Brat, D. J. and Van Meir, E. G. (2005). Hypoxia and the hypoxia-inducible-factor pathway in glioma growth and angiogenesis. *Neuro-Oncology* **2**, 134-153.

Keith, B. and Simon, M. C. (2007). Hypoxia-inducible factors, stem cells, and cancer. *Cell* **3**, 465-72.

Kenneth, N. S. and Rocha, S. (2008). Regulation of gene expression by hypoxia. *Biochemical Journal* 19-29.

Kenney, A. M., Cole, M. D. and Rowitch, D. H. (2003). Nmyc upregulation by sonic hedgehog signaling promotes proliferation in developing cerebellar granule neuron precursors. *Development* **1**, 15-28.

Kerjaschki, D., Bago-Horvath, Z., Rudas, M., Sexl, V., Schneckenleithner, C., Wolbank, S., Bartel, G., Krieger, S., Kalt, R., Hantusch, B., Keller, T., Nagy-Bojarszky, K., Huttary, N., Raab, I., Lackner, K., Krautgasser, K., Schachner, H., Kaserer, K., Rezar, S., Madlener, S., Vonach, C., Davidovits, A., Nosaka, H., Hammerle, M., Viola, K., Dolznig, H., Schreiber, M., Nader, A., Mikulits, W., Gnant, M., Hirakawa, S., Detmar, M., Alitalo, K., Nijman, S., Offner, F., Maier, T. J., Steinhilber, D. and Krupitza, G. (2011). Lipoxygenase mediates invasion of intrametastatic lymphatic vessels and propagates lymph node metastasis of human mammary carcinoma xenografts in mouse. *Journal of Clinical Investigation* **5**, 2000-2012.

Ketting, R. F., Fischer, S. E. J., Bernstein, E., Sijen, T., Hannon, G. J. and Plasterk, R. H. A. (2001). Dicer functions in RNA interference and in synthesis of small RNA involved in developmental timing in C-elegans. *Genes & Development* **20**, 2654-2659.

Kiani, M. F., Pries, A. R., Hsu, L. L., Sarelius, I. H. and Cokelet, G. R. (1994). Fluctuations in Microvascular Blood-Flow Parameters Caused by Hemodynamic Mechanisms. *American Journal of Physiology* **5**, H1822-H1828.

Kim, E. L., Wustenberg, R., Rubsam, A., Schmitz-Salue, C., Warnecke, G., Bucker, E. M., Pettkus, N., Speidel, D., Rohde, V., Schulz-Schaeffer, W., Deppert, W. and Giese, A. (2010). Chloroquine activates the p53 pathway and induces apoptosis in human glioma cells. *Neuro Oncol* **4**, 389-400.

Kim, J. W., Tchernyshyov, I., Semenza, G. L. and Dang, C. V. (2006). HIF-1-mediated expression of pyruvate dehydrogenase kinase: a metabolic switch required for cellular adaptation to hypoxia. *Cell Metab* **3**, 177-85.

Kim, J. Y. H., Sutton, M. E., Lu, D. J., Cho, T. A., Goumnerova, L. C., Goritchenko, L., Kaufman, J. R., Lam, K. K., Billet, A. L., Tarbell, N. J., Wu, J., Allen, J. C., Stiles, C. D., Segal, R. A. and Pomeroy, S. L. (1999). Activation of neurotrophin-3 receptor TrkC induces apoptosis in medulloblastomas. *Cancer Research* **3**, 711-719.

Kim, S. H., Xia, D. R., Kim, S. W., Holla, V., Menter, D. G. and DuBois, R. N. (2010). Human Enhancer of Filamentation 1 Is a Mediator of Hypoxia-Inducible Factor-1 alpha-Mediated Migration in Colorectal Carcinoma Cells. *Cancer Research* **10**, 4054-4063.

Kim, V. N., Han, J. and Siomi, M. C. (2009). Biogenesis of small RNAs in animals. *Nat Rev Mol Cell Biol* **2**, 126-39.

Kimura, H., Braun, R. D., Ong, E. T., Hsu, R., Secomb, T. W., Papahadjopoulos, D., Hong, K. L. and Dewhirst, M. W. (1996). Fluctuations in red cell flux in tumor microvessels can lead to transient hypoxia and reoxygenation in tumor parenchyma. *Cancer Research* **23**, 5522-5528.

King, M. C., Marks, J. H., Mandell, J. B. and Grp, N. Y. B. C. S. (2003). Breast and ovarian cancer risks due to inherited mutations in BRCA1 and BRCA2. *Science* **5645**, 643-646.

Klagsbrun, M. and Soker, S. (1993). Vegf/Vpf - the Angiogenesis Factor Found. *Current Biology* **10**, 699-702.

Kleihues, P. and Ohgaki, H. (2000). Phenotype vs genotype in the evolution of astrocytic brain tumors. *Toxicol Pathol* **1**, 164-70.

Kleinman, G. M., Hochberg, F. H. and Richardson, E. P. (1981). Systemic Metastases from Medulloblastoma - Report of 2 Cases and Review of the Literature. *Cancer* **10**, 2296-2309.

Kluiver, J., Poppema, S., de Jong, D., Blokzijl, T., Harms, G., Jacobs, S., Kroesen, B. J. and van den Berg, A. (2005). BIC and miR-155 are highly expressed in Hodgkin, priniary mediastinal and diffuse large B cell lymphomas. *Blood* **11**, 286a-286a.

Klymkowsky, M. W. and Savagner, P. (2009). Epithelial-Mesenchymal Transition A Cancer Researcher's Conceptual Friend and Foe. *American Journal of Pathology* **5**, 1588-1593.

Knappskog, S., Chrisanthar, R., Lokkevik, E., Anker, G., Ostenstad, B., Lundgren, S., Risberg, T., Mjaaland, I., Leirvaag, B., Miletic, H. and Lonning, P. E. (2012). Low expression levels of ATM may substitute for CHEK2/TP53 mutations predicting resistance towards anthracycline and mitomycin chemotherapy in breast cancer. *Breast Cancer Research* **2**,

Knappskog, S. and Lonning, P. E. (2012). P53 and its molecular basis to chemoresistance in breast cancer. *Expert Opinion on Therapeutic Targets* S23-S30.

Knight, S. W. and Bass, B. L. (2001). A role for the RNase III enzyme DCR-1 in RNA interference and germ line development in Caenorhabditis elegans. *Science* **5538**, 2269-2271.

Knobbe, C. B. and Reifenberger, G. (2003). Genetic alterations and aberrant expression of genes related to the phosphatidyl-inositol-3 '-kinase/protein kinase B (Akt) signal transduction pathway in glioblastomas. *Brain Pathology* **4**, 507-518.

Koch, C. A., Agyei, R., Galicia, S., Metalnikov, P., O'Donnell, P., Starostine, A., Weinfeld, M. and Durocher, D. (2004). Xrcc4 physically links DNA end processing by polynucleotide kinase to DNA ligation by DNA ligase IV. *Embo Journal* **19**, 3874-3885.

Koch, C. J. (1993). Unusual oxygen concentration dependence of toxicity of SR-4233, a hypoxic cell toxin. *Cancer Res* **17**, 3992-7.

Kool, M., Koster, J., Bunt, J., Hasselt, N. E., Lakeman, A., van Sluis, P., Troost, D., Schouten-van Meeteren, N., Caron, H. N., Cloos, J., Mrsic, A., Ylstra, B., Grajkowska, W., Hartmann, W., Pietsch, T., Ellison, D., Clifford, S. C. and Versteeg, R. (2008). Integrated Genomics Identifies Five Medulloblastoma Subtypes with Distinct Genetic Profiles, Pathway Signatures and Clinicopathological Features. *PLoS One* **8**,

Koong, A. C., Denko, N. C., Hudson, K. M., Schindler, C., Swiersz, L., Koch, C., Evans, S., Ibrahim, H., Le, Q. T., Terris, D. J. and Giaccia, A. J. (2000). Candidate genes for the hypoxic tumor phenotype. *Cancer Research* **4**, 883-887.

Koressaar, T. and Remm, M. (2007). Enhancements and modifications of primer design program Primer3. *Bioinformatics* **10**, 1289-1291.

Koritzinsky, M., Seigneuric, R., Magagnin, M. G., van den Beucken, T., Lambin, P. and Wouters, B. G. (2005). The hypoxic proteome is influenced by gene-specific changes in mRNA translation. *Radiotherapy and Oncology* **2**, 177-186.

Kortmann, R. D., Kuhl, J., Timmermann, B., Mittler, U., Urban, C., Budach, V., Richter, E., Willich, N., Flentje, M., Berthold, F., Slavc, I., Wolff, J., Meisner, C., Wiestler, O., Sorensen, N., Warmuth-Metz, M. and Bamberg, M. (2000). Postoperative neoadjuvant chemotherapy before radiotherapy as compared to immediate radiotherapy followed by maintenance chemotherapy in the treatment of medulloblastoma in childhood: Results of the German prospective randomized trial HIT '91. *International Journal of Radiation Oncology Biology Physics* **2**, 269-279.

Korwek, Z., Sewastianik, T., Bielak-Zmijewska, A., Mosieniak, G., Alster, O., Moreno-Villaneuva, M., Burkle, A. and Sikora, E. (2012). Inhibition of ATM blocks the etoposide-induced DNA damage response and apoptosis of resting human T cells. *DNA Repair* **11**, 864-873.

Koumenis, C., Alarcon, R., Hammond, E., Sutphin, P., Hoffman, W., Murphy, M., Derr, J., Taya, Y., Lowe, S. W., Kastan, M. and Giaccia, A. (2001). Regulation of p53 by hypoxia: dissociation of transcriptional repression and apoptosis from p53-dependent transactivation. *Mol Cell Biol* **4**, 1297-310.

Kraakman-van der Zwet, M., Overkamp, W. J. I., Friedl, A. A., Klein, B., Verhaegh, G. W. C. T., Jaspers, N. G. J., Midro, A. T., Eckardt-Schupp, F., Lohman, P. H. M. and Zdzienicka, M. Z. (1999). Immortalization and characterization of Nijmegen Breakage Syndrome fibroblasts. *Mutation Research-DNA Repair* **1**, 17-27.

Krig, S. R., Miller, J. K., Frietze, S., Beckett, L. A., Neve, R. M., Farnham, P. J., Yaswen, P. I. and Sweeney, C. A. (2010). ZNF217, a candidate breast cancer oncogene amplified at

20q13, regulates expression of the ErbB3 receptor tyrosine kinase in breast cancer cells. *Oncogene* **40**, 5500-5510.

Kruger, L., Demuth, I., Neitzel, H., Varon, R., Sperling, K., Chrzanowska, K. H., Seemanova, E. and Digweed, M. (2007). Cancer incidence in Nijmegen breakage syndrome is modulated by the amount of a variant NBS protein. *Carcinogenesis* **1**, 107-111.

Kulshreshtha, R., Ferracin, M., Wojcik, S. E., Garzon, R., Alder, H., Agosto-Perez, F. J., Davuluri, R., Liu, C. G., Croce, C. M., Negrini, M., Calin, G. A. and Ivan, M. (2007). A microRNA signature of hypoxia. *Molecular and Cellular Biology* **5**, 1859-1867.

Kuo, K. T., Chou, T. Y., Hsu, H. S., Chen, W. L. and Wang, L. S. (2012). Prognostic Significance of NBS1 and Snail Expression in Esophageal Squamous Cell Carcinoma. *Annals of Surgical Oncology* S549-S557.

Kuwabara, K., Ogawa, S., Matsumoto, M., Koga, S., Clauss, M., Pinsky, D. J., Lyn, P., Leavy, J., Witte, L., Josephsilverstein, J., Furie, M. B., Torcia, G., Cozzolino, F., Kamada, T. and Stern, D. M. (1995). Hypoxia-Mediated Induction of Acidic/Basic Fibroblast Growth-Factor and Platelet-Derived Growth-Factor in Mononuclear Phagocytes Stimulates Growth of Hypoxic Endothelial-Cells. *Proceedings of the National Academy of Sciences of the United States of America* **10**, 4606-4610.

Kwon, H. S. and Ott, M. (2008). The ups and downs of SIRT1. *Trends Biochem Sci* **11**, 517-25.

Laderoute, K. R., Alarcon, R. M., Brody, M. D., Calaoagan, J. M., Chen, E. Y., Knapp, A. M., Yun, Z., Denko, N. C. and Giaccia, A. J. (2000). Opposing effects of hypoxia on expression of the angiogenic inhibitor thrombospondin 1 and the angiogenic inducer vascular endothelial growth factor. *Clinical Cancer Research* **7**, 2941-2950.

Lahav, G., Rosenfeld, N., Sigal, A., Geva-Zatorsky, N., Levine, A. J., Elowitz, M. B. and Alon, U. (2004). Dynamics of the p53-Mdm2 feedback loop in individual cells. *Nature Genetics* **2**, 147-150.

Lamb, P. and Crawford, L. (1986). Characterization of the Human P53-Gene. *Mol Cell Biol* **5**, 1379-1385.

Lane, D. P. and Crawford, L. V. (1979). T-Antigen Is Bound to a Host Protein in Sv40-Transformed Cells. *Nature* **5701**, 261-263.

Lane, D. P. (1992). Cancer - P53, Guardian of the Genome. *Nature* **6381**, 15-16.

Laneve, P., Di Marcotullio, L., Gioia, U., Fiori, M. E., Ferretti, E., Gulino, A., Bozzoni, I. and Caffarelli, E. (2007). The interplay between microRNAs and the neurotrophin receptor tropomyosin-related kinase C controls proliferation of human neuroblastoma cells. *Proceedings of the National Academy of Sciences of the United States of America* **19**, 7957-7962.

Langdon, J. A., Lamont, J. M., Scott, D. K., Dyer, S., Prebble, E., Bown, N., Grundy, R. G., Ellison, D. W. and Clifford, S. C. (2006). Combined genome-wide allelotyping and copy number analysis identify frequent genetic losses without copy number reduction in medulloblastoma. *Genes Chromosomes & Cancer* **1**, 47-60.

Lavin, M. F. (2007). ATM and the Mre11 complex combine to recognize and signal DNA double-strand breaks. *Oncogene* **56**, 7749-7758.

Lawler, J. (2002). Thrombospondin-1 as an endogenous inhibitor of angiogenesis and tumor growth. *Journal of Cellular and Molecular Medicine* **1**, 1-12.

Lawlor, M. A. and Alessi, D. R. (2001). PKB/Akt: a key mediator of cell proliferation, survival and insulin responses? *Journal of Cell Science* **16**, 2903-2910.

Le Scodan, R., Cizeron-Clairac, G., Fourme, E., Meseure, D., Vacher, S., Spyratos, F., De la Lande, B., Cvitkovic, F., Lidereau, R. and Bieche, I. (2010). DNA Repair Gene Expression and Risk of Locoregional Relapse in Breast Cancer Patients. *International Journal of Radiation Oncology Biology Physics* **2**, 328-336.

Lee, J. W., Bae, S. H., Jeong, J. W., Kim, S. H. and Kim, K. W. (2004). Hypoxia-inducible factor (HIF-1)alpha: its protein stability and biological functions. *Exp Mol Med* **1**, 1-12.

Lee, M. J., Hatton, B. A., Villavicencio, E. H., Khanna, P. C., Friedman, S. D., Ditzler, S., Pullar, B., Robison, K., White, K. F., Tunkey, C., LeBlanc, M., Randolph-Habecker, J., Knoblaugh, S. E., Hansen, S., Richards, A., Wainwright, B. J., McGovern, K. and Olson, J. M. (2012). Hedgehog pathway inhibitor saridegib (IPI-926) increases lifespan in a mouse medulloblastoma model. *Proceedings of the National Academy of Sciences of the United States of America* **20**, 7859-7864.

Lee, M. Y., Chou, C. Y., Tang, M. J. and Shen, M. R. (2008). Epithelial-mesenchymal transition in cervical cancer: correlation with tumor progression, epidermal growth factor receptor overexpression, and snail up-regulation. *Clin Cancer Res* **15**, 4743-50.

Lee, R. C., Feinbaum, R. L. and Ambros, V. (1993). The C. elegans heterochronic gene lin-4 encodes small RNAs with antisense complementarity to lin-14. *Cell* **5**, 843-54.

Lee, Y., Jeon, K., Lee, J. T., Kim, S. and Kim, V. N. (2002). MicroRNA maturation: stepwise processing and subcellular localization. *Embo Journal* **17**, 4663-4670.

Lee, Y., Ahn, C., Han, J., Choi, H., Kim, J., Yim, J., Lee, J., Provost, P., Radmark, O., Kim, S. and Kim, V. N. (2003). The nuclear RNase III Drosha initiates microRNA processing. *Nature* **6956**, 415-9.

Levine, A. J., Momand, J. and Finlay, C. A. (1991). The p53 tumour suppressor gene. *Nature* **6326**, 453-6.

Levine, A. J. (1997). p53, the cellular gatekeeper for growth and division. *Cell* **3**, 323-331.

Lewis, B. P., Shih, I. H., Jones-Rhoades, M. W., Bartel, D. P. and Burge, C. B. (2003). Prediction of mammalian microRNA targets. *Cell* **7**, 787-98.

Lewis, B. P., Burge, C. B. and Bartel, D. P. (2005). Conserved seed pairing, often flanked by adenosines, indicates that thousands of human genes are microRNA targets. *Cell* **1**, 15-20.

Li, B., Shimizu, Y., Kobayashi, T., Terada, N., Yoshimura, K., Kamba, T., Mikami, Y., Inoue, T., Nishiyama, H. and Ogawa, O. (2012). Overexpression of ETS-1 is associated with malignant biological features of prostate cancer. *Asian Journal of Andrology* **6**, 860-863.

Li, J., Shi, M. X., Cao, Y., Yuan, W. S., Pang, T. X., Li, B. Z., Sun, Z., Chen, L. and Zhao, R. C. H. (2006). Knockdown of hypoxia-inducible factor-1 alpha in breast carcinoma MCF-7 cells results in reduced tumor growth and increased sensitivity to methotrexate. *Biochemical and Biophysical Research Communications* **4**, 1341-1351.

Li, L., Yuan, L., Luo, J., Gao, J., Guo, J. and Xie, X. (2013). MiR-34a inhibits proliferation and migration of breast cancer through down-regulation of Bcl-2 and SIRT1. *Clin Exp Med* **2**, 109-17.

Li, N., Fu, H. J., Tie, Y., Hu, Z., Kong, W., Wu, Y. G. and Zheng, X. F. (2009). miR-34a inhibits migration and invasion by down-regulation of c-Met expression in human hepatocellular carcinoma cells. *Cancer Letters* **1**, 44-53.

Li, P., Zhou, C., Xu, L. and Xiao, H. (2013). Hypoxia enhances stemness of cancer stem cells in glioblastoma: an in vitro study. *Int J Med Sci* **4**, 399-407.

Li, P. X., Maines-Bandiera, S., Kuo, W. L., Guan, Y., Sun, Y., Hills, M., Huang, G. Q., Collins, C. C., Leung, P. C. K., Gray, J. W. and Auersperg, N. (2007). Multiple roles of the candidate oncogene ZNF217 in ovarian epithelial neoplastic progression. *International Journal of Cancer* **9**, 1863-1873.

Liang, B. C. (1996). Effects of hypoxia on drug resistance phenotype and genotype in human glioma cell lines. *J Neurooncol* **2**, 149-55.

Lin, Q., Cong, X. Y. and Yun, Z. (2011). Differential Hypoxic Regulation of Hypoxia-Inducible Factors 1 alpha and 2 alpha. *Molecular Cancer Research* **6**, 757-765.

Lindahl, T. and Barnes, D. E. (2000). Repair of endogenous DNA damage. *Cold Spring Harbor Symposia on Quantitative Biology* 127-133.

Lingel, A., Simon, B., Izaurralde, E. and Sattler, M. (2004). Nucleic acid 3 '-end recognition by the Argonaute2 PAZ domain. *Nature Structural & Molecular Biology* **6**, 576-577.

Linzer, D. I. H. and Levine, A. J. (1979). Characterization of a 54k Dalton Cellular Sv40 Tumor-Antigen Present in Sv40-Transformed Cells and Uninfected Embryonal Carcinoma-Cells. *Cell* **1**, 43-52.

Liu, G. and Chen, X. B. (2006). Regulation of the p53 transcriptional activity. *Journal of Cellular Biochemistry* **3**, 448-458.

Liu, K., Bellam, N., Lin, H. Y., Wang, B., Stockard, C. R., Grizzle, W. E. and Lin, W. C. (2009). Regulation of p53 by TopBP1: a Potential Mechanism for p53 Inactivation in Cancer. *Molecular and Cellular Biology* **10**, 2673-2693.

Liu, L. L., Ning, X. X., Sun, L., Zhang, H. B., Shi, Y. Q., Guo, C. C., Han, S., Liu, J., Sun, S. R., Han, Z. Y., Wu, K. C. and Fan, D. M. (2008). Hypoxia-inducible factor-1 alpha contributes to hypoxia-induced chemoresistance in gastric cancer. *Cancer Science* **1**, 121-128.

Liu, L. P., Cash, T. P., Jones, R. G., Keith, B., Thompson, C. B. and Simon, M. C. (2006). Hypoxia-induced energy stress regulates mRNA translation and cell growth. *Molecular Cell* **4**, 521-531.

Liu, L. X., Marti, G. P., Wei, X. F., Zhang, X. J., Zhang, H. F., Liu, Y. V., Nastai, M., Semenza, G. L. and Harmon, J. W. (2008). Age-dependent impairment of HIF-1 alpha expression in diabetic mice: Correction with electroporation-facilitated gene therapy increases wound healing, angiogenesis, and circulating angiogenic cells. *Journal of Cellular Physiology* **2**, 319-327.

Lo, H. W., Hsu, S. C., Xia, W., Cao, X., Shih, J. Y., Wei, Y., Abbruzzese, J. L., Hortobagyi, G. N. and Hung, M. C. (2007). Epidermal growth factor receptor cooperates with signal transducer and activator of transcription 3 to induce epithelial-mesenchymal transition in cancer cells via up-regulation of TWIST gene expression. *Cancer Res* **19**, 9066-76.

Lodygin, D., Tarasov, V., Epanchintsev, A., Berking, C., Knyazeva, T., Korner, H., Knyazev, P., Diebold, J. and Hermeking, H. (2008). Inactivation of miR-34a by aberrant CpG methylation in multiple types of cancer. *Cell Cycle* **16**, 2591-2600.

Loh, Y. H., Wu, Q., Chew, J. L., Vega, V. B., Zhang, W. W., Chen, X., Bourque, G., George, J., Leong, B., Liu, J., Wong, K. Y., Sung, K. W., Lee, C. W. H., Zhao, X. D., Chiu, K. P., Lipovich, L., Kuznetsov, V. A., Robson, P., Stanton, L. W., Wei, C. L., Ruan, Y. J., Lim, B. and Ng, H. H. (2006). The Oct4 and Nanog transcription network regulates pluripotency in mouse embryonic stem cells. *Nature Genetics* **4**, 431-440.

LoRusso, P. M., Rudin, C. M., Reddy, J. C., Tibes, R., Weiss, G. J., Borad, M. J., Hann, C. L., Brahmer, J. R., Chang, I., Darbonne, W. C., Graham, R. A., Zerivitz, K. L., Low, J. A. and Von

Hoff, D. D. (2011). Phase I Trial of Hedgehog Pathway Inhibitor Vismodegib (GDC-0449) in Patients with Refractory, Locally Advanced or Metastatic Solid Tumors. *Clinical Cancer Research* **8**, 2502-2511.

Loscher, W. and Potschka, H. (2005). Drug resistance in brain diseases and the role of drug efflux transporters. *Nature Reviews Neuroscience* **8**, 591-602.

Lou, Y. M., McDonald, P. C., Oloumi, A., Chia, S., Ostlund, C., Ahmadi, A., Kyle, A., Keller, U. A. D., Leung, S., Huntsman, D., Clarke, B., Sutherland, B. W., Waterhouse, D., Bally, M., Roskelley, C., Overall, C. M., Minchinton, A., Pacchiano, F., Carta, F., Scozzafava, A., Touisni, N., Winum, J. Y., Supuran, C. T. and Dedhar, S. (2011). Targeting Tumor Hypoxia: Suppression of Breast Tumor Growth and Metastasis by Novel Carbonic Anhydrase IX Inhibitors. *Cancer Research* **9**, 3364-3376.

Louis, D. N., Ohgaki, H., Wiestler, O. D., Cavenee, W. K., Burger, P. C., Jouvet, A., Scheithauer, B. W. and Kleihues, P. (2007). The 2007 WHO classification of tumours of the central nervous system. *Acta Neuropathol* **2**, 97-109.

Lowe, S. W., Ruley, H. E., Jacks, T. and Housman, D. E. (1993). P53-Dependent Apoptosis Modulates the Cytotoxicity of Anticancer Agents. *Cell* **6**, 957-967.

Lowe, S. W., Bodis, S., Mcclatchey, A., Remington, L., Ruley, H. E., Fisher, D. E., Housman, D. E. and Jacks, T. (1994). P53 Status and the Efficacy of Cancer-Therapy in-Vivo. *Science* **5186**, 807-810.

Lu, Y., Ryan, S. L., Elliott, D. J., Bignell, G. R., Futreal, P. A., Ellison, D. W., Bailey, S. and Clifford, S. C. (2009). Amplification and Overexpression of Hsa-miR-30b, Hsa-miR-30d and KHDRBS3 at 8q24.22-q24.23 in Medulloblastoma. *PLoS One* **7**,

Lu, Z. M., Ghosh, S., Wang, Z. Y. and Hunter, T. (2003). Downregulation of caveolin-1 function by EGF leads to the loss of E-cadherin, increased transcriptional activity of beta-catenin, and enhanced tumor cell invasion. *Cancer Cell* **6**, 499-515.

Lund, E., Guttinger, S., Calado, A., Dahlberg, J. E. and Kutay, U. (2004). Nuclear export of microRNA precursors. *Science* **5654**, 95-98.

Luo, J. Y., Nikolaev, A. Y., Imai, S., Chen, D. L., Su, F., Shiloh, A., Guarente, L. and Gu, W. (2001). Negative control of p53 by Sir2 alpha promotes cell survival under stress. *Cell* **2**, 137-148.

Maclaine, N. J. and Hupp, T. R. (2009). The regulation of p53 by phosphorylation: A model for how distinct signals Integrate into the p53 pathway. *Aging-Us* **5**, 490-502.

MacLaine, N. J. and Hupp, T. R. (2011). How phosphorylation controls p53. *Cell Cycle* **6**, 916-921.

Mahaney, B. L., Meek, K. and Lees-Miller, S. P. (2009). Repair of ionizing radiation-induced DNA double-strand breaks by non-homologous end-joining. *Biochemical Journal* 639-650.

Makino, Y., Kanopka, A., Wilson, W. J., Tanaka, H. and Poellinger, L. (2002). Inhibitory PAS domain protein (IPAS) is a hypoxia-inducible splicing variant of the hypoxia-inducible factor-3 alpha locus. *Journal of Biological Chemistry* **36**, 32405-32408.

Manoranjan, B., Venugopal, C., McFarlane, N., Doble, B. W., Dunn, S. E., Scheinemann, K. and Singh, S. K. (2012). Medulloblastoma stem cells: where development and cancer cross pathways. *Pediatric Research* **4**, 516-522.

Mao, X. G., Yan, M., Xue, X. Y., Zhang, X., Ren, H. G., Guo, G., Wang, P., Zhang, W. and Huo, J. L. (2011). Overexpression of ZNF217 in glioblastoma contributes to the maintenance of

glioma stem cells regulated by hypoxia-inducible factors. *Laboratory Investigation* **7**, 1068-1078.

Margueron, R. and Reinberg, D. (2011). The Polycomb complex PRC2 and its mark in life. *Nature* **7330**, 343-349.

Marin, M. C., Jost, C. A., Brooks, L. A., Irwin, M. S., O'Nions, J., Tidy, J. A., James, N., McGregor, J. M., Harwood, C. A., Yulug, I. G., Vousden, K. H., Allday, M. J., Gusterson, B., Ikawa, S., Hinds, P. W., Crook, T. and Kaelin, W. G. (2000). A common polymorphism acts as an intragenic modifier of mutant p53 behaviour. *Nature Genetics* **1**, 47-54.

Markus, R., Reutens, D. C., Kazui, S., Read, S., Wright, P., Pearce, D. C., Tochon-Danguy, H. J., Sachinidis, J. I. and Donnan, G. A. (2004). Hypoxic tissue in ischaemic stroke: persistence and clinical consequences of spontaneous survival. *Brain* **Pt 6**, 1427-36.

Marmorstein, L. Y., Ouchi, T. and Aaronson, S. A. (1998). The BRCA2 gene product functionally interacts with p53 and RAD51. *Proceedings of the National Academy of Sciences of the United States of America* **23**, 13869-13874.

Martinez-lage, J. F., Salcedo, C., Corral, M. and Poza, M. (2002). Medulloblastomas in neurofibromatosis type 1. Case report and literature review. *Neurocirugia* **2**, 128-131.

Masciarelli, S., Fontemaggi, G., Di Agostino, S., Donzelli, S., Carcarino, E., Strano, S. and Blandino, G. (2013). Gain-of-function mutant p53 downregulates miR-223 contributing to chemoresistance of cultured tumor cells. *Oncogene*

Masson, N. and Ratcliffe, P. J. (2003). HIF prolyl and asparaginyl hydroxylases in the biological response to intracellular O-2 levels. *Journal of Cell Science* **15**, 3041-3049.

Matsumoto, T., Tani, E., Kaba, K., Kochi, N., Shindo, H., Yamamoto, Y., Sakamoto, H. and Furuyama, J. (1990). Amplification and expression of a multidrug resistance gene in human glioma cell lines. *J Neurosurg* **1**, 96-101.

Maxwell, P. H., Wiesener, M. S., Chang, G. W., Clifford, S. C., Vaux, E. C., Cockman, M. E., Wykoff, C. C., Pugh, C. W., Maher, E. R. and Ratcliffe, P. J. (1999). The tumour suppressor protein VHL targets hypoxia-inducible factors for oxygen-dependent proteolysis. *Nature* **6733**, 271-275.

McBride, O. W., Merry, D. and Givol, D. (1986). The gene for human p53 cellular tumor antigen is located on chromosome 17 short arm (17p13). *Proc Natl Acad Sci U S A* **1**, 130-4.

McCarty, M. F. and Whitaker, J. (2010). Manipulating Tumor Acidification as a Cancer Treatment Strategy. *Alternative Medicine Review* **3**, 264-272.

McCord, A. M., Jamal, M., Shankavaram, U. T., Lang, F. F., Camphausen, K. and Tofilon, P. J. (2009). Physiologic oxygen concentration enhances the stem-like properties of CD133+ human glioblastoma cells in vitro. *Mol Cancer Res* **4**, 489-97.

McManamy, C. S., Lamont, J. M., Taylor, R. E., Cole, M., Pearson, A. D. J., Clifford, S. C. and Ellison, D. W. (2003). Morphophenotypic variation predicts clinical behavior in childhood non-desmoplastic medulloblastomas. *Journal of Neuropathology and Experimental Neurology* **6**, 627-632.

Meco, D., Servidei, T., Riccardi, A., Ferlini, C., Cusano, G., Zannoni, G. F., Giangaspero, F. and Riccardi, R. (2009). Antitumor effect in medulloblastoma cells by gefitinib: Ectopic HER2 overexpression enhances gefitinib effects in vivo. *Neuro-Oncology* **3**, 250-259.

Meley, D., Spiller, D. G., White, M. R. H., McDowell, H., Pizer, B. and Sée, V. (2010). p53-mediated delayed NF-κB activity enhances etoposide-induced cell death in medulloblastoma. *Cell Death and Disease* **in press**,

Mellor, H. R. and Callaghan, R. (2008). Resistance to chemotherapy in cancer: A complex and integrated cellular response. *Pharmacology* **4**, 275-300.

Meng, A. X., Jalali, F., Cuddihy, A., Chan, N., Bindra, R. S., Glazer, P. M. and Bristow, R. G. (2005). Hypoxia down-regulates DNA double strand break repair gene expression in prostate cancer cells. *Radiotherapy and Oncology* **2**, 168-176.

Metzeler, K. H., Dufour, A., Benthaus, T., Hummel, M., Sauerland, M. C., Heinecke, A., Berdel, W. E., Buchner, T., Wormann, B., Mansmann, U., Braess, J., Spiekermann, K., Hiddemann, W., Buske, C. and Bohlander, S. K. (2009). ERG Expression Is an Independent Prognostic Factor and Allows Refined Risk Stratification in Cytogenetically Normal Acute Myeloid Leukemia: A Comprehensive Analysis of ERG, MN1, and BAALC Transcript Levels Using Oligonucleotide Microarrays. *Journal of Clinical Oncology* **30**, 5031-5038.

Meyn, M. S. (1997). Chromosome instability syndromes: Lessons for carcinogenesis. *Genetic Instability and Tumorigenesis* 71-148.

Minamishima, Y. A., Moslehi, J., Padera, R. F., Bronson, R. T., Liao, R. and Kaelin, W. G. (2009). A Feedback Loop Involving the Phd3 Prolyl Hydroxylase Tunes the Mammalian Hypoxic Response In Vivo. *Molecular and Cellular Biology* **21**, 5729-5741.

Mirabelli, C. K., Huang, C. H., Fenwick, R. G. and Crooke, S. T. (1985). Quantitative Measurement of Single-Strand and Double-Strand Breakage of DNA in Escherichia-Coli by the Antitumor Antibiotics Bleomycin and Talisomycin. *Antimicrobial Agents and Chemotherapy* **4**, 460-467.

Mohyeldin, A., Garzon-Muvdi, T. and Quinones-Hinojosa, A. (2010). Oxygen in Stem Cell Biology: A Critical Component of the Stem Cell Niche. *Cell Stem Cell* **2**, 150-161.

Momand, J., Zambetti, G. P., Olson, D. C., George, D. and Levine, A. J. (1992). The Mdm-2 Oncogene Product Forms a Complex with the P53 Protein and Inhibits P53-Mediated Transactivation. *Cell* **7**, 1237-1245.

Moynahan, M. E., Cui, T. Y. and Jasin, M. (2001). Homology-directed DNA repair, mitomycin-C resistance, and chromosome stability is restored with correction of a Brca1 mutation. *Cancer Research* **12**, 4842-4850.

Murphy, M., Ahn, J., Walker, K. K., Hoffman, W. H., Evans, R. M., Levine, A. J. and George, D. L. (1999). Transcriptional repression by wild-type p53 utilizes histone deacetylases, mediated by interaction with mSin3a. *Genes & Development* **19**, 2490-2501.

Nardinocchi, L., Puca, R., Sacchi, A. and D'Orazi, G. (2009). Inhibition of HIF-Ialpha activity by homeodomain-interacting protein kinase-2 correlates with sensitization of chemoresistant cells to undergo apoptosis. *Molecular Cancer*

Nefedova, Y., Cheng, P. Y., Alsina, M., Dalton, W. S. and Gabrilovich, D. I. (2004). Involvement of Notch-1 signaling in bone marrow stroma-mediated de novo drug resistance of myeloma and other malignant lymphoid cell lines. *Blood* **9**, 3503-3510.

Nefedova, Y., Sullivan, D. M., Bolick, S. C., Dalton, W. S. and Gabrilovich, D. I. (2008). Inhibition of Notch signaling induces apoptosis of myeloma cells and enhances sensitivity to chemotherapy. *Blood* **4**, 2220-2229.

Negri, T., Tarantino, E., Orsenigo, M., Reid, J. F., Gariboldi, M., Zambetti, M., Pierotti, M. A. and Pilotti, S. (2010). Chromosome Band 17q21 in Breast Cancer: Significant Association Between Beclin 1 Loss and HER2/NEU Amplification. *Genes Chromosomes & Cancer* **10**, 901-909.

Nichols, J., Zevnik, B., Anastassiadis, K., Niwa, H., Klewe-Nebenius, D., Chambers, I., Scholer, H. and Smith, A. (1998). Formation of pluripotent stem cells in the mammalian embryo depends on the POU transcription factor Oct4. *Cell* **3**, 379-391.

Nicholson, H. S., Kretschmar, C. S., Krailo, M., Bernstein, M., Kadota, R., Fort, D., Friedman, H., Harris, M. B., Tedeschi-Blok, N., Mazewski, C., Sato, J. and Reaman, G. H. (2007). Phase 2 study of temozolomide in children and adolescents with recurrent central nervous system tumors: a report from the Children's Oncology Group. *Cancer* **7**, 1542-50.

Nigro, J. M., Baker, S. J., Preisinger, A. C., Jessup, J. M., Hostetter, R., Cleary, K., Bigner, S. H., Davidson, N., Baylin, S., Devilee, P. and et al. (1989). Mutations in the p53 gene occur in diverse human tumour types. *Nature* **6250**, 705-8.

Nitta, M., Okamura, H., Aizawa, S. and Yamaizumi, M. (1997). Heat shock induces transient p53-dependent cell cycle arrest at G1/S. *Oncogene* **5**, 561-568.

Niwa, H., Miyazaki, J. and Smith, A. G. (2000). Quantitative expression of Oct-3/4 defines differentiation, dedifferentiation or self-renewal of ES cells. *Nature Genetics* **4**, 372-376.

Nobusawa, S., Watanabe, T., Kleihues, P. and Ohgaki, H. (2009). IDH1 mutations as molecular signature and predictive factor of secondary glioblastomas. *Clin Cancer Res* **19**, 6002-7.

Nonet, G. H., Stampfer, M. R., Chin, K., Gray, J. W., Collins, C. C. and Yaswen, P. (2001). The ZNF217 gene amplified in breast cancers promotes immortalization of human mammary epithelial cells. *Cancer Research* **4**, 1250-1254.

Northcott, P. A., Fernandez, A., Hagan, J. P., Ellison, D. W., Rutka, J. T., Croce, C. M., Kenney, A. M. and Taylor, M. D. (2009). The Mir-17/92 Polycistron Is Amplified and Upregulated in Sonic Hedgehog-Driven Medulloblastomas and Induced by N-Myc in Sonic Hedgehog-Treated Cerebellar Neural Precursors. *Neuro-Oncology* **6**, 924-924.

Northcott, P. A., Korshunov, A., Witt, H., Hielscher, T., Eberhart, C. G., Mack, S., Bouffet, E., Clifford, S. C., Hawkins, C. E., French, P., Rutka, J. T., Pfister, S. and Taylor, M. D. (2011). Medulloblastoma Comprises Four Distinct Molecular Variants. *Journal of Clinical Oncology* **11**, 1408-1414.

Northcott, P. A., Shih, D. J. H., Peacock, J., Garzia, L., Morrissy, A. S., Zichner, T., Stutz, A. M., Korshunov, A., Reimand, J., Schumacher, S. E., Beroukhim, R., Ellison, D. W., Marshall, C. R., Lionel, A. C., Mack, S., Dubuc, A., Yao, Y., Ramaswamy, V., Luu, B., Rolider, A., Cavalli, F. M. G., Wang, X., Remke, M., Wu, X. C., Chiu, R. Y. B., Chu, A., Chuah, E., Corbett, R. D., Hoad, G. R., Jackman, S. D., Li, Y. S., Lo, A., Mungall, K. L., Nip, K. M., Qian, J. Q., Raymond, A. G. J., Thiessen, N., Varhol, R. J., Birol, I., Moore, R. A., Mungall, A. J., Holt, R., Kawauchi, D., Roussel, M. F., Kool, M., Jones, D. T. W., Witt, H., Fernandez-L, A., Kenney, A. M., Wechsler-Reya, R. J., Dirks, P., Aviv, T., Grajkowska, W. A., Perek-Polnik, M., Haberler, C. C., Delattre, O., Reynaud, S. S., Doz, F. F., Pernet-Fattet, S. S., Cho, B. K., Kim, S. K., Wang, K. C., Scheurlen, W., Eberhart, C. G., Fevre-Montange, M., Jouvet, A., Pollack, I. F., Fan, X., Muraszko, K. M., Gillespie, G. Y., Di Rocco, C., Massimi, L., Michiels, E. M. C., Kloosterhof, N. K., French, P. J., Kros, J. M., Olson, J. M., Ellenbogen, R. G., Zitterbart, K., Kren, L., Thompson, R. C., Cooper, M. K., Lach, B., McLendon, R. E., Bigner, D. D., Fontebasso, A., Albrecht, S., Jabado, N., Lindsey, J. C., Bailey, S., Gupta, N., Weiss, W. A., Bognar, L., Klekner, A., Van Meter, T. E., Kumabe, T., Tominaga, T., Elbabaa, S. K., Leonard, J. R., Rubin, J. B., Liau, L. M., Van Meir, E. G., Fouladi, M., Nakamura, H., Cinalli, G., Garami, M., Hauser, P., Saad, A. G., Iolascon, A., Jung, S., Carlotti, C. G., Vibhakar, R., Ra, Y. S., Robinson, S., Zollo, M., Faria, C. C., Chan, J. A., Levy, M. L., Sorensen, P. H. B., Meyerson, M., Pomeroy, S. L., Cho, Y. J., Bader, G. D., Tabori, U., Hawkins, C. E., Bouffet, E., Scherer, S. W., Rutka, J. T.,

Malkin, D., Clifford, S. C., Jones, S. J. M., Korbel, J. O., Pfister, S. M., Marra, M. A. and Taylor, M. D. (2012). Subgroup-specific structural variation across 1,000 medulloblastoma genomes. *Nature* **7409**, 49-56.

Obach, M., Navarro-Sabate, A., Caro, J., Kong, X. G., Duran, J., Gomez, M., Perales, J. C., Ventura, F., Rosa, J. L. and Bartrons, R. (2004). 6-phosphofructo-2-kinase (pfkfb3) gene promoter contains hypoxia-inducible factor-1 binding sites necessary for transactivation in response to hypoxia. *Journal of Biological Chemistry* **51**, 53562-53570.

Oliner, J. D., Kinzler, K. W., Meltzer, P. S., George, D. L. and Vogelstein, B. (1992). Amplification of a gene encoding a p53-associated protein in human sarcomas. *Nature* **6381**, 80-3.

Olivier, M., Langerod, A., Carrieri, P., Bergh, J., Klaar, S., Eyfjord, J., Theillet, C., Rodriguez, C., Lidereau, R., Bieche, I., Varley, J., Bignon, Y., Uhrhammer, N., Winqvist, R., Jukkola-Vuorinen, A., Niederacher, D., Kato, S., Ishioka, C., Hainaut, P. and Borresen-Dale, A. L. (2006). The clinical value of somatic TP53 gene mutations in 1,794 patients with breast cancer. *Clinical Cancer Research* **4**, 1157-1167.

Oren, M. and Rotter, V. (1999). Introduction: p53 - the first twenty years. *Cellular and Molecular Life Sciences* **1**, 9-11.

Oren, M. (2003). Decision making by p53: life, death and cancer. *Cell Death Differ* **4**, 431-42.

Ortiz-Barahona, A., Villar, D., Pescador, N., Amigo, J. and del Peso, L. (2010). Genome-wide identification of hypoxia-inducible factor binding sites and target genes by a probabilistic model integrating transcription-profiling data and in silico binding site prediction. *Nucleic Acids Research* **7**, 2332-45.

Osaki, M., Oshimura, M. and Ito, H. (2004). PI3K-Akt pathway: Its functions and alterations in human cancer. *Apoptosis* **6**, 667-676.

Osisami, M. and Keller, E. T. (2013). SPDEF: a molecular switch for E-cadherin expression that promotes prostate cancer metastasis. *Asian Journal of Andrology* **5**, 584-585.

Ota, H., Tokunaga, E., Chang, K., Hikasa, M., Iijima, K., Eto, M., Kozaki, K., Akishita, M., Ouchi, Y. and Kaneki, M. (2006). Sirt1 inhibitor, Sirtinol, induces senescence-like growth arrest with attenuated Ras-MAPK signaling in human cancer cells. *Oncogene* **2**, 176-85.

Packer, R. J., Sutton, L. N., Elterman, R., Lange, B., Goldwein, J., Nicholson, H. S., Mulne, L., Boyett, J., Dangio, G., Wechslerjentzsch, K., Reaman, G., Cohen, B. H., Bruce, D. A., Rorke, L. B., Molloy, P., Ryan, J., Lafond, D., Evans, A. E. and Schut, L. (1994). Outcome for Children with Medulloblastoma Treated with Radiation and Cisplatin, Ccnu, and Vincristine Chemotherapy. *Journal of Neurosurgery* **5**, 690-698.

Padua, D., Zhang, X. H. F., Wang, Q. Q., Nadal, C., Gerald, W. L., Gomis, R. R. and Massague, J. (2008). TGF beta primes breast tumors for lung metastasis seeding through angiopoietin-like 4. *Cell* **1**, 66-77.

Pagnoux, C. and Guillevin, L. (2009). Azathioprine or Methotrexate Maintenance for ANCA-Associated Vasculitis THE AUTHORS REPLY. *New England Journal of Medicine* **13**, 1359-1359.

Pan, Y., Oprysko, P. R., Asham, A. M., Koch, C. J. and Simon, M. C. (2004). p53 cannot be induced by hypoxia alone but responds to the hypoxic microenvironment. *Oncogene* **29**, 4975-4983.

Panchision, D. M. (2009). The role of oxygen in regulating neural stem cells in development and disease. *J Cell Physiol* **3**, 562-8.

Papandreou, I., Cairns, R. A., Fontana, L., Lim, A. L. and Denko, N. C. (2006). HIF-1 mediates adaptation to hypoxia by actively downregulating mitochondrial oxygen consumption. *Cell Metab* **3**, 187-97.

Pardo, B., Gomez-Gonzalez, B. and Aguilera, A. (2009). DNA Repair in Mammalian Cells. *Cellular and Molecular Life Sciences* **6**, 1039-1056.

Parsels, L. A., Zellars, R. C., Loney, T. L., Parsels, J. D., Clarke, M. F., Merchant, A. K., Lawrence, T. S. and Maybaum, J. (1997). Prevention of fluorodeoxyuridine-induced cytotoxicity and DNA damage in HT29 colon carcinoma cells by conditional expression of wild-type p53 phenotype. *Molecular Pharmacology* **4**, 600-605.

Parsons, D. W., Jones, S., Zhang, X., Lin, J. C., Leary, R. J., Angenendt, P., Mankoo, P., Carter, H., Siu, I. M., Gallia, G. L., Olivi, A., McLendon, R., Rasheed, B. A., Keir, S., Nikolskaya, T., Nikolsky, Y., Busam, D. A., Tekleab, H., Diaz, L. A., Jr., Hartigan, J., Smith, D. R., Strausberg, R. L., Marie, S. K., Shinjo, S. M., Yan, H., Riggins, G. J., Bigner, D. D., Karchin, R., Papadopoulos, N., Parmigiani, G., Vogelstein, B., Velculescu, V. E. and Kinzler, K. W. (2008). An integrated genomic analysis of human glioblastoma multiforme. *Science* **5897**, 1807-12.

Parsons, D. W., Li, M., Zhang, X. S., Jones, S., Leary, R. J., Lin, J. C. H., Boca, S. M., Carter, H., Samayoa, J., Bettegowda, C., Gallia, G. L., Jallo, G. I., Binder, Z. A., Nikolsky, Y., Hartigan, J., Smith, D. R., Gerhard, D. S., Fults, D. W., VandenBerg, S., Berger, M. S., Marie, S. K. N., Shinjo, S. M. O., Clara, C., Phillips, P. C., Minturn, J. E., Biegel, J. A., Judkins, A. R., Resnick, A. C., Storm, P. B., Curran, T., He, Y. P., Rasheed, B. A., Friedman, H. S., Keir, S. T., McLendon, R., Northcott, P. A., Taylor, M. D., Burger, P. C., Riggins, G. J., Karchin, R., Parmigiani, G., Bigner, D. D., Yan, H., Papadopoulos, N., Vogelstein, B., Kinzler, K. W. and Velculescu, V. E. (2011). The Genetic Landscape of the Childhood Cancer Medulloblastoma. *Science* **6016**, 435-439.

Paulli, M., Viglio, A., Boveri, E., Pitino, A., Lucioni, M., Franco, C., Riboni, R., Rosso, R., Magrini, U., Marseglia, G. L. and Marchi, A. (2000). Nijmegen breakage syndrome-associated T-cell-rich B-cell lymphoma: Case report. *Pediatric and Developmental Pathology* **3**, 264-270.

Peck, B., Chen, C. Y., Ho, K. K., Di Fruscia, P., Myatt, S. S., Coombes, R. C., Fuchter, M. J., Hsiao, C. D. and Lam, E. W. SIRT inhibitors induce cell death and p53 acetylation through targeting both SIRT1 and SIRT2. *Mol Cancer Ther* **4**, 844-55.

Peck, B., Chen, C. Y., Ho, K. K., Di Fruscia, P., Myatt, S. S., Coombes, R. C., Fuchter, M. J., Hsiao, C. D. and Lam, E. W. F. (2010). SIRT Inhibitors Induce Cell Death and p53 Acetylation through Targeting Both SIRT1 and SIRT2. *Molecular Cancer Therapeutics* **4**, 844-855.

Peto, J., Collins, N., Barfoot, R., Seal, S., Warren, W., Rahman, N., Easton, D. F., Evans, C., Deacon, J. and Stratton, M. R. (1999). Prevalence of BRCA1 and BRCA2 gene mutations in patients with early-onset breast cancer. *Journal of the National Cancer Institute* **11**, 943-949.

Pfaff, E., Remke, M., Sturm, D., Witt, H., von Bueren, A. O., Wittmann, A., Schoettler, A., Scheurlen, W., Kulozik, A. E., Witt, O., von Deimling, A., Rutkowski, S., Hawkins, C., Tabori, U., Lichter, P., Korshunov, A. and Pfister, S. M. (2010). Tp53 Mutation Status Is a Potential Predictive Marker in Medulloblastoma. *Pediatric Blood & Cancer* **5**, 799-799.

Pfaffl, M. W., Horgan, G. W. and Dempfle, L. (2002). Relative expression software tool (REST (c)) for group-wise comparison and statistical analysis of relative expression results in real-time PCR. *Nucleic Acids Res* **9**,

Pierson, J., Hostager, B., Fan, R. and Vibhakar, R. (2008). Regulation of cyclin dependent kinase 6 by microRNA 124 in medulloblastoma. *Journal of Neuro-Oncology* **1**, 1-7.

Pinto, A. L. and Lippard, S. J. (1984). Binding of the Antitumor Drug Cis-Diamminedichloroplatinum(Ii) (Cisplatin) to DNA. *Biochimica Et Biophysica Acta* **3**, 167-180.

Piret, J. P., Cosse, J. P., Ninane, N., Raes, M. and Michiels, C. (2006). Hypoxia protects HepG2 cells against etoposide-induced apoptosis via a HIF-1-independent pathway. *Exp Cell Res* **15**, 2908-20.

Pisco, A. O., Brock, A., Zhou, J., Moor, A., Mojtahedi, M., Jackson, D. and Huang, S. (2013). Non-Darwinian dynamics in therapy-induced cancer drug resistance. *Nature Communications*

Pistollato, F., Rampazzo, E., Persano, L., Abbadi, S., Frasson, C., Denaro, L., D'Avella, D., Panchision, D. M., Della Puppa, A., Scienza, R. and Basso, G. (2010). Interaction of Hypoxia-Inducible Factor-1 alpha and Notch Signaling Regulates Medulloblastoma Precursor Proliferation and Fate. *Stem Cells* **11**, 1918-1929.

Pizer, B. and Clifford, S. (2008). Medulloblastoma: new insights into biology and treatment. *Archives of Disease in Childhood-Education and Practice Edition* **5**, 137-144.

Pollack, I. F., Stewart, C. F., Kocak, M., Poussaint, T. Y., Broniscer, A., Banerjee, A., Douglas, J. G., Kun, L. E., Boyett, J. M. and Geyer, J. R. (2011). A phase II study of gefitinib and irradiation in children with newly diagnosed brainstem gliomas: A report from the Pediatric Brain Tumor Consortium. *Neuro-Oncology* **3**, 290-297.

Polyak, K. and Weinberg, R. A. (2009). Transitions between epithelial and mesenchymal states: acquisition of malignant and stem cell traits. *Nature Reviews Cancer* **4**, 265-273.

Ponti, D., Costa, A., Zaffaroni, N., Pratesi, G., Petrangolini, G., Coradini, D., Pilotti, S., Pierotti, M. A. and Daidone, M. G. (2005). Isolation and in vitro propagation of tumorigenic breast cancer cells with stem/progenitor cell properties. *Cancer Research* **13**, 5506-5511.

Porter, A. G. and Janicke, R. U. (1999). Emerging roles of caspase-3 in apoptosis. *Cell Death and Differentiation* **2**, 99-104.

Powell, S. N. and Kachnic, L. A. (2003). Roles of BRCA1 and BRCA2 in homologous recombination, DNA replication fidelity and the cellular response to ionizing radiation. *Oncogene* **37**, 5784-5791.

Pugh, C. W., Tan, C. C., Jones, R. W. and Ratcliffe, P. J. (1991). Functional analysis of an oxygen-regulated transcriptional enhancer lying 3' to the mouse erythropoietin gene. *Proc Natl Acad Sci U S A* **23**, 10553-7.

Pugh, T. J., Weeraratne, S. D., Archer, T. C., Krummel, D. A. P., Auclair, D., Bochicchio, J., Carneiro, M. O., Carter, S. L., Cibulskis, K., Erlich, R. L., Greulich, H., Lawrence, M. S., Lennon, N. J., McKenna, A., Meldrim, J., Ramos, A. H., Ross, M. G., Russ, C., Shefler, E., Sivachenko, A., Sogoloff, B., Stojanov, P., Tamayo, P., Mesirov, J. P., Amani, V., Teider, N., Sengupta, S., Francois, J. P., Northcott, P. A., Taylor, M. D., Yu, F. R., Crabtree, G. R., Kautzman, A. G., Gabriel, S. B., Getz, G., Jager, N., Jones, D. T. W., Lichter, P., Pfister, S. M., Roberts, T. M., Meyerson, M., Pomeroy, S. L. and Cho, Y. J. (2012). Medulloblastoma exome sequencing uncovers subtype-specific somatic mutations. *Nature* **7409**, 106-110.

Purvis, J. E., Karhohs, K. W., Mock, C., Batchelor, E., Loewer, A. and Lahav, G. (2012). p53 Dynamics Control Cell Fate. *Science* **6087**, 1440-1444.

Quinlan, K. G. R., Verger, A., Yaswen, P. and Crossley, M. (2007). Amplification of zinc finger gene 217 (ZNF217) and cancer: When good fingers go bad. *Biochimica Et Biophysica Acta-Reviews on Cancer* **2**, 333-340.

Raffel, C. (2004). Medulloblastoma: Molecular genetics and animal models. *Neoplasia* **4**, 310-322.

Ragel, B. T., Couldwell, W. T., Gillespie, D. L. and Jensen, R. L. (2007). Identification of hypoxia-induced genes in a malignant glioma cell line (U-251) by cDNA microarray analysis. *Neurosurg Rev* **3**, 181-7; discussion 187.

Raghunand, N., Gatenby, R. A. and Gillies, R. J. (2003). Microenvironmental and cellular consequences of altered blood flow in tumours. *British Journal of Radiology* S11-S22.

Raica, M., Cimpean, A. M. and Ribatti, D. (2009). Angiogenesis in pre-malignant conditions. *Eur J Cancer* **11**, 1924-34.

Rampling, R., Cruickshank, G., Lewis, A. D., Fitzsimmons, S. A. and Workman, P. (1994). Direct Measurement of Po2 Distribution and Bioreductive Enzymes in Human-Malignant Brain-Tumors. *International Journal of Radiation Oncology Biology Physics* **3**, 427-431.

Rausch, T., Jones, D. T. W., Zapatka, M., Stutz, A. M., Zichner, T., Weischenfeldt, J., Jager, N., Remke, M., Shih, D., Northcott, P. A., Pfaff, E., Tica, J., Wang, Q., Massimi, L., Witt, H., Bender, S., Pleier, S., Cin, H., Hawkins, C., Beck, C., von Deimling, A., Hans, V., Brors, B., Eils, R., Scheurlen, W., Blake, J., Benes, V., Kulozik, A. E., Witt, O., Martin, D., Zhang, C., Porat, R., Merino, D. M., Wasserman, J., Jabado, N., Fontebasso, A., Bullinger, L., Rucker, F. G., Dohner, K., Dohner, H., Koster, J., Molenaar, J. J., Versteeg, R., Kool, M., Tabori, U., Malkin, D., Korshunov, A., Taylor, M. D., Lichter, P., Pfister, S. M. and Korbel, J. O. (2012). Genome Sequencing of Pediatric Medulloblastoma Links Catastrophic DNA Rearrangements with TP53 Mutations. *Cell* **1-2**, 59-71.

Raver-Shapira, N., Marciano, E., Meiri, E., Spector, Y., Rosenfeld, N., Moskovits, N., Bentwich, Z. and Oren, M. (2007). Transcriptional activation of miR-34a contributes to p53-mediated apoptosis. *Mol Cell* **5**, 731-43.

Read, T. A., Fogarty, M. P., Markant, S. L., McLendon, R. E., Wei, Z. Z., Ellison, D. W., Febbo, P. G. and Wechsler-Reya, R. J. (2009). Identification of CD15 as a Marker for Tumor-Propagating Cells in a Mouse Model of Medulloblastoma (vol 15, pg 135, 2009). *Cancer Cell* **3**, 267-267.

Ree, A. H., Tvermyr, M., Engebraaten, O., Rooman, M., Rosok, O., Hovig, E., Meza-Zepeda, L. A., Bruland, O. S. and Fodstad, O. (1999). Expression of a novel factor in human breast cancer cells with metastatic potential. *Cancer Research* **18**, 4675-4680.

Rice, M. C., Smith, S. T., Bullrich, F., Havre, P. and Kmiec, E. B. (1997). Isolation of human and mouse genes based on homology to REC2, a recombinational repair gene from the fungus Ustilago maydis. *Proceedings of the National Academy of Sciences of the United States of America* **14**, 7417-7422.

Riches, L. C., Lynch, A. M. and Gooderham, N. J. (2008). Early events in the mammalian response to DNA double-strand breaks. *Mutagenesis* **5**, 331-339.

Ripolles, L., Ortega, M., Ortuno, F., Gonzalez, A., Losada, J., Ojanguren, J., Soler, J. A., Bergua, J., Coll, M. D. and Caballin, M. R. (2006). Genetic abnormalities and clinical outcome in chronic lymphocytic leukemia. *Cancer Genetics and Cytogenetics* **1**, 57-64.

Rizzo, S., Hersey, J. M., Mellor, P., Dai, W., Santos-Silva, A., Liber, D., Luk, L., Titley, I., Carden, C. P., Box, G., Hudson, D. L., Kaye, S. B. and Brown, R. (2011). Ovarian Cancer Stem Cell-Like Side Populations Are Enriched Following Chemotherapy and Overexpress EZH2. *Molecular Cancer Therapeutics* **2**, 325-335.

Robles, A. I. and Harris, C. C. (2010). Clinical Outcomes and Correlates of TP53 Mutations and Cancer. *Cold Spring Harbor Perspectives in Biology* **3**,

Rocha, S. (2007). Gene regulation under low oxygen: holding your breath for transcription. *Trends in Biochemical Sciences* **8**, 389-397.

Rohwer, N. and Cramer, T. (2011). Hypoxia-mediated drug resistance: novel insights on the functional interaction of HIFs and cell death pathways. *Drug Resist Updat* **3**, 191-201.

Romer, J. and Curran, T. (2005). Targeting medulloblastoma: Small-molecule inhibitors of the sonic hedgehog pathway as potential cancer therapeutics. *Cancer Research* **12**, 4975-4978.

Roos, W. P., Batista, L. F., Naumann, S. C., Wick, W., Weller, M., Menck, C. F. and Kaina, B. (2007). Apoptosis in malignant glioma cells triggered by the temozolomide-induced DNA lesion O6-methylguanine. *Oncogene* **2**, 186-97.

Rossi, A., Caracciolo, V., Russo, G., Reiss, K. and Giordano, A. (2008). Medulloblastoma: From molecular pathology to therapy. *Clinical Cancer Research* **4**, 971-976.

Roy, M., Pear, W. S. and Aster, J. C. (2007). The multifaceted role of Notch in cancer. *Current Opinion in Genetics & Development* **1**, 52-59.

Rozen, S. and Skaletsky, H. (2000). Primer3 on the WWW for general users and for biologist programmers. *Methods Mol Biol* 365-86.

Ruark, E., Snape, K., Humburg, P., Loveday, C., Bajrami, I., Brough, R., Rodrigues, D. N., Renwick, A., Seal, S., Ramsay, E., Duarte, S. D., Rivas, M. A., Warren-Perry, M., Zachariou, A., Campion-Flora, A., Hanks, S., Murray, A., Pour, N. A., Douglas, J., Gregory, L., Rimmer, A., Walker, N. M., Yang, T. P., Adlard, J. W., Barwell, J., Berg, J., Brady, A. F., Brewer, C., Brice, G., Chapman, C., Cook, J., Davidson, R., Donaldson, A., Douglas, F., Eccles, D., Evans, D. G., Greenhalgh, L., Henderson, A., Izatt, L., Kumar, A., Lalloo, F., Miedzybrodzka, Z., Morrison, P. J., Paterson, J., Porteous, M., Rogers, M. T., Shanley, S., Walker, L., Gore, M., Houlston, R., Brown, M. A., Caufield, M. J., Deloukas, P., McCarthy, M. I., Todd, J. A., Turnbull, C., Reis, J. S., Ashworth, A., Antoniou, A. C., Lord, C. J., Donnelly, P., Rahman, N., Susceptibility, B. O. C. and Consor, W. T. C. C. (2013). Mosaic PPM1D mutations are associated with predisposition to breast and ovarian cancer. *Nature* **7432**, 406-U152.

Ruggiero, A., Cefalo, G., Garre, M. L., Massimino, M., Colosimo, C., Attina, G., Lazzareschi, I., Maurizi, P., Ridola, V., Mazzarella, G., Caldarelli, M., Di Rocco, C., Madon, E., Abate, M. E., Clerico, A., Sandri, A. and Riccardi, R. (2006). Phase II trial of temozolomide in children with recurrent high-grade glioma. *J Neurooncol* **1**, 89-94.

Russell, S. E. H., Hickey, G. I., Lowry, W. S., White, P. and Atkinson, R. J. (1990). Allele Loss from Chromosome-17 in Ovarian-Cancer. *Oncogene* **10**, 1581-1583.

Rutkowski, S., Bode, U., Deinlein, F., Ottensmeier, H., Warmuth-Metz, M., Soerensen, N., Graf, N., Emser, A., Pietsch, T., Wolff, J. E. A., Kortmann, R. D. and Kuehl, J. (2005). Treatment of early childhood medulloblastoma by postoperative chemotherapy alone. *New England Journal of Medicine* **10**, 978-986.

Rutkowski, S. (2006). Current chemotherapeutic procedure for the medulloblastoma. *Strahlentherapie Und Onkologie* 141-141.

Safran, M. and Kaelin, W. G. (2003). HIF hydroxylation and the mammalian oxygen-sensing pathway. *Journal of Clinical Investigation* **6**, 779-783.

Sahlgren, C., Gustafsson, M. V., Jin, S., Poellinger, L. and Lendahl, U. (2008). Notch signaling mediates hypoxia-induced tumor cell migration and invasion. *Proceedings of the National Academy of Sciences of the United States of America* **17**, 6392-6397.

Said, H. M., Hagemann, C., Staab, A., Stojic, J., Kuhnel, S., Vince, G. H., Flentje, M., Roosen, K. and Vordermark, D. (2007). Expression patterns of the hypoxia-related genes osteopontin, CA9, erythropoietin, VEGF and HIF-1alpha in human glioma in vitro and in vivo. *Radiotherapy and Oncology* **3**, 398-405.

Said, H. M., Hagemann, C., Carta, F., Katzer, A., Polat, B., Staab, A., Scozzafava, A., Anacker, J., Vince, G. H., Flentje, M. and Supuran, C. T. (2013). Hypoxia induced CA9 inhibitory targeting by two different sulfonamide derivatives including Acetazolamide in human Glioblastoma. *Bioorganic & Medicinal Chemistry* **13**, 3949-3957.

Saito, S., Goodarzi, A. A., Higashimoto, Y., Noda, Y., Lees-Miller, S. P., Appella, E. and Anderson, C. W. (2002). ATM mediates phosphorylation at multiple p53 sites, including Ser(46), in response to ionizing radiation. *Journal of Biological Chemistry* **15**, 12491-4.

Saito, S., Yamaguchi, H., Higashimoto, Y., Chao, C., Xu, Y., Fornace, A. J., Jr., Appella, E. and Anderson, C. W. (2003). Phosphorylation site interdependence of human p53 post-translational modifications in response to stress. *Journal of Biological Chemistry* **39**, 37536-44.

Sakaguchi, K., Herrera, J. E., Saito, S., Miki, T., Bustin, M., Vassilev, A., Anderson, C. W. and Appella, E. (1998). DNA damage activates p53 through a phosphorylation-acetylation cascade. *Genes & Development* **18**, 2831-2841.

Sakaguchi, K., Saito, S., Higashimoto, Y., Roy, S., Anderson, C. W. and Appella, E. (2000). Damage-mediated phosphorylation of human p53 threonine 18 through a cascade mediated by a casein 1-like kinase. Effect on Mdm2 binding. *Journal of Biological Chemistry* **13**, 9278-83.

Saldeen, J., Tillmar, L., Karlsson, E. and Welsh, N. (2003). Nicotinamide- and caspase-mediated inhibition of poly(ADP-ribose) polymerase are associated with p53-independent cell cycle (G2) arrest and apoptosis. *Molecular and Cellular Biochemistry* **1-2**, 113-122.

Sampath, J., Sun, D., Kidd, V. J., Grenet, J., Gandhi, A., Shapiro, L. H., Wang, Q., Zambetti, G. P. and Schuetz, J. D. (2001). Mutant p53 cooperates with ETS and selectively up-regulates human MDR1 not MRP1. *Journal of Biological Chemistry* **42**, 39359-67.

Sasabe, E., Zhou, X., Li, D. C., Oku, N., Yamamoto, T. and Osaki, T. (2007). The involvement of hypoxia-inducible factor-1 alpha in the susceptibility to gamma-rays and chemotherapeutic drugs of oral squamous cell carcinoma cells. *International Journal of Cancer* **2**, 268-277.

Schinkel, A. H. (1999). P-glycoprotein, a gatekeeper in the blood-brain barrier. *Advanced Drug Delivery Reviews* **2-3**, 179-194.

Schofield, C. J. and Ratcliffe, P. J. (2004). Oxygen sensing by HIF hydroxylases. *Nature Reviews Molecular Cell Biology* **5**, 343-354.

Schon, O., Friedler, A., Bycroft, M., Freund, S. M. V. and Fersht, A. R. (2002). Molecular mechanism of the interaction between MDM2 and p53. *Journal of Molecular Biology* **3**, 491-501.

Schreiber, M., Kolbus, A., Piu, F., Szabowski, A., Mohle-Steinlein, U., Tian, J. M., Karin, M., Angel, P. and Wagner, E. F. (1999). Control of cell cycle progression by c-Jun is p53 dependent. *Genes & Development* **5**, 607-619.

Scian, M. J., Stagliano, K. E. R., Anderson, M. A. E., Hassan, S., Bowman, M., Miles, M. F., Deb, S. P. and Deb, S. (2005). Tumor-derived p53 mutants induce NF-kappa B2 gene expression. *Molecular and Cellular Biology* **22**, 10097-10110.

See, V. P., B.; Meley, D. (2012). Molecular Mechanisms of Chemoresistance in Medulloblastoma. *Tumors of the Central Nervous System* 59-67.

Selten, G., Cuypers, H. T., Boelens, W., Robanusmaandag, E., Verbeek, J., Domen, J., Vanbeveren, C. and Berns, A. (1986). The Primary Structure of the Putative Oncogene Pim-1 Shows Extensive Homology with Protein-Kinases. *Cell* **4**, 603-611.

Semenza, G. L., Nejfelt, M. K., Chi, S. M. and Antonarakis, S. E. (1991). Hypoxia-inducible nuclear factors bind to an enhancer element located 3' to the human erythropoietin gene. *Proc Natl Acad Sci U S A* **13**, 5680-4.

Semenza, G. L. and Wang, G. L. (1992). A nuclear factor induced by hypoxia via de novo protein synthesis binds to the human erythropoietin gene enhancer at a site required for transcriptional activation. *Mol Cell Biol* **12**, 5447-54.

Semenza, G. L. (2000). Expression of hypoxia-inducible factor 1: Mechanisms and consequences. *Biochemical Pharmacology* **1**, 47-53.

Semenza, G. L. (2003). Targeting HIF-1 for cancer therapy. *Nat Rev Cancer* **10**, 721-32.

Semenza, G. L. (2012a). Molecular mechanisms mediating metastasis of hypoxic breast cancer cells. *Trends in Molecular Medicine* **9**, 534-543.

Semenza, G. L. (2012b). Hypoxia-Inducible Factors in Physiology and Medicine. *Cell* **3**, 399-408.

Sermeus, A., Cosse, J. P., Crespin, M., Mainfroid, V., de Longueville, F., Ninane, N., Raes, M., Remacle, J. and Michiels, C. (2008). Hypoxia induces protection against etoposide-induced apoptosis: molecular profiling of changes in gene expression and transcription factor activity. *Molecular Cancer*

Sermeus, A., Genin, M., Maincent, A., Fransolet, M., Notte, A., Leclere, L., Riquier, H., Arnould, T. and Michiels, C. (2012). Hypoxia-Induced Modulation of Apoptosis and BCL-2 Family Proteins in Different Cancer Cell Types. *Plos One* **11**,

Sharp, F. R. and Bernaudin, M. (2004). HIf1 and oxygen sensing in the brain. *Nature Reviews Neuroscience* **6**, 437-448.

Sharrocks, A. D. (2001). The ETS-domain transcription factor family. *Nature Reviews Molecular Cell Biology* **11**, 827-837.

Shepherd, F. A., Pereira, J. R., Ciuleanu, T., Tan, E. H., Hirsh, V., Thongprasert, S., Campos, D., Maoleekoonpiroj, S., Smylie, M., Martins, R., van Kooten, M., Dediu, M., Findlay, B., Tu, D. S., Johnston, D., Bezjak, A., Clark, G., Santabarbara, P., Seymour, L. and Trials, N. C. I. C. C. (2005). Erlotinib in previously treated non-small-cell lung cancer. *New England Journal of Medicine* **2**, 123-132.

Shilatifard, A. (2006). Chromatin modifications by methylation and ubiquitination: Implications in the regulation of gene expression. *Annual Review of Biochemistry* 243-269.

Shiloh, Y., Tabor, E. and Becker, Y. (1983). Abnormal Response of Ataxia-Telangiectasia Cells to Agents That Break the Deoxyribose Moiety of DNA Via a Targeted Free-Radical Mechanism. *Carcinogenesis* **10**, 1317-1322.

Shinohara, A., Ogawa, H. and Ogawa, T. (1992). Rad51 Protein Involved in Repair and Recombination in Saccharomyces-Cerevisiae Is a Reca-Like Protein. *Cell* **3**, 457-470.

Shvarts, A., Steegenga, W. T., Riteco, N., vanLaar, T., Dekker, P., Bazuine, M., vanHam, R. C. A., vanOordt, W. V., Hateboer, G., vanderEb, A. J. and Jochemsen, A. G. (1996). MDMX: A

novel p53-binding protein with some functional properties of MDM2. *Embo Journal* **19**, 5349-5357.

Shweiki, D., Itin, A., Soffer, D. and Keshet, E. (1992). Vascular Endothelial Growth-Factor Induced by Hypoxia May Mediate Hypoxia-Initiated Angiogenesis. *Nature* **6398**, 843-845.

Si, M. L., Zhu, S., Wu, H., Lu, Z., Wu, F. and Mo, Y. Y. (2007). miR-21-mediated tumor growth. *Oncogene* **19**, 2799-2803.

Siddik, Z. H. (2003). Cisplatin: mode of cytotoxic action and molecular basis of resistance. *Oncogene* **47**, 7265-79.

Singh, R. K., Gutman, M., Bucana, C. D., Sanchez, R., Llansa, N. and Fidler, I. J. (1995). Interferon-Alpha and Interferon-Beta down-Regulate the Expression of Basic Fibroblast Growth-Factor in Human Carcinomas. *Proc Natl Acad Sci U S A* **10**, 4562-4566.

Soderlund, K., Stal, O., Skoog, L., Rutqvist, L. E., Nordenskjold, B. and Askmalm, M. S. (2007). Intact Mre11/Rad50/Nbs1 complex predicts good response to radiotherapy in early breast cancer. *International Journal of Radiation Oncology Biology Physics* **1**, 50-58.

Solomon, J. M., Pasupuleti, R., Xu, L., McDonagh, T., Curtis, R., DiStefano, P. S. and Huber, L. J. (2006). Inhibition of SIRT1 catalytic activity increases p53 acetylation but does not alter cell survival following DNA damage. *Mol Cell Biol* **1**, 28-38.

Song, X. R., Liu, X. X., Chi, W. L., Liu, Y. L., Wei, L., Wang, X. W. and Yu, J. M. (2006). Hypoxia-induced resistance to cisplatin and doxorubicin in non-small cell lung cancer is inhibited by silencing of HIF-1 alpha gene. *Cancer Chemotherapy and Pharmacology* **6**, 776-784.

Sood, A. K., Saxena, R., Groth, J., Desouki, M. M., Cheewakriangkrai, C., Rodabaugh, K. J., Kasyapa, C. S. and Geradts, J. (2007). Expression characteristics of prostate-derived Ets factor support a role in breast and prostate cancer progression. *Human Pathology* **11**, 1628-1638.

Sowter, H. M., Ratcliffe, P. J., Watson, P., Greenberg, A. H. and Harris, A. L. (2001). HIF-1-dependent regulation of hypoxic induction of the cell death factors BNIP3 and NIX in human tumors. *Cancer Research* **18**, 6669-6673.

St Clair, W. H., Adams, J. A., Bues, M., Fullerton, B. C., La Shell, S., Kooy, H. M., Loeffler, J. S. and Tarbell, N. J. (2004). Advantage of protons compared to conventional X-ray or IMRT in the treatment of a pediatric patient with medulloblastoma. *International Journal of Radiation Oncology Biology Physics* **3**, 727-734.

Staab, A., Loeffler, J., Said, H. M., Diehlmann, D., Katzer, A., Beyer, M., Fleischer, M., Schwab, F., Baier, K., Einsele, H., Flentje, M. and Vordermark, D. (2007). Effects of HIF-1 inhibition by chetomin on hypoxia-related transcription and radiosensitivity in HT 1080 human fibrosarcoma cells. *Bmc Cancer*

Staal, S. P. (1987). Molecular-Cloning of the Akt Oncogene and Its Human Homologs Akt1 and Akt2 - Amplification of Akt1 in a Primary Human Gastric Adenocarcinoma. *Proceedings of the National Academy of Sciences of the United States of America* **14**, 5034-5037.

Stark, J. M., Pierce, A. J., Oh, J., Pastink, A. and Jasin, M. (2004). Genetic steps of mammalian homologous repair with distinct mutagenic consequences. *Molecular and Cellular Biology* **21**, 9305-9316.

Stein, L. D. (2004). Human genome - End of the beginning. *Nature* **7011**, 915-916.

Stephens, P. J., Greenman, C. D., Fu, B. Y., Yang, F. T., Bignell, G. R., Mudie, L. J., Pleasance, E. D., Lau, K. W., Beare, D., Stebbings, L. A., McLaren, S., Lin, M. L., McBride, D. J., Varela, I., Nik-Zainal, S., Leroy, C., Jia, M. M., Menzies, A., Butler, A. P., Teague, J. W., Quail, M. A.,

Burton, J., Swerdlow, H., Carter, N. P., Morsberger, L. A., Iacobuzio-Donahue, C., Follows, G. A., Green, A. R., Flanagan, A. M., Stratton, M. R., Futreal, P. A. and Campbell, P. J. (2011). Massive Genomic Rearrangement Acquired in a Single Catastrophic Event during Cancer Development. *Cell* **1**, 27-40.

Stetler-Stevenson, W. G. and Yu, A. E. (2001). Proteases in invasion: matrix metalloproteinases. *Seminars in Cancer Biology* **2**, 143-152.

Stiehl, D. P., Wirthner, R., Koditz, J., Spielmann, P., Camenisch, G. and Wenger, R. H. (2006). Increased prolyl 4-hydroxylase domain proteins compensate for decreased oxygen levels. Evidence for an autoregulatory oxygen-sensing system. *J Biol Chem* **33**, 23482-91.

Stiff, T., O'Driscoll, M., Rief, N., Iwabuchi, K., Lobrich, M. and Jeggo, P. A. (2004). ATM and DNA-PK function redundantly to phosphorylate H2AX after exposure to ionizing radiation. *Cancer Research* **7**, 2390-2396.

Stiles, C. D. and Rowitch, D. H. (2008). Glioma stem cells: a midterm exam. *Neuron* **6**, 832-46.

Stiller, C. A. (2007). Classification of childhood cancers. *Journal of Pediatric Hematology Oncology* S19-S20.

Stothard, P. (2000). The sequence manipulation suite: JavaScript programs for analyzing and formatting protein and DNA sequences. *Biotechniques* **6**, 1102, 1104.

Strano, S., Fontemaggi, G., Costanzo, A., Rizzo, M. G., Monti, O., Baccarini, A., Del Sal, G., Levrero, M., Sacchi, A., Oren, M. and Blandino, G. (2002). Physical interaction with human tumor-derived p53 mutants inhibits p63 activities. *Journal of Biological Chemistry* **21**, 18817-18826.

Strano, S., Dell'Orso, S., Di Agostino, S., Fontemaggi, G., Sacchi, A. and Blandino, G. (2007). Mutant p53: an oncogenic transcription factor. *Oncogene* **15**, 2212-2219.

Strauss, B. E., Shivakumar, C., Deb, S. P., Deb, S. and Haas, M. (1995). The MDR1 downstream promoter contains sequence-specific binding sites for wild-type p53. *Biochemical and Biophysical Research Communications* **3**, 825-831.

Strother, D., Ashley, D., Kellie, S. J., Patel, A., Jones-Wallace, D., Thompson, S., Heideman, R., Benaim, E., Krance, R., Bowman, L. and Gajjar, A. (2001). Feasibility of four consecutive high-dose chemotherapy cycles with stem-cell rescue for patients with newly diagnosed medulloblastoma or supratentorial primitive neuroectodermal tumor after craniospinal radiotherapy: Results of a collaborative study. *Journal of Clinical Oncology* **10**, 2696-2704.

Stupp, R., Mason, W. P., van den Bent, M. J., Weller, M., Fisher, B., Taphoorn, M. J., Belanger, K., Brandes, A. A., Marosi, C., Bogdahn, U., Curschmann, J., Janzer, R. C., Ludwin, S. K., Gorlia, T., Allgeier, A., Lacombe, D., Cairncross, J. G., Eisenhauer, E., Mirimanoff, R. O., European Organisation for, R., Treatment of Cancer Brain, T., Radiotherapy, G. and National Cancer Institute of Canada Clinical Trials, G. (2005). Radiotherapy plus concomitant and adjuvant temozolomide for glioblastoma. *N Engl J Med* **10**, 987-96.

Su, S. B., Motoo, Y., Iovanna, J. L., Xie, M. J., Mouri, H., Ohtsubo, K., Yamaguchi, Y., Watanabe, H., Okai, T., Matsubara, F. and Sawabu, N. (2001). Expression of p8 in human pancreatic cancer. *Clinical Cancer Research* **2**, 309-313.

Sullivan, R., Pare, G. C., Frederiksen, L. J., Semenza, G. L. and Graham, C. H. (2008). Hypoxia-induced resistance to anticancer drugs is associated with decreased senescence and requires hypoxia-inducible factor-1 activity. *Molecular Cancer Therapeutics* **7**, 1961-1973.

Sullivan, R. and Graham, C. H. (2009). Hypoxia prevents etoposide-induced DNA damage in cancer cells through a mechanism involving hypoxia-inducible factor 1. *Mol Cancer Ther* **6**, 1702-13.

Sun, F., Fu, H., Liu, Q., Tie, Y., Zhu, J., Xing, R., Sun, Z. and Zheng, X. (2008). Downregulation of CCND1 and CDK6 by miR-34a induces cell cycle arrest. *FEBS Lett* **10**, 1564-8.

Sun, G., Zhou, J., Yin, A., Ding, Y. and Zhong, M. (2008). Silencing of ZNF217 gene influences the biological behavior of a human ovarian cancer cell line. *International Journal of Oncology* **5**, 1065-1071.

Sun, H. Y., Dai, H. Q., Shaik, N. and Elmquist, W. F. (2003). Drug efflux transporters in the CNS. *Advanced Drug Delivery Reviews* **1**, 83-105.

Sun, M. K. (1999). Hypoxia, ischemic stroke, and memory deficits: Prospects for therapy. *Iubmb Life* **4**, 373-378.

Sun, Y. B., Cheung, J. M., Martel-Pelletier, J., Pelletier, J. P., Wenger, L., Altman, R. D., Howell, D. S. and Cheung, H. S. (2000). Wild type and mutant p53 differentially regulate the gene expression of human collagenase-3 (hMMP-13). *Journal of Biological Chemistry* **15**, 11327-11332.

Supuran, C. T. and Scozzafava, A. (2000). Carbonic anhydrase inhibitors: Aromatic sulfonamides and disulfonamides act as efficient tumor growth inhibitors - Part 95. *Journal of Enzyme Inhibition* **6**, 597-610.

Sutter, R., Shakhova, O., Bhagat, H., Behesti, H., Sutter, C., Penkar, S., Santuccione, A., Bernays, R., Heppner, F. L., Schuller, U., Grotzer, M., Moch, H., Schraml, P. and Marino, S. (2010). Cerebellar stem cells act as medulloblastoma-initiating cells in a mouse model and a neural stem cell signature characterizes a subset of human medulloblastomas. *Oncogene* **12**, 1845-1856.

Suva, M. L., Riggi, N., Janiszewska, M., Radovanovic, I., Provero, P., Stehle, J. C., Baumer, K., Le Bitoux, M. A., Marino, D., Cironi, L., Marquez, V. E., Clement, V. and Stamenkovic, I. (2009). EZH2 Is Essential for Glioblastoma Cancer Stem Cell Maintenance. *Cancer Research* **24**, 9211-9218.

Swietach, P., Wigfield, S., Supuran, C. T., Harris, A. L. and Vaughan-Jones, R. D. (2008). Cancer-associated, hypoxia-inducible carbonic anhydrase IX facilitates CO(2) diffusion. *Bju International* 22-24.

Tabori, U., Baskin, B., Shago, M., Alon, N., Taylor, M. D., Ray, P. N., Bouffet, E., Malkin, D. and Hawkins, C. (2010). Universal poor survival in children with medulloblastoma harboring somatic TP53 mutations. *Journal of Clinical Oncology* **8**, 1345-50.

Takagi, M., Absalon, M. J., McLure, K. G. and Kastan, M. B. (2005). Regulation of p53 translation and induction after DNA damage by ribosomal protein L26 and nucleolin. *Cell* **1**, 49-63.

Takata, M., Sasaki, M. S., Sonoda, E., Morrison, C., Hashimoto, M., Utsumi, H., Yamaguchi-Iwai, Y., Shinohara, A. and Takeda, S. (1998). Homologous recombination and non-homologous end-joining pathways of DNA double-strand break repair have overlapping roles in the maintenance of chromosomal integrity in vertebrate cells. *Embo Journal* **18**, 5497-5508.

Takekawa, M., Adachi, M., Nakahata, A., Nakayama, I., Itoh, F., Tsukuda, H., Taya, Y. and Imai, K. (2000). p53-inducible Wip1 phosphatase mediates a negative feedback regulation of p38 MAPK-p53 signaling in response to UV radiation. *Embo Journal* **23**, 6517-6526.

Tan, A. R., Yang, X. W., Hewitt, S. M., Berman, A., Lepper, E. R., Sparreboom, A., Parr, A. L., Figg, W. D., Chow, C., Steinberg, S. M., Bacharach, S. L., Whatley, M., Carrasquillo, J. A., Brahim, J. S., Ettenberg, S. A., Lipkowitz, S. and Swain, S. M. (2004). Evaluation of biologic end points and pharmacokinetics in patients with metastatic breast cancer after treatment with erlotinib, an epidermal growth factor receptor tyrosine kinase inhibitor. *Journal of Clinical Oncology* **15**, 3080-3090.

Tan, E. Y., Yan, M., Campo, L., Han, C., Takano, E., Turley, H., Candiloro, I., Pezzella, F., Gatter, K. C., Millar, E. K. A., O'Toole, S. A., McNeil, C. M., Crea, P., Segara, D., Sutherland, R. L., Harris, A. L. and Fox, S. B. (2009). The key hypoxia regulated gene CAIX is upregulated in basal-like breast tumours and is associated with resistance to chemotherapy. *British Journal of Cancer* **2**, 405-411.

Tanimoto, K., Makino, Y., Pereira, T. and Poellinger, L. (2000). Mechanism of regulation of the hypoxia-inducible factor-l alpha by the von Hippel-Lindau tumor suppressor protein. *Embo Journal* **16**, 4298-4309.

Tauchi, H., Kobayashi, J., Morishima, K., van Gent, D. C., Shiraishi, T., Verkaik, N. S., vanHeems, D., Ito, E., Nakamura, A., Sonodo, E., Takata, M., Takeda, S., Matsuura, S. and Komatsu, K. (2002). Nbs1 is essential for DNA repair by homologous recombination in higher vertebrate cells. *Nature* **6911**, 93-98.

Tavassoli, M., Ruhrberg, C., Beaumont, V., Reynolds, K., Kirkham, N., Collins, W. P. and Farzaneh, F. (1993). Whole Chromosome-17 Loss in Ovarian-Cancer. *Genes Chromosomes & Cancer* **3**, 195-198.

Tavazoie, S. F., Alarcon, C., Oskarsson, T., Padua, D., Wang, Q., Bos, P. D., Gerald, W. L. and Massague, J. (2008). Endogenous human microRNAs that suppress breast cancer metastasis. *Nature* **7175**, 147-52.

Taylor, C. T. and Pouyssegur, J. (2007). Oxygen, hypoxia, and stress. *Stress Responses in Biology and Medicine* 87-94.

Taylor, M. D., Northcott, P. A., Korshunov, A., Remke, M., Cho, Y. J., Clifford, S. C., Eberhart, C. G., Parsons, D. W., Rutkowski, S., Gajjar, A., Ellison, D. W., Lichter, P., Gilbertson, R. J., Pomeroy, S. L., Kool, M. and Pfister, S. M. (2012). Molecular subgroups of medulloblastoma: the current consensus. *Acta Neuropathol* **4**, 465-72.

Taylor, R. E., Bailey, C. C., Robinson, K., Weston, C. L., Ellison, D., Ironside, J., Lucraft, H., Gilbertson, R., Tait, D. M., Walker, D. A., Pizer, B. L., Imeson, J. and Lashford, L. S. (2003). Results of a randomized study of preradiation chemotherapy versus radiotherapy alone for nonmetastatic medulloblastoma: The International Society of Paediatric Oncology United Kingdom Children's Cancer Study Group PNET-3 study. *Journal of Clinical Oncology* **8**, 1581-1591.

Tazawa, H., Tsuchiya, N., Izumiya, M. and Nakagama, H. (2007). Tumor-suppressive miR-34a induces senescence-like growth arrest through modulation of the E2F pathway in human colon cancer cells. *Proc Natl Acad Sci U S A* **39**, 15472-7.

Teicher, B. A. (1994). Hypoxia and drug resistance. *Cancer Metastasis Rev* **2**, 139-68.

Testa, J. R. and Bellacosa, A. (2001). Commentary - AKT plays a central role in tumorigenesis. *Proceedings of the National Academy of Sciences of the United States of America* **20**, 10983-10985.

Thiery, J. P., Acloque, H., Huang, R. Y. J. and Nieto, M. A. (2009). Epithelial-Mesenchymal Transitions in Development and Disease. *Cell* **5**, 871-890.

Thollet, A., Vendrell, J. A., Payen, L., Ghayad, S. E., Ben Larbi, S., Grisard, E., Collins, C., Villedieu, M. and Cohen, P. A. (2010). ZNF217 confers resistance to the pro-apoptotic signals of paclitaxel and aberrant expression of Aurora-A in breast cancer cells. *Molecular Cancer*

Thomas, K. R. and Capecchi, M. R. (1990). Targeted Disruption of the Murine Int-1 Protooncogene Resulting in Severe Abnormalities in Midbrain and Cerebellar Development. *Nature* **6287**, 847-850.

Thompson, C. B. (2009). Metabolic Enzymes as Oncogenes or Tumor Suppressors. *New England Journal of Medicine* **8**, 813-815.

Thompson, L. H. and Schild, D. (2001). Homologous recombinational repair of DNA ensures mammalian chromosome stability. *Mutation Research-Fundamental and Molecular Mechanisms of Mutagenesis* **1-2**, 131-153.

Thompson, M. C., Fuller, C., Hogg, T. L., Dalton, J., Finkelstein, D., Lau, C. C., Chintagumpala, M., Adesina, A., Ashley, D. M., Kellie, S. J., Michael, D. T., Curran, T., Gajjar, A. and Gilbertson, R. J. (2006). Genornics identifies medulloblastoma subgroups that are enriched for specific genetic alterations. *Journal of Clinical Oncology* **12**, 1924-1931.

Thompson, T., Tovar, C., Yang, H., Carvajal, D., Vu, B. T., Xu, Q. L., Wahl, G. M., Heimbrook, D. C. and Vassilev, L. T. (2004). Phosphorylation of p53 on key serines is dispensable for transcriptional activation and apoptosis. *Journal of Biological Chemistry* **51**, 53015-53022.

Thorns, V., Walter, G. F. and Thorns, C. (2003). Expression of MMP-2, MMP-7, MMP-9, MMP-10 and MMP-11 in human astrocytic and oligodendroglial gliomas. *Anticancer Research* **5A**, 3937-3944.

Tian, H. and Cronstein, B. N. (2007). Understanding the mechanisms of action of methotrexate: implications for the treatment of rheumatoid arthritis. *Bull NYU Hosp Jt Dis* **3**, 168-73.

Toledo, F., Krummel, K. A., Lee, C. J., Liu, C. W., Rodewald, L. W., Tang, M. J. and Wahl, G. M. (2006). A mouse p53 mutant lacking the proline-rich domain rescues Mdm4 deficiency and provides insight into the Mdm2-Mdm4-p53 regulatory network. *Cancer Cell* **4**, 273-285.

Toledo, F. and Bardot, B. (2009). Cancer: Three birds with one stone. *Nature* **7254**, 466-7.

Tong, Y., Li, Q. G., Xing, T. Y., Zhang, M., Zhang, J. J. and Xia, Q. (2013). HIF1 regulates WSB-1 expression to promote hypoxia-induced chemoresistance in hepatocellular carcinoma cells. *Febs Letters* **16**, 2530-2535.

Trepel, M., Groscurth, P., Malipiero, U., Gulbins, E., Dichgans, J. and Weller, M. (1998). Chemosensitivity of human malignant glioma: Modulation by p53 gene transfer. *Journal of Neuro-Oncology* **1**, 19-32.

Treszezamsky, A. D., Kachnic, L. A., Feng, Z. H., Zhang, J. R., Tokadjian, C. and Powell, S. N. (2007). BRCA1- and BRCA2-deficient cells are sensitive to etoposide-induced DNA double-strand breaks via topoisomerase II. *Cancer Research* **15**, 7078-7081.

Tribius, S., Pidel, A. and Casper, D. (2001). ATM protein expression correlates with radioresistance in primary glioblastoma cells in culture. *International Journal of Radiation Oncology Biology Physics* **2**, 511-523.

Tsai, Y. P. and Wu, K. J. (2012). Hypoxia-regulated target genes implicated in tumor metastasis. *Journal of Biomedical Science*

Tsang, D. P. F. and Cheng, A. S. L. (2011). Epigenetic regulation of signaling pathways in cancer: Role of the histone methyltransferase EZH2. *Journal of Gastroenterology and Hepatology* **1**, 19-27.

Tsuchiya, S., Okuno, Y. and Tsujimoto, G. (2006). MicroRNA: Biogenetic and functional mechanisms and involvements in cell differentiation and cancer. *Journal of Pharmacological Sciences* **4**, 267-270.

Turner, D. P., Findlay, V. J., Kirven, A. D., Moussa, O. and Watson, D. K. (2008). Global gene expression analysis identifies PDEF transcriptional networks regulating cell migration during cancer progression. *Molecular Biology of the Cell* **9**, 3745-3757.

Tutt, A., Gabriel, A., Bertwistle, D., Connor, F., Paterson, H., Peacock, J., Ross, G. and Ashworth, A. (1999). Absence of Brca2 causes genome instability by chromosome breakage and loss associated with centrosome amplification. *Current Biology* **19**, 1107-1110.

Tuzi, N. L., Venter, D. J., Kumar, S., Staddon, S. L., Lemoine, N. R. and Gullick, W. J. (1991). Expression of Growth-Factor Receptors in Human Brain-Tumors. *British Journal of Cancer* **2**, 227-233.

Um, J. H., Kang, C. D., Bae, J. H., Shin, G. G., Kim, D. W., Kim, D. W., Chung, B. S. and Kim, S. H. (2004). Association of DNA-dependent protein kinase with hypoxia inducible factor-1 and its implication in resistance to anticancer drugs in hypoxic tumor cells. *Experimental and Molecular Medicine* **3**, 233-242.

Uniacke, J., Holterman, C. E., Lachance, G., Franovic, A., Jacob, M. D., Fabian, M. R., Payette, J., Holcik, M., Pause, A. and Lee, S. (2012). An oxygen-regulated switch in the protein synthesis machinery. *Nature* **7401**, 126-U154.

Uziel, T., Karginov, F. V., Xie, S. Q., Parker, J. S., Wang, Y. D., Gajjar, A., He, L., Ellison, D., Gilbertson, R. J., Hannon, G. and Roussel, M. F. (2009). The miR-17 similar to 92 cluster collaborates with the Sonic Hedgehog pathway in medulloblastoma. *Proceedings of the National Academy of Sciences of the United States of America* **8**, 2812-2817.

van Gent, D. C. and van der Burg, M. (2007). Non-homologous end-joining, a sticky affair. *Oncogene* **56**, 7731-40.

van Zijl, F., Krupitza, G. and Mikulits, W. (2011). Initial steps of metastasis: Cell invasion and endothelial transmigration. *Mutation Research-Reviews in Mutation Research* **1-2**, 23-34.

Vanankeren, S. C., Murray, D. and Meyn, R. E. (1988). Induction and Rejoining of Gamma-Ray-Induced DNA Single-Strand and Double-Strand Breaks in Chinese-Hamster Aa8 Cells and in 2 Radiosensitive Clones. *Radiation Research* **3**, 511-525.

Vara, J. A. F., Casado, E., de Castro, J., Cejas, P., Belda-Iniesta, C. and Gonzalez-Baron, M. (2004). PI3K/Akt signalling pathway and cancer. *Cancer Treatment Reviews* **2**, 193-204.

Varon, R., Reis, A., Henze, G., Von Einsiedel, H. G., Sperling, K. and Seeger, K. (2001). Mutations in the Nijmegen Breakage Syndrome gene (NBS1) in childhood acute lymphoblastic leukemia (ALL). *Cancer Research* **9**, 3570-3572.

Vasseur, S., Hoffmeister, A., Garcia-Montero, A., Mallo, G. V., Feil, R., Kuhbandner, S., Dagorn, J. C. and Iovanna, J. L. (2002). p8-deficient fibroblasts grow more rapidly and are more resistant to adriamycin-induced apoptosis. *Oncogene* **11**, 1685-1694.

Vaziri, H., Dessain, S. K., Eagon, E. N., Imai, S. I., Frye, R. A., Pandita, T. K., Guarente, L. and Weinberg, R. A. (2001). hSIR2(SIRT1) functions as an NAD-dependent p53 deacetylase. *Cell* **2**, 149-159.

Veikkola, T. and Alitalo, K. (1999). VEGFs, receptors and angiogenesis. *Seminars in Cancer Biology* **3**, 211-220.

Vendrell, J. A., Thollet, A., Nguyen, N. T., Ghayad, S. E., Vinot, S., Bieche, I., Grisard, E., Josserand, V., Coll, J. L., Roux, P., Corbo, L., Treilleux, I., Rimokh, R. and Cohen, P. A. (2012). ZNF217 Is a Marker of Poor Prognosis in Breast Cancer That Drives Epithelial-Mesenchymal Transition and Invasion. *Cancer Research* **14**, 3593-3606.

Venkitaraman, A. R. (2002). Cancer susceptibility and the functions of BRCA1 and BRCA2. *Cell* **2**, 171-182.

Verhaak, R. G., Hoadley, K. A., Purdom, E., Wang, V., Qi, Y., Wilkerson, M. D., Miller, C. R., Ding, L., Golub, T., Mesirov, J. P., Alexe, G., Lawrence, M., O'Kelly, M., Tamayo, P., Weir, B. A., Gabriel, S., Winckler, W., Gupta, S., Jakkula, L., Feiler, H. S., Hodgson, J. G., James, C. D., Sarkaria, J. N., Brennan, C., Kahn, A., Spellman, P. T., Wilson, R. K., Speed, T. P., Gray, J. W., Meyerson, M., Getz, G., Perou, C. M., Hayes, D. N. and Cancer Genome Atlas Research, N. (2010). Integrated genomic analysis identifies clinically relevant subtypes of glioblastoma characterized by abnormalities in PDGFRA, IDH1, EGFR, and NF1. *Cancer Cell* **1**, 98-110.

Vivanco, I. and Sawyers, C. L. (2002). The phosphatidylinositol 3-kinase-AKT pathway in human cancer. *Nature Reviews Cancer* **7**, 489-501.

Vogelstein, B., Lane, D. and Levine, A. J. (2000). Surfing the p53 network. *Nature* **6810**, 307-10.

Volinia, S., Calin, G. A., Liu, C. G., Ambs, S., Cimmino, A., Petrocca, F., Visone, R., Iorio, M., Roldo, C., Ferracin, M., Prueitt, R. L., Yanaihara, N., Lanza, G., Scarpa, A., Vecchione, A., Negrini, M., Harris, C. C. and Croce, C. M. (2006). A microRNA expression signature of human solid tumors defines cancer gene targets. *Proceedings of the National Academy of Sciences of the United States of America* **7**, 2257-2261.

Volk, E. L., Farley, K. M., Wu, Y., Li, F., Robey, R. W. and Schneider, E. (2002). Overexpression of wild-type breast cancer resistance protein mediates methotrexate resistance. *Cancer Research* **17**, 5035-5040.

Volpert, O. V., Dameron, K. M. and Bouck, N. (1997). Sequential development of an angiogenic phenotype by human fibroblasts progressing to tumorigenicity. *Oncogene* **12**, 1495-1502.

Walker, J. R., Corpina, R. A. and Goldberg, J. (2001). Structure of the Ku heterodimer bound to DNA and its implications for double-strand break repair. *Nature* **6847**, 607-14.

Wanami, L. S., Chen, H. Y., Peiro, S., Garcia de Herreros, A. and Bachelder, R. E. (2008). Vascular endothelial growth factor-A stimulates Snail expression in breast tumor cells: implications for tumor progression. *Exp Cell Res* **13**, 2448-53.

Wang, G. L., Jiang, B. H., Rue, E. A. and Semenza, G. L. (1995). Hypoxia-Inducible Factor-1 Is a Basic-Helix-Loop-Helix-Pas Heterodimer Regulated by Cellular O-2 Tension. *Proceedings of the National Academy of Sciences of the United States of America* **12**, 5510-5514.

Wang, J. and Lenardo, M. J. (2000). Roles of caspases in apoptosis, development, and cytokine maturation revealed by homozygous gene deficiencies. *Journal of Cell Science* **5**, 753-757.

Wang, Z. P., Bhattacharya, N., Mixter, P. F., Wei, W. Y., Sedivy, J. and Magnuson, N. S. (2002). Phosphorylation of the cell cycle inhibitor p21(Cip1/WAF1) by Pim-1 kinase. *Biochimica Et Biophysica Acta-Molecular Cell Research* **1**, 45-55.

Warburg, O. (1930). Note on the metabolism of tumours. *Biochemische Zeitschrift* 257-258.

Warburg, O. (1956a). Respiratory Impairment in Cancer Cells. *Science* **3215**, 269-270.

Warburg, O. (1956b). Origin of Cancer Cells. *Science* **3191**, 309-314.

Watanabe, T., Nobusawa, S., Lu, S., Huang, J., Mittelbronn, M. and Ohgaki, H. (2009). Mutational inactivation of the nijmegen breakage syndrome gene (NBS1) in glioblastomas is associated with multiple TP53 mutations. *J Neuropathol Exp Neurol* **2**, 210-5.

Wattel, E., Preudhomme, C., Hecquet, B., Vanrumbeke, M., Quesnel, B., Dervite, I., Morel, P. and Fenaux, P. (1994). P53 Mutations Are Associated with Resistance to Chemotherapy and Short Survival in Hematologic Malignancies. *Blood* **9**, 3148-3157.

Weemaes, C. M. R., Hustinx, T. W. J., Scheres, J. M. J. C., Vanmunster, P. J. J., Bakkeren, J. A. J. M. and Taalman, R. D. F. M. (1981). A New Chromosomal Instability Disorder - the Nijmegen Breakage Syndrome. *Acta Paediatrica Scandinavica* **4**, 557-564.

Weeraratne, S. D., Amani, V., Neiss, A., Teider, N., Scott, D. K., Pomeroy, S. L. and Cho, Y. J. (2011). miR-34a confers chemosensitivity through modulation of MAGE-A and p53 in medulloblastoma. *Neuro-Oncology* **2**, 165-175.

Wei, C. L., Wu, Q., Vega, V. B., Chiu, K. P., Ng, P., Zhang, T., Shahab, A., Yong, H. C., Fu, Y. T., Weng, Z. P., Liu, J. J., Zhao, X. D., Chew, J. L., Lee, Y. L., Kuznetsov, V. A., Sung, W. K., Miller, L. D., Lim, B., Liu, E. T., Yu, Q., Ng, H. H. and Ruan, Y. J. (2006). A global map of p53 transcription-factor binding sites in the human genome. *Cell* **1**, 207-219.

Wei, J. S., Song, Y. K., Durinck, S., Chen, Q. R., Cheuk, A. T., Tsang, P., Zhang, Q., Thiele, C. J., Slack, A., Shohet, J. and Khan, J. (2008). The MYCN oncogene is a direct target of miR-34a. *Oncogene* **39**, 5204-13.

Weidemann, A. and Johnson, R. S. (2008). Biology of HIF-1 alpha. *Cell Death and Differentiation* **4**, 621-627.

Weinberg, R. A. (1991). Tumor Suppressor Genes. *Science* **5035**, 1138-1146.

Welch, C., Chen, Y. and Stallings, R. L. (2007). MicroRNA-34a functions as a potential tumor suppressor by inducing apoptosis in neuroblastoma cells. *Oncogene* **34**, 5017-22.

Wen, J., Park, J. Y., Park, K. H., Chung, H. W., Bang, S., Park, S. W. and Song, S. Y. (2010). Oct4 and Nanog Expression Is Associated With Early Stages of Pancreatic Carcinogenesis. *Pancreas* **5**, 622-626.

Wenger, R. H., Camenisch, G., Desbaillets, I., Chilov, D. and Gassmann, M. (1998). Up-regulation of hypoxia-inducible factor-1 alpha is not sufficient for hypoxic/anoxic p53 induction. *Cancer Research* **24**, 5678-5680.

Wenger, R. H. (2002). Cellular adaptation to hypoxia: O-2-sensing protein hydroxylases, hypoxia-inducible transcription factors, and O-2-regulated gene expression. *Faseb Journal* **10**,

Wenger, R. H., Stiehl, D. P. and Camenisch, G. (2005). Integration of oxygen signaling at the consensus HRE. *Sci STKE* **306**, re12.

Weterings, E. and Chen, D. J. (2008). The endless tale of non-homologous end-joining. *Cell Res* **1**, 114-24.

Wiener, L., Feola, M., Templeton, J. Y., 3rd, Hamarman, H. M. and Venkataswamy, A. R. (1976). Monitoring tissue oxygenation of the heart after myocardial revascularization. *Am J Cardiol* **1**, 38-45.

Williams, A. C., Collard, T. J. and Paraskeva, C. (1999). An acidic environment leads to p53 dependent induction of apoptosis in human adenoma and carcinoma cell lines: implications for clonal selection during colorectal carcinogenesis. *Oncogene* **21**, 3199-3204.

Wong, A. K. C., Pero, R., Ormonde, P. A., Tavtigian, S. V. and Bartel, P. L. (1997). RAD51 interacts with the evolutionarily conserved BRC motifs in the human breast cancer susceptibility gene brca2. *Journal of Biological Chemistry* **51**, 31941-31944.

Wong, S. and Weber, J. D. (2007). Deacetylation of the retinoblastoma tumour suppressor protein by SIRT1. *Biochemical Journal* 451-460.

Woodburn, R. T., Azzarelli, B., Montebello, J. F. and Goss, I. E. (2001). Intense p53 staining is a valuable prognostic indicator for poor prognosis in medulloblastoma/central nervous system primitive neuroectodermal tumors. *Journal of Neuro-Oncology* **1**, 57-62.

Wouters, B. G., van den Beucken, T., Magagnin, M. G., Lambin, P. and Koumenis, C. (2004). Targeting hypoxia tolerance in cancer. *Drug Resistance Updates* **1**, 25-40.

Wu, X., Bayle, J. H., Olson, D. and Levine, A. J. (1993). The p53-mdm-2 autoregulatory feedback loop. *Genes Dev* **7A**, 1126-32.

Wykoff, C. C., Beasley, N. J. P., Watson, P. H., Turner, K. J., Pastorek, J., Sibtain, A., Wilson, G. D., Turley, H., Talks, K. L., Maxwell, P. H., Pugh, C. W., Ratcliffe, P. J. and Harris, A. L. (2000a). Hypoxia-inducible expression of tumor-associated carbonic anhydrases. *Cancer Research* **24**, 7075-7083.

Wykoff, C. C., Pugh, C. W., Maxwell, P. H., Harris, A. L. and Ratcliffe, P. J. (2000b). Identification of novel hypoxia dependent and independent target genes of the von Hippel-Lindau (VHL) tumour suppressor by mRNA differential expression profiling. *Oncogene* **54**, 6297-6305.

Xia, S., Yu, S. Y., Yuan, X. L. and Xu, S. P. (2004). [Effects of hypoxia on expression of P-glycoprotein and multidrug resistance protein in human lung adenocarcinoma A549 cell line]. *Zhonghua Yi Xue Za Zhi* **8**, 663-6.

Xie, X. H., Lu, J., Kulbokas, E. J., Golub, T. R., Mootha, V., Lindblad-Toh, K., Lander, E. S. and Kellis, M. (2005). Systematic discovery of regulatory motifs in human promoters and 3 ' UTRs by comparison of several mammals. *Nature* **7031**, 338-345.

Xu, J., Reumers, J., Couceiro, J. R., De Smet, F., Gallardo, R., Rudyak, S., Cornelis, A., Rozenski, J., Zwolinska, A., Marine, J. C., Lambrechts, D., Suh, Y. A., Rousseau, F. and Schymkowitz, J. (2011). Gain of function of mutant p53 by coaggregation with multiple tumor suppressors. *Nature Chemical Biology* **5**, 285-295.

Xu, J. S., Liu, Z. H. and Ornitz, D. M. (2000). Temporal and spatial gradients of Fgf8 and Fgf17 regulate proliferation and differentiation of midline cerebellar structures. *Development* **9**, 1833-1843.

Yamakuchi, M., Ferlito, M. and Lowenstein, C. J. (2008). miR-34a repression of SIRT1 regulates apoptosis. *Proc Natl Acad Sci U S A* **36**, 13421-6.

Yamakuchi, M. and Lowenstein, C. J. (2009). MiR-34, SIRT1 and p53: the feedback loop. *Cell Cycle* **5**, 712-5.

Yan, H., Parsons, D. W., Jin, G., McLendon, R., Rasheed, B. A., Yuan, W., Kos, I., Batinic-Haberle, I., Jones, S., Riggins, G. J., Friedman, H., Friedman, A., Reardon, D., Herndon, J., Kinzler, K. W., Velculescu, V. E., Vogelstein, B. and Bigner, D. D. (2009). IDH1 and IDH2 mutations in gliomas. *N Engl J Med* **8**, 765-73.

Yanaihara, N., Caplen, N., Bowman, E., Seike, M., Kumamoto, K., Yi, M., Stephens, R. M., Okamoto, A., Yokota, J., Tanaka, T., Colin, G. A., Liu, C. G., Croce, C. M. and Harris, C. C. (2006). Unique microRNA molecular profiles in lung cancer diagnosis and prognosis. *Cancer Cell* **3**, 189-198.

Yang, A. D., Camp, E. R., Fan, F., Shen, L., Gray, M. J., Liu, W., Somcio, R., Bauer, T. W., Wu, Y., Hicklin, D. J. and Ellis, L. M. (2006). Vascular endothelial growth factor receptor-1 activation mediates epithelial to mesenchymal transition in human pancreatic carcinoma cells. *Cancer Res* **1**, 46-51.

Yang, F., Van Meter, T. E., Buettner, R., Hedvat, M., Liang, W., Kowolik, C. M., Mepani, N., Mirosevich, J., Nam, S., Chen, M. Y., Tye, G., Kirschbaum, M. and Jove, R. (2008). Sorafenib inhibits signal transducer and activator of transcription 3 signaling associated with growth arrest and apoptosis of medulloblastomas. *Molecular Cancer Therapeutics* **11**, 3519-3526.

Yang, M. H., Chiang, W. C., Chou, T. Y., Chang, S. Y., Chen, P. M., Teng, S. C. and Wu, K. J. (2006). Increased NBS1 expression is a marker of aggressive head and neck cancer and overexpression of NBS1 contributes to transformation. *Clinical Cancer Research* **2**, 507-515.

Yang, X. (2003). Regulation of p53 responses by post-translational modifications. *Cell Death and Differentiation* **4**, 400-403.

Yannone, S. M., Khan, I. S., Zhou, R. Z., Zhou, T., Valerie, K. and Povirk, L. F. (2008). Coordinate 5' and 3' endonucleolytic trimming of terminally blocked blunt DNA double-strand break ends by Artemis nuclease and DNA-dependent protein kinase. *Nucleic Acids Res* **10**, 3354-65.

Yi, R., Qin, Y., Macara, I. G. and Cullen, B. R. (2003). Exportin-5 mediates the nuclear export of pre-microRNAs and short hairpin RNAs. *Genes & Development* **24**, 3011-3016.

Yokota, N., Nishizawa, S., Ohta, S., Date, H., Sugimura, H., Namba, H. and Maekawa, M. (2002). Role of Wnt pathway in medulloblastoma oncogenesis. *International Journal of Cancer* **2**, 198-201.

Yuan, X., Curtin, J., Xiong, Y., Liu, G., Waschsmann-Hogiu, S., Farkas, D. L., Black, K. L. and Yu, J. S. (2004). Isolation of cancer stem cells from adult glioblastoma multiforme. *Oncogene* **58**, 9392-400.

Zagzag, D., Zhong, H., Scalzitti, J. M., Laughner, E., Simons, J. W. and Semenza, G. L. (2000). Expression of hypoxia-inducible factor 1 alpha in brain tumors - Association with angiogenesis, invasion, and progression. *Cancer* **11**, 2606-2618.

Zenz, T., Mohr, J., Eldering, E., Kater, A. P., Buhler, A., Kienle, D., Winkler, D., Durig, J., van Oers, M. H. J., Mertens, D., Dohner, H. and Stilgenbauer, S. (2009). miR-34a as part of the resistance network in chronic lymphocytic leukemia. *Blood* **16**, 3801-3808.

Zhang, H., Bosch-Marce, M., Shimoda, L. A., Tan, Y. S., Baek, J. H., Wesley, J. B., Gonzalez, F. J. and Semenza, G. L. (2008). Mitochondrial autophagy is an HIF-1-dependent adaptive metabolic response to hypoxia. *J Biol Chem* **16**, 10892-903.

Zhang, H., Wong, C. C. L., Wei, H., Gilkes, D. M., Korangath, P., Chaturvedi, P., Schito, L., Chen, J., Krishnamachary, B., Winnard, P. T., Raman, V., Zhen, L., Mitzner, W. A., Sukumar, S. and Semenza, G. L. (2012). HIF-1-dependent expression of angiopoietin-like 4 and L1CAM mediates vascular metastasis of hypoxic breast cancer cells to the lungs. *Oncogene* **14**, 1757-1770.

Zhu, H., Chen, X. P., Luo, S. F., Guan, J., Zhang, W. G. and Zhang, B. X. (2005). Involvement of hypoxia-inducible factor-1-alpha in multidrug resistance induced by hypoxia in HepG2 cells. *Journal of Experimental & Clinical Cancer Research* **4**, 565-574.

Zhukova, N., Ramaswamy, V., Remke, M., Pfaff, E., Shih, D. J., Martin, D. C., Castelo-Branco, P., Baskin, B., Ray, P. N., Bouffet, E., von Bueren, A. O., Jones, D. T., Northcott, P. A., Kool, M., Sturm, D., Pugh, T. J., Pomeroy, S. L., Cho, Y. J., Pietsch, T., Gessi, M., Rutkowski, S., Bognar, L., Klekner, A., Cho, B. K., Kim, S. K., Wang, K. C., Eberhart, C. G., Fevre-Montange, M., Fouladi, M., French, P. J., Kros, M., Grajkowska, W. A., Gupta, N., Weiss, W. A., Hauser, P., Jabado, N., Jouvet, A., Jung, S., Kumabe, T., Lach, B., Leonard, J. R., Rubin, J. B., Liau, L. M., Massimi, L., Pollack, I. F., Shin Ra, Y., Van Meir, E. G., Zitterbart, K., Schuller, U., Hill, R. M., Lindsey, J. C., Schwalbe, E. C., Bailey, S., Ellison, D. W., Hawkins, C., Malkin, D., Clifford, S. C., Korshunov, A., Pfister, S., Taylor, M. D. and Tabori, U. (2013). Subgroup-specific prognostic implications of TP53 mutation in medulloblastoma. *Journal of Clinical Oncology* **23**, 2927-35.

Zinkernagel, A. S., Johnson, R. S. and Nizet, V. (2007). Hypoxia inducible factor (HIF) function in innate immunity and infection. *Journal of Molecular Medicine-Jmm* **12**, 1339-1346.

Zou, J., Li, P., Lu, F., Liu, N., Dai, J. J., Ye, J. J., Qu, X., Sun, X. L., Ma, D. X., Park, J. and Ji, C. Y. (2013). Notch1 is required for hypoxia-induced proliferation, invasion and chemoresistance of T-cell acute lymphoblastic leukemia cells. *Journal of Hematology & Oncology*

Zurawel, R. H., Allen, C., Wechsler-Reya, R., Scott, M. P. and Raffel, C. (2000). Evidence that haploinsufficiency of Ptch leads to medulloblastoma in mice. *Genes Chromosomes & Cancer* **1**, 77-81.

Appendix

1.1 Significant transcripts analysis on MatLAB

The following coding is for selecting significantly expressed transcripts.

Additional functions including: profile searches, kmeans clustering and hierarchy clustering.

MATLAB CODES:

```
function                                          cfrunwithprofileID
(fulldata,allgenenames,alltranscriptsIDs)



%%%%%%%%%%%%%%%%%%%%%%%%%%%%%%%%%%%%%%%%%%%%%%%%%%%%%%%%%%%%%%%%%%%%
%%%

% This bit sets up the microarray analysis, reading in data
and setting up
% any empty vectors or matrices that need to be defined.

%%%%%%%%%%%%%%%%%%%%%%%%%%%%%%%%%%%%%%%%%%%%%%%%%%%%%%%%%%%%%%%%%%%%
%%%



includeborderlinetranscripts = 1;   % =1 if you want to allow
borderline transcripts

clusteranalysis = 1;              % =1 to carry out a cluster
analysis

profilesearch = 1;    % =1 to search for a specific profile

profile = [0,1,0,0];  % the specific profile to search for



%%%%%%%%%%%%%%%%%%%%%%%%%%%%%%%%%%%%%%%%%%%%%%%%%%%%%%%%%%%%%%%%%%%%
%%%

probes = 3;      % there are three probes for every transcripts
```

```
p = fulldata;   % This reads in the input matrix to the p data
matrix

datalength = length(p(:,1));  % this works out how many data
points there are


a = 2;  %this will start the analysis at row 2 (row 1 in title
is the time points header)


number_of_sig_transcripts = (datalength-1)/probes; % works out
how many transcripts to be tested


time_points = 4; % tells us for how many time points the
experiment covered

time = [0 6 64 96]; % lets us know the time points of the
experiment


count = 0;  % starts the count of expressed transcript at zero

bordercount = 0; % starts the count for borderline transcript
at zero


results = [];  % sets up the results matrix for any transcript
which are found

               % to be significantly different in stats test

borderresults = []; % sets up the same for borderline
transcript



probevec1 = zeros(3,1); % empty vector for all 12 transcript
measurements of T0

probevec2 = zeros(3,1); % empty vector for all 12 transcript
measurements of T6

probevec3 = zeros(3,1); % empty vector for all 12 transcript
measurements of T64

probevec4 = zeros(3,1); % empty vector for all 12 transcript
measurements of T96

anovamatrix = zeros(3,4);   % empty matrix to store above
vectors


vec1 = zeros(9,1); % empty vector for all 12 gene measurements
of T0

vec2 = zeros(9,1); % empty vector for all 12 gene measurements
of T6
```

```
vec3 = zeros(9,1); % empty vector for all 12 gene measurements
of T64
vec4 = zeros(9,1); % empty vector for all 12 gene measurements
of T96



sigtranscriptresults = []; % used to store profiles for
expressing transcript
borderlinetranscripresults = [];



%%%%%%%%%%%%%%%%%%%%%%%%%%%%%%%%%%%%%%%%%%%%%%%%%%%%%%%%%%%%%%%%%%%%%%%
%%%%
% this section does the actual analysis to see if a transcript
expression
% profile shows significant change over time
%


for i = 1:number_of_sig_transcripts


% This bit reads in the data for each time point into a vector
% this is then placed in the matrix anova matrix read for
stats test



%%%
%%% PROBE 1 %%%%%%%%%%%%%%%%%%%%%%%%%%
%%%
    probevec1(1:3) = p(a,1:3);
    probevec2(1:3) = p(a,4:6);
    probevec3(1:3) = p(a,7:9);
    probevec4(1:3) = p(a,10:12);

    anovamatrix(:,1) = probevec1;
    anovamatrix(:,2) = probevec2;
    anovamatrix(:,3) = probevec3;
    anovamatrix(:,4) = probevec4;



% gets the p value of above profiles for probe 1
```

```
    pvalue1 = anova1(log2(anovamatrix),[],'off');



%%%
%%% PROBE 2 %%%%%%%%%%%%%%%%%%%%%%%%%%
%%%
    probevec1(1:3) = p(a+1,1:3);
    probevec2(1:3) = p(a+1,4:6);
    probevec3(1:3) = p(a+1,7:9);
    probevec4(1:3) = p(a+1,10:12);

    anovamatrix(:,1) = probevec1;
    anovamatrix(:,2) = probevec2;
    anovamatrix(:,3) = probevec3;
    anovamatrix(:,4) = probevec4;


% gets the p value of above profiles for probe 1

    pvalue2 = anova1(log2(anovamatrix),[],'off');



%%%
%%% PROBE 3 %%%%%%%%%%%%%%%%%%%%%%%%%%
%%%
    probevec1(1:3) = p(a+2,1:3);
    probevec2(1:3) = p(a+2,4:6);
    probevec3(1:3) = p(a+2,7:9);
    probevec4(1:3) = p(a+2,10:12);

    anovamatrix(:,1) = probevec1;
    anovamatrix(:,2) = probevec2;
    anovamatrix(:,3) = probevec3;
    anovamatrix(:,4) = probevec4;
```

```
% gets the p value of above profiles for probe 1

    pvalue3 = anova1(log2(anovamatrix),[],'off');




%%%%%%%%%%%%%%%%%%%%%%%%%%%%%%%%%%%%%%%%%%%%%%%%%%%%%%%%%%%%%%%%%%%%%%%
%%%%
%
% This next bit records those genes which have a low p value
in the matrix
% results.    It also counts how many transcripts are
significant and records
% their names.  Change the p value below for a different level
of significance



    if pvalue1 < 0.01 && pvalue2 < 0.01 && pvalue3 < 0.01

        vec1(1:9) = [p(a,1:3),p(a+1,1:3),p(a+2,1:3)];
        vec2(1:9) = [p(a,4:6),p(a+1,4:6),p(a+2,4:6)];
        vec3(1:9) = [p(a,7:9),p(a+1,7:9),p(a+2,7:9)];
        vec4(1:9) = [p(a,10:12),p(a+1,10:12),p(a+2,10:12)];

       count = count+1;
       sigtranscript(count) = allgenenames(a-1);
       sigtranscript2(count) = alltranscriptsIDs(a-1);



%%% Delete as appropriate below to use either mean or median
for
%%% expression values of a transcript at a particular time
point

      results(count,:)                                          =
log2([mean(vec1),mean(vec2),mean(vec3),mean(vec4)]);
      rawresults(count,:)                                       =
[mean(vec1),mean(vec2),mean(vec3),mean(vec4)];
```

```
    end



%%%
%%% This next section tests for transcripts which may express
but have one faulty
%%% probe.  The expression criteria is change from 0.01 to
0.001 but this
%%% time only 2 of the 3 probes have to pass the condition
%%%
%%%


if includeborderlinetranscripts == 1;


    pvaluevec = [pvalue1 pvalue2 pvalue3];


    if min(pvaluevec) < 0.01 && median(pvaluevec) < 0.01 &&
max(pvaluevec) > 0.01


        bordercount = bordercount +1 ;


        vec1(1:9) = [p(a,1:3),p(a+1,1:3),p(a+2,1:3)];
        vec2(1:9) = [p(a,4:6),p(a+1,4:6),p(a+2,4:6)];
        vec3(1:9) = [p(a,7:9),p(a+1,7:9),p(a+2,7:9)];
        vec4(1:9) = [p(a,10:12),p(a+1,10:12),p(a+2,10:12)];


       count = count+1;
       sigtranscript(count) = allgenenames(a-1);
       sigtranscript2(count) = alltranscriptsIDs(a-1);
       bordertranscript(bordercount) = allgenenames(a-1);




%%% Delete as appropriate below to use either mean or median
for
%%% expression values of a transcript at a particular time
point


      results(count,:)                                    =
log2([mean(vec1),mean(vec2),mean(vec3),mean(vec4)]);
```

```
      borderresults(bordercount,:)                                  =
log2([mean(vec1),mean(vec2),mean(vec3),mean(vec4)]);

      rawresults(count,:)                                           =
[mean(vec1),mean(vec2),mean(vec3),mean(vec4)];


    end


end


%%%%%%%%%%%%%%%%%%%%%%%%%%%%%%%%%%%%%%%%%%%%%%%%%%%%%%%%%%%%%%
%%%%%%%%%%%%%%%%%




    a=a+3;   % the analysis for this gene is done, we move a
along 3 for next gene



end



%%%%%%%%%%%%%%%%%%%%%%%%%%%%%%%%%%%%%%%%%%%%%%%%%%%%%%%%%%%%%%
%%%%%%%%%%%%%%%%%

%

% We now have all expressing transcripts.  The next section
filters out only

% those transcripts which show a satisfactory level of
expression

%

%%%%%%%%%%%%%%%%%%%%%%%%%%%%%%%%%%%%%%%%%%%%%%%%%%%%%%%%%%%%%%
%%%%%%%%%%%%%%%%%

%


expressingcount = 0; % initially no transcripts are said to be
expressing


minfoldchange = 1; % This is the minimum required fold change
for a

                   % significant transcript to be called an
expressing transcript
```

```
                    % (1 relates to a 2fold change on log2
scale)



% Below we go through each significant transcript profile from
results matrix

% and get the min and max.  the ratio between these has to be
greater than

% the minimum fold change to be included in the
expressingresults matrix

% which holds the profiles for all expressing transcript.


for j = 1:length(results(:,1))


    minimum = min(results(j,:));   % gets max expression of
transcript

    maximum = max(results(j,:));   % gets min expression of
transcript


    change = maximum - minimum;    % works out the ratio



% this bit stores those gene names that meet the condition in

% expressinggenes and the corresponding profile in expressing
results.  The

% count also moves up by 1.


    if change > minfoldchange


       expressingcount = expressingcount +1;


       sigtranscriptresults(expressingcount,:) = results(j,:);

       rawexpressingresults(expressingcount,:)                =
rawresults(j,:);



       expressinggenes(expressingcount) = sigtranscript(j);

       expressinggenes2(expressingcount) = sigtranscript2(j);


    end
```

```
end




if includeborderlinetranscripts == 1

borderexpressingcount = 0;

for q = 1:length(borderresults(:,1))

    minimum = min(borderresults(q,:));   % gets max expression
of transcript
    maximum = max(borderresults(q,:));   % gets min expression
of transcript

    change = maximum -minimum;    % works out the ratio



% this bit stores those gene names that meet the condition in
% expressinggenes and the corresponding profile in expressing
results.  The
% count also moves up by 1.

    if change > minfoldchange

       borderexpressingcount = borderexpressingcount +1;

       borderlinetranscripresults(borderexpressingcount,:)    =
borderresults(q,:);

       borderexpressinggenes(borderexpressingcount)           =
bordertranscript(q);
```

```
    end



end


end



%%%%%%%%%%%%%%%%%%%%%%%%%%%%%%%%%%%%%%%%%%%%%%%%%%%%%%%%%%%%%%%%%
%%%%%%%%%%%%%%%%%
%
% We now have all that we need to say that a transcript is
expressed by a given
% fold change, and that it has already been found to change
over time to a
% satisfactory p value.
%
% This section is optional and can be commented out.  It takes
a specific
% profile and looks at each expressed gene for any which match
the criteria.
%
% for example the profile [0,0,0,1] looks for any transcript
which only
% express at the last time point when compared to T0.
%
%%%%%%%%%%%%%%%%%%%%%%%%%%%%%%%%%%%%%%%%%%%%%%%%%%%%%%%%%%%%%%%%%
%%%%%%%%%%%%%%%%%
% %
% %
% %

if profilesearch == 1
```

```
profilecount = 0;       % intially zero as before

for k = 1:length(sigtranscriptresults(:,1))

% we set each time pont to zero first and then work out the
normalised values

    binary_results = [0,0,0,0];

    normalised_profile(1:4)   =   sigtranscriptresults(k,:)   -
sigtranscriptresults(k,1);



    % following this we go through each time point and if a
particular time
    % point meets the condition then we change it to a 1

    for l = 1:time_points

        if (normalised_profile(l))>minfoldchange

            binary_results(l) = 1;

        end

         if (normalised_profile(l))< -1*(minfoldchange)

            binary_results(l) = -1;

        end


    end


    % We now compare a genes binary profile to the desired
profile
    % if they match we save the transcript name in
profileexpressinggenes and we
```

```
    % move the count up by 1

        if binary_results(1:4) == profile(1:4)

        profilecount = profilecount+1;

        profileexpressinggenes(profilecount)                    =
expressinggenes(k);
        profileexpressingIDs(profilecount)                      =
expressinggenes2(k);
        end

end



if profilecount >0

profilecount
dlmwrite('Matching_Profile_Expressed_Genes_Names.txt',char(pro
fileexpressinggenes),'')
dlmwrite('Matching_Profile_Expressed_transcript_IDs.txt',char(
profileexpressingIDs),'')

end

end

% %
% %
%%%%%%%%%%%%%%%%%%%%%%%%%%%%%%%%%%%%%%%%%%%%%%%%%%%%%%%%%%%%%%%%%%%%%%%%
%%%%%%%%%%%%%%%%%
%
%
% Now all the analysis is done and we just need to return the
desired
% aspects of the analysis.
%
% Below we print out to screen the number of sig transcript
(count) and the
```

```
% number of expressing transcript (expressinggenes).  We also
write to file a
% text file of all expressing genes as well as the profiles
associated with
% each.
%
% Note that for particular profiles, if the above section is
uncommented
% then these gene names too are written to file and the count
is printed to
% the screen
%
%%%%%%%%%%%%%%%%%%%%%%%%%%%%%%%%%%%%%%%%%%%%%%%%%%%%%%%%%%%%%%%%%
%%%%%%%%%%%%%%%%%
%
%
%
%
%
%%%%%%%%%%%%%%%%%%%%%%%%%%%%%%%%%%%%%%%%%%%%%%%%%%%%%%%%%%%%%%%%%
%%%%%%%%%%%%%%%%%

if clusteranalysis == 1

    normalisedexpressingresults = [];

% % %     for d = 1:length(rawexpressingresults(:,1))
%    %    %                                  mean_expression    =
mean(rawexpressingresults(d,:));
%   %   %                        normalisedexpressingresults(d,:)   =
[(rawexpressingresults(d,1)/mean_expression)
(rawexpressingresults(d,2)/mean_expression)
(rawexpressingresults(d,3)/mean_expression)
(rawexpressingresults(d,4)/mean_expression)
(rawexpressingresults(d,5)/mean_expression)];
% % %     end

    for d = 1:length(sigtranscriptresults(:,1))
    mean_expression = mean(sigtranscriptresults(d,:));
    normalisedexpressingresults(d,:)                               =
[(sigtranscriptresults(d,1)/mean_expression)
(sigtranscriptresults(d,2)/mean_expression)
```

```
(sigtranscriptresults(d,3)/mean_expression)
(sigtranscriptresults(d,4)/mean_expression)];
    end




% % %     %%%
% % %     %%% heirarchal clustering
% % %     %%%
% % %
%       %       %                                   corrdist      =
pdist(normalisedexpressingresults,'euclidean');
% % %     clustertree = linkage(corrdist,'average');
% % %     clusters = cluster(clustertree,'maxclust',16);
% % %
% % %     f = figure('visible','off');
% % %     for c = 1:16
% % %        subplot(4,4,c)
%                                 %                                   %
plot(time,normalisedexpressingresults((clusters==c),:)');
% % %        axis tight
% % %     end
% % %     saveas(f,'heirarchal_clusters.pdf');
% % %     close(f)
% % %
%                                 %                                   %
fprintf(fopen('heirarchalclusters.txt','w'),'%d\n',clusters);
% % %
% % %




    %%%
    %%% k means clustering
    %%%


    [cidx,ctrs]                                                       =
kmeans(normalisedexpressingresults,16,'dist','sqEuclidean','re
p',15,'disp','final');
```

```
    newf = figure('visible','off');
    for c = 1:16
       subplot(4,4,c)
       plot(time,normalisedexpressingresults((cidx==c),:)');
       axis tight
    end
    saveas(newf,'kmeans_clusters.pdf');
    close(newf)

fprintf(fopen('kmeansclusters.txt','w'),'%d\n',cidx);



    newerf = figure('visible','off');
    for c = 1:16
       subplot(4,4,c)
       plot(time,ctrs(c,:)');
       axis tight
       axis off
    end
    saveas(newerf,'kmeans_clusters_profiles.pdf');
    close(newerf)

end

%%%%%%%%%%%%%%%%%%%%%%%%%%%%%%%%%%%%%%%%%%%%%%%%%%%%%%%%%%%%%%%%%%%%%%%%%%%%%%%%
%%%%%%%%%%%%%%%%%

count
expressingcount


dlmwrite('Sig_Expressed_Gene_Names.txt',char(expressinggenes),
'')
dlmwrite('Sig_Expressed_Gene_IDs.txt',char(expressinggenes2),'
')
csvwrite('Sig_Expression_Profiles.csv',sigtranscriptresults)
csvwrite('Raw_Expression_Profiles.csv',rawexpressingresults)



if bordercount > 0
```

```
dlmwrite('Borderline_Expressed_Gene_Names.txt',char(borderexpr
essinggenes),'')
csvwrite('Borderline_Expression_Profiles.csv',borderlinetransc
ripresults)
end



end
```

1.2 Coding for producing heatmaps

The following coding are for generating heat maps on data which are not normalised by the average means (this is the general case when using MATLAB clustergram built in functions). In another word, this part of the coding is for producing a heatmap where the time points are normalised to T0 control.

CODES:

```
function output = clustergramscalebar (data,names,scalebar)



output = clustergram(data,'ColumnLabels',[0 6 64
96],'DisplayRatio',[1/10,1/3],'RowLabels',names,'Cluster',1,'C
olormap',scalebar);


set(output,'Standardize',3)




end


% when running this function, create a temp folder name then
save the file
% eg DNArepair = clustergram (list of data,list of
names,upmatrix)
% 'DNArepair' folder will be created in the temporary
workspce, save this
% file
```

1.3 Extracting transcripts ID and gene names

In order to extract data from the microarray, we

The microarray data are listed by transcripts IDs and gene names, in order extract data, we need these information first. However, when we look at pathway of interest, only the Gene ID's are provided. Therefore, the following section describes how to extract gene names and transcript ID number from a gene ID list exported from KEGG pathway, the matlab coding is also provided.

1. From KEGG, export and save the gene ID of a particular pathway as a text file

2. Open up Matlab and load the following files:- Gene_Names_full, AllIDs, Data_full, Transcript_full and"Gene ID of interest.text"

3. Run 'search by Gene_IDs.m'

MATLAB CODES:-

```
function Search_by_Gene_IDs
(data_full,AllGeneIDnumbers,GeneNames,TranscriptsIDs,GeneIDsof
Interest)


probes = 3;              % there are three probes for every
transcript
p = data_full;    % This reads in the input matrix to the p
data matrix
datalength = length(p(:,1));  % this works out how many data
points there are


a = 2;  %this will start the analysis at row 2 (row 1 is time
points)


number_of_transcripts = (datalength-1)/probes; % works out how
many genes to be tested
number_of_interestinggenes = length(GeneIDsofInterest);


count = 0;  % starts the count of expressed genes at zero


vec1 = zeros(9,1); % empty vector for all 12 gene measurements
of T0
```

```
vec2 = zeros(9,1); % empty vector for all 12 gene measurements
of T6
vec3 = zeros(9,1); % empty vector for all 12 gene measurements
of T64
vec4 = zeros(9,1); % empty vector for all 12 gene measurements
of T96


for i = 1:number_of_transcripts

    for j = 1:number_of_interestinggenes




         if AllGeneIDnumbers(a) == GeneIDsofInterest(j)


            vec1(1:9)                                          =
sort([p(a,1:3),p(a+1,1:3),p(a+2,1:3)]);
            vec2(1:9)                                          =
sort([p(a,4:6),p(a+1,4:6),p(a+2,4:6)]);
            vec3(1:9)                                          =
sort([p(a,7:9),p(a+1,7:9),p(a+2,7:9)]);
            vec4(1:9)                                          =
sort([p(a,10:12),p(a+1,10:12),p(a+2,10:12)]);


            count = count+1;
            genename(count) = GeneNames(a);
            transcriptname(count) = TranscriptsIDs(a);
            geneID(count)=AllGeneIDnumbers(a);


            rawresults(count,:)                                =
[mean(vec1(2:8)),mean(vec2(2:8)),mean(vec3(2:8)),mean(vec4(2:8
))];



         end


    end


    a=a+3;   % the analysis for this gene is done, we move a
along 3 for next gene
```

```
end

geneID=geneID';

count

dlmwrite('Gene_Names_Interest.txt',char(genename),'')
dlmwrite('Transcript_IDs_Interest.txt',char(transcriptname),''
)
csvwrite('Gene_IDs_Interest.csv',geneID)
csvwrite('Raw_Expression_Profiles_Interest.csv',rawresults)

end
```

1.4 MICROARRAY CANONICAL PATHWAY ANALYSIS

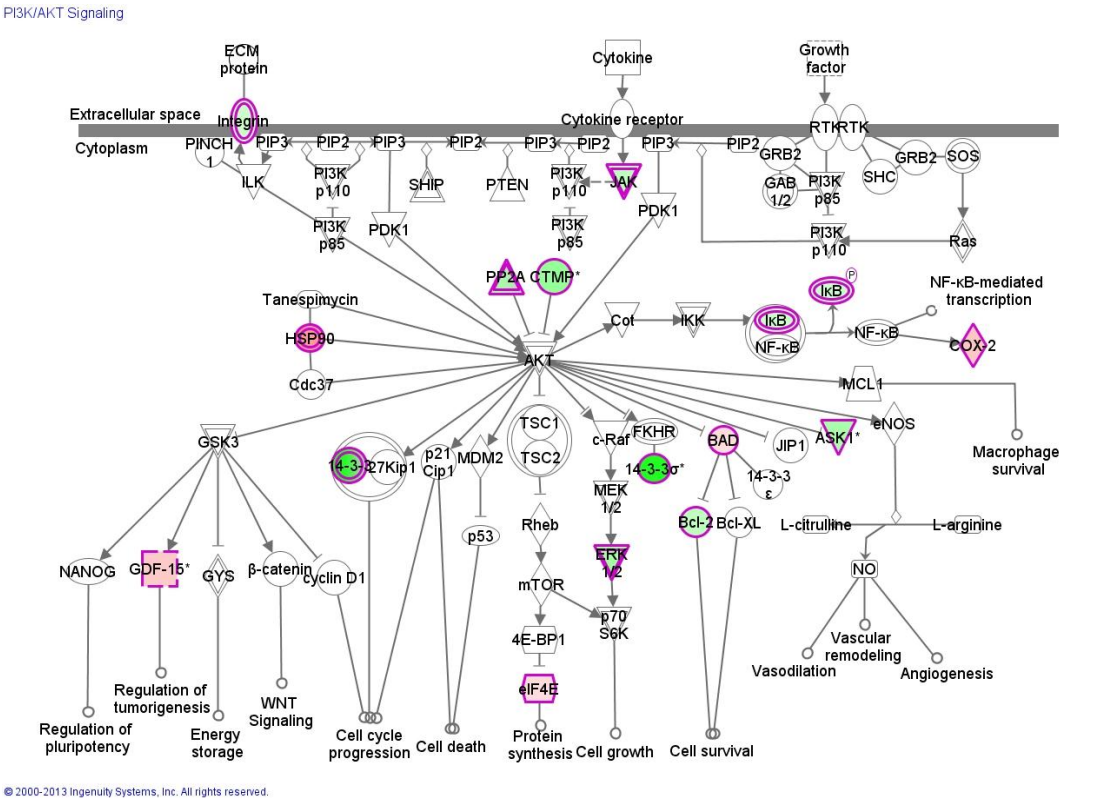

PI3K/Akt pathway obtained from IPA. *A component pathway of the PI3K/Akt pathway, highlighting the genes which are regulated (highlighted in purple) in chronic hypoxia. Expressed genes are shaded in red, repressed genes are shaded in green*